

$^{18}\text{O}/^{16}\text{O}$ AND D/H STUDIES ON THE
INTERACTIONS BETWEEN HEATED METEORIC GROUND WATERS AND
IGNEOUS INTRUSIONS: WESTERN SAN JUAN MOUNTAINS, COLORADO
AND THE ISLE OF SKYE, SCOTLAND

Thesis by
Richard W. Forester

In Partial Fulfillment of the Requirements
for the Degree of
Doctor of Philosophy

California Institute of Technology
Pasadena, California

1975

(Submitted January 21, 1975)

Acknowledgements

I am indebted to Dr. Hugh Taylor for guidance, and for hundreds of stimulating and heated discussions (held in six countries) throughout the course of this research. Many of his ideas and suggestions have been incorporated into this study.

Dr. Samuel Epstein kindly provided mass spectrometer and laboratory facilities.

I thank S. Epstein, L.T. Silver, A.L. Albee, W.B. Kamb, G.G. Goles, D.E. White, J.R.O'Neil, A.R. McBirney, D.L. Norton, R.F. Gans, B.R. Doe, R.E. Zartman, S.M.F. Sheppard, D. Wenner, J. Hall, T.O. Early, P.L. Knauth, and J. Laird for valuable discussions.

Hugh Taylor and S.M.F. Sheppard kindly helped collect samples from Scotland. Other samples were generously contributed by R.P. Sharp, A.L. Albee, J.D. Hudson, R. Todhunter, A. Bateman, A.R. McBirney, F.N. Earll, R.B. Farquharson, R.L. Armstrong, P. Rodda, J.T. Fyles, and S. Moorbath.

I thank Joop Goris and Jane Young for helping with the mass spectrometric analyses. E.V. Nenow, D. Smith, P. Yanagisawa and, in particular, C. Bauman, maintained the high vacuum equipment in working order. I thank A. Gancarz, who generously gave of his time, and skillfully manipulated the Caltech microprobe.

I would like to thank my wife, Gert, for her encouragement, for typing several earlier drafts of this manuscript, and for drafting some of the figures for the thesis.

During part of this research, I was supported by the Phelps Dodge Fund and an ARCS scholarship. Research funds were also provided by Dr. Hugh Taylor from NSF Grants GA-12945 and GA 30997X.

ABSTRACT

Detailed oxygen, hydrogen and carbon isotope studies have been carried out on igneous and metamorphic rocks of the Stony Mountain complex, Colorado, and the Isle of Skye, Scotland, in order to better understand the problems of hydrothermal meteoric water-rock interaction.

The Tertiary Stony Mountain stock (~1.3 km in diameter), is composed of an outer diorite, a main mass of biotite gabbro, and an inner diorite. The entire complex and most of the surrounding country rocks have experienced various degrees of ^{18}O depletion (up to 10 per mil) due to interaction with heated meteoric waters. The inner diorite apparently formed from a low- ^{18}O magma with $\delta^{18}\text{O} \approx +2.5$, but most of the isotopic effects are a result of exchange between H_2O and solidified igneous rocks. The low- ^{18}O inner diorite magma was probably produced by massive assimilation and/or melting of hydrothermally altered country rocks. The $\delta^{18}\text{O}$ values of the rocks generally increase with increasing grain size, except that quartz typically has $\delta^{18}\text{O} = +6$ to $+8$, and is more resistant to hydrothermal exchange than any other mineral studied. Based on atom % oxygen, the outer diorites, gabbros, and volcanic rocks exhibit integrated water/rock ratios of 0.3 ± 0.2 , 0.15 ± 0.1 , and 0.2 ± 0.1 , respectively. Locally, water/rock ratios attain values greater than 1.0. Hydrogen isotopic analyses of sericites, chlorites, biotites, and amphiboles range from -117 to -150. δD in biotites varies inversely with $\text{Fe}/\text{Fe}+\text{Mg}$, as predicted by Suzuoki

and Epstein (1974), and positively with elevation, over a range of 600 m. The calculated δD of the mid-to-late-Tertiary meteoric waters is about -100. Carbonate $\delta^{13}C$ values average -5.5 (PDB), within the generally accepted range for deep-seated carbon.

Almost all the rocks within 4 km of the central Tertiary intrusive complex of Skye are depleted in ^{18}O . Whole-rock $\delta^{18}O$ values of basalts (-7.1 to +8.4), Mesozoic shales (-0.6 to +12.4), and Precambrian sandstones (-6.2 to +10.8) systematically decrease inward towards the center of the complex. The Cuillin gabbro may have formed from a ^{18}O -depleted magma (depleted by about 2 per mil); $\delta^{18}O$ of plagioclase (-7.1 to +2.5) and pyroxene (-0.5 to +3.2) decrease outward toward the margins of the pluton. The Red Hills epigranite plutons have $\delta^{18}O$ quartz (-2.7 to +7.6) and feldspar (-6.7 to +6.0) that suggest about 3/4 of the exchange took place at subsolidus temperatures; profound disequilibrium quartz-feldspar fractionations (up to 12) are characteristic. The early epigranites were intruded as low- ^{18}O melts (depletions of up to 3 per mil) with $\delta^{18}O$ of the primary, igneous quartz decreasing progressively with time. The Southern Porphyritic Epigranite was apparently intruded as a low- ^{18}O magma with $\delta^{18}O \approx -2.6$. A good correlation exists between grain size and $\delta^{18}O$ for the unique, high- ^{18}O Beinn an Dubhaich granite which intrudes limestone having a $\delta^{18}O$ range of +0.5 to +20.8, and $\delta^{13}C$ of -4.9 to -1.0. The δD values of sericites (-104 to -107), and amphiboles, chlorites,

and biotites (-105 to -128) from the igneous rocks, indicate that Eocene surface waters at Skye had $\delta D \approx -90$. The average water/rock ratio for the Skye hydrothermal system is approximately one; at least 2000 km^3 of heated meteoric waters were cycled through these rocks.

Thus these detailed isotopic studies of two widely separated areas indicate that (1) ^{18}O -depleted magmas are commonly produced in volcanic terranes invaded by epizonal intrusions; (2) most of the ^{18}O -depletion in such areas are a result of subsolidus exchange (particularly of feldspars); however correlation of $\delta^{18}\text{O}$ with grain size is generally preserved only for systems that have undergone relatively minor meteoric-hydrothermal exchange; (3) feldspar and calcite are the minerals most susceptible to oxygen isotopic exchange, whereas quartz is very resistant to oxygen isotope exchange; biotite, magnetite, and pyroxene have intermediate susceptibilities; and (4) basaltic country rocks are much more permeable to the hydrothermal convective system than shale, sandstone, or the crystalline basement complex.

TABLE OF CONTENTS

	Page
1 INTRODUCTION	1
1.1 Object of the research	1
1.2 Basis of the research	3
1.3 Isotopic variations in natural waters	14
1.4 Previous work	14
2 THEORETICAL CONSIDERATIONS	21
2.1 Notation	22
2.2 Theory of isotopic fractionation	24
2.3 Oxygen isotope fractionations	24
2.4 Hydrogen isotope fractionations	24
3 EXPERIMENTAL PROCEDURES	29
3.1 Sample collection	29
3.2 Petrographic examination and preparation of samples	29
3.3 Oxygen extraction	32
3.4 Hydrogen extraction	33
3.5 Mass spectrometric and other correction factors	34
4 A MODEL FOR METEORIC HYDROTHERMAL CONVECTION	38
4.1 General statement	38
4.2 Active geothermal systems	38
Steamboat Springs, Nevada	38
Salton Sea Geothermal Area, California	41
Wairakei Geothermal Area, New Zealand	43
4.3 Theory of convective fluid flow in the vicinity of an igneous intrusion	46
General statement	46
Mathematical formulation	50
4.4 Summary	57
5 THE STONY MOUNTAIN STOCK, WESTERN SAN JUAN MOUNTAINS, SOUTHWESTERN COLORADO, U.S.A.	59
5.1 General geological setting	59
5.2 Mid-Cenozoic volcanic and tectonic history of the Western San Juan Mountains	61
5.3 Geology of Stony Mountain stock	66
6 ISOTOPIC RESULTS: WESTERN SAN JUAN MOUNTAINS, COLORADO	76
6.1 Regional isotopic relationships	76
6.2 Isotopic relationships in the volcanic country rocks	95
6.3 Hydrogen isotope systematics	101

	Page
6.4 Oxygen isotopic variations within the Stony Mtn. complex	113
6.5 Effect of grain size	116
6.6 Effect of fractures and hydrothermal veins	124
6.7 Effect of mineralogy	126
6.8 Oxygen isotopic relationships among minerals	127
6.9 Mineral-whole rock ^{18}O relationships	139
6.10 Carbon and oxygen isotope ratios in carbonates	140
6.11 Water/rock ratios	143
Method of calculation	143
Gabbros	148
Outer diorite	153
Tertiary volcanic rocks	155
Veins	158
6.12 Low- ^{18}O magma hypothesis	159
7 THE SCOTTISH TERTIARY IGNEOUS PROVINCE	170
7.1 Introduction	170
7.2 Isle of Skye, Scotland	170
7.3 Pre-Tertiary geology of Skye	174
Lewisian	174
Torridonian	178
Durness Limestone	178
Mesozoic	179
7.4 The Tertiary igneous rocks of Skye	179
Introduction	179
Cuillin gabbro complex	180
Western Red Hills	186
Eastern Red Hills	191
8 ISOTOPIC RESULTS: ISLE OF SKYE, SCOTLAND	196
8.1 Introduction	196
8.2 Hydrogen isotope systematics	219
8.3 Lewisian gneiss	226
8.4 Torridonian sedimentary rocks	228
8.5 Cambro-Ordovician Durness limestone	231
8.6 Mesozoic sediments	237
8.7 Basaltic country rocks and dikes	241
Water/rock ratios	246
8.8 Cuillin gabbro complex	251
General statement	251
Plagioclase	251
Pyroxene	259
Plagioclase-pyroxene fractionations	261
Magnetite	263
Olivine	264
Summary	265

	Page
8.9 Broadford gabbro	266
8.10 Coire Uaigneich granophyre	268
8.11 Western Red Hills	273
8.12 Eastern Red Hills	301
8.13 Water/rock ratios in the Skye epigranites	307
8.14 Lead and strontium isotopic studies in Skye	309
9 OTHER SCOTTISH TERTIARY PLUTONIC CENTERS AND MISCELLANEOUS LOCALITIES	315
9.1 Isle of Mull	315
General geology	315
Isotopic results	324
9.2 Northern Granite Complex, Arran	331
9.3 Miscellaneous localities	334
Little Chief Granite porphyry stock, California	334
Clark County, Nevada	336
Coryell Syenite, British Columbia	336
Miscellaneous samples	337
 BIBLIOGRAPHY	 338

Chapter 1
INTRODUCTION

1.1 Object of the research

Taylor (1968) was the first to realize the full importance and extent of the high-temperature interaction of meteoric ground waters with intrusive igneous rocks, notably on his study of the Tertiary ring-dike complexes at Skye, Mull and Ardnamurchan, Inner Hebrides, Scotland. Taylor (1968) and Taylor and Forester (1971) found that (1) essentially all the rocks analyzed from these intrusive centers were low in ^{18}O , and (2) the ^{18}O fractionations among coexisting minerals were abnormal and therefore the mineral assemblage was not in oxygen isotope equilibrium. They concluded that these rocks had undergone interaction with heated meteoric waters, and pointed out that prime conditions for such an interaction would be shallow-level (epizonal) intrusions emplaced in a highly permeable country rock, such as the well-jointed plateau basalt flows of the Inner Hebrides. Hydrogen isotope studies by Taylor and Epstein (1968) confirmed these conclusions, and further ^{18}O analyses approximately delineated the areal extent of low ^{18}O rocks around intrusive centers in the volcanic fields of the San Juan Mountains, Colorado (Forester and Taylor, 1972; Taylor, 1974a), and the Western Cascade Range, Oregon (Taylor, 1971).

The above-described studies supplied little information concerning the detailed mechanism of meteoric water-rock interactions. Therefore, it is important to carry out comprehensive isotopic studies in a specific locality where the geology is well understood, but nevertheless complex enough to permit a wide variety of geological situations to occur. No such detailed investigations have yet been made on intrusive centers where there have been extensive interactions with meteoric ground waters. With the above criteria in mind, two areas were selected for detailed examination, the Scottish Tertiary igneous complex at Skye (Harker, 1904; Richey, 1961; Brown, 1969; Stewart, 1965) and a small gabbro-diorite pluton at Stony Mountain (Dings, 1941) in the San Juan Mountains.

The objectives of the present study are to try to discern:

- (1) the timing of the meteoric water-rock interactions in terms of the geological events;
- (2) whether or not any mineral pair can be useful as an ^{18}O geothermometer in these types of geologic environments;
- (3) the relative susceptibilities of the various minerals to isotopic exchange;
- (4) the effect of the water-rock interaction on mineralogy and texture;

- (5) the optimum conditions necessary for the interaction, and the relative importance of the various geological variables, such as water/rock ratios, type of country rock, degree of fracturing, grain size of the minerals, mineralogy, etc.;
- (6) the temperatures involved in this exchange process; and
- (7) whether or not the liquid silicate melt was contaminated with meteoric waters, or whether the interaction took place entirely with solid rocks, together with an attempt to place semi-quantitative limits on the importance of both effects.

1.2 Basis of the research

There are essentially two premises that provide the basis for this whole work: (1) $\delta^{18}\text{O}$ and δD values in primary, unaltered igneous rocks are relatively constant throughout the world, and (2) meteoric waters and other surface-derived waters in general have $\delta^{18}\text{O}$ and δD values that are in marked contrast to those in average igneous rocks.

The $^{18}\text{O}/^{16}\text{O}$ ratios of most igneous rocks of various ages throughout the world lie in the range $\delta = +5.5$ to $+10.0$ (Figure 1-1). In striking contrast to these rocks, some geologic complexes exhibit widely divergent and

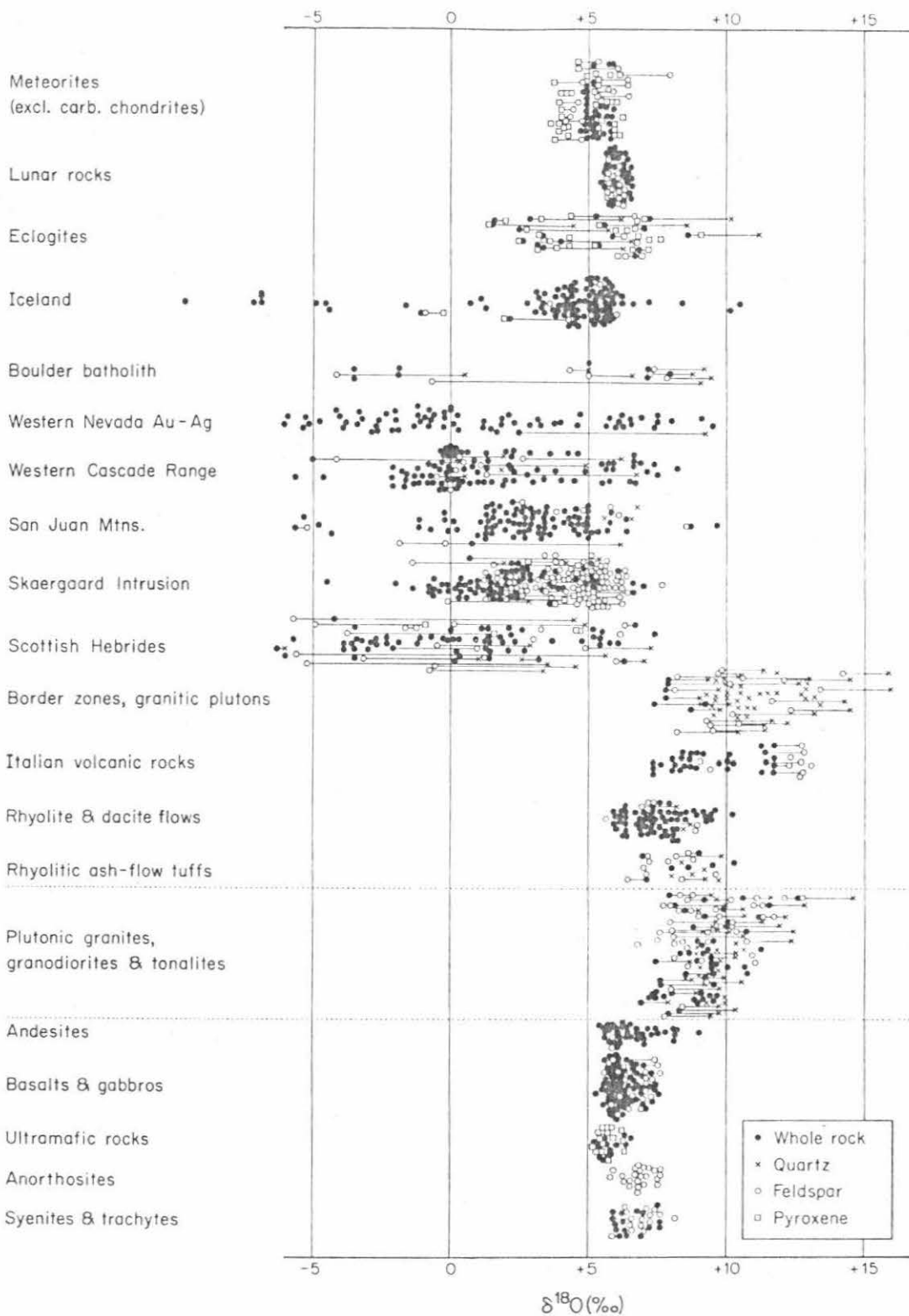


Figure 1-1. Mineral and whole rock $\delta^{18}\text{O}$ analyses of igneous rocks from a wide variety of localities (after Taylor, 1974b).

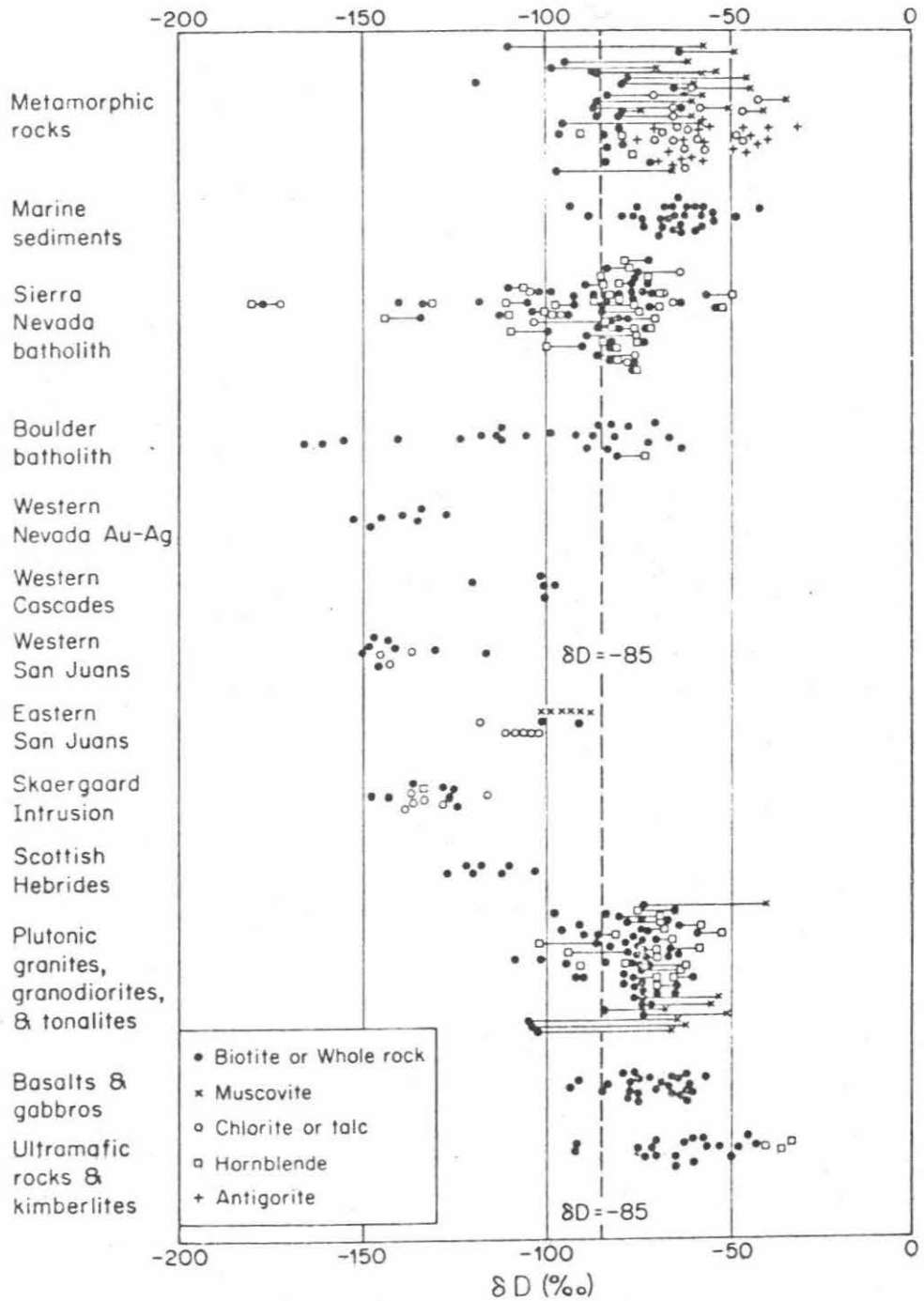


Figure 1-2. A plot of δD analyses from igneous, metamorphic, and hydrothermally altered rocks from a wide variety of localities. Compilation from Taylor (1974b).

abnormally low $\delta^{18}\text{O}$ values, along with disequilibrium fractionations between coexisting minerals. These same complexes also exhibit abnormally low δD values (Figure 1-2). These areas have, in general, two geologic features in common: (1) they occur in relatively young (usually Tertiary), highly fractured volcanic piles, and (2) these volcanic lavas have been intruded by epizonal plutons. The only way in which such low δ -values could arise is through the interaction between 'normal' igneous rocks and low- ^{18}O , low-D, meteoric waters. This thesis is an attempt to better understand the interaction, by examining several of these anomalous areas in detail.

1.3 Isotopic variations in natural waters

In the present type of study it is important to have an understanding of the isotopic variations in natural waters that might be involved in igneous rock-water interactions. Much work has been carried out on natural waters during the last twenty years.

Meteoric waters include rain, melted snow and ice, lakes and rivers; in other words, all fresh water derived from the atmosphere. Early work on the isotopic variations of water by Epstein and Mayeda (1953) and Friedman (1953) were followed up by Craig (1961), who showed that meteoric ground waters

exhibit excellent systematics, and can be described by the equation

$$\delta D = 8\delta^{18}O + 10 \quad (\text{Figure 1-3}).$$

Because of liquid-vapor equilibrium fractionations in H_2O , the water in an air mass is depleted in the heavy isotopes of oxygen and hydrogen relative to the ocean from which it is derived. As the air mass moves inland across the continents and precipitation occurs, there is a progressive depletion in ^{18}O and deuterium in the clouds because of these fractionation effects. On the continents these effects are reflected in the surface waters; the higher the elevation or latitude, the lower the δD and $\delta^{18}O$ values of the waters. Figure 1-4 represents a rough contour map for average δD values in North America. Note the marked topographic effect shown by both the Sierra Nevada and the Rocky Mountains.

Those surface waters that plot off the meteoric water line (closed basins on Figure 1-3) have undergone evaporation in arid climates, a process dominated by the kinetics of rapid molecular exchange between liquid and vapor (Craig et al., 1963).

Present-day ocean waters are singularly uniform in their isotopic composition. Only in the areas of restricted circulation, such as the Red Sea where evaporation is an important process (Craig, 1966) or where ocean water is contaminated by meltwater or river water discharge, will oceanic

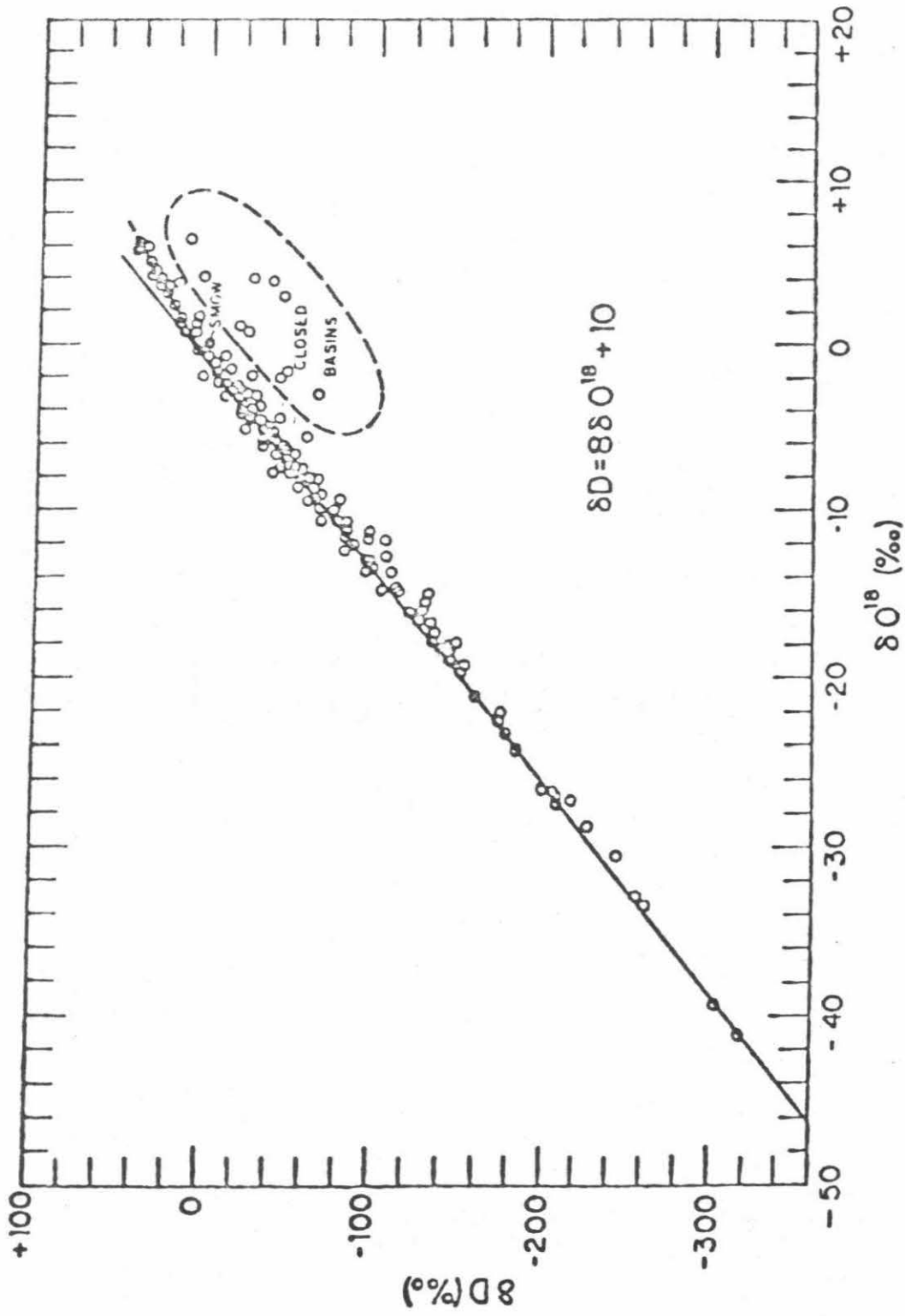


Figure 1-3. δD and $\delta^{18}O$ variations in meteoric waters, after Craig (1961).

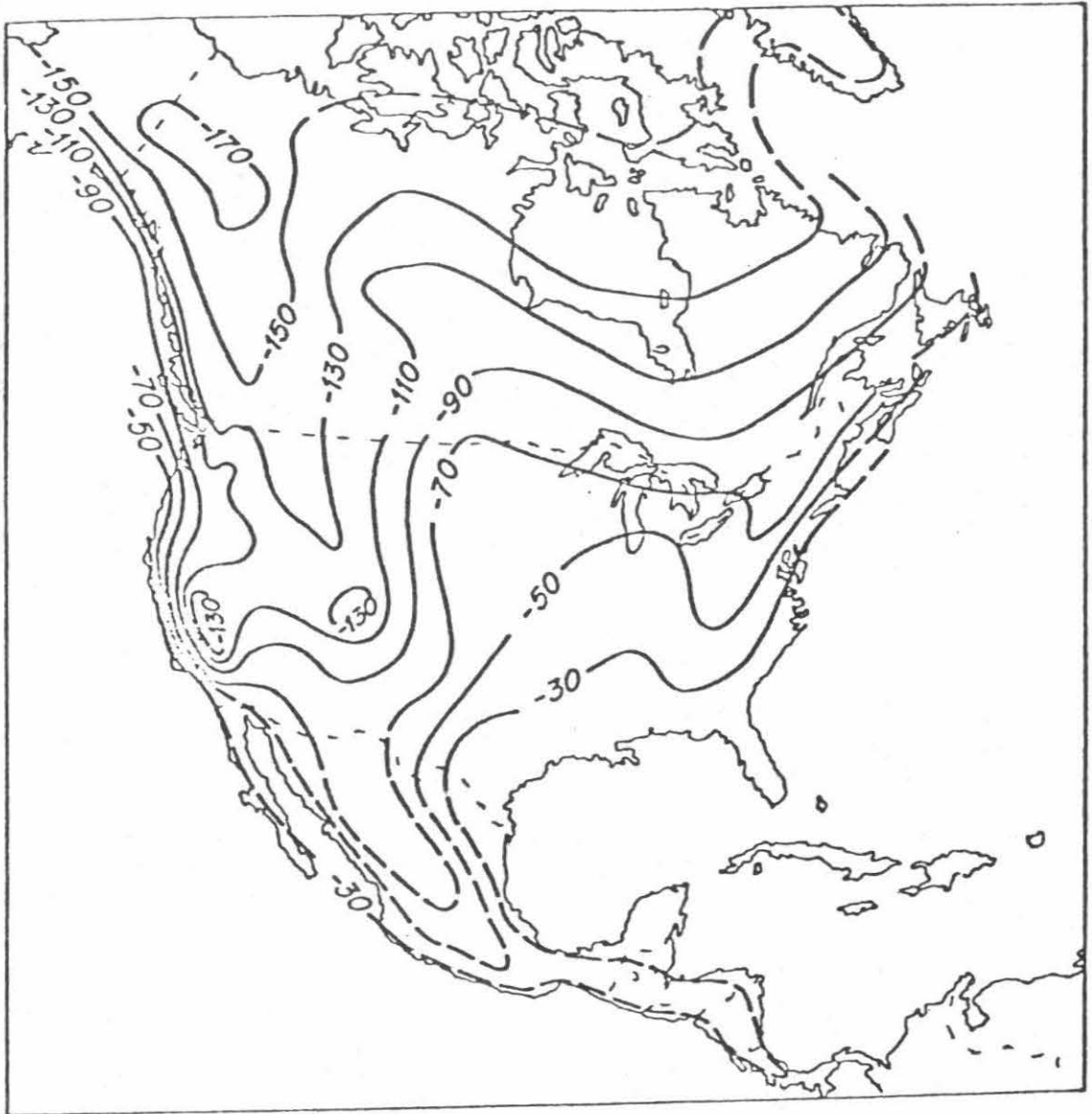


Figure 1-4. Map of North and Central America showing the approximate average δD values of meteoric waters. Compilation after Taylor (1974b), based on data of Freidman *et al.* (1964), Dansgaard (1964), and Hitchon and Krouse (1972).

δ -values differ significantly from those of mean ocean water.

It is now well established that almost all geothermal waters in hot spring areas throughout the world are essentially of surface origin. Craig et al. (1956) discovered that, compared with the local meteoric waters, near-neutral, chloride-type hot springs are characterized by an enrichment in ^{18}O , but have essentially the same hydrogen isotopic composition (Figure 1-5). This was interpreted as an exchange of oxygen between the isotopically heavy country rocks and the isotopically depleted ground waters. The country rocks, having approximately 30 times less atom % hydrogen with respect to an equal volume of water, would have a negligible effect on the δD of the water, thus giving rise to the characteristic "oxygen isotope shift" shown in Figure 1-5 (see also Craig, 1963; 1966). Isotopic patterns in the acid-type hot springs (Figure 1-6) show similar features, but are accompanied by some systematic changes in D/H ratios, a result of non-equilibrium kinetic effects in evaporation.

The isotopic compositions of formation waters (Figure 1-7) have been studied by Degens et al. (1964), Graf et al. (1965), Clayton et al. (1966), and Hitchon and Friedman (1969). Clayton et al. (1966) concluded that the saline formation waters in the mid-continent region of North America are predominantly of local meteoric origin. They suggested that the original connate waters were flushed out during compaction

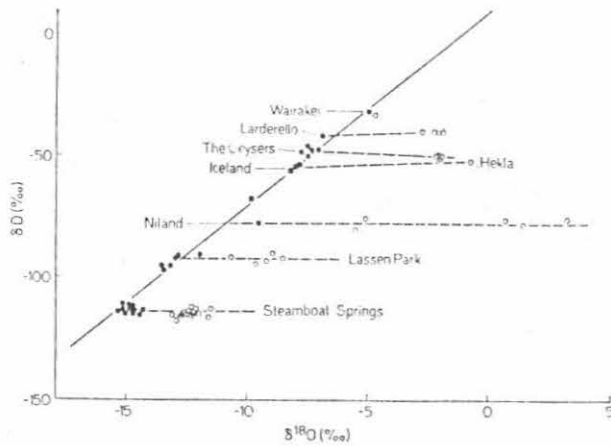


Figure 1-5

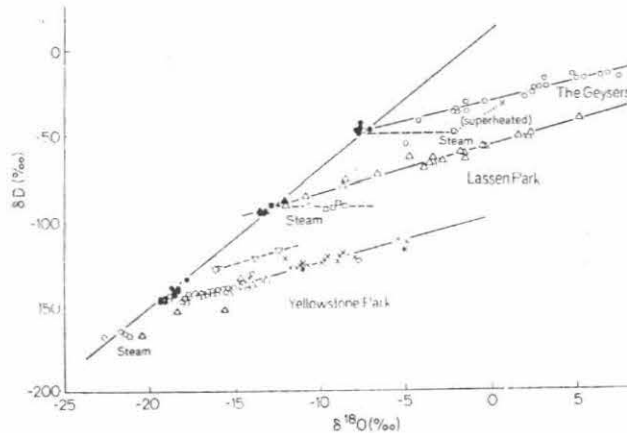


Figure 1-6

Figure 1-5. δD vs $\delta^{18}O$ plot for near-neutral, chloride-type geothermal waters (open circles) and local precipitation (solid circles). The meteoric water line is also shown. After Craig et al. (1956); Craig, (1963).

Figure 1-6. δD vs $\delta^{18}O$ plot for acid geothermal waters and steam. The solid symbols represent local meteoric waters. After Craig (1963).

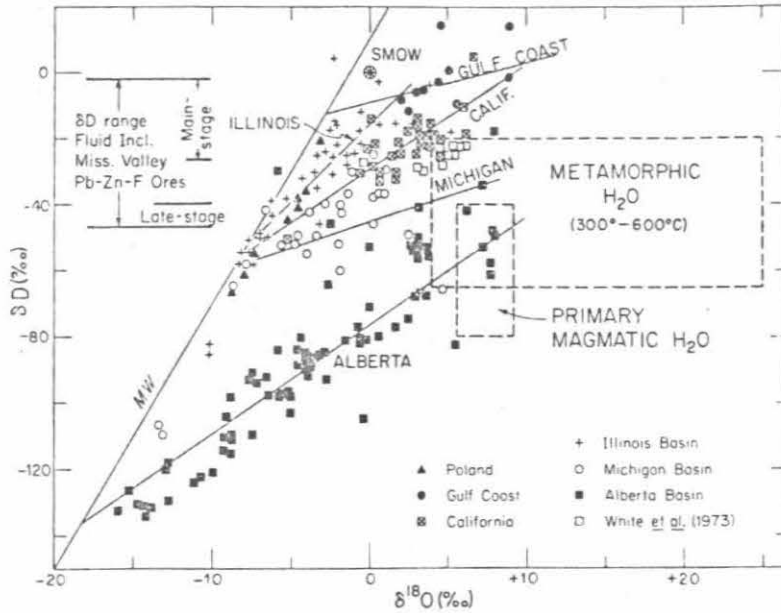


Figure 1-7. Plot of δD vs $\delta^{18}O$ for formation waters from Gulf Coast, Illinois, and Michigan basins (Clayton *et al.*, 1966), the Alberta basin (Hitchon and Friedman, 1969), the California Tertiary (Kharaka *et al.*, 1973) and Poland (Dowgiallo and Tongiorgi, 1972). The calculated fields of primary magmatic waters and metamorphic waters are also shown, along with some possible modern metamorphic waters from California (White *et al.*, 1973). MW = meteoric water line.

of the sedimentary section and cycling of ground waters. Hitchon and Friedman (1969) however, explained the formation waters as having originated by mixing connate (sea) water with surface waters. Exchange between limestones and water causes the main ^{18}O shift, while exchange of deuterium between H_2S and water explains some of the δD variation. Another possible fractionation process that may account for part of the isotopic variations seen in Figure 1-7 is ultra-filtration (Coplen and Hanshaw, 1973). Note that some of these samples come from great depths (over 3.5 km), and these waters represent direct evidence for the involvement of waters of meteoric origin in deep-seated geological processes.

Those waters that have equilibrated with rocks at the P and T of metamorphism may be defined as metamorphic waters. Since we cannot directly measure this type of water, we apply an appropriate fractionation factor to the measured D/H ratio in hydrous minerals of metamorphic rocks (see Figure 1-2) and come up with the field shown in Figure 1-7. The large variation in $\delta^{18}\text{O}$ (+5 to +25) is mainly due to the highly variable oxygen isotopic compositions of the metamorphic parent rocks. The δD values however, lie in the restricted range -20 to -65.

Magmatic waters are those solutions that have equilibrated with igneous materials at magmatic temperatures. Because most igneous rocks have relatively uniform $\delta^{18}\text{O}$ and δD

values (Figures 1-1 and 1-2) the field for primary magmatic waters is similarly constrained (Figure 1-7).

A fundamental problem exists in defining the δD range of H_2O in natural silicate melts. If all of the hydrogen in a silicate melt is ultimately incorporated into the hydrous mineral phases that crystallize from the magma, then the δD value of "magmatic water" will be given by the bulk isotopic analyses of the minerals themselves. On the other hand, equilibrium mineral-water hydrogen isotope fractionation factors are roughly 0.975 at $700^\circ C$ (Suzuoki and Epstein, 1970). Therefore the field of "primary magmatic water" shown in Figure 1-7 is here defined as the calculated water in equilibrium with the minerals of 'normal' igneous rocks at temperatures $\geq 700^\circ C$. The H_2O given off during the late stages of crystallization of a water-rich magma would probably have such a δD value.

1.4 Previous work

Although in disfavor until recently, the idea that meteoric ground waters may have interacted with igneous intrusions and their associated country rocks is not particularly new. It has long been thought plausible, for example, that meteoric waters have passed through hot igneous rocks and have given rise to geysers and hot springs. Lawson (1914)

and Van Hise (1902) argued for a ground water origin for the deposition of ores in and near intrusive bodies, but since that time, largely due to the influence of W. Lindgren, J.F. Kemp and other geologists, the magmatic origin of hydrothermal ore deposits was almost universally accepted.

The first clear-cut chemical evidence to indicate that meteoric ground waters were the principal constituents of almost all hot spring waters, and that abundant exchange had occurred with rocks, was that of Craig et al. (1956; see Sect. 1-3).

Clayton et al. (1968a) did an oxygen isotope study on the fine-grained sandstones and siltstones of the Colorado River delta in the Salton Sea geothermal area. They concluded that the carbonate and silicate minerals had exchanged oxygen with the local meteoric waters, and were in isotopic equilibrium at temperatures ranging from 340°C down to approximately 150°C. The fine-grained quartz, however, proved to be very resistant to oxygen isotope exchange and it only moved about 50% of the way toward equilibrium at 340°C. Approximately equal volumes of water and rock were involved in this exchange process.

The first igneous rocks with anomalous $\delta^{18}\text{O}$ values attributable to exchange with meteoric waters were found by Taylor and Epstein (1963) in the chilled marginal gabbro of

the Skaergaard Intrusion, Greenland. The mineral assemblage in this rock was also found not to be in isotopic equilibrium because the plagioclase $\delta^{18}\text{O}$ value was lower than in the co-existing clinopyroxene. In addition, Garlick and Epstein (1966) also observed such ^{18}O disequilibrium and attributed the large variation of $^{18}\text{O}/^{16}\text{O}$ found in various samples of hydrothermal quartz from Butte, Montana to the mixing of meteoric water with magmatic water.

Taylor (1968) re-interpreted some of the conclusions of Taylor and Epstein (1963) on the Skaergaard Intrusion, suggesting that meteoric ground waters had contaminated the later stages of crystallization of the Skaergaard magma, thus producing the trend of ^{18}O depletion as one moved upward in the Layered Series. He also suggested that the Precambrian Seychelles Islands granite could have exchanged with meteoric waters, to explain its anomalously low $\delta^{18}\text{O}$ value of quartz (+4.1) and microperthite (+2.6). However, the main mass of data that led to a better understanding of low- ^{18}O igneous rocks came from the Tertiary Igneous Complexes of Skye, Mull and Ardnamurchan of northwest Scotland. Taylor (1968) concluded that the optimum conditions for exchange between heated meteoric waters and igneous rocks could be met when well-jointed country rocks (e.g. plateau basalts) are intruded by plutons at shallow depths of the earth's crust.

These conditions were met in the Scottish Tertiary Igneous Province and Taylor (1968) postulated that although most of the exchange took place after crystallization, some of this interaction was between meteoric waters and silicate melts.

Taylor and Epstein (1968) gave further evidence for the interaction of meteoric waters with shallow-level igneous rocks by showing that the hydrous phases from these plutons are commonly depleted in deuterium relative to those in "normal" igneous rocks (see Figure 1-7).

Sheppard et al. (1969; 1971) and Sheppard and Taylor (1973; 1974) presented strong isotopic evidence for the existence of a meteoric-hydrothermal component during the formation of the alteration assemblages in porphyry copper deposits. They were able to distinguish between hypogene and supergene clay minerals, and showed that the δD and $\delta^{18}O$ values of the Tertiary clays exhibit a well defined correlation with present-day δD and $\delta^{18}O$ values of meteoric waters. Sheppard et al. (1969) emphasized that to clearly distinguish between magmatic- and meteoric-hydrothermal fluids, we need to go to areas where the local meteoric waters provide a strong D/H contrast to D/H ratios thought to be characteristic of magmatic waters ($\delta D \approx -50$, Sheppard and Epstein, 1970; see Figure 1-7).

A pertinent ^{18}O study on the Scottish Tertiary rocks by Taylor and Forester (1971) presented evidence that most of

the low- ^{18}O rocks underwent exchange in the solid state, and that quartz was the most resistant, and alkali feldspar the least resistant, to isotopic exchange. This conclusion led to the realization that feldspar, being readily exchanged, can monitor hydrothermal effects, whereas quartz does not.

Some of the other isotopic studies that have demonstrated the involvement of heated low- ^{18}O meteoric waters with igneous rocks include Beckinsale (1974), Bethke et al. (1973), Eslinger and Savin (1973), Forester and Taylor (1972), Hall et al. (1973), Landis et al. (1972), Matsuhisa et al. (1972; 1973), Muehlenbachs et al. (1974), Ohmoto and Rye (1970), O'Neil et al. (1973), Sugisaki and Jensen (1971), Taylor (1971; 1973), Taylor and Forester (1973), and Wenner and Taylor (1974).

Rocks that have interacted with sea water have been described by Robinson and Badham (1974), Robinson and Ohmoto (1973), Ohmoto et al. (1970) and Wenner and Taylor (1973). Formation waters were the dominant hydrothermal fluids responsible for the Mississippi Valley deposits studied by Hall and Friedman (1969), Pinckney and Rye (1972) and Heyl et al. (1973). A review of these low- ^{18}O occurrences is given by Taylor (1974b).

Other than the many situations described above, which are all readily attributed to interaction with meteoric waters, there are only three other types of geologic occurrences

involving rocks with anomalously low- $^{18}\text{O}/^{16}\text{O}$ ratios: (1) certain eclogites, (2) various rocks in contact-metamorphic skarns that are associated with decarbonation reactions and (3) low- ^{18}O magmas. Several B-Type eclogites associated with migmatitic gneisses were shown to have $\delta^{18}\text{O}$ values as low as +1.5 (Vogel and Garlick, 1970). These low- ^{18}O eclogites were interpreted as having formed from basaltic rocks which have previously undergone high-temperature exchange with ocean water or meteoric water, before being carried down into the mantle along a subduction zone. The group III A-type eclogites from the Roberts Victor kimberlite pipe have $\delta^{18}\text{O}$ values as low as +2.2 and have been interpreted as products of a pressure-dependent crystal-melt isotopic fractionation (Garlick *et al.* 1971). Whatever their exact origin, it is clear that we do not yet have a proper understanding of these low- ^{18}O eclogites.

Unusually low- $^{18}\text{O}/^{16}\text{O}$ ratios are found in the calcsilicate skarns and rocks that are associated with decarbonation metamorphism. For example, wollastonite from an Adirondack skarn zone has a $\delta^{18}\text{O}$ value of -0.9 (Taylor, 1969). In these and other cases however, the geologic occurrence is usually sufficient to explain these low- ^{18}O values as a product of decarbonation whereby the liberated CO_2 carries off oxygen enriched by roughly 5 per mil over the residual calcsilicate minerals (e.g. see Shieh and Taylor, 1969b).

The first evidence for the existence of low- ^{18}O magmas was presented by Forester and Taylor (1972). They postulated that the inner diorite intrusion of the Stony Mountain stock in southwestern Colorado was emplaced with a $\delta^{18}\text{O} \approx +2.8$. This requires exchanging an amount of meteoric water equal to about 25% of that of the inner diorite silicate melt (based on atom % oxygen).

Muehlenbachs et al. (1974) and Muehlenbachs (1973) have reported $\delta^{18}\text{O}$ values as low as +0.4 for a pumice, and +2.8 for a glassy obsidian from Iceland. Glassy, fresh volcanic rocks from Iceland leave little doubt about the existence of low- ^{18}O magmas in nature. The main problem is the mechanism(s) through which these low- ^{18}O melts are generated. Recently, Friedman et al. (1974) have described large-scale interaction between meteoric water and magma in ash-flow tuffs from Nevada, Colorado, and Yellowstone National Park. The $\delta^{18}\text{O}$ values of these magmas decrease as a function of time, indicating continued contamination of the silicate melt. The effect has been to decrease by 2 per mil the original 'normal' $\delta^{18}\text{O}$ value of 7,000 km³ of magma in 6×10^5 years. It seems likely that all of these low- ^{18}O magmas are also the result of some type of meteoric-water interaction, but the exact details remain obscure. This problem is discussed in detail below.

Chapter 2

THEORETICAL CONSIDERATIONS

2.1 Notation

All isotopic analyses in this work are given in per mil in the familiar δ -notation,

$$\delta = \left(\frac{R_{\text{sample}} - R_{\text{standard}}}{R_{\text{standard}}} \right) 10^3$$

where R represents the $^{18}\text{O}/^{16}\text{O}$, D/H or $^{13}\text{C}/^{12}\text{C}$ ratio. The standard for oxygen and hydrogen is SMOW (Craig, 1961) while that for carbon is CO_2 evolved from the Chicago PDB Belemnite standard by reacting it with 100% H_3PO_4 at 25.2°C (Urey et al., 1951; McCrea, 1950).

The fractionation (or enrichment) factor α for two substances A and B is defined as $\alpha_{A-B} = R_A/R_B$. We can then write the relationship between α and δ as

$$\alpha_{A-B} = \frac{1000 + \delta_A}{1000 + \delta_B}$$

Theoretical calculations predict that for reactions among gaseous species $\ln\alpha$ follows a $1/T^2$ dependence at temperatures of geological interest, and most experimentally determined mineral - H_2O fractionations also closely approximate a $1/T^2$ relationship. It is therefore convenient to report fractionations as Δ , defined here as

$$\Delta_{A-B} = 10^3 \ln\alpha_{A-B}$$

Note that, inasmuch as α is usually close to unity, we can use the first term in the power series

$$\ln(1+x) = x - 1/2 x^2 + 1/3 x^3 - \dots,$$

to give an approximate value for $\Delta_{A-B} \approx \delta_A - \delta_B$.

Throughout the text, the δD and $\delta^{18}O$ values of specific minerals will be given as $\delta^{18}O_K$, $\delta^{18}O_Q$, δD_{H_2O} , etc. where the subscript identifies the mineral as defined in the abbreviations in Table 6-1. Note that $\delta^{18}O_R$ is the whole-rock $\delta^{18}O$ value, and $\delta^{18}O_{H_2O}$ is the $\delta^{18}O$ value of the H_2O fluid (usually a calculated value).

2.2 Theory of isotopic fractionation

Urey and Rittenberg (1933) were the first to point out the possibility of calculating isotopic equilibrium constants from spectroscopic data alone. Today most calculations of fractionation factors for isotopic exchange reactions are modeled after those of Urey (1947) and Bigeleisen and Mayer (1947), who related the mass-dependent vibrational frequencies to partition functions.

Consider the exchange reaction



where X and Y are molecules which have a common element.

Subscripts 1 and 2 denote that the molecule exclusively contains only the light or the heavy isotope respectively. The

equilibrium constant K for the reaction, at a specific temperature is given by

$$K = \left(\frac{Q_{X_2}}{Q_{X_1}} \right)^a / \left(\frac{Q_{Y_2}}{Q_{Y_1}} \right)^b ,$$

where Q = statistical mechanical partition function. The Q 's can be expressed in terms of the fundamental vibrational frequencies of the isotopic molecules involved. In general, $K = \alpha^n$, where n is the maximum number of exchangeable atoms taking part in the isotopic exchange reaction.

Bigeleisen and Mayer (1947) predicted that, at low temperatures, $\ln K$ would follow a $1/T$ dependence, while at high temperatures, $\ln K$ would vary as $1/T^2$. At infinitely high T , K approaches unity.

Note that oxygen isotope fractionation factors should be essentially pressure-independent, inasmuch as isotopic substitution represents a practically zero volume change. This has been experimentally verified by Hoering (1961) on the bicarbonate - H_2O system up to 4 kbs, and by Clayton et al. (1972a) for calcium carbonate- H_2O to 20 kbs. This pressure-independent characteristic not only simplifies oxygen isotope studies in natural systems, but establishes it as a powerful tool in unravelling geochemical processes.

2.3 Oxygen isotope fractionations

Experimentally determined mineral-H₂O oxygen isotope fractionation curves, as well as some empirically determined curves, are given in Figure 2-1. Figure 2-2 provides some calculated ¹⁸O/¹⁶O fractionation curves of particular interest. The most sensitive mineral pair for oxygen isotope geothermometry is quartz-magnetite (Figure 2-1), while quartz-alkali feldspar fractionations are extremely insensitive at the temperatures of formation of igneous and metamorphic rocks. The most accurately known mineral-H₂O fractionation curves are those for feldspar-H₂O (O'Neil and Taylor, 1967), muscovite-H₂O (O'Neil and Taylor, 1969) and calcite-H₂O (O'Neil *et al.*, 1969). These systems equilibrate fairly readily, compared to quartz-H₂O and magnetite-H₂O which involve experimental difficulties with respect to attainment of oxygen isotope equilibrium.

2.4 Hydrogen isotope fractionations

Some of the hydrogen isotope fractionations in silicate-H₂O systems investigated to date are shown in Figure 2-3, along with some empirical curves for low-temperature mineral assemblages. Note that in general, the values of 1000 ln α are much larger than those in the oxygen isotope systems.

The results of Suzuki and Epstein (1970; 1974; see Figure 2-3) demonstrate the importance of Mg, Fe and Al con-

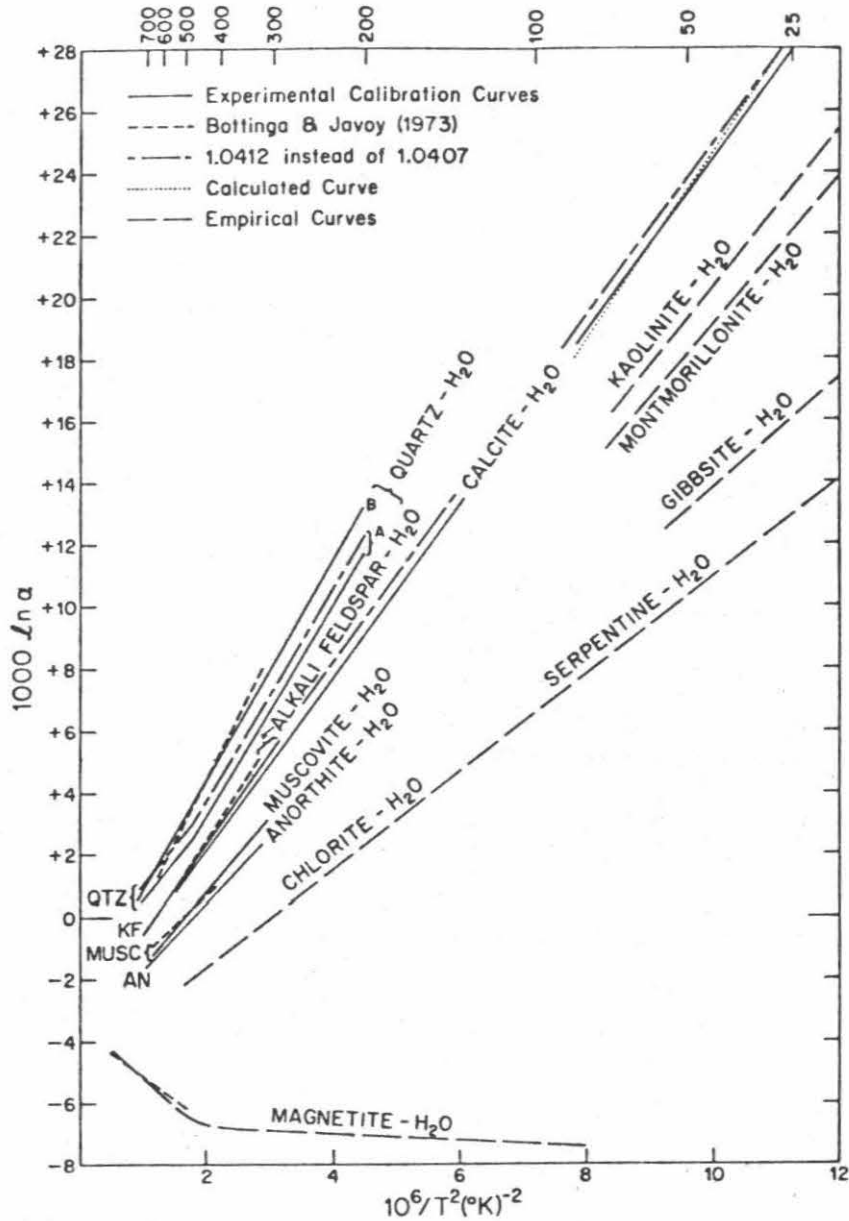


Figure 2-1. Experimentally determined equilibrium oxygen isotope fractionation curves for various mineral- H_2O systems, along with some empirically derived and calculated curves. Compilation is from Taylor (1974b).

Figure 2-2. Calculated equilibrium oxygen isotope fractionation factors as a function of temperature for $\text{CO}_2\text{-H}_2\text{O}$ and $\text{CO}_2\text{-calcite}$ (Bottinga, 1968), $^{34}\text{S}\text{O}_2\text{-H}_2\text{O}$ and $^{13}\text{C}\text{O}_2\text{-CO}$ (Urey, 1947), together with the experimentally determined curve for liquid water-vapor water (Horibe and Craig, in Craig 1963, solid line; Bottinga and Craig, 1968, dashed line). After Taylor (1974b).

Figure 2-3. Equilibrium hydrogen isotope fractionation curves for various mineral- H_2O systems. For temperatures above 400°C , the curves are based on laboratory experiments of Suzuoki and Epstein (1970, 1974). For temperatures below 400°C , the curves are based on empirical extrapolations to estimated values at earth-surface temperatures (Savin and Epstein, 1970; Lawrence and Taylor, 1971; Wenner and Taylor, 1973) and on some preliminary laboratory experiments by Sheppard and Taylor (unpub. data, 1969) on kaolinite- H_2O at 300°C . After Taylor (1974b).

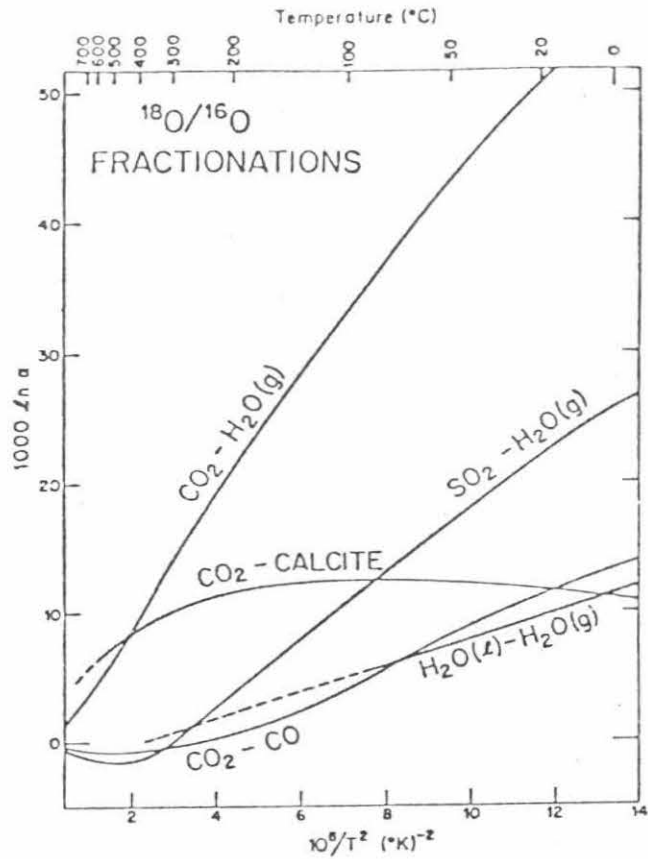


Figure 2-2

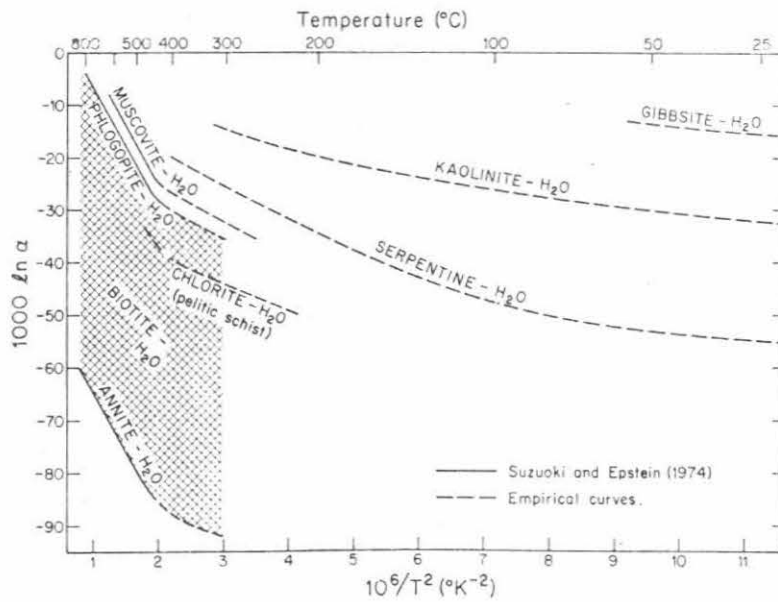


Figure 2-3

tents of the OH-bearing silicates on the D/H fractionations. At a specified temperature, Al and Mg-rich minerals concentrate deuterium relative to Fe-rich minerals.

It is of interest to note that, because of the essentially parallel nature of the fractionation curves in Figure 2-3, hydrogen isotope geothermometry on these silicate phases is virtually precluded. On the other hand, if we can obtain temperatures of formation by some independent means, the curves can be used to calculate the δD values of coexisting H_2O at equilibrium.

Chapter 3

EXPERIMENTAL PROCEDURES

3.1 Sample collection

Except for those samples reported in Taylor and Forester (1971) almost all of the samples analyzed in this work were collected by the author. The Stony Mountain samples were collected in the late summer of 1969, while the samples from Skye, Mull and Ardnamurchan were obtained in a trip to Scotland in 1970. Additional samples from Skye were collected during a brief return trip in July, 1971.

3.2 Petrographic examination and preparation of samples

Nearly all of the samples analyzed in this research were examined in thin section. Pertinent petrographic data are given along with the isotopic data in the appropriate tables. X-ray diffraction techniques were used to identify and estimate the type and relative amounts of carbonate that were present.

In most cases, handpicking of mineral grains from the gently crushed rock was sufficient to give pure mineral separates. A Frantz magnetic separator was also used, but because of the ubiquitous presence of dust-like magnetite in some of the samples, the Frantz separator could not always provide a sufficiently pure separate. On the other hand, these same inclusions provided a simple way of separating

different portions of the same mineral (e.g. plagioclase) from a hand specimen on the basis of their differing magnetic susceptibilities.

After handpicking, most quartz separates were treated with hydrofluoric acid and then cleaned ultrasonically. Because many of the handpicked feldspar grains contained quartz intergrowths, and because the $\delta^{18}\text{O}$ values of the co-existing quartz and feldspar are in general quite different because the two minerals are drastically out of oxygen isotopic equilibrium, it was important to correct for this effect. This was done by (a) examining the oxygen yields produced during F_2 reaction of the feldspars and (b) making grain mounts of the analyzed feldspar separates and estimating their quartz contents. The largest such correction, 0.9 per mil, was applied to the feldspar of SK-177. Most corrections amounted only to about 0.2 or 0.3 per mil.

Magnetite, olivine and epidote react with fluorine only with great difficulty. Therefore, these minerals were ground to a very fine powder and reacted with fluorine at the highest possible temperatures ($\sim 630^\circ\text{C}$). The magnetite was separated from the other minerals by first obtaining a rough hand-magnetic separate from the sample, and grinding this sample to a fine grain size. The grains were then placed in a beaker and the non-magnetic grains were washed away while the magnetite was held at the bottom of the beaker by a hand magnet. This process was repeated many times until an essentially pure magnetite separate was recovered.

Whole-rock powders were prepared by first grinding a few small chips of the rock sample in the mortar, then discarding this sample. In this way, the mortar was "contaminated" with a sample of the same rock that was to be ground for isotopic analysis.

Some of the samples, especially the hydrothermally altered volcanic country rocks, contain small but significant amounts of calcite. Inasmuch as the fluorination of carbonates may give non-predictable results, it was decided to remove the carbonate from some of these whole-rock samples prior to fluorination. To test the effect of removing the calcite with hydrochloric acid on the $\delta^{18}\text{O}$ value of the residue, three experiments were performed.

(1) A sample of M1-22 ($\delta^{18}\text{O}_R = +4.4$), which does not contain calcite, was treated with 3.7 N HCl for about 20 seconds, filtered and thoroughly washed with warm distilled water and the residue dried. The residue had $\delta^{18}\text{O}_R = +4.5$ (i.e. indistinguishable from the untreated sample).

(2) A sample of M1-52 which contained a small (<5%) amount of calcite was directly reacted with F_2 and gave a $\delta^{18}\text{O}_R = +5.6$. The sample was then treated with HCl as above in experiment (1); the acid-treated sample had the same $\delta^{18}\text{O}$ value, +5.6. It thus appears that small amounts of carbonate do not significantly affect the $\delta^{18}\text{O}_R$ values.

(3) Equal amounts (~20 mg) each of basalt SK-168 ($\delta^{18}\text{O} = +0.4$) and calcite SK-48 ($\delta^{18}\text{O} = +19.2$) were mixed together

and acid-treated as in the above experiments. The filtered residue was analyzed and found to be essentially indistinguishable from SK-168, with $\delta^{18}\text{O} = +0.5$.

Most of the amphiboles, chlorites, and biotites analyzed for D/H were essentially monomineralic concentrates. A pure separate is not entirely necessary however, as long as the contaminating minerals are anhydrous, or only contribute insignificantly to the total H_2 yield. In fact, all the white mica analyses were extracted from whole rock or feldspar concentrates, where sericite is the dominant (or sole) hydrous mineral. The identification and relative amounts of the various hydrous phases in the D/H analyses were checked by utilizing optical and X-ray techniques, as well as examining the H_2 yields produced during fusion of the sample.

3.3 Oxygen extraction

Almost all of the oxygen extractions from silicates and oxides were performed using fluorine as the reaction reagent (Taylor and Epstein, 1962a); some samples, however, were reacted with bromine pentafluoride (Clayton and Mayeda, 1963; Garlick, 1964). All samples were loaded into the nickel reaction vessels in a drybox and reacted at $450^\circ - 630^\circ\text{C}$ with excess fluorine to liberate free oxygen. The O_2 was quantitatively converted to CO_2 by combustion with a resistance-heated graphite rod. The CO_2 was then cycled through a

mercury diffusion pump to remove any trace amounts of F or Br compounds that may have been present. The CO_2 was then analyzed mass spectrometrically.

The tank F_2 used as a reagent in this research contains small amounts of oxygen and nitrogen. The oxygen typically amounts to about 4.7 μmoles , based on the normal amount of fluorine placed in a reaction vessel ($2/3$ atm F_2 in a 50 cm^3 volume). This contaminant oxygen has $\delta^{18}\text{O} = +9$ and thus all oxygen extractions by the fluorine method were corrected for this contaminant. The typical correction was approximately 0.1 per mil.

Carbonates were reacted with 100% H_3PO_4 at 25.2°C according to the method described by McCrea (1950). Coexisting calcite and dolomite were analyzed for $\delta^{18}\text{O}$ and $\delta^{13}\text{C}$ utilizing the technique of Epstein *et al.* (1963).

3.4 Hydrogen extraction

The hydrogen was extracted from OH-bearing phases utilizing techniques similar to that described by Friedman (1953) and Godfrey (1962). The samples were degassed under high vacuum at 200°C for about two hours and then heated by an induction heater to about 1300°C to liberate H_2O and H_2 . The H_2O was converted to H_2 by passing it through a uranium furnace at about 700°C .

The RF field from the working coil induces a current flow in the platinum crucible and thus the crucible and contained sample are heated. The outer glass envelope is heated somewhat by radiation from the crucible so fans were used to cool the container.

During fusion of the sample, the evolved gas is ionized and discharged within the glass envelope due to the high frequency field. This discharge may result in spurious δD values, possibly because some of the ionized gas may be driven into the walls of the glass envelope or because of interactions with the vacuum grease. However, if the glass envelope vessel is isolated from the rest of the system during dehydration, the pressure buildup prevents gaseous discharge and allows complete sample fusion in about 15 minutes. This technique, suggested by R.L. Armstrong, was used for all samples. As shown by Wenner (1970), this technique gives the same isotopic results as the low pressure method of Godfrey (1962).

After the H_2 was collected, the sample was reheated to insure complete dehydration. The total volume of H_2 was measured and the gas was analyzed mass spectrometrically.

3.5 Mass spectrometric and other correction factors

All CO_2 samples were analyzed in a 60° , single focusing, double collecting mass spectrometer of the type described by

Nier (1947) and McKinney et al. (1950). Inasmuch as isotopic composition measurements are carried out on carbon dioxide gas, correction factors were applied to relate the mass 46/ (44+ 45) and 45/44 ratios to $^{18}\text{O}/^{16}\text{O}$ and $^{13}\text{C}/^{12}\text{C}$ ratios (Craig, 1957).

All samples extracted by the fluorine or bromine penta-fluoride method were compared to Rose Quartz Pegmatite Standard with a $\delta^{18}\text{O} = +8.45$ (H.P. Taylor, unpublished data). This Caltech standard was analyzed 80 times during the course of this research. Inasmuch as all the CO_2 samples prepared by this method have the same carbon composition (that of the spectroscopically pure graphite rod used in the burning), the ^{13}C correction factor is zero, and the ^{17}O correction factor, after Craig (1957), is

$$\delta_c^{18}\text{O} = 1.001 \delta_m^{18}\text{O} ,$$

where δ_c = corrected δ -value

and δ_m = raw machine δ -value, corrected only for instrumental effects.

Because the Caltech mass spectrometer reference standard gas was 24.5 per mil heavier than SMOW at the time of this research, a multiplicative correction factor of 1.0245 must be applied to change to the SMOW standard. $\delta^{18}\text{O}$ value for any sample x is given by

$$\delta_{x\text{-SMOW}} = \left(\delta_x^{\text{RAW}} - \delta_{R Q \text{ STD}}^{\text{RAW}} \right) (1.0245) (\text{Bkgd}) + 8.45$$

where δ = fluorine-corrected, raw δ -values
and Bkgd = multiplicative background correction factor,
measured each day and typically about 1.02.

This factor includes the instrumental effects of valve mixing and leakage.

The following fractionation factors were used to convert the $\delta^{18}\text{O}$ values of evolved CO_2 from carbonate to $\delta^{18}\text{O}$ values of the total carbonate.

$$\alpha_{\text{CO}_2} - \text{calcite} = 1.01025$$

$$\alpha_{\text{CO}_2} - \text{dolomite} = 1.01110$$

These values are modified after Sharma and Clayton (1965); see Clayton et al. (1968b). The analytical precision for oxygen and carbon in this work is ± 0.2 per mil.

The hydrogen mass spectrometric analyses were performed on a Nier-McKinney type instrument with a side arm for collecting the mass 2 beam. The raw δ -values were corrected for leakage and background. A correction for the contaminating H_3^+ ions was included following the pressure effect method described by Friedman (1953). Taking into consideration the Caltech working standard correction factor, the equation which converts the raw δ -values to SMOW is given by

$$\delta_{\text{x-SMOW}} = 0.9405 \delta_{\text{x-MS}} - 68.75$$

where $\delta_{\text{x-MS}}$ = δ D-value of the sample relative to the Caltech machine standard hydrogen gas. During the course of this work a water standard was run six times and a Caltech biotite

standard was run five times. The analytical precision for D/H analyses in this work is ± 2 per mil.

Chapter 4

A MODEL FOR METEORIC HYDROTHERMAL CONVECTION

4.1 General statement

It is now clear that most rocks that are anomalously depleted in ^{18}O have undergone large-scale exchange with heated, low ^{18}O meteoric ground waters. It is equally obvious that the isotopic exchange processes that are presently going on in modern geothermal systems (e.g. Wairakei, Steamboat Springs, and Salton Sea) although at a more shallow level, are essentially analogous to those that have occurred in geothermal systems of the past (e.g. Tertiary plutonic centers of NW Scotland and Western Cascades). This chapter describes some active geothermal systems, and also discusses some qualitative theories regarding the modeling of convective fluid flow in the vicinity of an igneous intrusion.

4.2 Active geothermal systemsSteamboat Springs, Nevada

The geology of the Steamboat Springs region consists of a Mesozoic (?) metasedimentary and volcanic basement intruded by Cretaceous granodiorite. After deep erosion, Cenozoic volcanism produced more than the 100 cubic miles of flows, tuffs and tuff-breccias of intermediate composition. During and after these eruptions, lake and stream deposits accumulated.

Most of the rocks in the thermal area have been hydrothermally altered. A large hot magma chamber has evolved heat and some mineral constituents for a period of at least 10^5 years (White et al., 1964; White, 1968a).

White (1968a; 1973) has illustrated a simple hot-spring system which is reproduced in Figure 4-1. If the cold down-flowing limb of the convection system has an average temperature of 45°C with a density of 0.990, and the hot, upward-flowing part has an average temperature of only 170°C with a density of 0.9000, the driving force related to thermal expansion over the 10,000 feet is equivalent to nearly 400 psi (White, 1968a). Thus the main factor in driving this huge convection system is the density contrast between the cold downflowing part of the system and the hot, less dense, upflowing part of the system. In most hot-spring systems, pressure, salinity, and bulk permeability are less important than temperature.

The isotopic composition of alkaline and neutral hot-spring waters and condensed steam from the Steamboat Springs area set an upper limit on the amount of water of magmatic origin at approximately 5 per cent (Craig et al., 1956; White et al., 1963). The total heat flow of the Steamboat Springs thermal area is estimated to be 1.2×10^7 cal sec^{-1} , equivalent to at least 150 times the mean heat flow at the surface of the earth (White, 1968a).

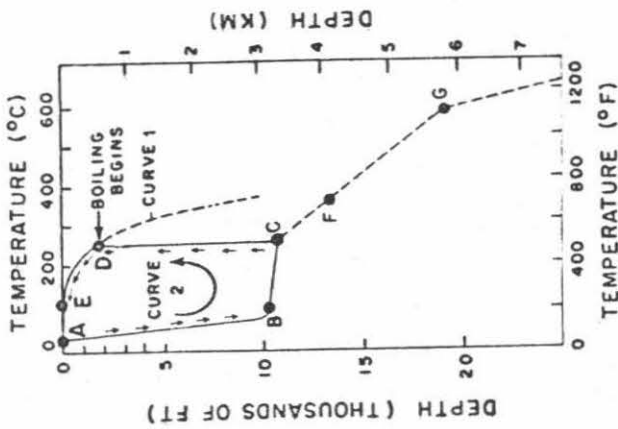
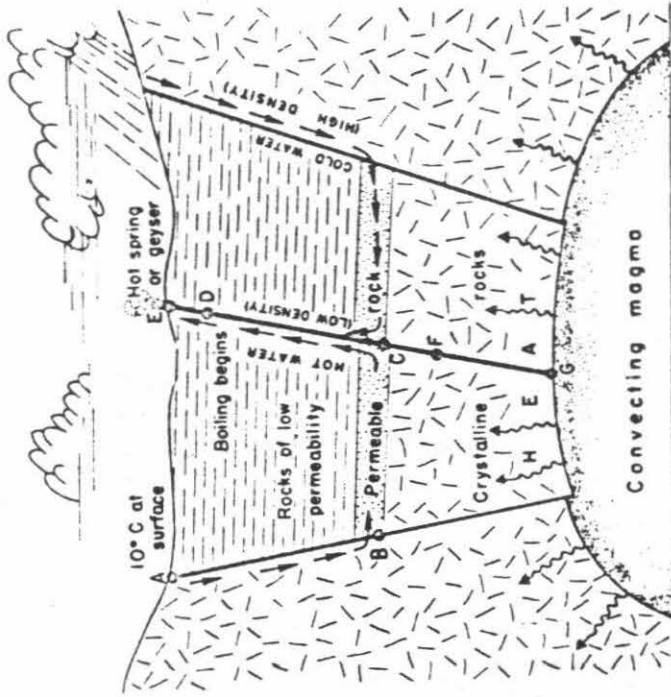


Figure 4-1. Model of a simple, high-temperature geothermal system with deeply circulating meteoric water assumed to be heated entirely by conduction (from White, 1968a; 1973). Curve 1 is the reference curve for the boiling point of pure water. Curve 2 shows the temperature profile along a typical circulation route from point A (recharge) to point E (discharge).

Salton Sea Geothermal Area, California

The Salton Sea geothermal field is situated near the southeastern edge of the Salton Sea in the Imperial Valley, and near the axis of a major structural depression that extends northwestward from the Gulf of California. The main rock units are those deposited by the Colorado River as part of its delta, and consist of Tertiary and Quaternary sands, silts and clays (Muffler and White, 1969). These deltaic sediments are approximately 20,000 feet thick (Kovach et al., 1962; Biehler et al., 1964). Five late Quaternary rhyolitic domes intrude the sediments (White, 1968b). The hot-spring activity is an expression of the general positive heat flow anomaly that characterizes the Salton Trough.

Temperatures within the geothermal reservoir range up to 360°C at 7100 feet (Helgeson, 1968). Wells in the reservoir have produced a remarkably saline brine containing up to 259,000 ppm (by weight) dissolved solids. The main constituents are Cl, Na, Ca, K, Fe and Mn. The thermal brine is estimated to be 5 km³ in volume (White, 1968b).

Thermodynamic and geochemical calculations by Helgeson (1967) demonstrated that the sulfur, oxygen and CO₂ fugacities are of the order of 10⁻¹⁰, 10⁻³⁰ and 2.8 atmospheres respectively. The pH of the brine was calculated to be 4.7 at 300°C.

Within the Salton Sea geothermal region, the original sediments are being metamorphosed to low grade rocks of the greenschist facies. Above 300°C the typical metamorphic

assemblage is quartz + epidote + chlorite + K-feldspar + albite ± K-mica (Muffler and White, 1969).

Craig (1963; 1966) concluded from the isotopic composition of waters in the Salton Sea geothermal area that the source is local precipitation with $\delta^{18}\text{O} = -11$. The near-neutral, geothermal subsurface waters exhibit a remarkable 14 per mil oxygen isotope shift, nearly twice the maximum shift so far observed in any other modern geothermal field. Helgeson (1968) however, suggested that the geothermal brines had their source from Colorado River water originally trapped in the deltaic sediments. In this regard, it is interesting to note that Coplen (1973) demonstrated, from oxygen and hydrogen isotope compositions of water samples from the Dunes geothermal anomaly, Imperial Valley, that the water in the Dunes system was derived from the Colorado River. Clayton et al. (1968a) demonstrated that the carbonates in the Salton Sea geothermal area have equilibrated with the meteoric waters to temperatures at least as low as 150°C. They estimated that a volume of water at least equal to that of the exchanged sediments had passed through the system.

Helgeson (1968) has clearly demonstrated that convective heat transfer is required to account for the temperature-depth profiles observed in the reservoir. His calculations show that thermal convection of pore fluids is the major mechanism of heat and mass transfer in the geothermal area. Magmatic heat is the main energy source that drives the convective

system (White, 1965). A possible simplified model for the Salton Sea geothermal system (after White, 1968b) is shown in Figure 4-2.

Wairakei Geothermal Area, New Zealand

The hydrothermal areas at Wairakei are associated with the still-active Central Volcanic District. Actively subsiding tectonic depressions are filled with approximately 5 km of rhyolites, pyroclastic pumice, ignimbrites and breccias and overlie the greywacke basement (Grindley, 1961).

The isotopic composition of the waters at Wairakei is unique in that there is only a small ^{18}O -shift away from the local meteoric water (Banwell, 1963b; Craig, 1963). Banwell (1963b) suggested the small effect was a combination of (1) a large total volume of circulated water compared to the exchanged rock, and (2) Wairakei is a relatively old system ($\sim 5 \times 10^5$ years), and thus the rocks adjoining the hydrothermal conduits have probably undergone extensive ^{18}O exchange already.

Elder (1965) demonstrated that convection is the dominant mode of heat transfer. With a temperature of approximately 400°C at the base of the 5 km-deep Taupo depression, heat flow by conduction is about 2×10^{-6} cal cm^{-2} sec^{-1} . The regional average heat flux is $50 \mu\text{cal cm}^{-2}$ sec^{-1} (Thompson, 1960). Banwell (1963a) considered the problem of conductive and convective heat transfer from a magma chamber to both roof rocks

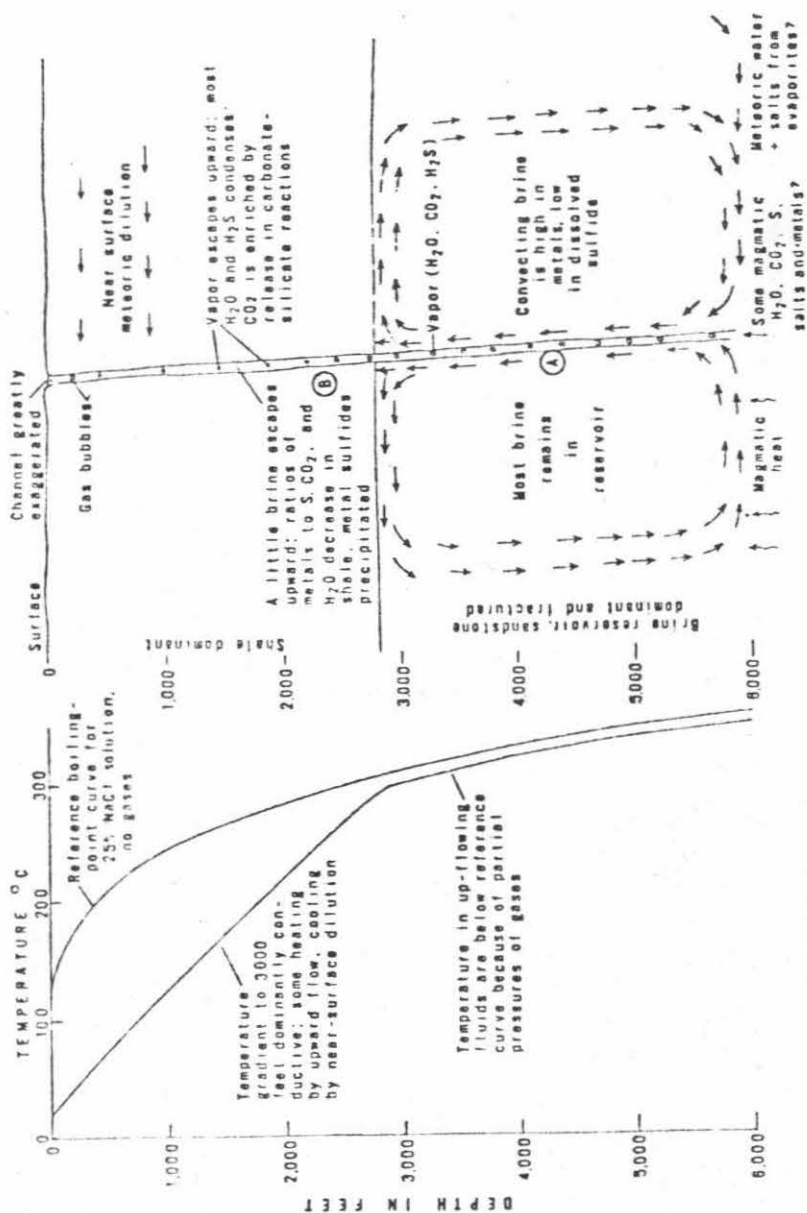


Figure 4-2. Simplified model for the Salton Sea geothermal system (from White, 1968b).

and circulating water. He suggested that volcanic steam may be necessary to account for the heat flow in the Wairakei area. The main problem was to provide a reasonable model with a sufficiently large area for heat conduction to account for continuous water circulation over 10^5 years. Isotopic evidence rules out large amounts of 'magmatic' water in the system. As White (1957) has pointed out however, the heat flow, chemical composition and isotopic data are all compatible if the volcanic steam is diluted about 15 times by meteoric water.

Another source of heat that has generally been neglected in models of this type is the exothermic nature of many hydration and devitrification reactions (Ellis, 1967). The heats of reaction, in calories per gram, of silica glass to quartz, albite glass to albite, and alkali feldspar to mica are -83.5, -46, and -40, respectively (Cumberlidge and Saull, 1959; Kracek and Neuvonen, 1952; Hemley, 1959). In general, the devitrification of glassy volcanic rocks and the formation of hydrated products such as chlorites and micas from anhydrous minerals causes an evolution of heat on the order of several tens of calories per gram. Ellis (1967) calculated that, for the New Zealand Taupo Volcanic Zone containing 0.1 gram of water per cubic centimeter of rock, the adiabatic temperature rise due to hydration reactions alone would be of the order of 300°C . Thus, the heat available from rock alteration is approximately 3×10^{17} cal/km³. This heat is

appreciable compared with that contained in a cooling rock unit and can significantly prolong the life of a geothermal system.

A simple model of the Wairakei system, based on the data of Thompson et al. (1961), was given by Elder (1965) and is shown in Figure 4-3. The temperature distribution with depth at Wairakei has revealed a body of water-saturated rock at least 1.4 km thick. Isotherms and flow lines are shown in a cross-section through the modern geothermal area at Wairakei in Figure 4-4 (after Elder, 1965; Spooner and Fyfe, 1973). Note the 'mushroom' form of the pattern which is just what one would expect from outward flowing lobes of hot water and is strikingly similar to calculated models of convective flow by Wooding (1957) and Donaldson (1962) and to model experiments of Elder (1965).

4.3 Theory of convective fluid flow in the vicinity of an igneous intrusion

General Statement

It is clear from the previous discussion on modern geothermal systems that simple conductive heat transfer models cannot correctly describe these near-surface environments. The heat flow studies demand convective heat transfer by circulating water, inasmuch as conductive heat transfer cannot, by itself, account for the geothermal anomalies. The isotopic data demonstrate that almost all of this water is derived

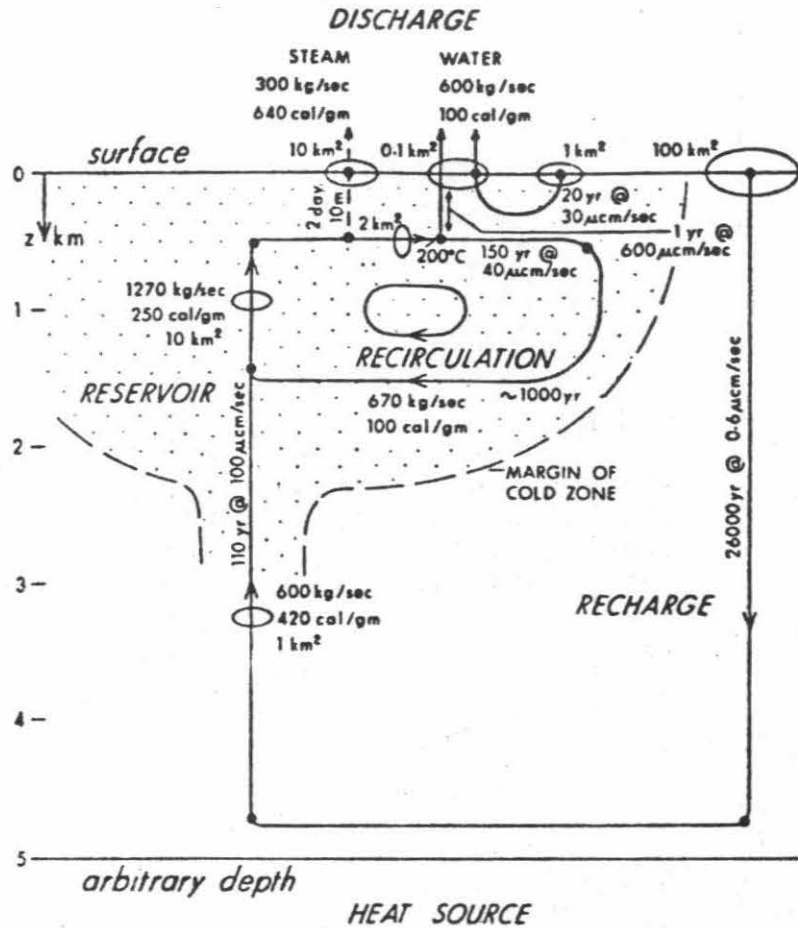


Figure 4-3. Schematic model of Wairakei geothermal system. Based on the data of Thompson *et al.*, 1961 (from Elder, 1965).

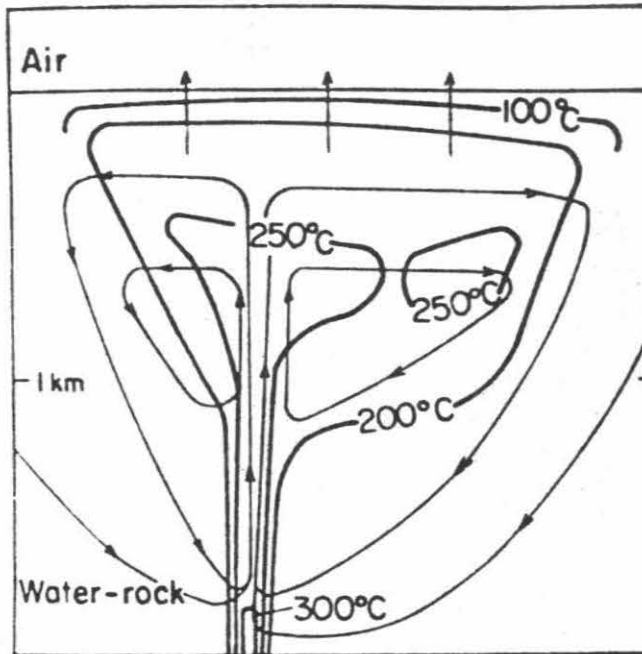


Figure 4-4. Vertical section of the upper 2 km of the Wairakei geothermal system, showing the measured isotherms and approximate flow lines (from Spooner and Fyfe, 1973; after Banwell, 1961 and Elder, 1965).

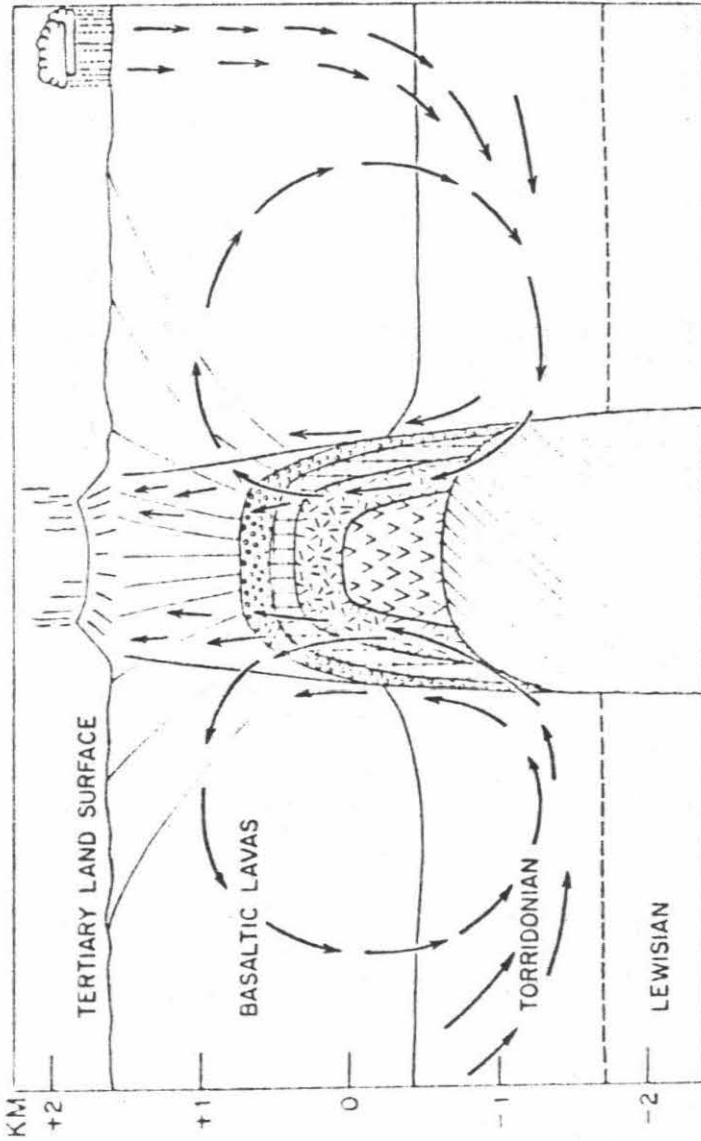


Figure 4-5.

Generalized geologic section through a typical ring-dike complex at Skye (modified after Thompson, 1969). Checked patterns indicate a series of ring dikes above a gabbro pluton. Cone-sheet fractures are shown extending upward to the caldera and the Tertiary land surface. The vertical scale is exaggerated relative to the horizontal. The heavy arrows show schematically how meteoric waters would be set in motion by the heat emanating from the hot igneous rocks and magmas (see text). The circulation is in reality undoubtedly much more complicated than that shown. With certain modifications in the thicknesses of the plateau lavas and Mesozoic sediments, and the absence of Torridonian and the presence of Moine schists, the diagram also applies to Mull and Ardnamurchan (after Taylor and Forester, 1971).

from local ground waters and that large-scale exchange has occurred between these waters and the rocks in the geothermal system. A simple model that could be used to effect such an interaction would be similar to that used by Banwell (1963a) and White (1968a; b) to represent the Wairakei, Salton Sea, and Steamboat Springs geothermal systems (see Figure 4-1). Similar models have been utilized for the deeper portions of ancient systems by Sheppard et al. (1969), Taylor and Forester (1971) and Taylor (1971). Meteoric ground waters are heated in the vicinity of a crystallizing and cooling igneous pluton and set into convective motion (see Figure 4-5). The igneous pluton then is the energy source that drives the convective circulation system. The mathematical model thus involves the solution of non-isothermal convective fluid flow through a porous medium.

It should be kept in mind that since any thermal disturbance may set the adjacent waters into convective motion, these models apply equally well to oceanic environments as well as continental ones. Sea water hydrothermal systems have been considered by Elder (1965), Palmason (1967), Muehlenbachs and Clayton (1972), Spooner and Fyfe (1973), and Wenner and Taylor (1973).

Mathematical Formulation

Consider a homogeneous permeable layer. The steady-state equation that describes fluid flow is given by Darcy's Law,

$$\nabla P = \rho g z - \frac{\nu}{k} V \quad (4-1)$$

where P = pressure

ρ = density of fluid

g = gravitational acceleration

z = vertical coordinate

ν = kinematic viscosity of the fluid

k = permeability of the medium

V = mass flow rate

For the flow to be zero,

$$\nabla P = \rho g z \quad (4-2)$$

$$\text{and thus } \frac{\partial P}{\partial x} = \frac{\partial P}{\partial y} = 0 \quad (4-3)$$

since gravitation varies only in the z direction. Thus the flow can be zero only if the fluid density is constant in the horizontal x - y plane, and any thermal disturbance (e.g. an igneous intrusion with near vertical walls) will demand convective flow in the medium.

The first term on the right hand side of equation (4-1) is the pressure effect in the vertical z direction. The next term is the pressure drop due to fluid flow in the x - y plane only, and is equal to $\text{grad } P$ in this plane.

The steady-state equation of continuity for an incompressible fluid with no sources or sinks is

$$\nabla \cdot V = 0 \quad (4-4)$$

We now must consider the equation of conservation of energy. The fundamental partial differential equation for heat conduction with no heat source is

$$\frac{\partial T}{\partial t} = \kappa \nabla^2 T \quad (4-5)$$

where $T(x, y, z, t)$ = temperature

t = time

κ = thermal diffusivity; $\kappa = \frac{K}{\rho c}$

where K is the thermal conductivity, and c is the specific heat and ∇^2 = Laplacian operator.

The thermal diffusivities of rocks are so small (on the order of $10^{-2} \text{ cm}^2 \text{ sec}^{-1}$ at normal P and T) that more than 10^5 years would be required to conduct heat from a depth of 2 km to the surface. A much more rapid heat transfer mechanism is that of convection. Convection is material transfer in a fluid under the influence of gravity, where density variations are the result of non-isothermal conditions. As the masses move, heat is transferred. Note that gravity never takes a holiday (Bowen, 1928, p. 24).

Let us now modify equation (4-5) to include the effects of convection. Because $T = T(x, y, z, t)$, the total derivative of temperature is written

$$dT = \frac{\partial T}{\partial x} dx + \frac{\partial T}{\partial y} dy + \frac{\partial T}{\partial z} dz + \frac{\partial T}{\partial t} dt \quad (4-6)$$

Dividing both sides of equation (4-6) by dt , and defining a set of terms V_j , where

$$V_j = dj/dt \quad (j = \text{coordinates } x, y, \text{ or } z),$$

$$\text{we have} \quad \frac{dT}{dt} = V_x \frac{\partial T}{\partial x} + V_y \frac{\partial T}{\partial y} + V_z \frac{\partial T}{\partial z} + \frac{\partial T}{\partial t}$$

$$\text{or} \quad \frac{dT}{dt} = \frac{\partial T}{\partial t} + V \cdot \text{grad } T \quad (4-7)$$

As we are now considering a moving element of fluid, the term $\partial T/\partial t$ in (4-5) must be replaced by dT/dt as given in (4-7). Thus

$$\frac{\partial T}{\partial t} = \kappa \nabla^2 T - V \cdot \text{grad } T \quad (4-8)$$

For two-dimensional space, the energy balance equation is

$$\frac{\partial T}{\partial t} + V_x \frac{\partial T}{\partial x} + V_z \frac{\partial T}{\partial z} = \kappa \nabla^2 T \quad (4-9)$$

Equations (4-1), (4-4), and (4-8) have been recast in a coupled set of two-dimensional nonhomogeneous linear partial differential equations of the second order, and solved for temperature and stream potential as a function of time by Cathles and Norton (1974), using finite difference methods. The input for their computer program included the initial and boundary conditions for temperature and fluid flow and the Rayleigh number, R . The Rayleigh number is a dimensionless parameter that combines both the fluid and media properties into a ratio; the numerator contains factors that tend to enhance heat transfer by convection, while the denominator contains factors that favor conduction:

$$R = \frac{k\alpha(\Delta T)gh}{\nu\kappa} \quad (4-10)$$

where α = coefficient of volumetric expansion,

ΔT = temperature difference in the column,

h = thickness of the homogeneous porous medium, and
the other symbols have been previously defined.

For a medium of infinite extent bounded above and below by impervious layers, Lapwood (1948) predicted that the critical value of R for the onset of convection is $4\pi^2$. Experimental work by Elder (1965; 1967) demonstrated that heat transfer is entirely by conduction when $R < 40$, consistent with the study by Lapwood. Palmason (1967) calculated R to be 190 for the upper 2 km of the volcanic rocks in Iceland, where water circulation controls to a large extent the surface heat flow.

In the model presented by Cathles and Norton (1974) a constant Rayleigh number was used; this is in spite of the fact that equation (4-10) contains a number of fluid properties strongly dependent on P and T . Donaldson (1962) and Wooding (1957) utilized explicit functions for density, although their basic model was not as relevant to the actual geological situation as that of Cathles and Norton. In order to define a more realistic model, Norton (personal communication, 1974) is now in the process of including explicit functions for α , ν , and ρ in terms of P and T , and introducing the factor of anisotropic permeability as a system parameter. As it is, Cathles and Norton (1974) still present the best available mathematical model for pluton-driven, convective flow.

Their model assumes a pluton 2 km wide, 2.75 km high, and buried 2.75 km below the surface. The assumed permeability of the pluton is 0.15 millidarcies while that of the country rock is 0.3 millidarcies. Initially, the pluton is assumed to be 750°C hotter than the country rocks. Their results defined fluid velocities on the order of 30m/y at the top of the pluton. The volume of water cycled through the upper part of the pluton, where the streamlines are most closely spaced, is approximately 3 times the volume of the upper part of the pluton. The pluton was found to cool to 20% of its initial temperature in 10^5 years. As pointed out by Elder (1965), because free convection in a porous medium can involve a very large heat flow, bodies may cool several orders of magnitude more rapidly by convection.

We can also calculate the time-integrated W/R ratio for an interacting water-rock system, inasmuch as any system must obey the law of conservation of energy. The total heat lost from the cooling and crystallizing pluton will be

$$(m_R c_R) \Delta T_R + (L_x + H) m_R$$

while the heat gain of the water is

$$(m_W c_W) \Delta T_W + L_V m_W$$

where subscripts R, W refer to rock and water respectively,

m_R, m_W = mass

c_R, c_W = specific heat capacity (0.26 and 1.0 cal gm⁻¹ °C⁻¹ respectively)

$\Delta T_R, \Delta T_W$ = mean temperature change (assumed in this example to be 750°C for R, 300°C for W)

H = heat of hydration reactions ($\sim 30 \text{ cal gm}^{-1}$)

L_x = latent heat of crystallization ($\sim 100 \text{ cal gm}^{-1}$)

L_v = latent heat of vaporization ($\sim 500 \text{ cal gm}^{-1}$ in a vapor-dominated system; zero in a hot water system)

Assuming no other sources or sinks and equating the two expressions above, we have

$$\frac{m_W}{m_R} = \frac{c_R \Delta T_R + L_x + H}{c_W \Delta T_W + L_v}$$

Substituting the reasonable values given above, we obtain

$m_W/m_R \approx 0.4$ for a vapor-dominated system, and $m_W/m_R \approx 1.1$ for a hot water system. These are equivalent to atomic oxygen (W/R) ratios of 0.8 and 2.1 respectively. These ratios will vary, depending on the contributions from hydration reactions, the temperature intervals chosen, and the latent heat from the pluton (i.e. percent of crystals at time of intrusion). These however are minor contributions, and therefore it is reasonable to expect systems which have experienced significant meteoric-hydrothermal alteration to be characterized by a time-integrated atomic oxygen W/R ratio of about 1 to 2. It is interesting to note that, for almost all "fossil hydrothermal" systems studied to date, the minimum, calculated W/R ratios cluster about unity (see Taylor, 1974b, Figure 27).

4.4 Summary

In summary, a hydrothermal system is composed of a heat source and a recirculation system, and possibly with a recharge and surface discharge system. In the circulation system, the dilute, relatively cool meteoric waters are heated in the vicinity of the intrusion and, as a consequence of their lowered density, rise. This water is replaced by additional radially inflowing cool ground water moving towards the heat source (Figure 4-5). The heated ground waters exchange oxygen with the minerals in the country rocks and the intrusion. During passage through these rocks, the initially dilute waters may dissolve various elements (notably Na, Ca, K, Cl and Mg) and in some cases may develop into a brine. The density increase of the fluid due to increased salinity may be more than compensated by the effect of temperature on its density.

The convective system could be such that the same H₂O would cycle through the rocks repeatedly. With high temperature exchange, this water would increase in ¹⁸O with each cycle and in time lose its ¹⁸O/¹⁶O contrast with the rocks through which it passed. Of course, new influx of unexchanged ground waters could always take place, although the access routes may change with time. Thus rain waters, snow, lakes, rivers and ground waters in the catch basin in general will recharge the circulatory flow system. This replenishment by

fresh meteoric ground waters may effectively maintain a strong $^{18}\text{O}/^{16}\text{O}$ contrast between the waters and the exchanging rocks. At the same time, water may be lost from the system by discharging through springs (or as steam) at the earth's surface, in a similar fashion as is seen today in Yellowstone, Steamboat Springs, Wairakei or other geothermal regions.

It should be pointed out that this model is the antithesis of the classical process in which water is thought to have been given off by a crystallizing and cooling magma and added to the country rocks.

Chapter 5

THE STONY MOUNTAIN STOCK, WESTERN SAN JUAN MOUNTAINS,
SOUTHWESTERN COLORADO, U.S.A.5.1 General geological setting

The Western San Juan Mountains of Colorado are largely composed of Tertiary volcanic rocks, but also include a Precambrian crystalline complex, and sedimentary rocks ranging in age from Cambrian to Tertiary (Figure 5-1). The Precambrian rocks of the Needle Mountains include the Vallecito Conglomerate which is at least 750 meters thick. This is overlain by the Irving Greenstone and the Uncompahgre Formation, with a minimum thickness of 2500 meters, chiefly composed of very pure quartzites, with lesser amounts of slate and shale (Cross et al., 1905; Barker, 1969). The lower Paleozoic section comprises just a few hundred meters of largely marine carbonates, but the younger sedimentary section (Pennsylvanian to Early Eocene) is made up of approximately 1000 meters of clastic rocks. Some Cretaceous units contain abundant volcanic debris. These volcanic rocks are probably related to the Late Cretaceous or Early Paleocene intrusive granodiorites and quartz monzonites in the vicinity of Ouray and in the La Plata and Rico Mountains (Larson and Cross, 1956).

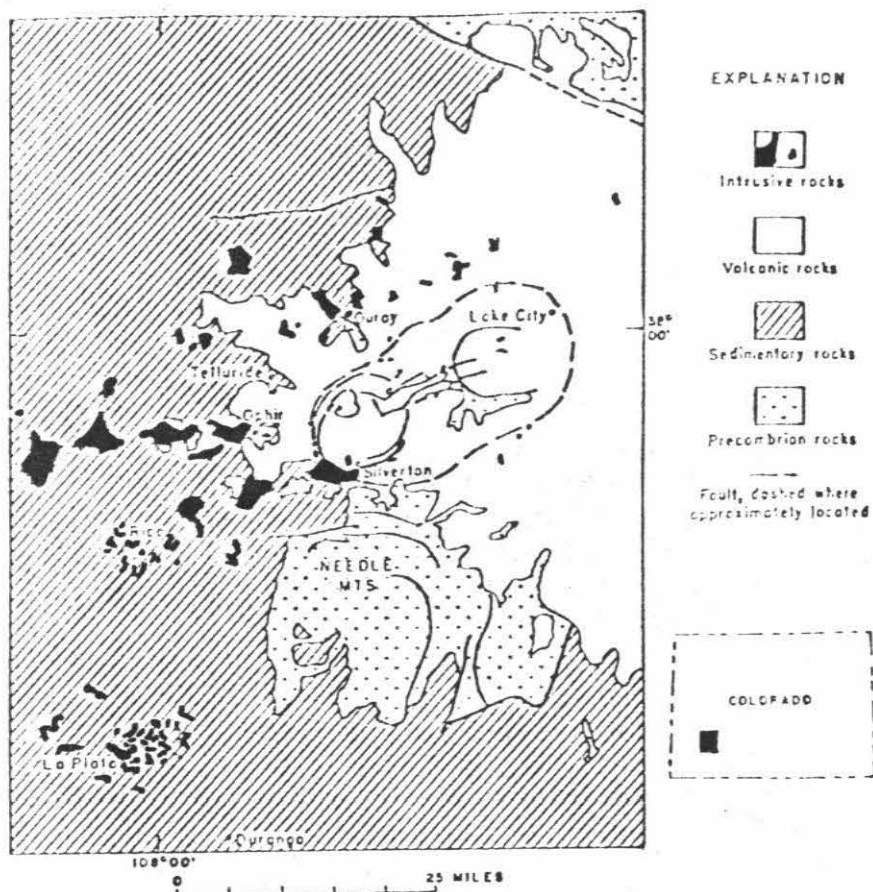


Figure 5-1. Generalized geologic map of the Western San Juan Mountains, Colorado (from Luedke and Burbank, 1968). Elliptical dash line is rim of San Juan volcanic depression.

5.2 Mid-Cenozoic volcanic and tectonic history of the Western San Juan Mountains

The Tertiary volcanic rocks of the Western San Juan Mountains are composed of three major units, approximately 2.4 km thick and comprising more than 6000 km³ in volume. The stratigraphic relationships were first determined by Cross and Purington (1899) and Cross et al. (1905) with further amplification by Larsen and Cross (1956). The three principal episodes of major volcanic activity have been called old, middle, and young by Luedke and Burbank (1968; see Table 5-1). The volcanic rocks are largely Oligocene in age (Lipman et al., 1970; see Table 5-2). Preliminary geochronological studies on the ages of mineralization in the Western San Juan Mountains indicate that much of the productive mineralization structurally associated with the Silverton caldera appears to have been active 6-10 m.y. later than the formation of the caldera 28 m.y. ago (Lipman, personal communication, 1973).

The old unit, the San Juan Formation, is composed of up to 900 meters of rhyodacitic tuff breccia with minor volcanic conglomerate, tuff, rhyodacitic lava flows and flow breccias, rhyodacitic to quartz-laticitic welded ash-flow tuffs and basaltic andesite lava flows and autobreccia (Larsen and Cross, 1956; Luedke and Burbank, 1963; 1968). It is estimated to have had a volume between 3000 and 5000 km³ and to have been deposited over more than 8000 km².

Table 5-1*

Tertiary Volcanic Stratigraphy
of the Western San Juan Mountains

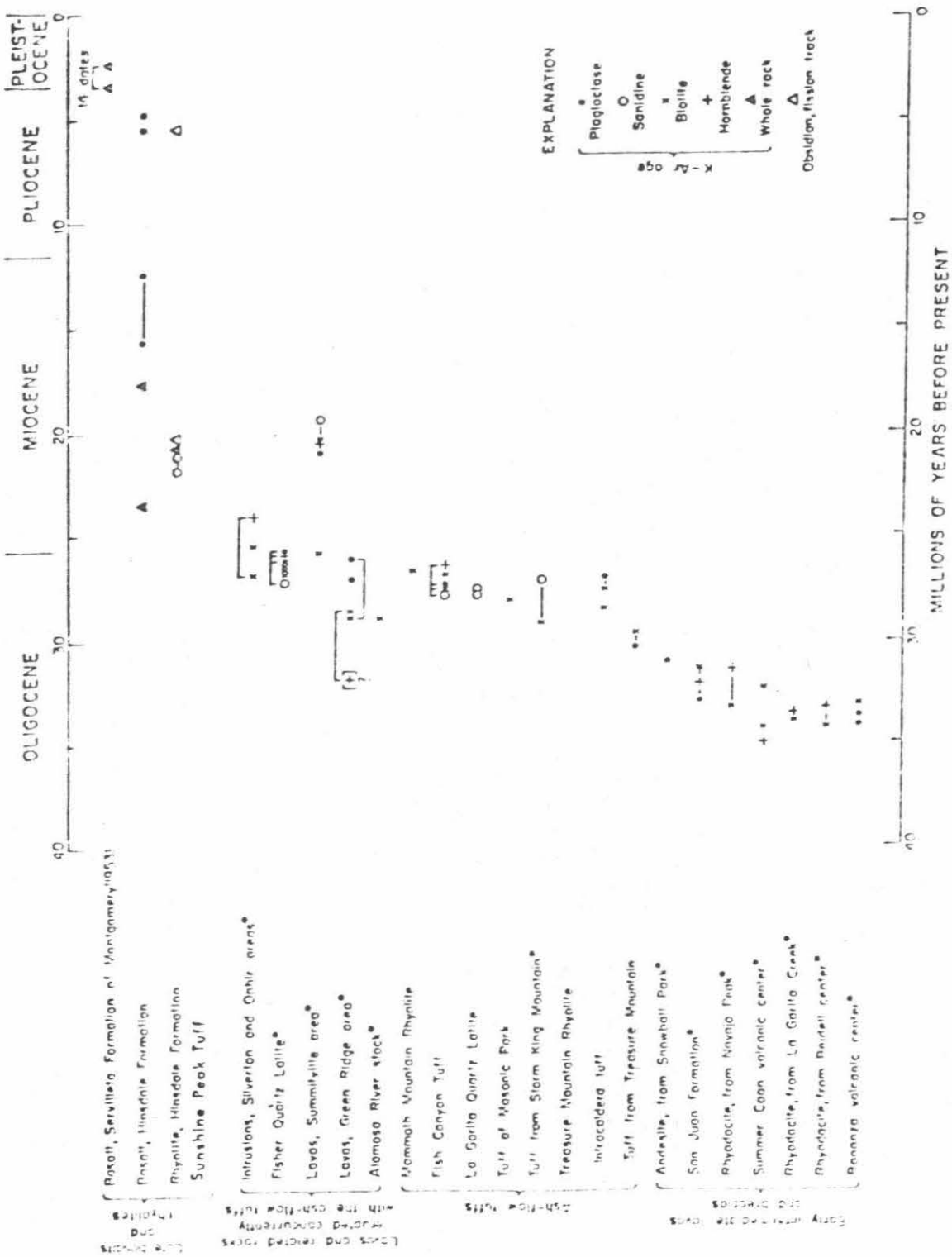
UNIT	GROUP	FORMATION
Young	Potosi Volcanic Group	Gilpin Peak Tuff
		Hensen Formation
Middle	Silverton Volcanic Group	Burns Formation
		Eureka Tuff
		Picayune Formation
Old		San Juan Formation

* A revised volcanic stratigraphy and nomenclature has recently been proposed by Lipman et al., (1973). Rocks of the San Juan Formation are called "early intermediate-composition lavas and breccias". The Picayune Formation is considered to be a vent-facies accumulation in the San Juan Formation. Gilpin Peak Tuff is called "lower ash-flow sheets".

Table 5-2

Compilation of ages of minerals and rocks from the San Juan volcanic field, arranged in generalized stratigraphic sequence. Tie lines connect phases of same sample; brackets indicate geologically improbable date; •, stratigraphic relations to other units of subgroup are uncertain. Data from Lipman et al. (1970), and Mehnert et al. (1973a; b).

Table 5-2



The middle unit of Luedke and Burbank (1968), the Silverton Volcanic Group, ranges in composition from basaltic andesite to rhyolite and consists of lava flows, breccias and welded ash-flow tuffs. It covered an estimated 1900 km^2 and had a volume of about 1700 km^3 .

The third major volcanic episode, the young unit, consists of welded ash-flow tuff in the Potosi Volcanic Group. The rocks range in composition from rhyodacite to rhyolite, but are predominantly quartz latites. They covered an estimated 6500 to 9100 km^2 and had a total volume of at least 1700 to 2500 km^3 .

Late in the history of the old volcanic episode there developed a major subsidence structure known as the San Juan volcanic depression (Figure 5-1). The principal development of this 40 km -long by 20 km -wide crustal block occurred after the eruption of a large-scale ash-flow, the Eureka Tuff (Table 5-1). Major resurgent doming of the crustal block took place before the deposition of the Burns Formation and formed an elongate graben structure (the Eureka graben) together with radial fractures along the crest of the dome.

The young volcanic episode, during the major ash-flow eruptions, resulted in the subsidence of two nearly circular crustal blocks called the Silverton and Lake City cauldrons within the San Juan volcanic depression (Figure 5-1). The cauldron floors were arched and distended as a result of the Eureka graben structure. Extensive radial and concentric

fracturing occurred, and dikes and plutons were intruded along these fracture zones; one example of such an intrusive body is the Stony Mountain-Mt. Sneffels center (Figure 5-2). During the final stages of the main volcanic-plutonic activity, pervasive hydrothermal alteration and mineralization occurred (Burbank, 1941). Minor eruptions of basalt and rhyolite continued through Miocene and Pliocene time.

5.3 Geology of Stony Mountain stock

The Stony Mountain stock, about 1.3 km in diameter, intrudes horizontally bedded volcanic rocks about 10 km NW of the ring-fault zone rim of the Silverton cauldron (Figure 5-2; Plate 5-1). The stock was first mapped by Cross (1899) and later in more detail by Dings (1941). It also is included in the quadrangle map of Burbank and Luedke (1966). A geologic map of the Stony Mountain stock (Dings, 1941; Burbank, 1941) is shown in Figure 5-3; the geological contacts are superimposed on the topographic map in Figure 5-4.

The lowermost volcanic unit is the San Juan Tuff, the old volcanic unit of Luedke and Burbank (1968). Up to 380 meters of this unit are exposed in the vicinity of the Stony Mountain stock. It is made up largely of rhyodacitic tuffs, breccias, and agglomerates whose fragments are primarily very fine-grained andesite. The Silverton Volcanic Group, the middle unit, is represented only by the basal Picayune Formation,

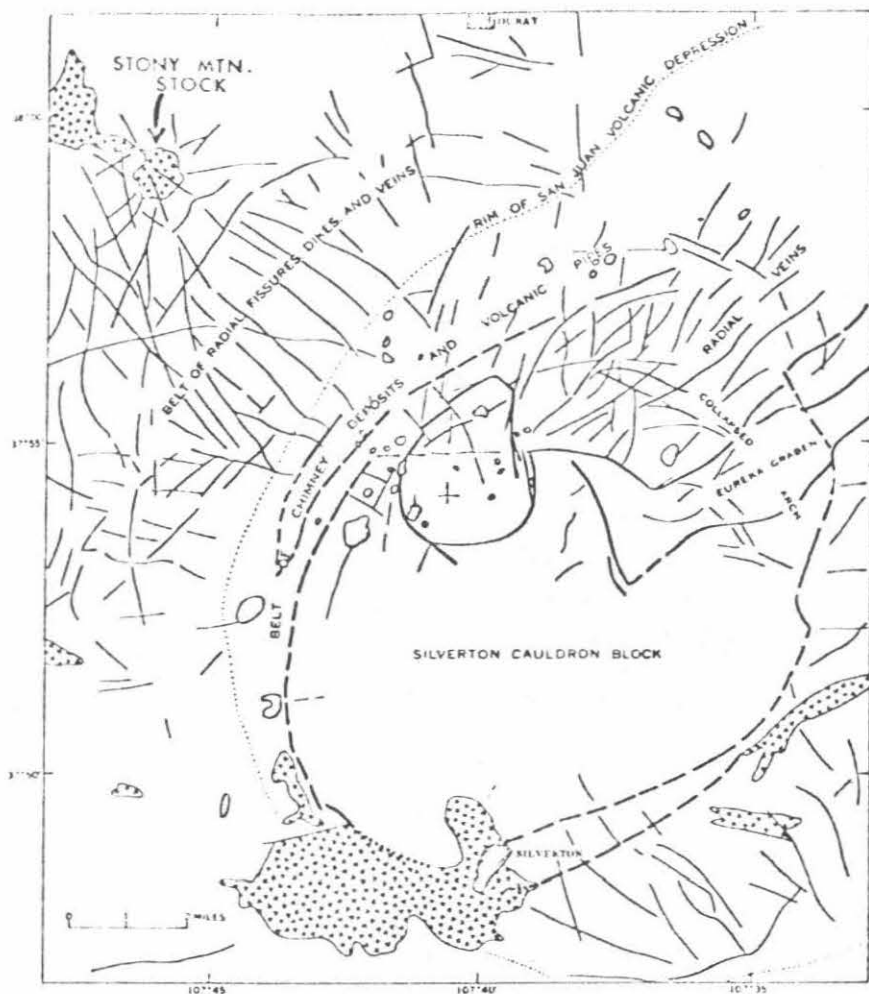


Figure 5-2. Structural map of the Silverton cauldron and vicinity. Larger plutonic bodies, v-pattern; smaller intrusive bodies and volcanic pipes, stippled pattern; faults, heavy lines; radial fissures, dikes, and veins, light lines (after Luedke and Burbank, 1968).

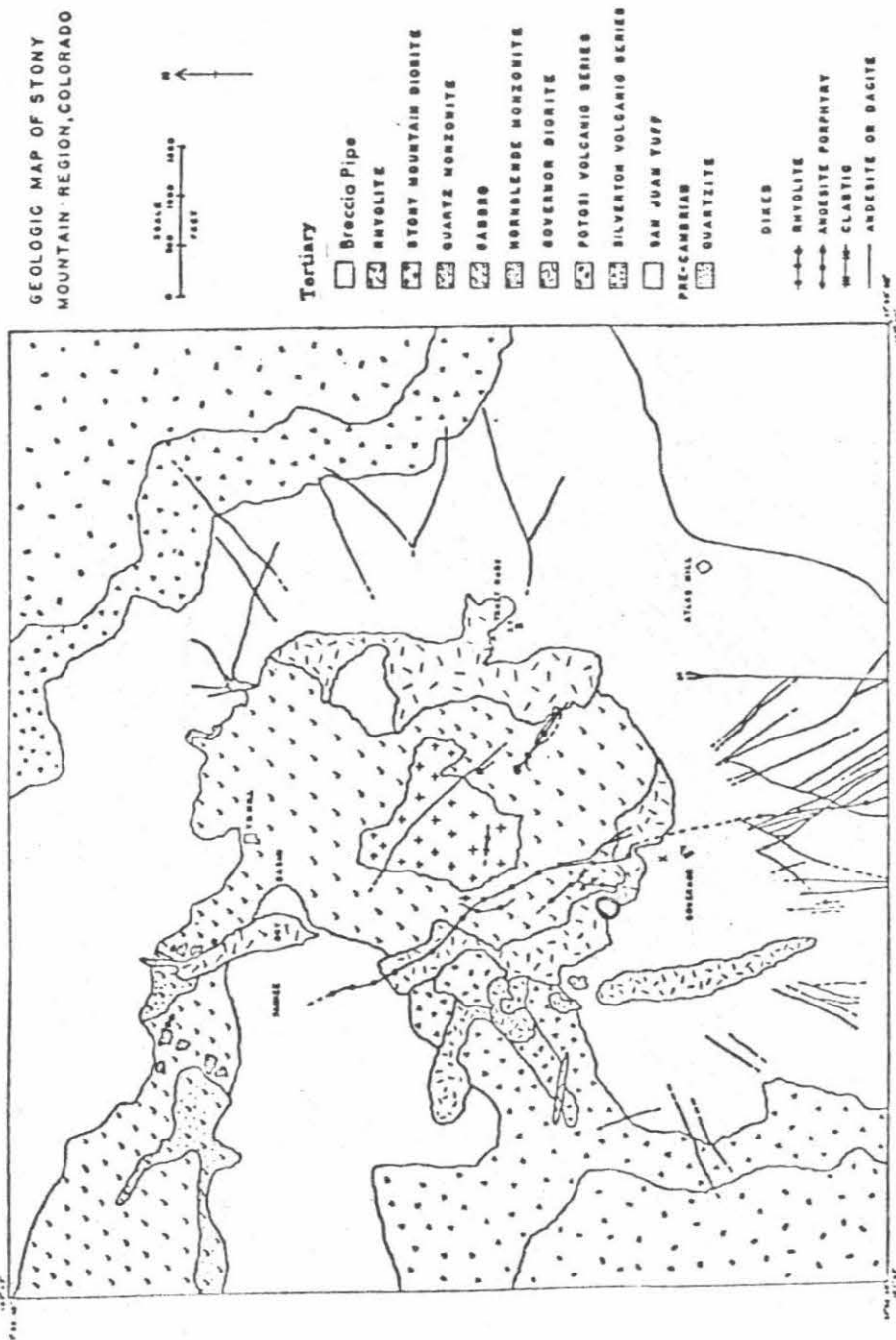


Figure 5-3. Geologic map of the Stony Mountain region (revised from Dings, 1941).

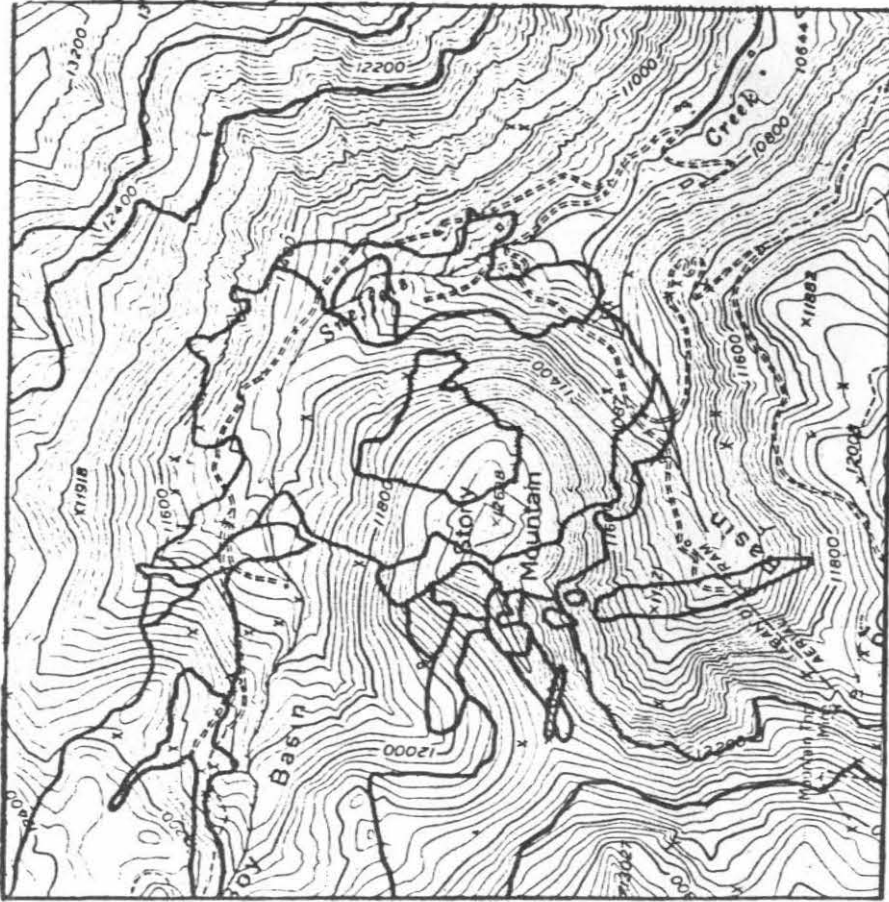


Figure 5-4. Topographic expression of the Stony Mountain region, in relation to the geologic map (see Figure 5-3). Contour interval is 40'.



Plate 5-1. Stony Mountain, Colorado, as seen from the southwest. The cliff-forming outcrop across the middle of the photograph is the outer diorite ring dike. It is cut by the rust-colored, circular breccia pipe. The top of the mountain (12,698') consists of gabbro, while the inner diorite forms the shoulder to the east.

which disconformably overlies the San Juan Tuff. It is composed of about 150 meters of dark, porphyritic, pyroxene-bearing andesitic to rhyodacitic tuffs, breccias and flows in this area. The Picayune Formation is here separated from the overlying Potosi Volcanic Group by an erosional unconformity. The Potosi Group is represented by the Gilpin Peak Tuff, composed predominantly of quartz-latitude ash-flow tuffs. A thickness of about 100 meters of the Gilpin Peak Tuff is exposed in the immediate vicinity of the Stony Mountain stock, but 400 meters of the type section are still exposed on nearby Potosi Peak. Generally, the volcanic rocks in the vicinity of the Stony Mountain-Mt. Sneffels intrusion are extensively hydrothermally altered and contain sericitized feldspars, carbonate and epidote. Chlorite and uralite are the common alteration products of the mafic minerals.

The sequence of intrusion of the Stony Mountain complex, as first established by Dings (1941) is the following: (1) an outer, 150-meter thick, arcuate ring-dike of fine-grained diorite, with a minor amphibole monzonite differentiate exposed near the NW portion of the stock; (2) the main mass of medium-grained gabbro, grading into a quartz diorite to the north and with a quartz monzonite facies in the connecting arm extending towards Mt. Sneffels; (3) a central plug, about 0.5 km across, of fine-grained diorite; and (4) a tabular rhyolite mass about 500 meters long and 100 meters wide.

The term outer diorite will be retained for the outermost and oldest intrusive unit of the Stony Mountain complex, although chemically and mineralogically it is closer to a quartz diorite or a granodiorite (see Table 5-3). The outer diorite usually contains 1 mm phenocrysts of clinopyroxene, orthopyroxene and plagioclase, set in a aphanitic groundmass of pyroxene, opaques, plagioclase, orthoclase, quartz and apatite. The common alteration products are sericite, chlorite, calcite, epidote and magnetite. The hornblende monzonite body grades imperceptibly into the outer diorite. The hornblende phenocrysts are typically set in an altered groundmass of feldspar, chlorite, calcite and opaques. A mineralized breccia pipe (Burbank, 1933) perforates the SW portion of the outer diorite ring dike. It is largely composed of dolomite, quartz, and white mica, with smaller amounts of pyrite, chalcopyrite, hematite and sphalerite. Fragments of San Juan Tuff appear to make up a large part of this breccia.

The greater part of the intrusion is made up of a gabbroic rock that has a variable chemical composition. The southern half of this intrusive unit is a relatively fresh, uniform, dark grayish-green biotite gabbro, usually with hypersthene and containing only small amounts of sericite, chlorite and uralite as alteration products. The northern part of the unit is generally a gray quartz diorite, and is slightly finer-grained than the southern gabbros (0.9 vs 1.4 mm). In the arm extending towards Mt. Sneffels (Sneffels Arm Gabbro) the rock

Table 5-3
 Chemical Analyses* and Norms of Rocks
 from the Stony Mountain Region

	1	2	3	4	5	6
SiO ₂	47.32	52.05	60.15	60.23	61.36	63.91
Al ₂ O ₃	16.71	17.96	18.03	15.56	16.36	17.07
Fe ₂ O ₃	6.92	4.09	2.73	3.20	3.59	4.39
FeO	5.94	6.33	3.27	3.08	1.45	1.51
MgO	5.69	5.03	2.18	2.73	1.75	.81
CaO	8.51	8.64	5.78	4.21	3.59	4.47
Na ₂ O	2.70	2.99	3.53	4.43	4.04	3.48
K ₂ O	2.02	1.61	2.76	3.42	3.64	3.74
H ₂ O+	.24		.09	.10	1.34	
H ₂ O-	1.04	.97	.53	1.10	1.56	.33
TiO ₂	1.50		.65	.79	.51	
P ₂ O ₅	.96	.31		.34	.36	.21
MnO	.08	.43		.14	.07	
CO ₂			.19	.44	.64	
ZrO ₂				.00		
SO ₃	.19					
BaO	.07			.11	.12	
SrO	.06				.12	
Total	99.95	100.41	99.89	99.92	100.51	99.92
Q	0.84	1.50	13.26	9.84	16.98	19.74
or	11.68	9.45	16.68	20.02	21.13	21.68
ab	22.53	25.15	29.34	37.20	34.06	29.34
an	27.80	30.86	25.02	12.79	10.84	20.29
C					1.84	
di	6.16	8.44	3.16	5.31		
hy	14.04	17.43	6.34	6.12	4.40	2.00
mt	9.98	6.03	3.94	4.64	3.48	4.87
il	2.89		1.22	1.52	.91	
hm					1.28	1.12
ap	2.35	.67		.67	1.01	.67

Table 5-3 (Cont'd)

* All analyses taken from Larsen and Cross (1956, p.232)

1. Gabbro porphyry. Near Mt. Sneffels, Telluride, Colo.
2. Gabbro. From summit of Stony Mountain in the Telluride quadrangle.
3. Granodiorite (Governor diorite of Dings). From the northeastern part of the Telluride quadrangle, 290 ft due west of the Summit of Stony Mountain at an altitude of 12,510 ft.
4. Hornblende granodiorite (monzonite). From Stony Mountain in the northeastern part of the Telluride quadrangle.
5. Granodiorite porphyry. From the large dike in the east border of the Ouray quadrangle on the east side of Porphyry basin.
6. Granodiorite. From the east base of Sultan Mountain in the Silverton quadrangle.

is a quartz-bearing diorite that is gradational into, as well as being cut by, two masses of pink to green-gray quartz monzonite. The quartz monzonite is composed largely of andesine, orthoclase and quartz and contains relatively abundant chlorite, sericite, carbonate, epidote and uralite.

A tabular, pink rhyolite mass, with quartz and orthoclase phenocrysts, was the latest major intrusion in this area. Various dikes, mainly of andesite, form a radial pattern around the Stony Mountain stock.

Numerous Precambrian quartzite xenoliths, up to 50 meters long, occur within the dioritic gabbro in the connecting arm between Mt. Sneffels and Stony Mountain. These inclusions were probably derived from quartzites of the Uncompahgre Formation, which crop out just south of the town of Ouray (see Luedke and Burbank, 1962).

Chapter 6

ISOTOPIC RESULTS: WESTERN SAN JUAN MOUNTAINS, COLORADO

6.1 Regional isotopic relationships

All the $^{18}\text{O}/^{16}\text{O}$, $^{13}\text{C}/^{12}\text{C}$ and D/H analyses pertaining to the Western San Juan Mountains and, in particular, to the Stony Mountain stock are presented in Tables 6-1 and 6-2. The regional data are presented in Figure 6-1, and all samples analyzed in the vicinity of the Stony Mountain stock are plotted on the map in Figure 6-2 and the generalized cross-section in Figure 6-3.

An average whole rock $\delta^{18}\text{O} \approx +4$ and $\delta\text{D} \approx -145$ characterizes most of the igneous rocks in the Silverton-Ouray district, with the notable exception of those samples along the eastern and southeastern portion of the Silverton caldera ring fracture which have an average $\delta^{18}\text{O} \approx -5$ (Figure 6-1). All of these rocks are generally lower in both $\delta^{18}\text{O}$ and δD than the rocks of the Eastern San Juan Mountains, where the altered volcanic and intrusive rocks typically have $\delta\text{D} \approx -110$, (Taylor, 1974a). Both areas have thus interacted with heated meteoric ground waters in Oligocene-Miocene time, the western region showing whole-rock $\delta^{18}\text{O}$ depletions of more than 12 per mil, while the eastern area exhibits local depletions up to 5 per mil. Taylor (1974a) suggested several reasons for the isotopic contrast: (1) the Silverton area may have represented

Table 6-1

Oxygen and carbon isotope analyses of whole-rocks and minerals from the
Stony Mountain stock and vicinity and the Western San Juan Mountains,
Colorado

Sample ² (SM-)	Mineral ³	$\delta^{18}O$ (‰) ⁴	Remarks ⁵
<u>Stony Mountain Stock and Vicinity</u>			
Quartzite ¹			
122	Q	+11.3	Essentially pure qtz; quartzite xenolith in gabbro.
123	Q	+11.8	As above. Strike N40°W, dip 50°S.
124	Q	+10.6±0.1(2)	As above. Strike N, dip 90°.
San Juan Tuff			
2	WR	+0.1	
4	WR* Ct	+3.4 +1.8	($\delta^{13}C = -5.8$).
13	WR	+4.3±0.0(2)	
69	WR	+2.5	Turbid to opaque feld phenos (1mm) now largely <u>sericite</u> , qtz, <u>mag</u> & <u>ct</u> . Fractures, lined with mag, cut rock. Grain size ≈20μ.
83b	WR	+1.4	Xenolith (12mx3m) in gabbro. 1mm seriz feld phenos; mafics now largely <u>chl</u> ; gdmass of <u>sericite</u> , <u>carbonate</u> , qtz, opaques.
118	WR	+2.9	
134a	WR	+2.4	
143	WR	+1.0	
147	F	+2.3	Plag phenos (1-2mm), quite fresh; strong oscillatory zoning. Px phenos (1mm) most with <u>mag</u> alteration, in gdmass of feld, qtz and opaques.
148	WR	-0.7	
154	WR* Ct	+1.7 +2.3	($\delta^{13}C = -5.3$).
165c	WR* Ct	+2.7 +4.3	($\delta^{13}C = -7.5$).
168	WR	+1.6	

Table 6-1 (Cont'd)

Sample (SM-)	Mineral	$\delta^{18}O$ (‰)	Remarks
169	WR Ct	-1.1 -0.7	Pheno (6mm) of amph now largely altered to chl, ct & mag. Gdmass (0.01mm) of <u>chl</u> , <u>sericite</u> , <u>ct</u> , <u>qtz</u> & <u>mag</u> . Ct veinlet cuts rock. Amyg of qtz-ct-feld-mag. ($\delta^{13}C = -3.9$).
171	Q WR	+7.1 +3.1	Xenocrysts & phenos of oscillatory zoned dusty plag (0.5mm) & almost totally altered mafics, now largely <u>biot</u> , <u>mag</u> , <u>chl</u> , & <u>ep</u> with minor remnant <u>cpx</u> , in an aphanitic gdmass of feld, qtz, <u>ep</u> , <u>chl</u> , <u>sericite</u> & apatite.
173	WR Ct	-0.2 -1.8	($\delta^{13}C = -5.5$).
185	WR	+2.0	
187b	WR (matrix)	+1.3	Conglomeratic volcanic; fragments largely altered; <u>sericite</u> , <u>ct</u> , <u>chl</u> , <u>mag</u> , <u>qtz</u> , <u>feld</u> , <u>hem</u> .
195	WR	-0.1	Subhorizontal bedding.
197	WR	+0.2	
202	WR	+1.3	Volcanic fragments (& xenocrysts) with oscillatory zoned plag; mafics now <u>chl</u> , in a gdmass of feld, qtz, mag & <u>sericite</u> .
216	WR Ct	+2.6 +0.3	1cm-sized fragments & matrix altered to assemblage of feld, qtz, <u>sericite</u> , <u>chl</u> , <u>mag</u> , <u>ep</u> & <u>ct</u> . ($\delta^{13}C = -5.5$).
216 I	WR	+1.6±0.1(2)	Same as SM-216.
216II	WR	+2.9	Same as SM-216.
Picayune Formation			
36	WR	+2.6	Phenos of cpx (3mm, 10%, generally fresh but some altered to chl), plag (2mm, 35%, partly altered to sericite) & mag (6mm, 1%) in a gdmass (<0.4mm, 50%) of plag, mag, qtz, <u>chl</u> & <u>sericite</u> . A few amyg filled with colloform ct & qtz.
155	WR	+1.3	Altered pyrox pheno, up to 5mm long in seriz plag-rich gdmass.
163	WR	+1.7±0.1(2)	Similar to SM-155.

Table 6-1 (Cont'd)

Sample (SM-)	Mineral	$\delta^{18}O$ (‰)	Remarks
Gilpin Peak Tuff			
42	WR*	+3.0	$(\delta^{13}C = -5.5)$.
	Ct	+5.2	
54	WR	+3.5	
156	WR	+1.6	Mafic pheno now largely altered to <u>chl</u> ; similar to SM-157.
157	WR	+2.6±0.1(2)	Seriz feld & altered mafic (<u>chl</u>) pheno (1-2mm) in gray-green matrix of <u>sericite</u> , <u>chl</u> , <u>ct</u> , feld, qtz, & mag.
158a	WR	+3.5	5cm from a 3cm-thick dike.
162	WR	+4.1	Plag (40%, 2mm) & px (5%, 6mm) in a gdmass (55%, $\leq 10\mu$) of feld, qtz, <u>sericite</u> , <u>chl</u> , mag, & <u>ct</u> . Plag pheno often are zoned (avg An_{30}) some with turbid cores, cloudy central regions & v turbid rims. Most are v turbid throughout. Minor amyg filled with fg qtz & feld.
Outer Diorite			
3a	WR	+1.6±0.1(2)	Fractured, blocky, fg diorite. 1m from SM-4.
12	WR	+3.7	Equigranular fg diorite.
41	WR	+2.2	Pheno of cpx (10%, 3-4mm), mag (5%, 0.2 mm) & plag (25%, 0.8mm) in brownish gdmass (60%, 0.1mm) of feld, <u>sericite</u> , qtz & mag. Cpx altered along cracks & rims to <u>chl</u> . Plag is only partly clear mostly cloudy or turbid due to alteration (mainly <u>sericite</u> & <u>ep</u>).
58	F WR	+5.9 +4.7	Pheno of plag (40%, up to 5mm) & altered mafics (5% <u>chl</u> , mag, biot) in a crushed gdmass (50%, 0.2mm) of feld, qtz, mag, <u>sericite</u> & <u>chl</u> . Generally plag is quite clear & fresh, oscillatory zoned, & only partially seriz along features, cracks, some rims & cores. A few rock fragments are present.
77	F WR	+2.9 +3.4	

Table 6-1 (Cont'd)

Sample (SM-)	Mineral	$\delta^{18}\text{O}$ (‰)	Remarks
89	WR	-1.1	Pheno of amph (30%, 2mm), cpx (5%, 0.5 mm) & plag (5%, 0.6mm) in a gdmass (55%, 40 μ) of feld, mag, cpx, qtz, <u>sericite</u> , & <u>chl</u> . The pheno are cracked & partly altered to mag, <u>chl</u> & <u>sericite</u> . Minor qtz & zeolites in cavities; within 0.5m of major vein.
166	WR	+5.8 \pm 0.0(2)	Pheno of oscillatory zoned, clear to partly cloudy & seriz plag (35%, 1mm), fresh cpx (5%, 6mm), altered mafics (<u>chl</u> 5%) & amph (5%) in a gdmass (30%, 15 μ) of feld, qtz, mag, <u>ep</u> , <u>sericite</u> & apatite.
167	WR	+5.9 \pm 0.1(2)	Similar to SM-166.
178	WR	+5.3	Seriate plag (up to 1mm), oscillatory zoned, clear to partly seriz; qtz, mag, px, <u>chl</u> & <u>ep</u> . Thin (1mm) fracture goes through rock. Unusually qtz-rich rock.
180	M WR	-0.8 \pm 0.1(2) +2.9	Pheno of highly oscillatory zoned, clear to partly cloudy plag (25%, 0.4mm), cpx (2%, 0.4mm), mag (1%, 0.2mm) & opx (<1%) in an aphanitic gdmass (70%) of feld, qtz, mag, apatite, <u>ep</u> & <u>sericite</u> . Rock has v small m cavities.
181	WR	+4.5	Thin <u>chl</u> -qtz-sericite veinlets cut rock. Dusty zoned plag & altered cpx (now <u>chl</u> , <u>ep</u> , mag, ct) with interstitial cloudy to turbid feld, qtz, mag, <u>sericite</u> & <u>ct</u> .
198	WR	+2.7	
200	p WR (gdmass)	+6.1 +5.8	Glomeroporphyritic pheno of cpx, zoned plag, & opx (30%, up to 7mm) in a fg gdmass (70%) of zoned plag, mag, px, <u>biot</u> , apatite, qtz & <u>sericite</u> . A v fresh rock except for the seriz of gdmass feld.
203	WR	+4.5	

Table 6-1 (Cont'd)

Sample (SM-)	Mineral	$\delta^{18}\text{O}$ (‰)	Remarks
Hornblende Monzonite			
44	WR	+3.3±0.2(3)	Similar to SM-49.
49	WR*	+3.3	Feld & mafics altered to <u>sericite</u> , <u>ct</u> , <u>chl</u> , & <u>mag</u> with <u>qtz</u> seemingly the only primary mineral left from the original rock. ($\delta^{13}\text{C}=-6.2$).
	Ct	+3.9	
Gabbro			
63	F	+4.8	Low magnetic fraction ~50% of bulk plag.
64	F	+6.0	High magnetic fraction ~50% of bulk plag. Hypidiomorphic-granular rock with clear to partly dusty zoned plag (1.5mm), px (1.2mm), biot (1mm), mag (0.15mm), K, qtz, apatite, <u>sericite</u> & <u>zeolite</u> . Px shows an opaque-rich patchy schiller-type alteration pattern, but generally quite fresh. The variation of included dust-like material, probably mainly mag, has allowed the separation of two plag fractions analyzed here.
	F	+5.3	
	F	+5.6	
	(calc'd avg)		
	P	+5.6	
	B	+5.6	
	M	+1.7	
	WR	+5.4±0.0(3)	
82	F	+4.6	
84	F	+6.0	Similar to SM-64 except plag (2mm) is slightly more cracked & px (1.6mm) is significantly more altered to <u>chl</u> .
	P	+4.5	
	WR	+5.0	
90	F	+2.6	Hypidiomorphic-granular rock traversed by many thin fractures & veinlets (<u>chl</u> , <u>ct</u> , <u>sericite</u>). Diffusely zoned plag (1.9mm) generally dusty to cloudy, largely due to seriz. Px & biot largely altered to <u>chl</u> . Minor K, qtz & apatite.
	WR	+3.2	
91a	WR	+2.6	Similar to SM-90. Plag (3mm) is partly seriz along fractures, cracks & cleavage. Mag is mostly associated with altered mafics (<u>chl</u>). Rock is 0.5cm from inner diorite contact, which is knife sharp.
91c	WR	+3.0	12.5cm from inner diorite contact. 1cm from inner diorite contact. Similar to SM-91a.
	WR	+3.0	
98a	WR	+1.4±0.2(2)	

Table 6-1 (Cont'd)

Sample (SM-)	Mineral	$\delta^{18}O$ (‰)	Remarks
101	F P B M WR	+5.2±0.0(3) +5.5±0.1(3) +5.5±0.1(2) +2.0±0.0(3) +5.0±0.1(3)	Hypidiomorphic-granular with diffusely zoned An ₆₂₋₃₀ , clear to dusty plag (50%, 0.9mm), cpx (10%, 0.5mm), biot (2%, 0.7mm) mag, apatite, <u>chl</u> , qtz & <u>zeolite</u> . Thin fractures cut rock. See Plate 8-1a.
111	F F F M WR	+4.2 +4.1 +4.0 +1.5 +3.7±0.2(4)	Low magnetic fraction (~25% of bulk plag). Intermediate magnetic fraction (~50% of bulk plag). High magnetic fraction (~25% of bulk plag). Hypidiomorphic-granular diorite with v dusty seriate plag (avg 0.6mm). Px with secondary mag, & <u>chl</u> , biot, mag, K, qtz, <u>sericite</u> , apatite & <u>ep</u> . Fractures cut rock. Variation of dusty inclusions in plag has allowed for 3 separate fractions of plag to be separated.
113	Q M WR	+8.3 +1.6 +4.5	Similar to SM-111 except plag (60%, 1mm) is clear to partly dusty. Minor <u>uralite</u> after px & <u>zeolite</u> in this qtz diorite.
131	WR	+3.4	Similar to SM-113 except seriz has made some of the plag & K quite cloudy. <u>Chl</u> & <u>ep</u> are the main mafic phases.
138	WR	+5.0	Similar to SM-111 with oscillatory zoned dusty plag (0.7mm). Px partly altered to <u>chl</u> , <u>ep</u> & <u>mag</u> . Weak pilotaxitic texture. Qtz diorite.
139	WR	+5.3±0.3(4)	Similar to SM-138. Plag (65%, 0.6 mm) dusty or cloudy. Minor <u>uralite</u> .
140	WR	+4.4	Similar to SM-138 except slightly coarser grained. Plag (1.3mm) ranges from clear to dusty or cloudy, sometimes fractured & cracked with accompanying <u>sericite</u> & <u>chloritization</u> .
146	F B WR	+6.1±0.2(4) +4.7 +5.9	Hypidiomorphic-granular rock with oscillatory zoned dusty plag (70%, 1.3mm), cpx (15%, 0.4mm), biot (6%, 0.3mm), opx (2%, 0.4mm), mag (2%), <u>chl</u> , qtz & apatite (especially as needle-like inclusions in plag).

Table 6-1 (Cont'd)

Sample (SM-)	Mineral	$\delta^{18}\text{O}$ (‰)	Remarks
159	F P WR	+6.5 +5.7 +5.7	Top of Stony Mtn. Hypidiomorphic-granular qtz gabbro with zoned, fractured, & dusty plag (3.1mm), partially chloritized cpx & opx (2mm) biot, mag, qtz, sericite, apatite & zeolite.
183	F WR	+5.8±0.0(2) +4.9	Hypidiomorphic-granular rock, with zoned dusty plag (60%, 0.9mm) cut by minute chl-veinlets, & partially seriz; cpx (10%, 0.5mm) with alteration products chl, biot & mag, with patchy surface of different birefringence; chl (20%), mostly pseudo-morphic after cpx; biot, K, qtz, mag, apatite & zeolite.
Quartz Monzonite			
109	Q F M WR	+6.3±0.2(2) +2.1 -1.1 +2.3±0.1(2)	Diffusely zoned cloudy seriz plag (30%, 0.8mm), An54-31, poikilitically enclosed by K (45%, 1mm). Cpx (10%, 0.8mm) altered in part to mag & chl, with patchy biref. Mag, biot, qtz, sericite, ep, apatite & ct. F corrected for 7% qtz.
112	Q F WR	+8.3±0.1(2) +3.2 +3.5	Similar to SM-109, except mafics now largely chl. F corrected for 15% qtz.
125	WR	+2.1±0.0(2)	As above; some pyrite present.
Inner Diorite			
91a	WR WR	+1.9 +2.1	4cm from gabbro contact. 0.5cm from gabbro contact.
91c	WR WR	+1.4 +1.9	12.5cm from gabbro contact. 1cm from gabbro contact.
94	WR	+3.3	Pilotaxitic texture; zoned, clear to dusty plag, px, mag, biot, chl, qtz, & apatite.
95	WR	+2.7	
96	WR	+2.7	
97	WR	+1.3	
99b	F P (calc'd) M WR	+3.1±0.1(2) +2.2 -0.2 +2.8±0.0(2)	Pilotaxitic structure; zoned, clear to partly dusty fresh plag (65%, 0.4mm); cpx & opx are fresh; mag, K, qtz, chl, apatite, sericite. Veinlets of chl (0.5mm) cut the rock.

Table 6-1 (Cont'd)

Sample (SM-)	Mineral	$\delta^{18}\text{O}$ (‰)	Remarks
Rhyolite			
103	q k WR	+7.8±0.0(2) -1.6±0.1(2) +2.3	Pheno of euhedral qtz (15%, 2mm) with β -morphology, & cloudy K (15%, 1mm) somewhat altered to sericite in a gdmass (70%, 0.01mm) of very dusty to cloudy feld, qtz, <u>mag</u> & <u>sericite</u> .
Breccia Pipe			
81	Q WR D	+9.4 +5.0 +2.2	Essentially composed to qtz, both as 0.5 mm grains, & in aphanitic gdmass with dolomite & <u>white mica</u> . Opaques include pyrite, <u>chalcopyrite</u> , specular hematite, & <u>leucoxene</u> . ($\delta^{13}\text{C}=-4.7$)
Dikes			
179d	WR	+2.9	Inclusion-rich plag pheno (20%, up to 1 cm) with opaque inclusions oriented parallel to (010) of host plag, & chl-sericite alteration along cracks & cleavages; in gdmass (80%, 0.03mm) of dusty plag, <u>chl</u> , <u>opaque</u> , <u>ct</u> & <u>sericite</u> . This porphyritic andesitic dike is 3m wide; sample from center of dike.
188	WR	+1.5	Central portion of andesitic dike, 3m thick; strike N40°E; dip 65°S. Similar to SM-179d.
215	WR	-0.2	Similar to SM-179d. Andesitic dike, porphyritic, 1m thick. Strike E, dip 90°. Sample is 15cm from conglomeratic volcanic contact.
Veins			
74d	Q	-1.8	Major vein, with banded cryptocrystalline massive white qtz; blue fluorite, pyrite & galena in vuggy, comb-like structure.
116	Q	+5.1	Major vein cutting San Juan Tuff, trending N65°W, dip 90°. Sample is of euhedral vug qtz; associated with galena & pyrite.

Table 6-1 (Cont'd)

Sample (SM-)	Mineral	$\delta^{18}O$ (‰)	Remarks
<u>Western San Juan Mtns.</u>			
Col-1-8	WR	+1.8	Propylitized diorite porphyry, on Telluride-Rico highway, 2.6 mi N of Trout Lake.
Col-2-8 A (+chl)	WR	+8.7	Slightly chloritized quartz diorite porphyry, north side of Telluride-Rico highway, 2 mi W of Ophir, 2.2 mi N of Trout Lake.
	F	+8.6	
		+6.9	
Col-8-8	WR	+9.6	Diorite porphyry, just N of La Plata, 2.2 mi N of Kroeger campground & 8.4 mi N of junction with U.S. 160.
Col-11-8	WR	+5.9	Granodiorite porphyry at contact with Hermosa Formation, Silverton-Durango highway, 7 mi S of Col-13-8.
Col-13-8	WR	+6.4	Augite-biotite mg quartz monzonite, 1 mi SW of Silverton on Silverton-Durango highway.
	Q	+8.8	
	K	+6.6	
	B	+3.9	
Col-13-8a	WR	+5.1	Leucocratic fg granitic dike cutting Col-13-8.
Col-14-8	WR	+0.8	Porphyritic quartz monzonite, somewhat propylitized, just NE of Silverton at mouth of Cement Creek.
	Q	+6.3	
	K	-0.2	
	F	-1.9	
	Chl	-4.1	
Col-16-8	WR	-5.6	Chloritized granodiorite porphyry. Animas River canyon, mouth of Cunningham Creek.
	F	-5.2	
	Chl	-7.6	
SJ-25	WR	-5.3	Altered rhyolite, Burns Formation, Animas River canyon, mouth of Eureka Gulch, 7 mi NE of Silverton.
SJ-26	WR	-4.8	Altered rhyolite, Burns Formation, Animas River canyon, mouth of Maggie Gulch, 6 mi ENE of Silverton.
SJ-33	WR	-4.3	Altered rhyolite, Burns Formation, resistant ridge overlooking Animas River canyon, 2.5 mi NE of Silverton.

Table 6-1 (Cont'd)

Sample (SM-)	Mineral	$\delta^{18}\text{O}$ (‰)	Remarks
Col-3R (88316)	Q	+2.2	Vein quartz from an ore body in the Gold King mine, 6 mi N of Silverton.
SJ-14	WR	+2.3	Altered Treasure Mtn. rhyolite, roadcut on U.S. highway 550, 1.1 mi S of Red Mtn. Pass.
SJ-12	WR	+3.0	Silverton Volcanic Group, roadcut on U.S. highway 550, 0.9 mi N of Red Mtn. Pass.
SJ-10	WR	+4.6	Silverton Volcanic Group, roadcut on U.S. highway 550, 2.5 mi N of Red Mtn. Pass (San Juan Co. line).
Col-17-8	WR	+2.9	Fresh, unaltered mg pyroxene gabbro from Stony Mtn., 6 mi SW of Ouray (see Forester & Taylor, 1972, and Dings, 1941).
	F	+3.3	
	B	+4.0	
	M	+2.1	
Col-18-8	WR	+3.2	Highly propylitized diorite porphyry (Kmp on map) in Canyon Creek, 3 mi SW of Ouray.
Col-19-8	WR	+3.8	Slightly chloritized & uralitized gabbro dike, N-trending, 1.0 mi N of Cedar Hill Cemetery, N of Ouray.
SJ-1	Q	-1.7	Euhedral comb quartz.
SJ-17	WR	+5.7	
SJ-19	WR	+3.0	
S-4	K	+2.7	Silverton quartz monzonite, 1 mi SW of Silverton on the Silverton-Durango highway.
	M	+0.5	
YAG-738	Mafics	+1.8	Cretaceous diorite porphyry, 37°59'5" (N Lat), 107°42'30" (W Long).
	WR	+4.5	
YAG-741	WR	+4.5	Silverton Volcanic Group, felsite porphyry Burns Formation, 1.5 mi S of Red Mtn. Pass.
YAG-739	WR	+2.4	San Juan Tuff, altered andesite tuff, 37°58'40" (N Lat), 107°43'0" (W Long).

1. The unit names given are not necessarily the rock types.
2. All sample numbers without letter prefix are SM- .
All Col- samples are from Taylor (1974a).
All SJ- samples are from Taylor (1974a), except SJ-1, SJ-17, and SJ-19.
YAG samples provided by Armstrong (see Armstrong, 1969).
3. Abbreviations are WR = whole rock; F = plagioclase feldspar; K = alkali feldspar; Q = quartz; q, k, p = quartz, alkali feldspar, and pyroxene phenocrysts, respectively; B = biotite; Chl = chlorite; Ct = calcite; D = dolomite; A = amphibole; M = magnetite; P = pyroxene; Calc'd = calculated; avg = average; * = acid-treated to remove carbonate.
4. $\delta^{18}\text{O}$ values relative to SMOW; the number in parenthesis is the number of separate determinations; error is the average deviation from the mean.
5. Abbreviations are vfg = very fine grained; pheno = phenocrysts; gdmass = groundmass; amyg = amygdules; qtz = quartz; plag = plagioclase; mag = magnetite; biot = biotite; ct = calcite; chl = chlorite; seriz = sericitized; amph = amphibole; feld = feldspar; hem = hematite; cpx = clinopyroxene; px = pyroxene; ep = epidote; opx = orthopyroxene; K = alkali feldspar. Minerals that are underlined are secondary phases. Dusty feldspar (usually plagioclase) has scattered, dust-like inclusions which are probably largely magnetite (see Plate 8-1). Cloudy feldspar is due mainly to mild sericitization, while in turbid feldspar, the mineral seems to be dominated by the white micas. The extreme effect leads to an opaque-like appearance of the feldspar (see Plate 8-2).

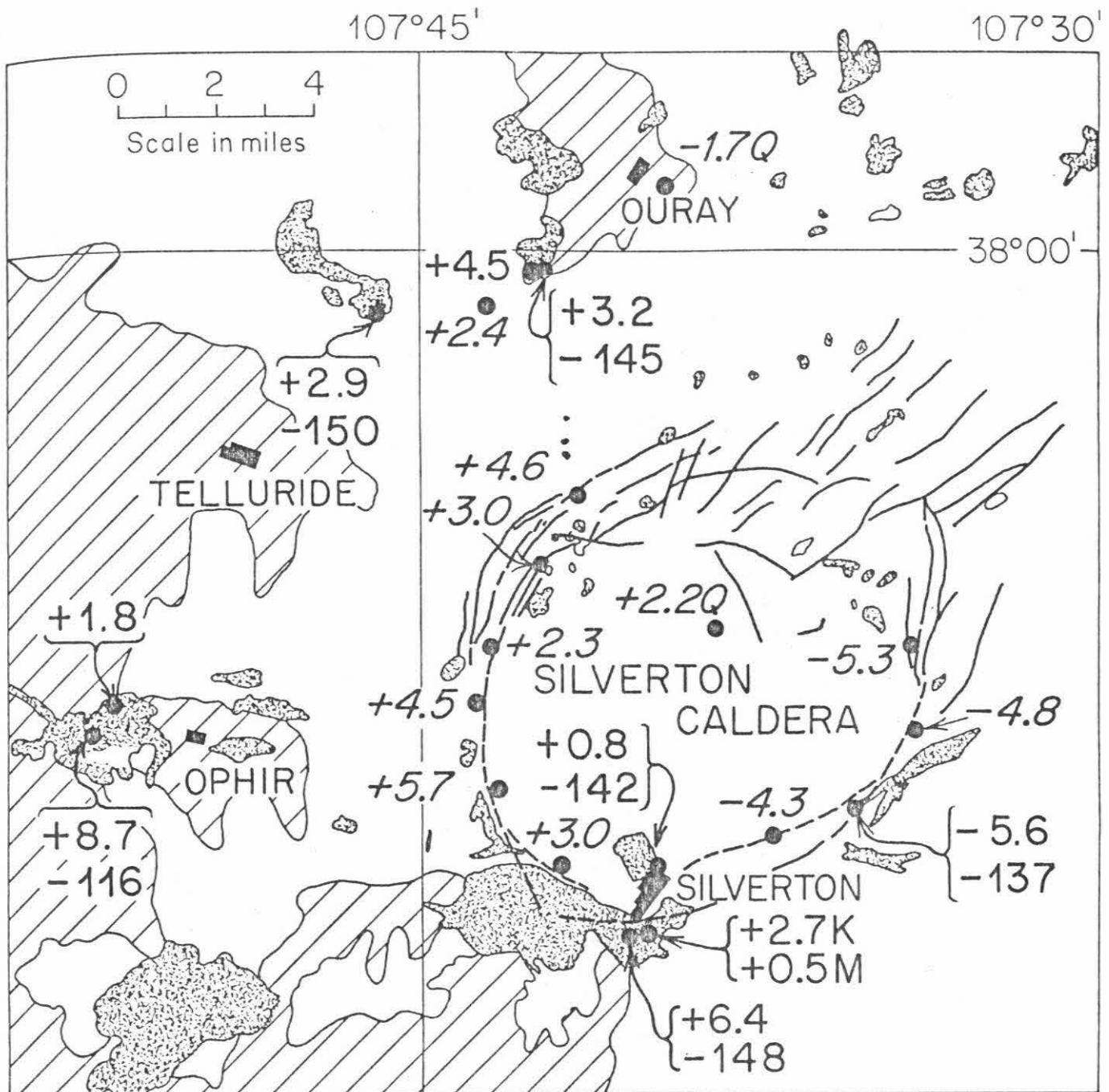


Figure 6-1. $\delta^{18}\text{O}$ and δD analyses of igneous rocks from the Western San Juan Mountains, Colorado. The $\delta^{18}\text{O}$ values are all whole-rock samples, except Q = quartz, K = alkali feldspar, and M = magnetite. Data on volcanic rocks (blank pattern) are shown in italics and for intrusive rocks (stippled pattern) in regular lettering. The Phanerozoic sedimentary rocks are shown in a diagonal-lined pattern. Large negative numbers are δD values on chlorite or biotite. Data from Taylor, 1974a, Forester and Taylor, 1972, and this work.

Figure 6-2. Geologic map of the Stony Mountain region, (revised after Dings, 1941), showing most of the $\delta^{18}O$ analyses obtained in the present study. Only at the inner diorite-gabbro contact are the data generalized (see Table 6-1).

Figure 6-3. A highly schematic cross section through the Stony Mountain intrusive complex on the right and the Sneffels Arm extension on the left, based principally on a geologic map by Dings (1941), showing all the whole-rock $\delta^{18}O$ data obtained in the present research. All samples are plotted at their exact elevations, but their spatial relationships are only diagrammatic, as all data-points have been projected onto the plane of the section, assuming cylindrical symmetry in the vicinity of the main ring complex. Generalized $\delta^{18}O$ contours are shown as heavy black lines at $\delta^{18}O = +5, +3, +1$ and -1 per mil. The reconstructed Tertiary land surface is drawn on the basis that the maximum thickness of Gilpin Peak Tuff (GPT) exposed anywhere in this vicinity is about 400 m on Potosi Peak. The total original thickness was probably about 520 m (see Luedke and Burbank, 1968). Also note that the Stony Mountain stock was probably intruded very soon after the deposition of the Gilpin Peak Tuff (Lipman *et al.*, 1970). PF = Picayune Formation (Silverton Group). SJT = San Juan Tuff. The central diorite intrusion and the San Juan Tuff are both shown as blank pattern. The gabbro is cross-hatched. The outer diorite is the large dotted pattern; the finer dotted pattern is the quartz monzonite and monzonite. The elongate body that cross-cuts the Sneffels Arm gabbro and quartz monzonite is a late rhyolite. Dikes are shown as lines of rectangular bars. Veins are shown as thin, wavy lines (after Forester and Taylor, 1972).

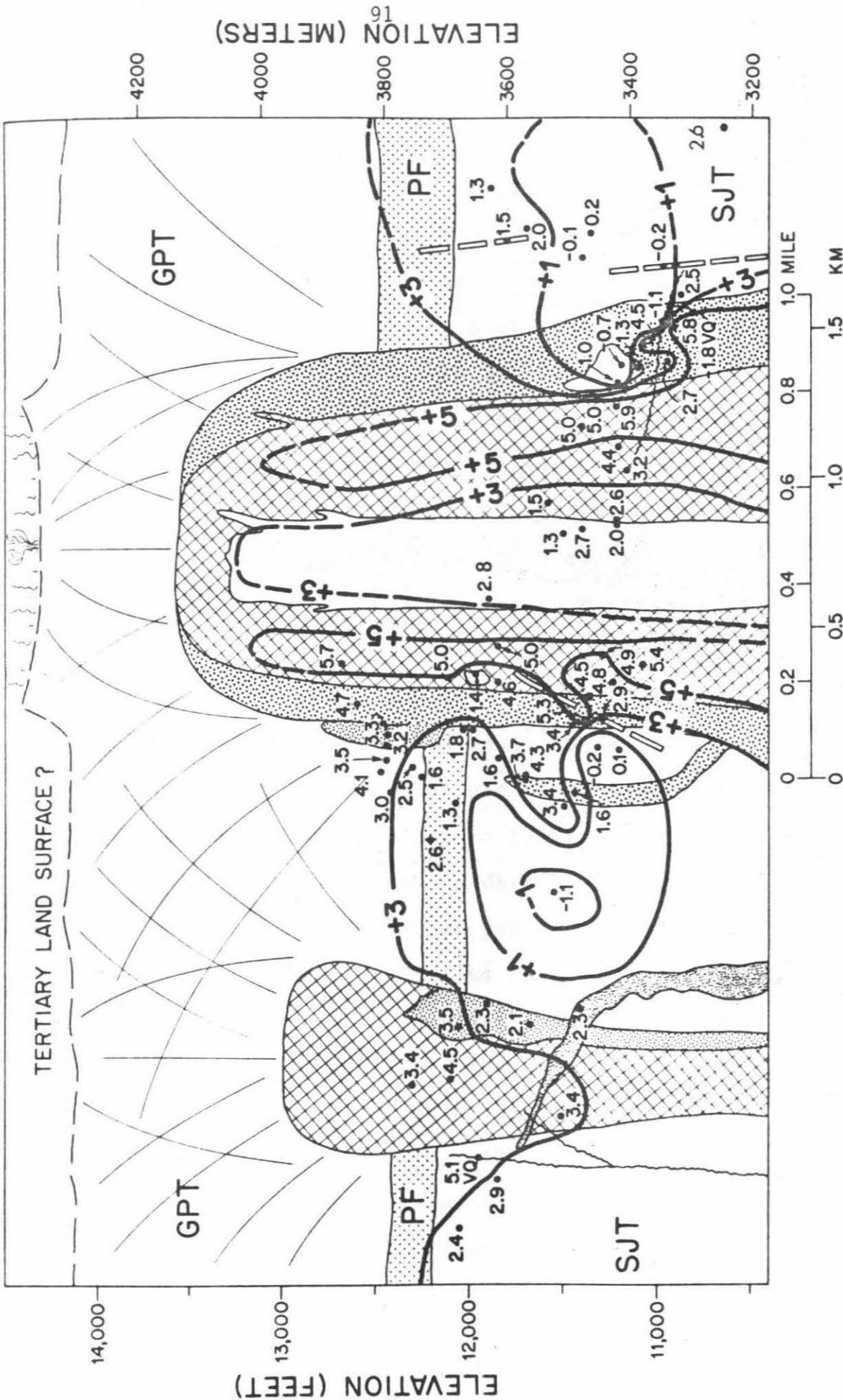


Figure 6-3

a volcanic plateau appreciably higher in elevation than the Eastern San Juans (as is the case today); (2) the mid-Tertiary topographic barriers may have been such that the Silverton-Ouray area received most of its precipitation from Pacific storms, whereas the southeastern San Juans obtained most of their rainfall and snowfall from the Gulf of Mexico (also generally true today in the two areas); and (3) the meteoric-hydrothermal systems may have terminated at different times in the two areas. Note that Bethke et al. (1973), in a study of the fluid inclusions from the Creede district, Eastern San Juans, concluded that the ore fluid was dominantly meteoric water with $\delta D \approx -58$.

Let us examine how the regional ^{18}O -depletion in the Silverton area could have taken place, in the light of the tectonic and volcanic evolution in the Western San Juans. Section A of Figure 6-4 (from Luedke and Burbank, 1968) represents the eruption of the San Juan Formation. The San Juan volcanic depression (see also Figure 5-3) formed by a major subsidence (arrow in Section B) and the Silverton Volcanic Group was confined within the structure. Graben faults and radial fractures formed as a result of resurgence (Section C), with accompanied volcanism. The young unit (Potosi Volcanic Group) was erupted, largely as voluminous ash flows, with subsequent subsidence of the Silverton and Lake City cauldrons, as shown by the arrow in Section D, Figure 6-4. Further resurgence, doming and graben formation (Section E)

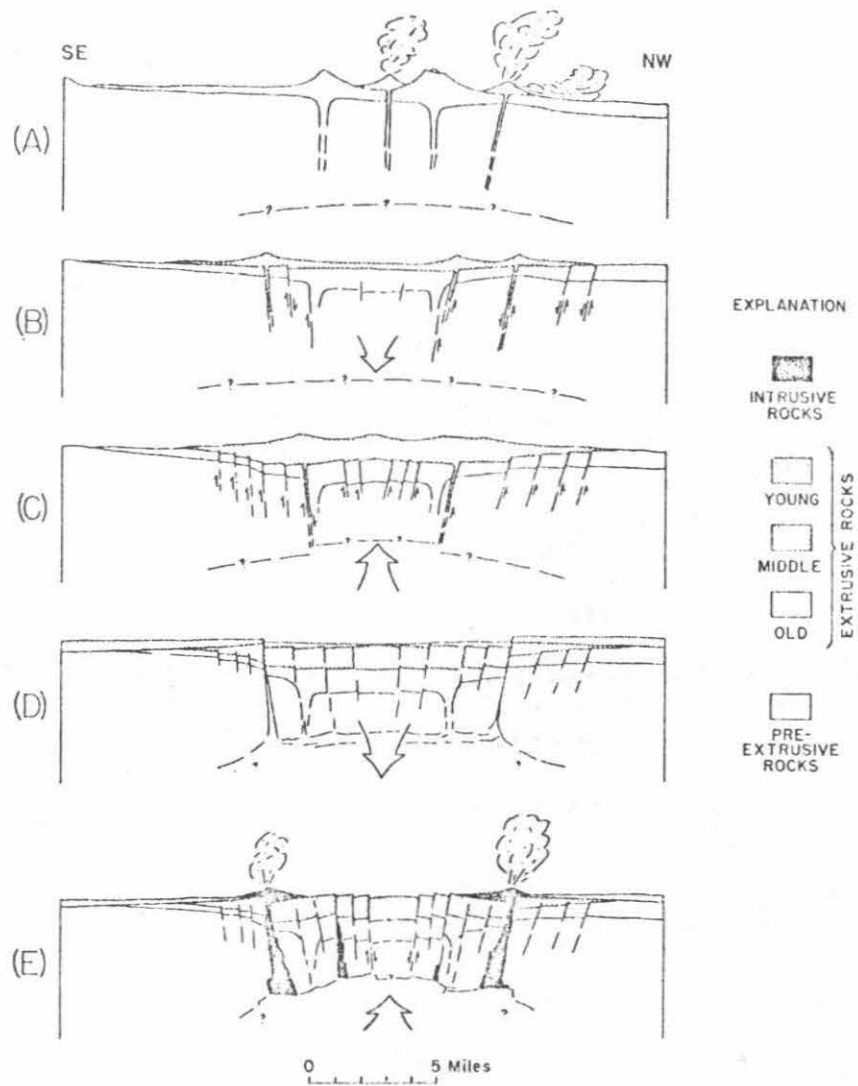


Figure 6-4. Schematic structure sections showing the generalized volcanic and structural evolution of the Western San Juans (after Luedke and Burbank, 1968).

resulted in intrusive activity, especially along the radial and concentric fractures related to the subsided blocks.

From the above account of the volcanic and structural evolution, it is evident that subsequent to the formation of the San Juan volcanic depression, a highly fractured and jointed volcanic pile developed over an extensive magma chamber of batholithic dimensions. This gigantic heat source, along with the cooling pile of lava flows, could have provided sufficient energy to heat up, drive, and circulate meteoric ground waters throughout a very large volume of rock. Thus, pervasive oxygen isotopic interactions with heated meteoric waters could have occurred in the volcanic pile, perhaps accounting for a reduction in the average regional $\delta^{18}\text{O}$ value of from about +7 or +8 to about +4. The hydrothermal convection systems produced by the many stocks and smaller intrusions in this area (only the larger bodies are shown in Figure 6-1) could also be important. Therefore the regional ^{18}O depletion in part may be a result of the combined effects of many overlapping meteoric-hydrothermal alteration systems produced by the myriads of stocks present throughout the area.

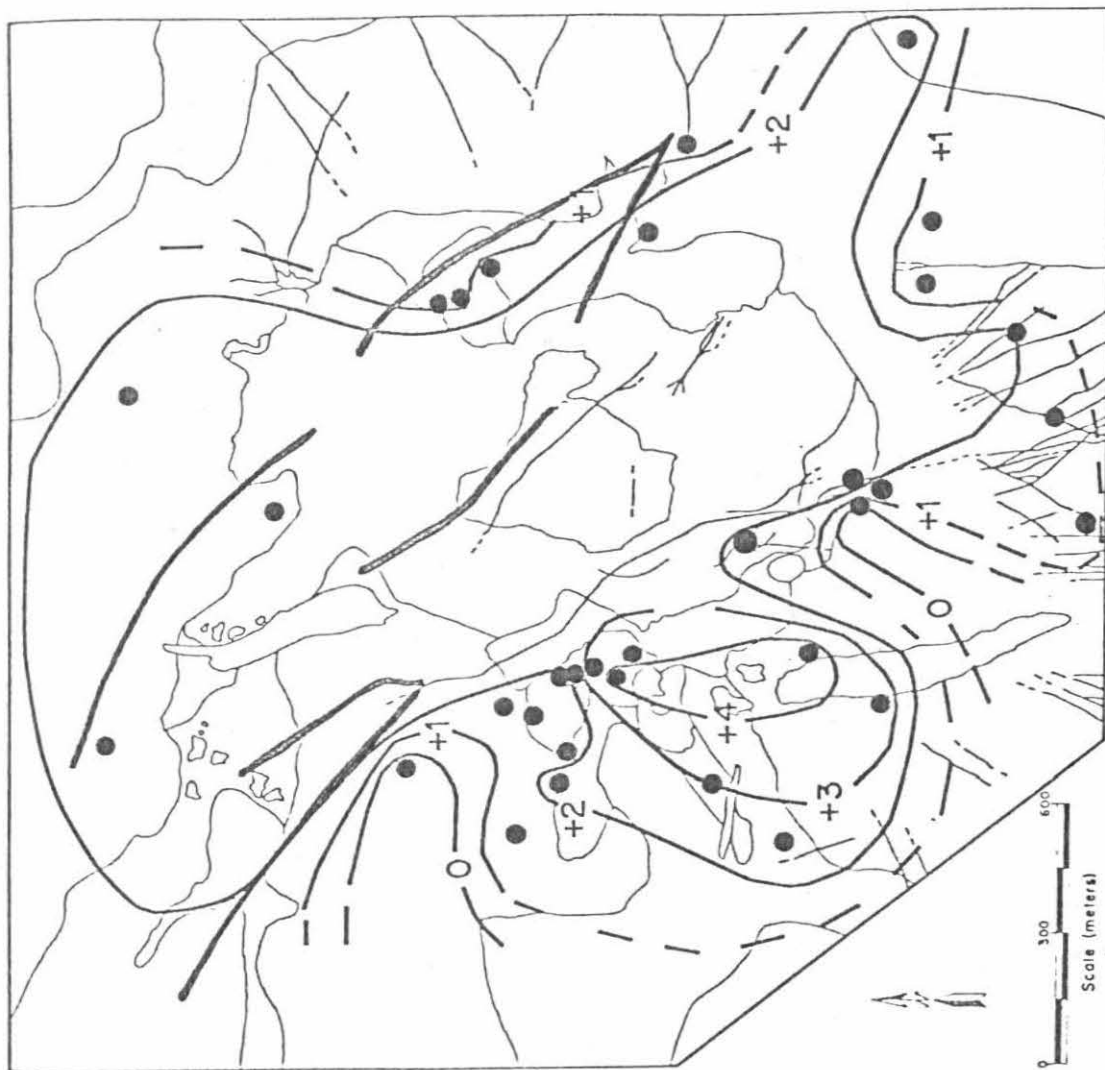
One other way to account for some of the ^{18}O -depletions in the volcanic rocks is through the interaction of meteoric waters and magmas to produce low- ^{18}O silicate melts. It is thus possible that some of the primary ash-flow tuff magmas had $\delta^{18}\text{O}$ values as low as +4 when they erupted. This possi-

bility has been suggested by Friedman et al. (1974) as an explanation for low- ^{18}O ash-flow tuffs in Nevada, Colorado and Wyoming.

6.2 Isotopic relationships in the volcanic country rocks

Thirty-three whole rock $\delta^{18}\text{O}$ analyses of volcanic and dike rocks immediately surrounding the Stony Mountain stock are plotted in Figure 6-5 and contoured (see also Figure 6-3). The main features shown by the isotopic data are the following: (1) the San Juan Tuff displays the lowest $\delta^{18}\text{O}$, with values ranging from +4.3 to -1.1 and averaging +1.6 (23 samples, with a standard deviation of 1.4); (2) there is a general increase in ^{18}O content of the volcanic rocks as we go upward in the sequence. The three $\delta^{18}\text{O}$ values of the Picayune Formation average +1.9, while six samples of the uppermost volcanic unit, the Gilpin Peak Tuff, average +3.1; and (3) the dike rocks have $\delta^{18}\text{O}$ values similar to those of the rocks they intrude.

There are several explanations possible for the isotopic pattern displayed in Figure 6-5. In our model for the interaction of heated meteoric ground waters with igneous rocks, we note that convective circulation of the ground waters is such that the heated, and thus less dense, waters move upward in the vicinity of the intrusion (heat source). Unless there is vastly more oxygen in the supply of water than the amount



TERTIARY

- Mineralized breccia pipe
- Rhyolite
- Inner diorite
- Quartz monzonite
- Gabbro
- Hornblende monzonite
- Outer diorite
- Gilpin Peak Tuff
- Picoyune Formation
- San Juan Tuff

PRECAMBRIAN

- Quartzite
- Dyke
- Major vein or mineralized fracture

Figure 6-5. Whole rock $\delta^{18}O$ contours of volcanic and dike rocks in the vicinity of the Stony Mountain stock. Black dots are sample localities.

of oxygen in the rock through which the water passes, the water must increase its $\delta^{18}\text{O}$ value due to high temperature isotopic exchange with the igneous country rocks. Thus, by the time it has passed through the lower volcanic units and reached the volcanics at higher elevations, the water will no longer show the same degree of "isotopic contrast" relative to 'normal' igneous $\delta^{18}\text{O}$ values that it had when it first entered the hydrothermal convective system. The correlation between $\delta^{18}\text{O}$ and elevation thus may be due to the water having undergone appreciable isotopic exchange by the time it reached the higher elevations; other factors being equal, if it had a higher $\delta^{18}\text{O}$ value it would not have as great an isotopic effect on the country rocks with which it exchanges.

Other important possibilities are that there was a general increase in temperature with depth, or that more water may have passed through the older volcanics (San Juan Tuff) than the younger volcanic rocks. The latter might come about if the San Juan Tuff was the main aquifer in the vicinity of the Stony Mountain Stock. Either higher temperatures or a larger water/rock ratio for the San Juan Tuff would give rise to more depleted $\delta^{18}\text{O}$ values, other things being equal.

The San Juan Tuff is also slightly finer grained than the other volcanic units (see Figure 6-10). Obviously, isotopic exchange would be facilitated by finer grained materials,

other things being equal. The smaller the grain size, the larger is the surface area that the minerals present to the exchanging fluid phase. Further, the finer the grain size of the minerals, the more numerous are the channelways (grain boundary contacts) for the aqueous fluid. This would also facilitate isotopic exchange.

The fact that the dike rocks are similar in $\delta^{18}\text{O}$ to the volcanic rocks of comparable grain size suggests that the dikes were intruded either at an early stage or possibly while the igneous rocks in the area were still hot, and the meteoric-hydrothermal convection systems were still working. If the entire area had cooled down before the dikes were emplaced, the dikes themselves would not represent sufficiently large "heat engines" to cause such extensive high-temperature exchange with the meteoric waters. This is in accord with the geologic evidence that most of the dikes are associated in time with the outer diorite period of ring intrusion (Dings, 1941). It must be pointed out however, that dikes emplaced into plutonic environments tend to approach the $\delta^{18}\text{O}$ values of the rocks they intrude (Shieh and Taylor, 1969a; Turi and Taylor, 1971), so some of the exchange conceivably could have been with the liquid dike magmas after the country rocks became heated.

All of the volcanic rocks in the vicinity of the Stony Mountain stock have been lowered in ^{18}O by at least 4 per mil,

and some must have been depleted by at least 8 or 9 per mil. This is because 'normal' volcanic rocks with such chemical compositions have restricted and well-defined ranges of $\delta^{18}\text{O}$ values (Taylor, 1968), typically +6 to +9 (Figure 1-1). The question arises then as to how much of this ^{18}O depletion is due to the presence of the plutonic igneous centers, and how much of it is due to ^{18}O exchange before the plugs and stocks were intruded. On a regional scale, these questions are not entirely inseparable, inasmuch as essentially simultaneous intrusive and extrusive igneous activity occurred throughout the evolution of the Western San Juan volcanic field, and both types of igneous activity presumably set up hydrothermal-convective systems. On a smaller scale however, it may be possible to separate these two events. Thus the volcanic rocks in the immediate vicinity of the Stony Mountain stock are characterized by an average $\delta^{18}\text{O} < +2$. Before emplacement of the many stocks along the caldera ring fracture and before intrusion of other stocks such as the Stony Mountain complex, this volcanic terrain probably had $\delta^{18}\text{O}$ values greater than +4. The regional ^{18}O depletion may have occurred prior to this intrusive episode or it may represent a regional ^{18}O lowering due to the effects of overlapping alteration systems produced by the many intrusions in this district. In any case, a 2 to 3 per mil depletion in ^{18}O was apparently produced in the volcanic country rocks immediately surrounding the Stony

Mountain complex, presumably attributable to the meteoric-hydrothermal system established by this single ring-dike complex.

Although it is also conceivable that the "early" regional ^{18}O depletion is due in part to original eruptions of low- ^{18}O melts ($\delta^{18}\text{O} \approx +4$), this cannot represent a general explanation for all the Western San Juan volcanic rocks because there are several samples with normal or near-normal $\delta^{18}\text{O}$ values (e.g. SJ-17). Post-crystallization hydrothermal alteration is the most plausible explanation of the $\delta^{18}\text{O}$ data, in the light of the results obtained on sample SM-171. This sample has the most positive whole-rock $\delta^{18}\text{O}$ value (+3.1) of all the San Juan Tuff samples analyzed in the vicinity of the Stony Mountain stock. It has a $\delta^{18}\text{O}_Q = +7.1$ and thus the quartz presumably had a $\delta^{18}\text{O}$ at least as high as +7.1 before the Stony Mountain complex was emplaced. In an original equilibrium mineral assemblage such quartz would be expected to coexist with a whole-rock $\delta^{18}\text{O} \approx +6.2$ or higher (Taylor, 1968), so that the magmatic or whole-rock $\delta^{18}\text{O}$ of SM-171 must have originally been at least as high as +6.2. The original value probably was higher than +6.2 inasmuch as the quartz also may have been lowered in ^{18}O because of its exceedingly fine grain size (0.02 mm). Aphanitic volcanic rocks of this type typically have a $\delta^{18}\text{O}$ of +6

to +9, so essentially all of the ^{18}O lowering of this rock probably occurred subsequent to its crystallization. The San Juan Tuff magma may not have been isotopically homogeneous, but if it was, all the $\delta^{18}\text{O}$ effects in the vicinity of Stony Mountain, as well as most of the regional $\delta^{18}\text{O}$ effects, must be due to subsolidus exchange.

6.3 Hydrogen isotope systematics

The hydrogen isotope data (Table 6-2) clearly confirm that meteoric-hydrothermal waters exchanged appreciably with essentially all the rocks in the Stony Mountain area.

In natural mineral assemblages and in laboratory equilibration experiments, sericite is found to concentrate deuterium relative to biotite and amphibole while chlorite generally has an intermediate δD value (Taylor and Epstein, 1966; Suzuki and Epstein, 1974). This general order of enrichment in δD is also displayed by the hydrous phases in the Stony Mountain region except that each phase is drastically depleted in deuterium with respect to 'normal' igneous and metamorphic rocks (on the order of 60 per mil, Figure 6-6). The white mica analyses, including samples from the volcanic rocks as well as the intrusive complex, are extremely uniform: $\delta\text{D} = -117, -118$ and -120 . The volcanic rocks, with chlorite as the dominant hydrous phase, are also very uniform at $-140, -146$ and -147 . The chlorite sample with the highest δD also

Table 6-2

HYDROGEN ISOTOPE ANALYSES FROM THE STONY MOUNTAIN STOCK AND VICINITY, AND THE WESTERN SAN JUAN MOUNTAINS, COLORADO.

Unit	Sample Number ¹	Mineral	$\delta D(\text{‰})^2$	Description ³
Quartz Monzonite	SM-109	Whole Rock	-133	Biotite (85%), sericite and epidote (10%); trace of chlorite.
	SM-64	Biotite	-139 ± 1 (2)	
	SM-84	Whole Rock	-132	Biotite (65%), amphibole (15%), chlorite (15%), and sericite (5%).
Gabbro	SM-113	Biotite Whole Rock	-129 -132	Biotite (90%), chlorite (5%), and amphibole (5%).
	SM-146	Biotite	-146 ± 2 (2)	
	SM-159	Biotite	-119 ± 0 (2)	
	Col-17-8	Biotite	-150	
Outer Diorite	SM-58	Whole Rock	-117	White mica (85%), chlorite (10%) and biotite (5%).
	SM-89	Amphibole	-138	

Table 6-2 (Cont'd)

Unit	Sample Number	Mineral	$\delta D(\text{‰})$	Description
Horn- blende Monzon- ite	SM-49	Whole Rock	-120	White mica (85%) and chlorite (15%).
	SM-162	Whole Rock	-118	White mica (98%) and chlorite (2%).
Gillpin Peak Tuff	SM-169	Whole Rock	-147	Chlorite (75%), amphibole (15%), and sericite (10%).
	SM-187b	Whole Rock	-140	Chlorite (65%) and sericite (35%).
San Juan Tuff	SM-216	Whole Rock	-146	Chlorite (85%), sericite (10%), and epidote (5%).
	<u>Western San Juan Mountains</u>			
	Col-2-8	Chlorite and biotite	-116	Chloritized quartz diorite porphyry.
	Col-13-8	Biotite	-148	Augite-biotite quartz monzonite.
	Col-14-8	Chlorite	-142	Porphyritic quartz monzonite.

Table 6-2 (Cont'd)

Sample Number	Mineral	δD (‰)	Description
Col-16-8	Chlorite	-137	Chloritized granodiorite porphyry.
Col-18-8	Chlorite	-145	Propylitized diorite porphyry.

1. All samples with prefix Col are from Taylor (1974a).
2. δD values are relative to SMOW; the number in parentheses indicates the number of separate determinations; error is the average deviation from the mean.
3. More detailed descriptions are given in Table 6-1. Hydrous mineral % are estimated contributions to the δD value.

has some white mica present; this may account for its heavier δD value inasmuch as white mica is known to concentrate deuterium with respect to chlorite. The only amphibole analyzed for D/H has a δ -value of -138.

In contrast to the other hydrous minerals, the biotites cover a large range of δD values, from -119 to -150. It is interesting that the -119 value comes from an unusually coarse grained gabbro (SM-159) with one of the highest $\delta^{18}O_R$ values found at Stony Mtn. and also with the most 'normal' plagioclase-pyroxene ^{18}O fractionation. This biotite may therefore have undergone only partial hydrogen isotope exchange. Also, this sample comes from the top of Stony Mtn.; thus it may have come into contact with cooler meteoric-hydrothermal solutions, which would favor less complete exchange. However, it is probably not possible to account for the entire 31 per mil δD variation of the biotites solely on the basis of partial exchange or mixing between magmatic H_2O and meteoric H_2O . All these rocks to some extent have been depleted in ^{18}O , which demands appreciable quantities of heated meteoric waters (see Section 6-11). Inasmuch as water has several tens of times more atom per cent hydrogen than the rocks, the initial (magmatic) hydrogen isotope values would in almost all cases be completely wiped out. Except for sample SM-159, the present variation of δD in the biotites must therefore reflect variables other than significant mixing of waters of magmatic and meteoric origin.

If the isotopic composition of the meteoric water was constant, then part of the 31 per mil variation in the biotites may be explained by variations in temperature. Using the relationship between hydrogen isotopic fractionation factors and temperature as given by Suzuoki and Epstein (1970), to explain the entire effect would require a temperature variation of about 400°C. It is unlikely that these few random samples of the gabbro would have undergone such drastic differences in cooling history or subsolidus deuteric effects. Also, this would imply an upward increase in temperature in the volcanic section, because of the relation between elevation and δD shown in Figures 6-7b and 6-8. A more plausible explanation lies in the fact that hydrogen isotope fractionations depend not only on temperature but on the type of cation to which the OH is bonded (Suzuoki and Epstein, 1974). Thus, at a given temperature, annite would be expected to have a different value of δD than phlogopite equilibrated with the same water. The relationship determined by Suzuoki and Epstein (1974) is:

$$10^3 \ln \alpha_{\text{Mineral-H}_2\text{O}} = -22.4 \left(\frac{10^6}{T^2} \right) + 28.2 + 2X_{\text{Al}} - 4X_{\text{Mg}} - 68X_{\text{Fe}}$$

where X represents the mole fractions of various cations in the biotite. Thus at equilibrium, for a given temperature and $\delta D_{\text{H}_2\text{O}}$, a biotite with a higher ratio of Fe/Mg would contain

- Figure 6-6. Plot of δD vs $\delta^{18}O$ for sericites, biotites, amphiboles, and chlorites from the Stony Mountain region, Colorado. The field of 'normal' biotites and hornblendes is also shown, along with the meteoric water line (Craig, 1961) and the kaolinite line (Savin and Epstein, 1970a).
- Figure 6-7a. Plot of δD vs $Fe/(Fe + Mg)$ for four biotites from the Stony Mountain gabbro. The size of the box indicates the analytical precision. The sample with highest δD value (SM-159) may be only partially exchanged (see text).
- Figure 6-7b. Plot of δD vs elevation for biotites from the Stony Mountain gabbro. Height of bar indicates error on the δD analysis.

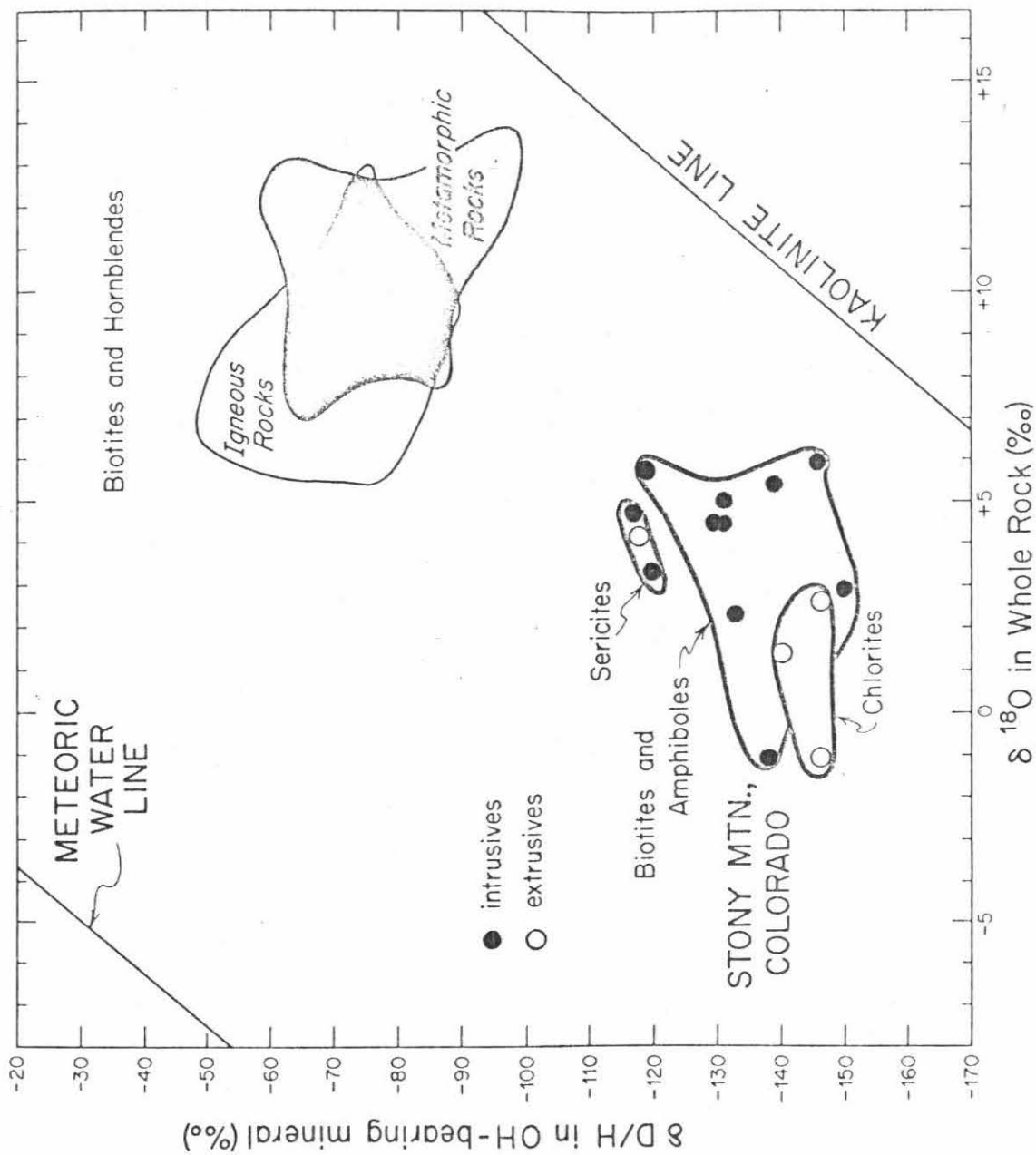


Figure 6-6

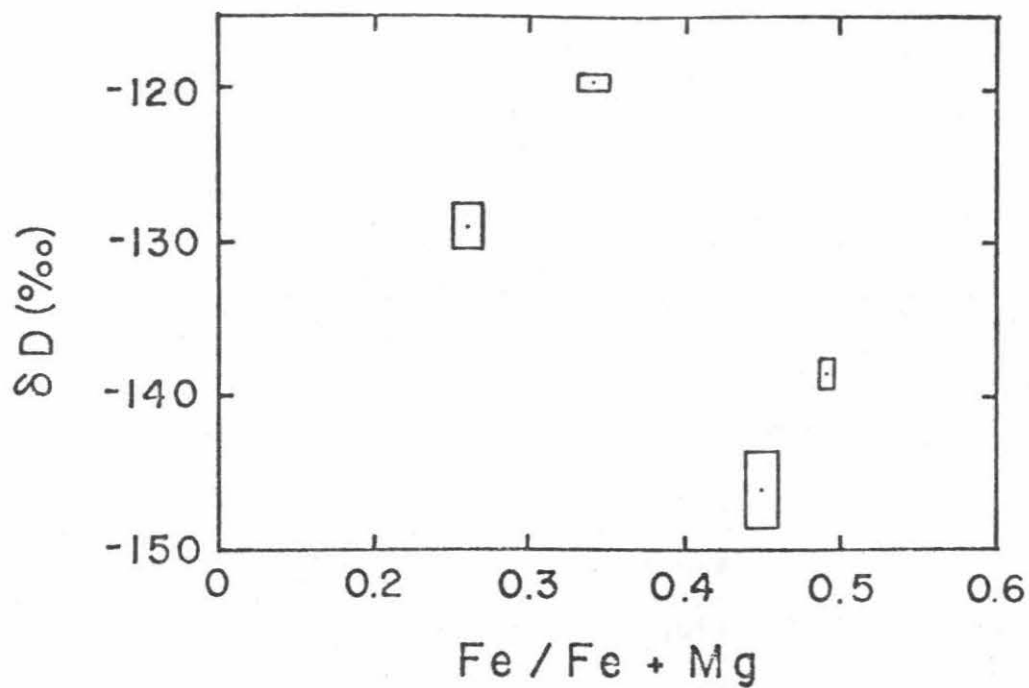


Figure 6-7a

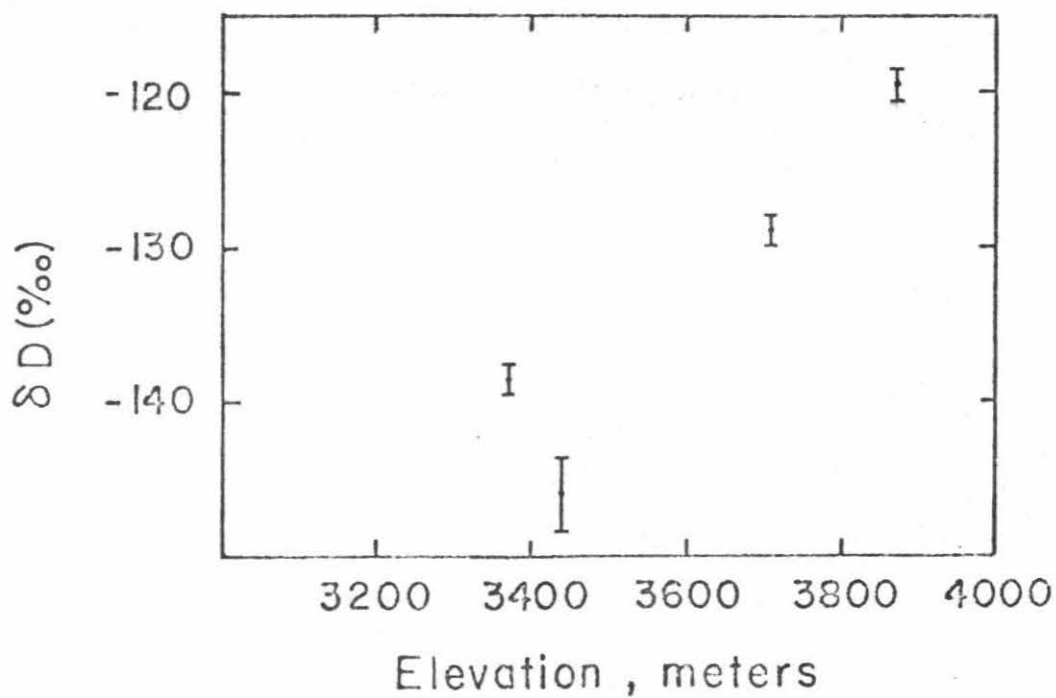


Figure 6-7b

less deuterium than one that had a lower ratio of Fe/Mg. In Figure 6-7a we plot δD vs $Fe/(Fe + Mg)$ for four pure biotite separates from the Stony Mountain gabbro. The $Fe/(Fe + Mg)$ ratios (Table 6-3) were determined on the Caltech MAC Model 5-SA3 probe which is completely automated and interfaced with a PDP-8/L computer. The accelerating voltage was 15Kv and a large spot ($\sim 15\mu$) was used. Although the correlation is not perfect, the two biotites with the highest $Fe/(Fe + Mg)$ ratios have the lowest concentration of deuterium. Excluding SM-159 for the reasons given above, and assuming that the other three biotite samples last equilibrated with waters at about $500^{\circ}C$, we can use the equation given above to calculate δD values of the waters coexisting with these three biotites. The values range from -100 to -110 (Table 6-3). Applying the same calculation to SM-159, we obtain $\delta D_{H_2O} = -90$; this is probably a little too heavy, again perhaps suggesting that this sample was only partially equilibrated with the meteoric waters. Thus, simply by assuming a constant δD value of about -100 to -110 for the meteoric waters and an equilibration temperature of approximately $500^{\circ}C$, most of the δD variations of the Stony Mountain biotites can be adequately explained. Applying the meteoric water equation of Craig (1961) this gives an initial $\delta^{18}O_{H_2O} \approx -14$ to -15 .

Table 6-3

Fe/(Fe + Mg) values for Stony Mountain biotites

	δD (per mil)	Fe/Fe + Mg \pm mean deviation	Elevation (meters)	Calc. δD_{H_2O} @ 500°C
SM-64	$-139 \pm 1(2)$	$0.49 \pm 0.00(6)^*$	3371	-100
SM-113	-129	$0.26 \pm 0.01(9)$	3706	-103
SM-146	$-146 \pm 2(2)$	$0.45 \pm 0.01(10)$	3438	-110
SM-159	$-119 \pm 0(2)$	$0.34 \pm 0.01(8)$	3870	-90

* Number of separate points analyzed.

Applying the same equation to the white mica analyses, but assuming a lower equilibration temperature of about 350°C and $X_{Al} \approx 1$, the calculated δD_{H_2O} values are also about -100, in agreement with the value calculated using the biotite data. It seems reasonable to assume a lower equilibration temperature for the sericites than for the biotites because the former came from more highly altered rocks and are much finer-grained. Thus, they probably formed at lower temperatures and/or they would have probably continued to exchange D/H down to lower temperatures.

The fact that hydrogen isotope fractionation depends on, among other things, the type of cation to which the OH is bonded, may account for the chlorite samples having less deuterium than expected on the basis of the D/H data on high-Al chlorites from pelitic schists obtained by Taylor and Epstein (1966). Similar systematics in hydrogen isotope ratios have also been found at Skaergaard, East Greenland (Taylor and Forester, 1974). The chlorites from regionally metamorphosed pelitic schists, in general, have both lower Fe/Mg ratios and higher Al contents than chlorites occurring as amygdale fillings or associated with alteration of igneous rocks (Albee, 1962). Both of these chemical effects would favor lower δD values in the chlorites from igneous rocks than in the chlorites from metasedimentary rocks.

The correlation between δD of the biotites and the elevation at which these samples are found (Figure 6-7b) also seems to hold when the hydrogen isotope data for all of the samples are plotted against their respective elevations (Figure 6-8). The reason for this relationship is not known, but it is probably in part a result of the fact that the white mica samples come from a rather restricted range of elevations. Figures 6-7a and 6-7b imply an anticorrelation between the elevation of the biotite sample and its Fe/(Fe + Mg) ratio, and the latter conceivably could be controlling the δD values as explained above. However, there is no obvious reason why the Fe/(Fe + Mg) ratio should increase with depth and this may reflect lack of sampling.

6.4 Oxygen isotopic variations within the Stony Mtn. complex

Forty-six whole rock $\delta^{18}O$ values of the intrusive ring complex of Stony Mtn. are plotted and contoured in Figure 6-9. The outer diorite and hornblende monzonite range from +5.9 to -1.1, and average +3.7 (16 samples) with a standard deviation of 1.8. The gabbros and quartz monzonites range from +5.9 to +1.4 and average +4.0 (20 samples; standard deviation = 1.3). Nine samples of the inner diorite range only from +3.3 to +1.3 and have an average $\delta^{18}O_R = +2.2$, with a standard deviation of 0.7. As shown by the $\delta^{18}O$ contour lines, the data are extremely

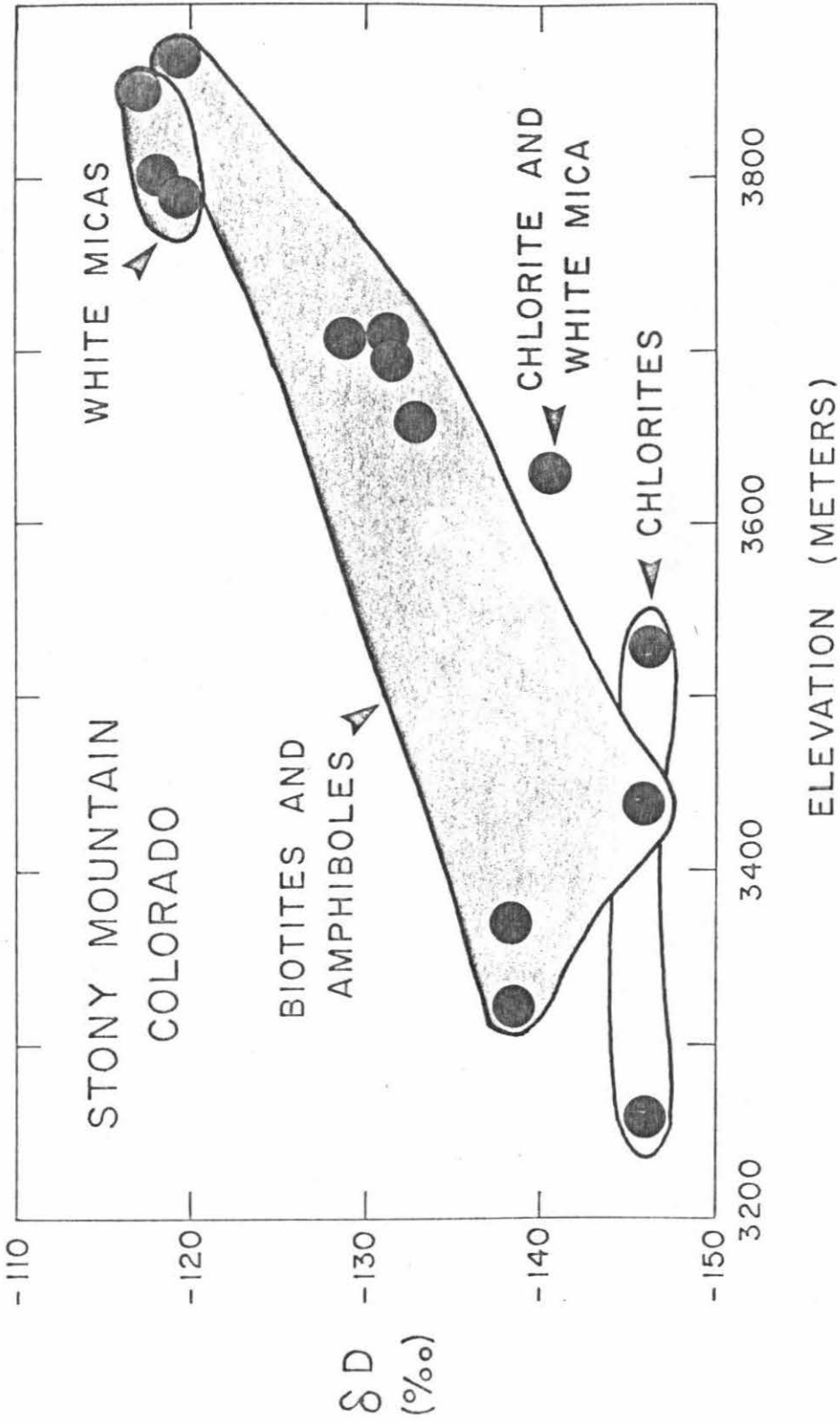


Figure 6-8. Plot of δD vs elevation for OH-bearing minerals from the Stony Mountain region, Colorado.



- | | |
|--------------------------------------|--------------------------|
| TERTIARY | |
| <input type="checkbox"/> | Mineralized breccia pipe |
| <input type="checkbox"/> | Rhyolite |
| <input type="checkbox"/> | Inner diorite |
| <input type="checkbox"/> | Quartz monzonite |
| <input type="checkbox"/> | Gabbro |
| <input type="checkbox"/> | Hornblende monzonite |
| <input type="checkbox"/> | Outer diorite |
| <input type="checkbox"/> | Galpin Peak Tuff |
| <input type="checkbox"/> | Picayune Formation |
| <input type="checkbox"/> | San Juan Tuff |
| PRECAMBRIAN | |
| <input type="checkbox"/> | Quartzite |
| — Dyke | |
| — Major vein or mineralized fracture | |

Figure 6-9. Whole rock $\delta^{18}O$ contours of the Stony Mtn. intrusive complex. All samples within the central (hatched) contour have $\delta^{18}O < +2$.

systematic; the lowest $\delta^{18}\text{O}$ values occur either at the margin of the complex, conforming roughly with outcrops of the outer diorite, or else they are confined to the central core of the stock. Note also that those samples with $\delta^{18}\text{O} > +5$, that lie between the two +5 contour lines, define an annular region in the middle of the intrusive complex that conforms fairly well to the position of the gabbro ring dike (see also Figure 6-3).

6.5 Effect of grain size

It appears that, to a first approximation, the oxygen isotope systematics in the Stony Mtn. complex can be explained principally on the basis of the grain size of the various igneous units, as might be expected if the exchange took place at subsolidus temperatures. Figure 6-10 is a plot of the average ^{18}O depletion in the various rock types at Stony Mtn. vs the average grain size of these rock types. The average ^{18}O depletion is estimated by subtracting the measured $\delta^{18}\text{O}$ of each rock type from the probable initial $\delta^{18}\text{O}$ value. The latter are estimated from typical values measured in 'normal' igneous rock types in other areas (Taylor, 1968) as follows: The San Juan Tuff, Picayune Formation, Gilpin Peak Tuff, quartz monzonite, rhyolite and breccia pipe are assumed to have had $\delta^{18}\text{O} = +8.5$; outer and inner diorites, dikes and hornblende monzonite, $\delta^{18}\text{O} = +7.5$; and gabbro $\delta^{18}\text{O} = +6.5$.

These are somewhat arbitrary choices, but they are based on the following considerations.

Assuming that the original magma was isotopically homogeneous, the outer diorite magma must have had a $\delta^{18}\text{O} > +6.1$ when intruded, since this is the value of a pyroxene phenocryst in SM-200. The groundmass in this rock has a $\delta^{18}\text{O} = +5.8$ but in 'normal' igneous rocks a pyroxene is invariably lighter than the whole-rock value, not heavier as in the disequilibrium case here. Therefore, the $\delta^{18}\text{O}$ of the outer diorite magma was probably originally about +7.0 to +8.0 and could not have been lower than +6.5. Similarly, the gabbro clearly must have originally had $\delta^{18}\text{O} > +6.0$ because the plagioclase of SM-159 has $\delta^{18}\text{O} = +6.5$ and plagioclase is known to be extremely susceptible to hydrothermal ^{18}O exchange (see below). This high an original $\delta^{18}\text{O}$ for the gabbro is also confirmed by a granodioritic phase of the gabbro (SM-113) which has a quartz $\delta^{18}\text{O} = +8.3$. Quartz monzonite sample SM-112 has a quartz $\delta^{18}\text{O} = +8.3$, so the initial whole-rock $\delta^{18}\text{O}$ value of the quartz monzonite must have been at least as high as +7.5. The rhyolite has quartz phenocrysts with $\delta^{18}\text{O} = +7.8$, compatible with the original magma having a $\delta^{18}\text{O} \approx +7.0$ or higher. However, inasmuch as the quartz $\delta^{18}\text{O}$ may have been lowered slightly, and because many aphanitic

rhyolites elsewhere in the world have $\delta^{18}\text{O} \approx +8.5$, the latter value is assumed here. The breccia pipe has a $\delta^{18}\text{O}_0 = +9.4$, so again an initial whole-rock value of +8.5 has been adopted. The inner diorite has a very narrow range of $\delta^{18}\text{O}$ values, but for the purpose of Figure 6-10, we have assumed it had the same initial $\delta^{18}\text{O}$ value as the outer diorite. It will later be argued, however, that this was a rather exceptional intrusion emplaced as an 'abnormal' low- ^{18}O magma.

The correlation observed in Figure 6-10 is suspect since only average values have been used for a given rock unit. In Figure 6-11 are plotted representative individual samples from some of the units and it is now clear that, within most of the units, $\delta^{18}\text{O}$ depletions as well as grain sizes cover a large spectrum of values and the correlation is no longer so evident. Except for the inner diorite, the finer-grained rocks show a restricted range of grain sizes but a large range in $\delta^{18}\text{O}$ depletion values, whereas the coarser-grained rocks, notably the gabbros, exhibit a spectrum of grain sizes but are not as variable in $\delta^{18}\text{O}$ depletion as the finer-grained rocks.

The gabbro unit, because it exhibits a wide range in grain size, affords a useful test of the importance of this variable in the exchange process as well as testing whether or not exchange largely occurred at subsolidus temperatures. In Figure 6-12, eight representative samples of analyzed

- Figure 6-10. Plot of average $\delta^{18}\text{O}$ depletion vs average grain size for the various rock units in the Stony Mtn. region (see text).
- Figure 6-11. Plot of estimated $\delta^{18}\text{O}$ depletion vs average grain size for representative samples of rock units in the Stony Mtn. region. Note the restricted range shown by the inner diorite samples.
- Figure 6-12. $\delta^{18}\text{O}_F$ vs average grain size for the Stony Mtn. gabbro. Circles are analyzed plagioclases; squares are calculated from analyzed whole-rock samples by adding 0.4 per mil to $\delta^{18}\text{O}_R$ (see text).

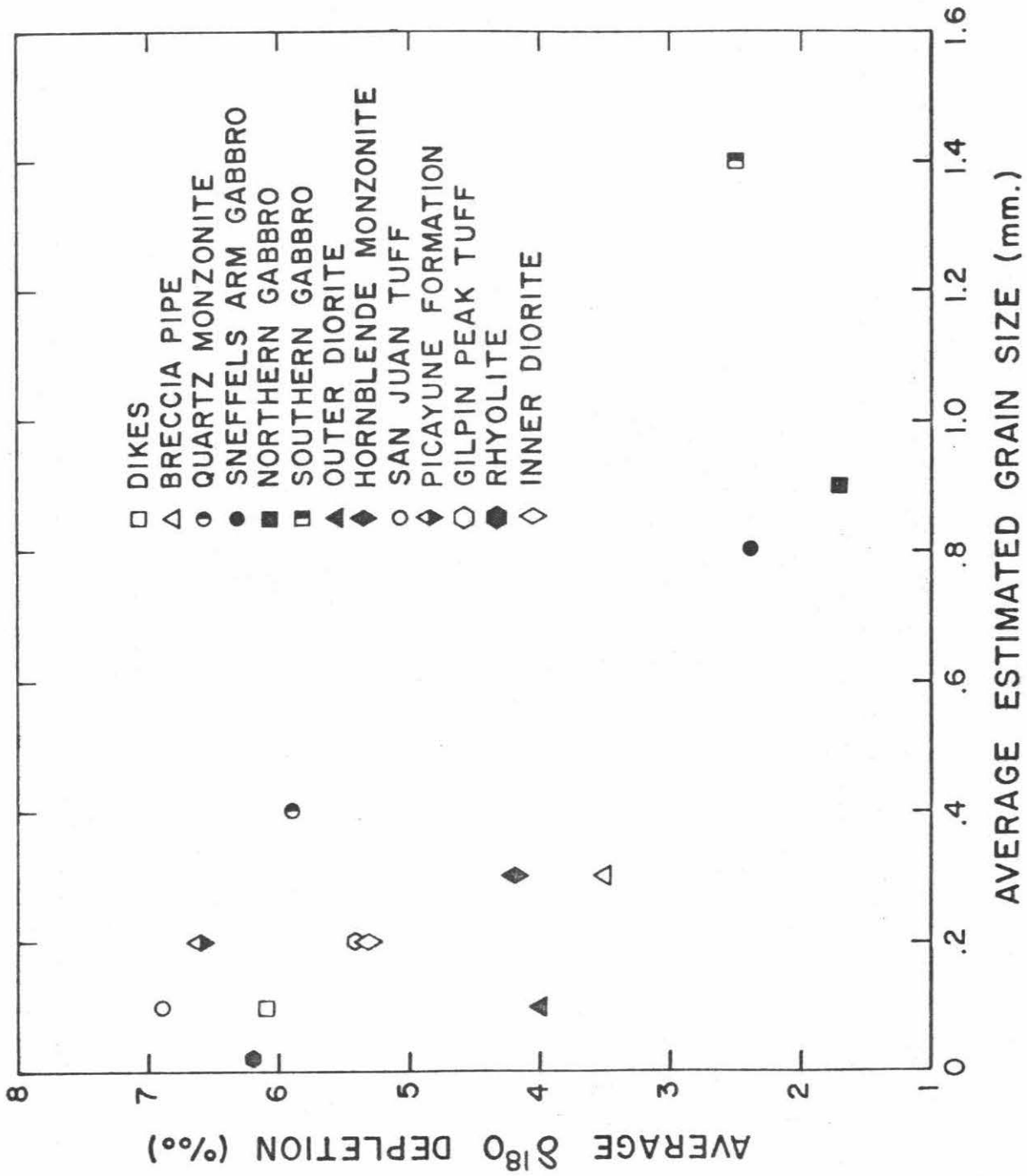


Figure 6-10

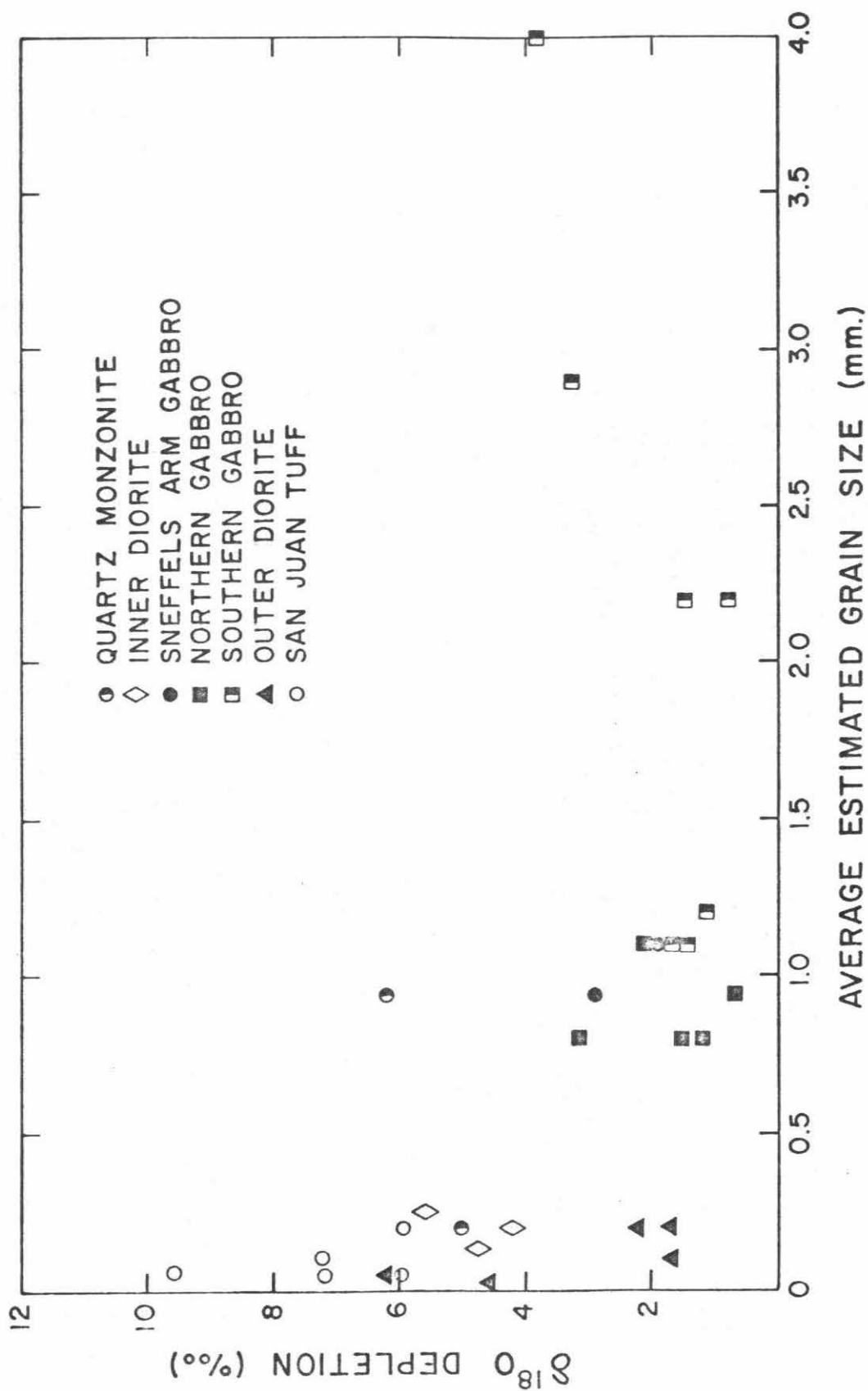


Figure 6-11

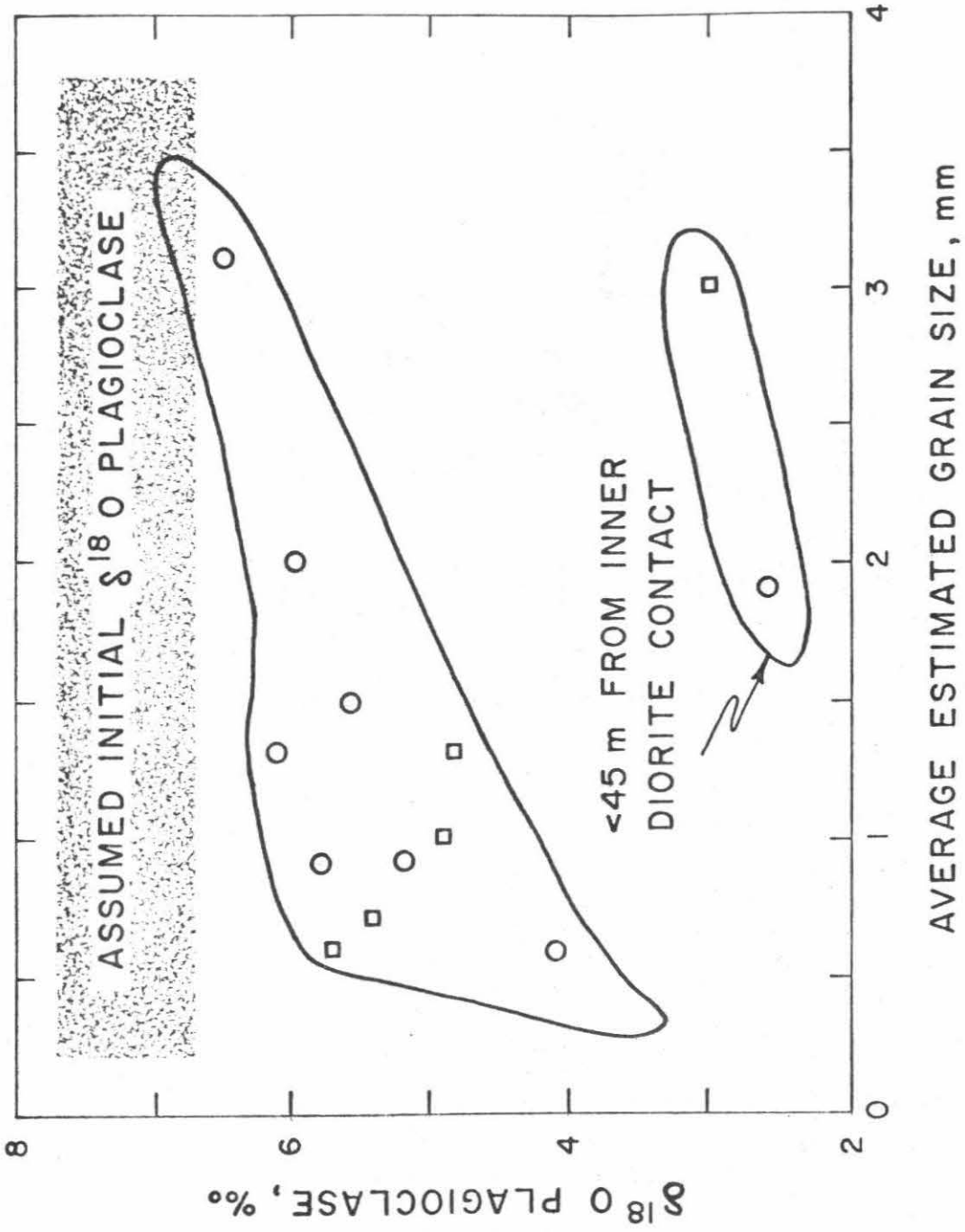


Figure 6-12

plagioclases, along with five estimated values based on analyses of whole-rock samples, are plotted against average grain size. For plotting purposes, it is assumed that the plagioclase is 0.4 per mil heavier than the whole rock $\delta^{18}\text{O}$ value, this being the average difference in eight gabbro samples where both the plagioclase and the whole rock values were measured. There is a correlation between $\delta^{18}\text{O}_F$ and grain size (except for two samples discussed below) which indicates that almost all of the ^{18}O lowering can be accounted for by exchange in the solid state and that, other things being equal, the larger the grain size the better preserved are the initial $\delta^{18}\text{O}$ values. The two samples that clearly fall off this trend, SM-90 and SM-91a, are respectively 45 and 0 meters from the contact with the intrusion of diorite. Thus these two samples, along with SM-98a, emphasize that the central portions of the gabbro have been significantly affected by the nearby later intrusion of the low- ^{18}O inner diorite. Thus they have experienced an oxygen isotope exchange event that did not affect, to any great extent, the other samples. It is also interesting to note that those samples close to the contact with the inner diorite provide $\delta^{18}\text{O}$ evidence of the relative ages of the two units because it is likely that the $\delta^{18}\text{O}$ values of the gabbros were lowered during or after the intrusion of the diorite.

Grain size is obviously an important variable in determining the final isotopic composition of a rock that is under-

going oxygen isotopic exchange at subsolidus temperatures. It is equally obvious, however, that grain size alone cannot account for the isotopic patterns shown in Figure 6-10 or 6-11.

6.6 Effect of fractures and hydrothermal veins

The size, abundance and location of fractures and hydrothermal veins will have two important effects on the exchange process: (1) they will, to a certain extent, control the circulation of the meteoric-hydrothermal solutions and (2) because most of the water will be moving along these fractures, rocks in close proximity to them will be affected to a greater degree than those at large distances, other things being equal.

The main structural features in the northwest San Juan Mountains are the persistent veins, fractures and dikes that generally trend $N45^{\circ}W$ and are related to the northwestern side of the Silverton caldera (Figure 5-2). Many of these fractures are filled with vein and dike material and represent economically significant ore bodies (Mayor and Fisher, 1972). The Stony Mountain stock has imposed a radial set of dikes upon this pattern (Dings, 1941) and, in addition, the intrusive rocks are crisscrossed by myriads of tiny fractures and veinlets. These would allow easy access for the heated ground waters and thus promote oxygen exchange with the minerals in the Stony Mountain complex. A sample situated right at the

wall of the fracture will be exposed to the highest water/rock ratio because of the large quantity of H_2O passing through that channelway, whereas rocks further away from the fracture would be subjected to smaller water/rock ratios.

A possible example of this effect is seen in SM-89 which was collected within 0.5 m of a major mineralized fracture (Circassian vein, Burbank, 1941). This outer diorite sample has by far the lowest $\delta^{18}O_R$ value found anywhere in that unit, namely -1.1, yet is equivalent in grain size and mineralogy to most other samples of the diorite. It is concluded that its close proximity to the major fracture allowed the rock to experience an ^{18}O depletion of about 9 per mil. Another possible example is the inner diorite sample SM-97 with $\delta^{18}O = +1.3$; it was collected within 10 m of a major vein system in the district (see Figure 6-2).

The vein minerals themselves were apparently deposited from meteoric-hydrothermal solutions. Evidence of this is seen in samples SM-74d, SM-116, SJ-1 and Col-3R. Cryptocrystalline vein quartz of SM-74d has $\delta^{18}O = -1.8$. If this was deposited at about $300^\circ C$, application of the oxygen isotope fractionation curve for the quartz-water system of Clayton *et al.* (1972b) indicates that water would have a $\delta^{18}O \approx -9$. The euhedral comb quartz crystals of SJ-1 have a $\delta^{18}O = -1.7$ and if crystallized in equilibrium with H_2O at $300^\circ C$ it also would have formed from a water with $\delta^{18}O \approx -9$.

Similarly, the euhedral quartz crystals from a vein just south of the Yankee Boy Vein (Burbank, 1941) have $\delta^{18}\text{O} = +5.1$ and at 300°C this would have formed in equilibrium with a water of $\delta^{18}\text{O} \approx -2$. Quartz from the Gold King mine (+2.2; Taylor, 1974a) must have been deposited from a fluid with $\delta^{18}\text{O} \approx -5$ to -10 , if the temperature of deposition was in the range $200^\circ - 400^\circ\text{C}$. Even more striking in this regard is a vein dickite ($\delta^{18}\text{O} = -6.2$, $\delta\text{D} = -141$; Sheppard *et al.*, 1969) from the Ouray area. Based on data from these various samples it seems clear that most of the minerals in the hydrothermal vein systems from the Silverton-Ouray area were deposited from fluids that were dominantly meteoric in origin. This is very reasonable for epithermal mineral deposits in volcanic regions, based on recent studies in western Nevada by Taylor (1973) and O'Neil and Silberman (1973).

6.7 Effect of mineralogy

From both laboratory experiments, and based on $^{18}\text{O}/^{16}\text{O}$ analyses of coexisting minerals, it is apparent that all minerals do not present the same susceptibility to oxygen isotopic exchange (O'Neil and Taylor, 1967; Clayton *et al.*, 1972b; Taylor, 1968). One of the clearest examples of this in the Stony Mountain area is shown by the coexisting quartz and alkali feldspar phenocrysts in the intrusive rhyolite. The phenocrysts of quartz and alkali feldspar are both about

1 to 2 mm in size, yet $\delta^{18}\text{O}_Q = +7.8$ whereas $\delta^{18}\text{O}_K = -1.6$. In 'normal' rhyolites the alkali feldspar is typically only about 0.8 to 1.0 per mil lower in ^{18}O than the coexisting quartz. Thus, in this Stony Mtn. sample the feldspar has been depleted in ^{18}O by at least 8.4 per mil.

In the Stony Mtn. mineral assemblages, quartz consistently has the heaviest $^{18}\text{O}/^{16}\text{O}$ ratio and is most normal in its oxygen isotopic composition; the $\delta^{18}\text{O}_Q$ values range from +11.8 to +6.3 (excluding vein quartz). The highest $\delta^{18}\text{O}$ values (+11.8, +11.3, +10.6) are from quartzite inclusions in the Sneffels Arm Gabbro and are within the $\delta^{18}\text{O}$ range for sandstones and quartzites found elsewhere (Garlick and Epstein, 1967; Anderson, 1967; Taylor and Epstein, 1962b; Clayton and Mayeda, 1963). It is abundantly clear that quartz is the most resistant of the common rock-forming minerals to oxygen isotope exchange. This has also been shown by Taylor (1968; 1971); Forester and Taylor (1972); Taylor and Forester (1971); Clayton et al. (1968a) and Garlick and Epstein (1966; 1967).

6.8 Oxygen isotopic relationships among minerals

The oxygen isotopic fractionations between coexisting minerals in the rocks of the Stony Mountain intrusive complex are, in general, indicative of non-equilibrium. All coexisting mineral data from the gabbros, quartz monzonites and an inner

diorite are plotted in Figure 6-13. The $\delta^{18}\text{O}$ values of various pairs of coexisting minerals from the Stony Mountain complex are also plotted in Figure 6-14abcd.

In Figure 6-13, the samples are arranged in order of decreasing $\delta^{18}\text{O}_F$. The column at the extreme left represents the hypothetical original Stony Mountain gabbro immediately after crystallization, with all minerals initially in oxygen isotopic equilibrium.

In the plagioclase-pyroxene plot (Figure 6-14a) the four mineral pairs are all from the gabbro unit. Typical plagioclase-pyroxene fractionations ($1000 \ln \alpha$) in quenched mafic igneous rocks are about 0.6 (Anderson *et al*, 1971; Garlick, 1966) whereas the corresponding fractionations in mineralogically equivalent intrusive rocks are approximately twice as large (about 1.1, Taylor, 1968; 1969), indicating subsolidus exchange has taken place during the slow cooling of these plutonic rocks. In Figure 6-14a this 0.6 to 1.1 per mil range of plagioclase-pyroxene fractionations are plotted as a tentative "equilibrium" band and compared to data from the literature. Thus, any points falling within the "equilibrium" band, depending on their δ -values, would represent (1) a 'normal' unaltered mineral assemblage of gabbro, (2) crystallization of a low- ^{18}O gabbro melt, or (3) a normal gabbro in which both the coexisting plagioclase and pyroxene have been lowered in ^{18}O by equal amounts at subsolidus temperatures.

Figure 6-13. $\delta^{18}\text{O}$ values for all coexisting minerals from the Stony Mountain gabbros, two quartz monzonite samples (SM-109; 112), a rhyolite (SM-103), and an inner diorite (SM-99b). The first column represents the $\delta^{18}\text{O}$ values of coexisting minerals from a hypothetical original gabbro. Except for the rhyolite and inner diorite, all samples are arbitrarily arranged in a sequence according to decreasing $\delta^{18}\text{O}_F$. Note that the feldspar of SM-103 is K-feldspar (Table 6-1).

Figure 6-14. $\delta^{18}\text{O}$ data for coexisting plagioclase-pyroxene (6-14a), plagioclase-biotite (6-14b), plagioclase-magnetite (6-14c), and quartz-feldspar (6-14d) from the Stony Mtn. complex, compared to other values from the literature. The 'equilibrium' bands shown in this series of diagrams are based largely on analyses of coexisting minerals from igneous rocks by Taylor (1968) and Anderson *et al.* (1971). Additional references are given in the appropriate diagrams. The stippled band in 6-14c represents the range of both plutonic and volcanic equilibrium values.

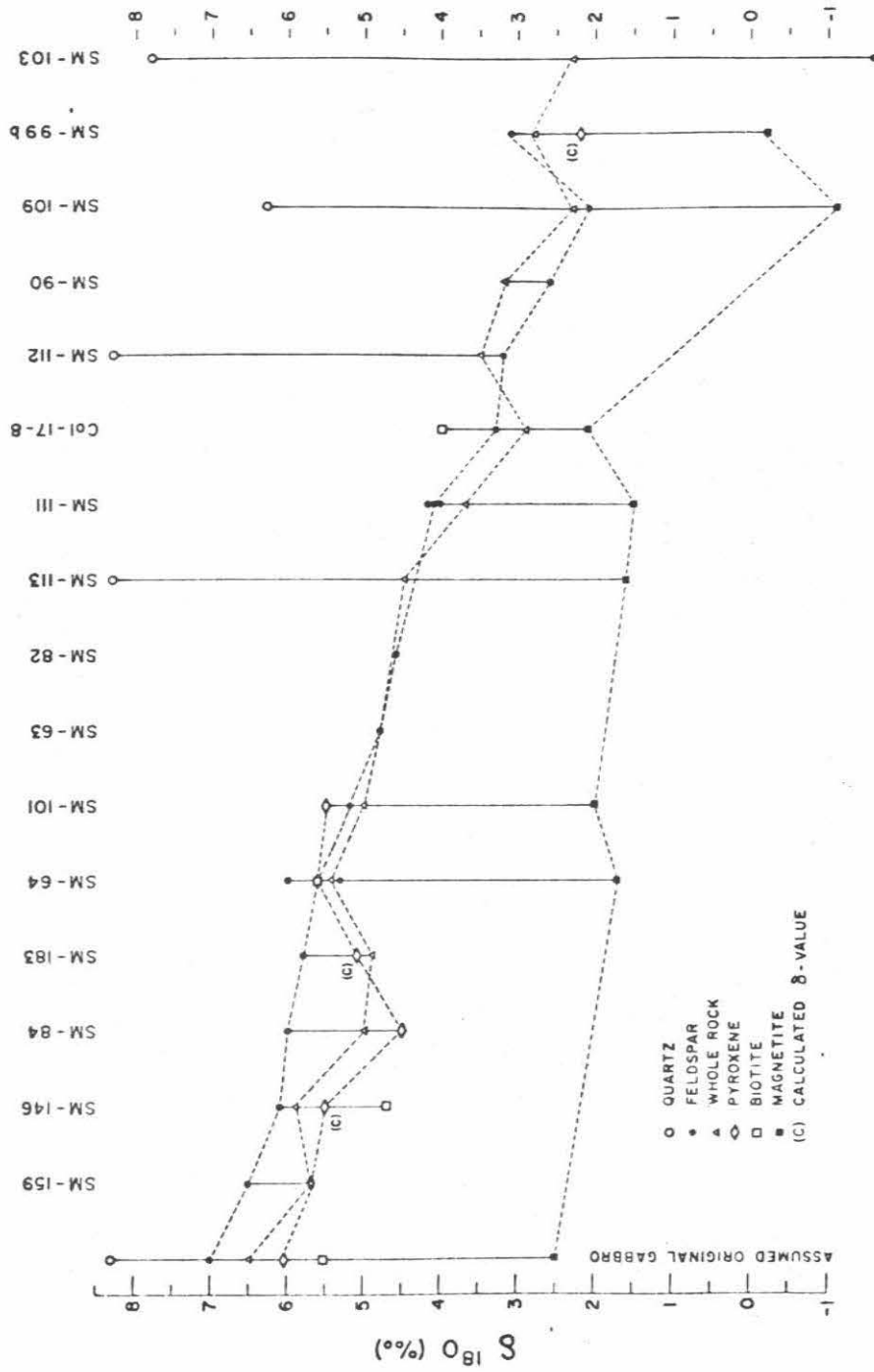


Figure 6-13

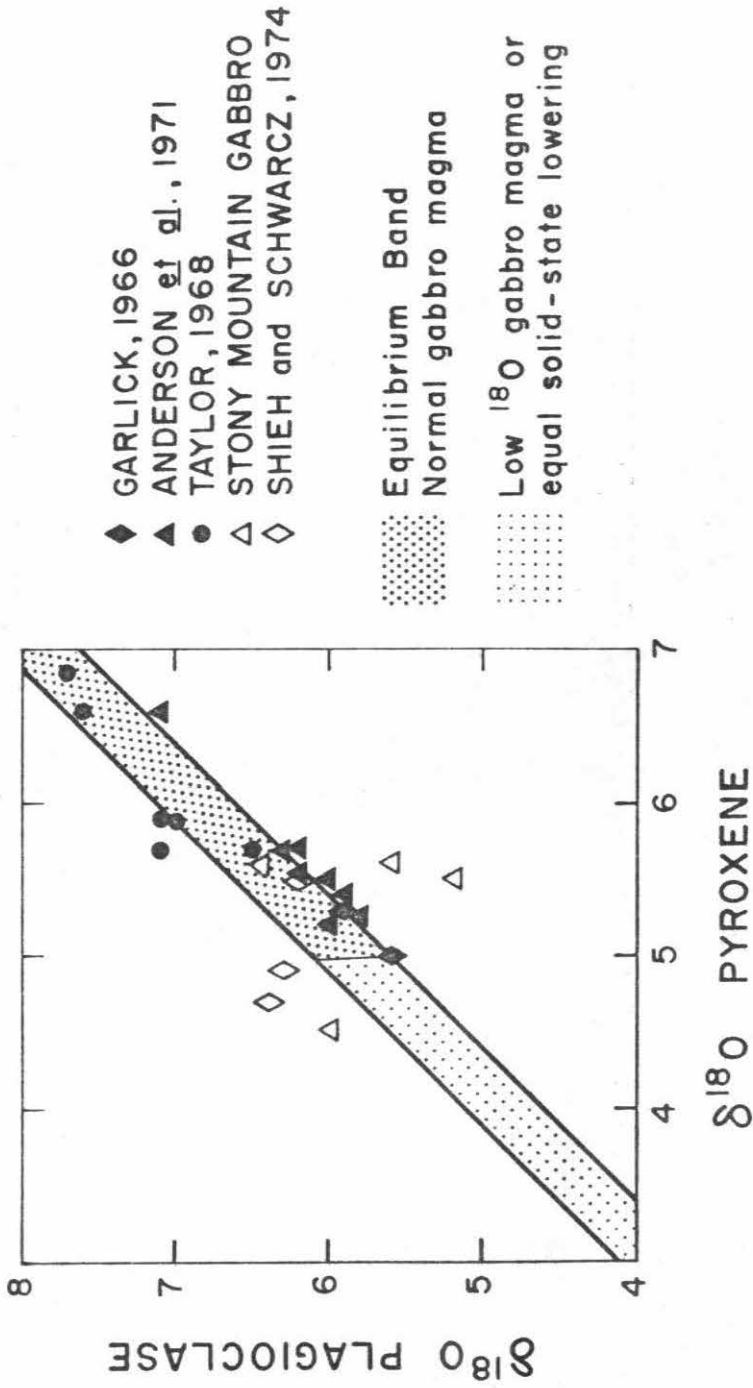
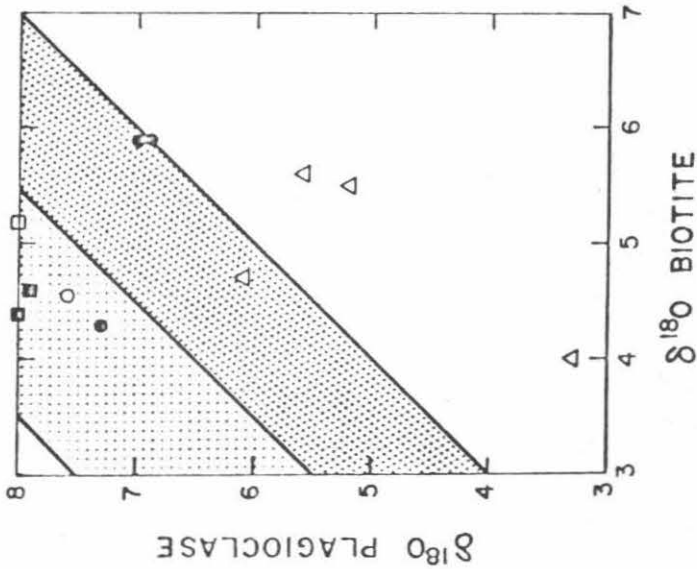
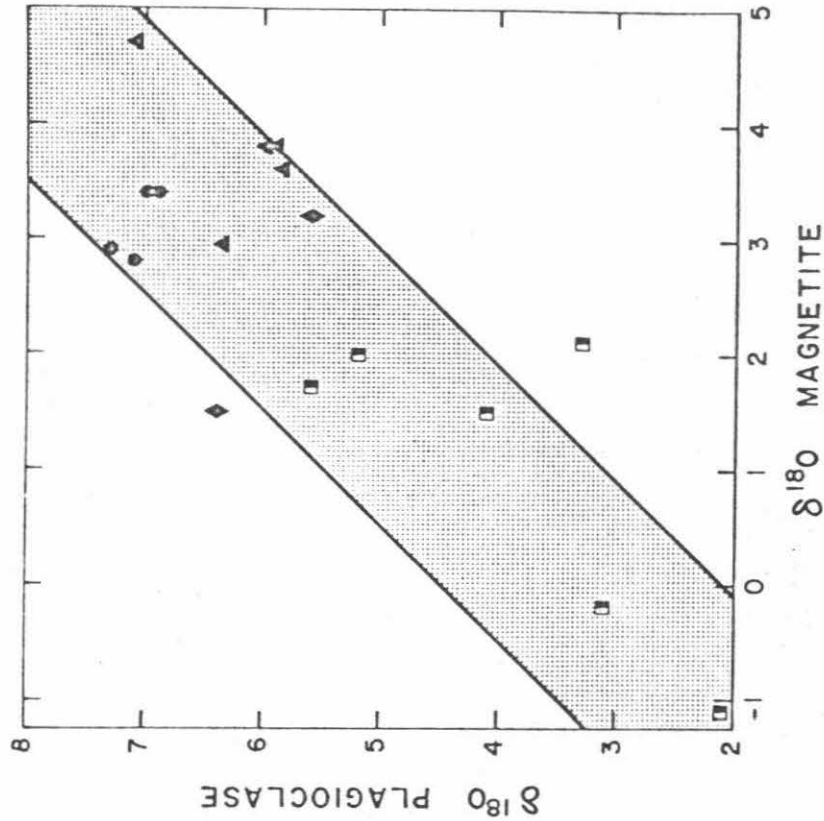


Figure 6-14a



- TAYLOR, 1968
- TAYLOR and EPSTEIN, 1962
- TURI and TAYLOR, 1971
- SHIEH and TAYLOR, 1969 a
- △ STONY MOUNTAIN GABBRO (δ-14b)
- ▲ ANDERSON et al., 1971
- ◆ GARLICK, 1966
- ▣ STONY MOUNTAIN (δ-14c)

⋯ PLUTONIC
 ⋮ VOLCANIC

Figure 6-14b

Figure 6-14c

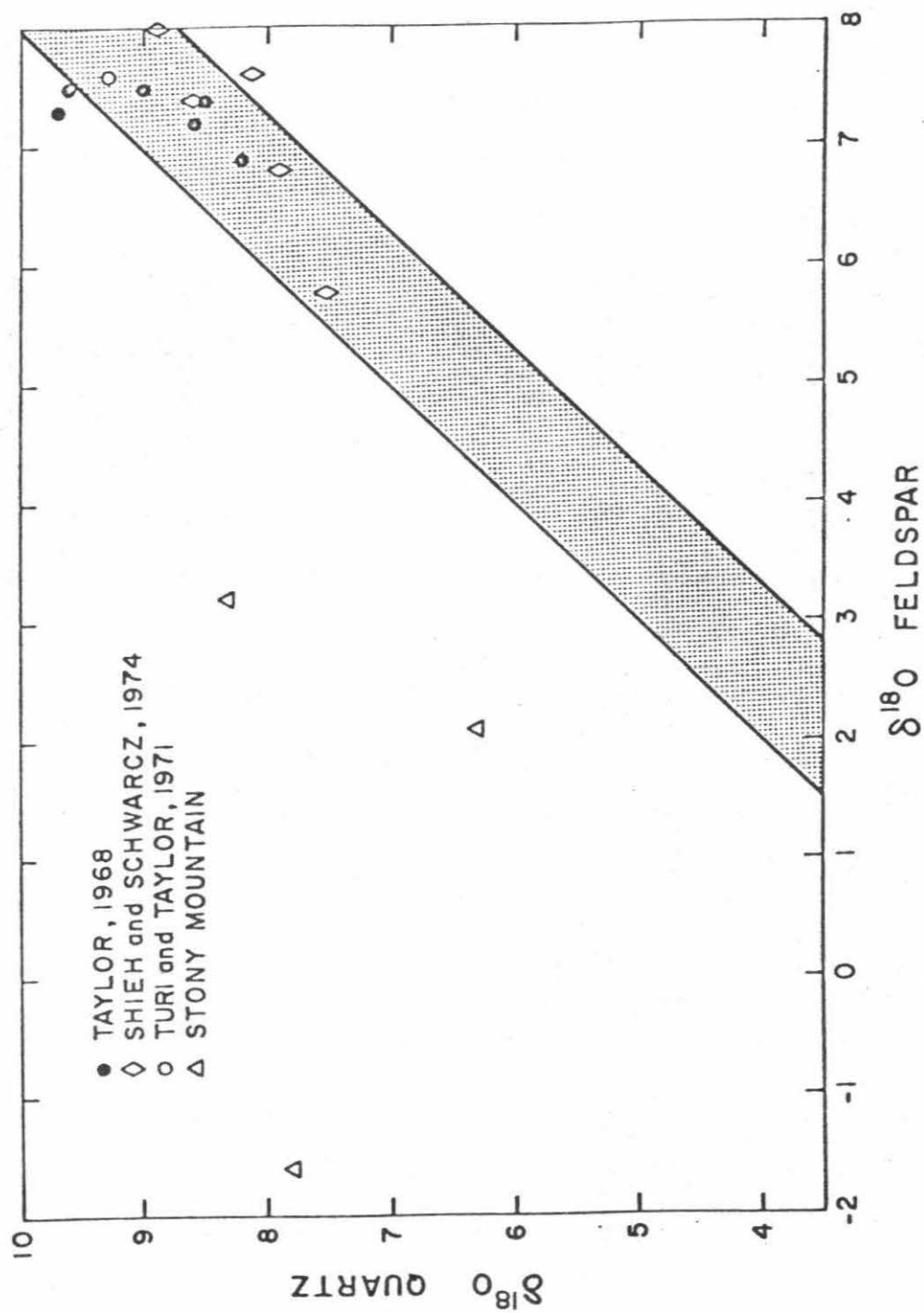


Figure 6-14d

Note that almost all of the analyses of coexisting minerals from the literature fall within the "equilibrium" band. However, only one Stony Mountain sample falls within this zone. This sample is the aforementioned SM-159 from the very top of Stony Mountain (3870 m); it contains the most ^{18}O -rich plagioclase and pyroxene of any gabbro in the complex and its biotite has the highest δD value (see Figures 6-2 and 6-7). As mentioned previously, this rock could represent crystallization from a normal basaltic magma having $\delta^{18}\text{O} \approx +6.0$. Nevertheless, it is also plausible to suggest the pyroxene and plagioclase have each been lowered in $\delta^{18}\text{O}$ by a small amount (perhaps 0.5 per mil?) at subsolidus temperatures, because (a) the δD of the biotite in SM-159 is -119 and thus it has been at least partially affected by Tertiary meteoric hydrothermal solutions, and (b) texturally, although the rock is one of the least altered gabbro samples, it does show evidence of having been slightly altered (see Table 6-1). In any case, if there has been any subsolidus exchange it must have occurred at high temperatures ($>500^\circ\text{C}$) because the plagioclase-pyroxene ^{18}O fractionation is indicative of equilibrium at high temperatures. Part of the reason for the excellent preservation of the oxygen isotopic ratios in SM-159 may lie in the fact that both pyroxene (~ 2 mm) and plagioclase (~ 3 mm) are among the coarsest in grain size of all the minerals in the Stony Mountain complex.

The two data points in Figure 6-14a that lie below the "equilibrium" band represent samples where the plagioclase has undergone more ^{18}O depletion than the coexisting pyroxene, compatible with the known fact that feldspar is more susceptible to oxygen isotopic exchange than any other rock-forming mineral. The data point lying above the band represents a sample where pyroxene has apparently undergone slightly more ^{18}O depletion than the coexisting plagioclase. Unfortunately, the pyroxene separate analyzed from this rock was not pure; it is intimately intergrown with, and altered to, chlorite. Such chlorite would be expected to have a very low $\delta^{18}\text{O}$ value, probably accounting for the anomalously low $\delta^{18}\text{O}$ value of this pyroxene concentrate.

In Figure 6-14b coexisting plagioclase and biotite pairs are plotted and compared to data points from the literature. Unaltered plutonic rocks typically have $\Delta_{\text{F-B}} = 2.5$ to 4.5 (Taylor and Epstein, 1962b; Taylor, 1968; Shieh and Taylor, 1969a). Volcanic rocks usually have smaller fractionations; Taylor (1968) gives analyses of two volcanic rocks that have $\Delta_{\text{F-B}} = 2.1$ and 1.0 . The four gabbro samples from Stony Mtn. have $\Delta_{\text{F-B}}$ values of -0.7 , -0.3 , 0.0 , and $+1.4$. This indicates that biotite was more resistant to exchange with circulating meteoric-hydrothermal fluids than was plagioclase. However, a problem arises when it is realized that if the plagioclase was initially about $+7.0$, then based on data on plutonic rocks

from other occurrences, the initial $\delta^{18}\text{O}$ of the coexisting biotite should be about +5.0 or less. Yet two of the biotites have $\delta^{18}\text{O} = +5.5$ and +5.6 (Figure 6-13), indicating a lack of any ^{18}O depletion and perhaps even a small ^{18}O enrichment. A possible way out of this dilemma is to assume that the gabbro originally had $\delta^{18}\text{O}_F \geq +7.5$.

There is reason to believe that biotite should be somewhat susceptible to low temperature, retrograde isotopic exchange (Schwarcz et al., 1970; Garlick and Epstein, 1967). However, there is no correlation between $\delta^{18}\text{O}_B$ and the grain sizes of the biotites. Experimental work on equilibrium oxygen isotope fractionations involving biotite has not yet been done, so inferences must be based solely on data from natural assemblages. The scatter of points in the Δ_{F-B} vs Δ_{Q-B} of Figure 17 of Shieh and Taylor (1969a) may be due to a variety of reasons: variations in Fe/Mg of the biotites, different oxygen fugacities at the time of crystallization, retrograde exchange effects and variations in the An content of the coexisting plagioclase. Also, volcanic biotites are often deficient in hydroxyl with respect to biotites in plutonic rocks (Friedman et al., 1964) and this may in part account for a variation in Δ -values (Taylor, 1968). The above complications might be responsible for the apparently anomalously high $\delta^{18}\text{O}_B$ values from the two Stony Mtn. gabbros.

As shown in Figure 6-14c, an approximately linear relationship exists between $\delta^{18}\text{O}$ values of coexisting plagioclase and magnetite from Stony Mountain. Only one data point falls outside the zone of 'normal' igneous fractionations and in this sample plagioclase has clearly suffered more ^{18}O depletion than did the coexisting magnetite. All of the other data points fall within the "equilibrium" band defined for mafic volcanic and plutonic rocks. Thus all but one of the $\Delta_{\text{F-M}}$ values measured in the Stony Mtn. complex are remarkably uniform: 3.9, 3.2 and 2.6 for the gabbro, 3.3 for the inner diorite, and 3.2 for a quartz monzonite. Using the experimentally determined oxygen isotope geothermometer for plagioclase - H_2O (O'Neil and Taylor, 1969) with the empirical calibration for magnetite - H_2O by Anderson *et al.* (1971), the above Δ -values give temperatures of 770° , 880° , 1005° , 880° and 910°C , respectively. These isotopic temperatures are all reasonable values ($\pm 100^\circ\text{C}$) for crystallization of such igneous rocks. The $\delta^{18}\text{O}_{\text{F}}$ in these samples, however, is 1 to 5 per mil lower than 'normal' igneous plagioclase and, in general, the plagioclase is not in isotopic equilibrium with the other coexisting minerals (Figure 6-13). Except for the inner diorite, these calculated temperatures thus are meaningless, unless (1) both the magnetite and the plagioclase in each rock suffered approximately the same amount of subsolidus ^{18}O lowering, and (2) hydrothermal exchange occurred at $T \geq 800^\circ\text{C}$.

In these particular rock samples, magnetite and plagioclase might have exhibited equal apparent susceptibility to oxygen isotopic exchange because the magnetite is an order of magnitude smaller in grain size than the plagioclase, and the magnetite in most of these samples is a composite of several generations of magnetite formation - original igneous magnetite and 'deuteric' or 'alteration' magnetite as described by Dings (1941). In fact, it is possible that none of the original igneous magnetite has exchanged at all, the measured $\delta^{18}O_M$ value simply being the composite of unadulterated igneous magnetite ($\delta^{18}O_M \approx +2.5$; see Figure 6-13) and magnetite produced during the hydrothermal alteration by heated meteoric waters ($\delta^{18}O_M \approx -6$). A mass balance calculation shows that this would require about 90% of the magnetite to be totally unexchanged.

The breccia pipe exhibits an abnormally large disequilibrium $\Delta_{Q-D} = 7.2$. It is likely that the quartz has retained its initial $\delta^{18}O$ value (+9.4) whilst the dolomite continued to exchange with meteoric waters down to lower temperatures.

In Figure 6-14d, $\delta^{18}O_Q$ is plotted vs $\delta^{18}O_F$ in two quartz monzonite samples and one rhyolite; these values are compared with the 'normal' quartz-feldspar fractionations in igneous rocks, which range from 0.7 to 2.0 (shaded portion of the diagram). The samples from the Stony Mountain complex are all drastically out of oxygen isotope equilibrium, with $\Delta_{Q-F} = 4.2$,

5.1 and 9.4. Because of the near-equal grain size and large disequilibrium fractionation displayed by the quartz and feldspar, almost all of the oxygen isotopic exchange could have taken place at subsolidus temperatures. Quartz is clearly very resistant to oxygen isotope exchange compared with alkali feldspar.

The general pattern that emerges from the discussion in this section is that (1) quartz is very resistant to isotopic exchange; (2) feldspar is very susceptible to exchange, and (3) most of the other rock-forming minerals are intermediate in their resistance to exchange; fine-grained magnetite, biotite, and pyroxene all exhibit approximately the same susceptibility (see Figure 6-13). Magnetite is, however, probably more resistant to exchange than pyroxene or biotite of equivalent grain size, and in the Stony Mtn. rocks its isotopic relationships are complicated by more than one generation of formation.

6.9 Mineral-whole rock ^{18}O relationships

In normal fresh volcanic rocks the plagioclase-groundmass fractionations are very slightly positive or zero, whereas the pyroxene-groundmass fractionations are negative (Garlick, 1966; Anderson et al., 1971). At Stony Mtn., even the outer diorites with the most normal $\delta^{18}\text{O}$ values exhibit isotopic reversals. For example, SM-200 is an apparently fresh porphyritic outer diorite sample with $\delta^{18}\text{O}_p = +6.1$ and the groundmass with $\delta^{18}\text{O} =$

+5.8. Another outer diorite specimen has $\delta^{18}O_F = +2.9$ and $\delta^{18}O_R = +3.4$. Samples SM-112, SM-90 and SM-109 all show plagioclase-whole rock $\delta^{18}O$ reversals (Figure 6-13). Although all these samples have experienced ^{18}O depletion, note that this would not be obvious had we only done one analysis from SM-200 (e.g. just the pyroxene). Thus, in an area known to have experienced meteoric-hydrothermal alteration, we must be cautious in pronouncing a rock 'normal' solely on the basis of one analysis (especially of a resistant phase).

6.10 Carbon and oxygen isotope ratios in carbonates

Carbonate is a minor but ubiquitous phase in the altered volcanic and intrusive rocks of the Stony Mountain complex. In Figure 6-15, $\delta^{13}C$ is plotted vs $\delta^{18}O$ for eight calcites and one dolomite. There is a very slight tendency for $\delta^{13}C$ to increase with decreasing $\delta^{18}O$. However, if the most positive and most negative $\delta^{13}C$ values are thrown out, then $\delta^{13}C$ is seen to be independent of $\delta^{18}O$ with an average value of -5.5.

The $\delta^{13}C$ value of -5.5 is within the generally accepted range for deep-seated carbon from carbonatites (Taylor et al., 1967; Conway and Taylor, 1969; Deines, 1970). In a recent analysis of carbon isotope values from carbonatites, kimberlites and diamonds, Deines and Gold (1973) estimated the best average $\delta^{13}C$ value for primitive carbon to be about -5.2.

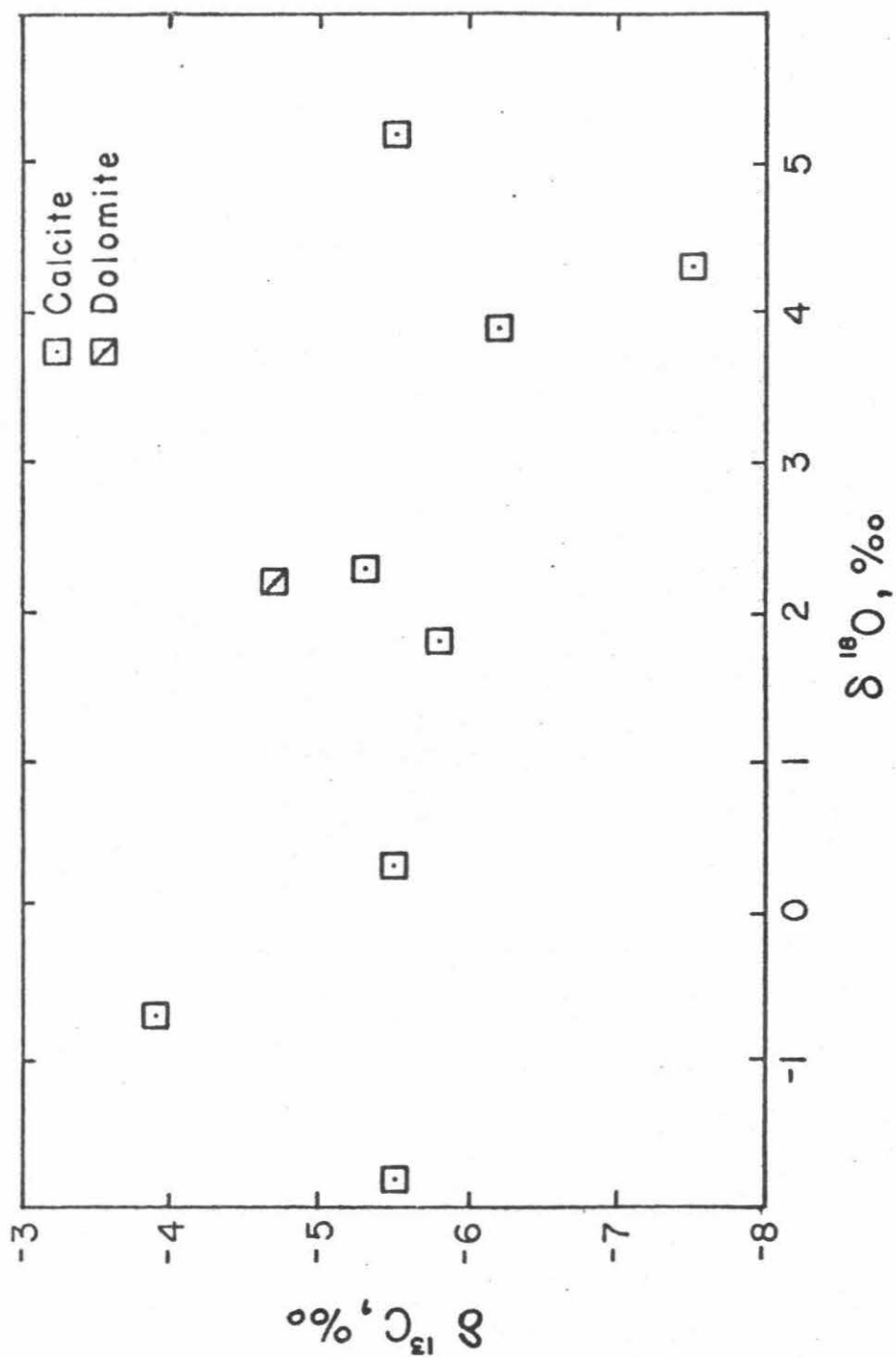


Figure 6-15. Plot of $\delta^{13}\text{C}$ vs $\delta^{18}\text{O}$ for carbonates from the volcanic and plutonic rocks of the Stony Mtn. region.

Thus the isotopic data in the Stony Mountain area are compatible with the carbon in these altered igneous rocks having been derived from primary igneous source materials.

The $\delta^{18}\text{O}$ variations of the carbonates are best explained in terms of varying $^{18}\text{O}/^{16}\text{O}$ ratios of the meteoric ground waters that were undergoing exchange with the igneous rocks but, in part, they may also be due to temperature variations. For example, using the experimentally derived equilibrium ^{18}O fractionation curve for calcite-water of O'Neil et al. (1969), the $\delta^{18}\text{O}$ variation of the calcites from +5.2 to -1.8 may be explained by their having last exchanged oxygen at 250°C with a fluid varying in $\delta^{18}\text{O}$ from about -3 to -10. These carbonates could also have formed from a fluid of constant $\delta^{18}\text{O}_{\text{H}_2\text{O}} \approx -8$, if the temperatures varied from about 325° to 150°C. The actual situation probably was a combination of these two extremes with the isotopic composition of the waters and the temperature of exchange varying between narrow limits, around $\delta^{18}\text{O} \approx -7$ and $T \approx 250^\circ\text{C}$. The temperature at which the $\delta^{18}\text{O}$ of calcite is finally 'frozen in' is expected to be lower than for any of the silicate minerals (including the feldspars) because of the much faster kinetics of hydrothermal exchange in the calcite- H_2O system.

As noted by Forester and Taylor (1972), the $\delta^{18}\text{O}$ values of the calcites are all close to the $\delta^{18}\text{O}$ values obtained in the whole-rock silicate samples from which the calcites were

separated. This is illustrated in Figure 6-16. A similar relationship was found by Clayton et al. (1968a) between the calcites and silicates of the Colorado River deltaic sediments in the Salton Sea geothermal area, and by Taylor (1973) from the altered volcanic rocks at Tonopah, Nevada. The reason for the similarity of $\delta^{18}\text{O}$ values is that both the carbonates and the silicates have largely equilibrated with the heated ground waters at similar temperatures (see section on W/R ratio). The dominant silicate in the igneous rock is feldspar, which at these temperatures at equilibrium would have an $^{18}\text{O}/^{16}\text{O}$ ratio very close to that of calcite. At equilibrium, quartz would be relatively enriched in ^{18}O but chlorite and opaque oxides would be depleted in ^{18}O with respect to the carbonate so that overall, the whole-rock values would closely resemble the carbonate $\delta^{18}\text{O}$ values. The similarity in the $\delta^{18}\text{O}_\text{C}$ and $\delta^{18}\text{O}_\text{R}$ values implies that the Stony Mtn. rocks were not affected by late, extremely low-temperature hydrothermal events of any major importance; if they had been, the $\delta^{18}\text{O}_\text{C}$ values would indicate this, because fine-grained calcites are so readily exchanged (see O'Neil et al., 1969; Fornaseri and Turi, 1969).

6.11 Water/rock ratios

Method of calculation

It is possible to set approximate minimum estimates of the amounts of water that have passed through these abnormally

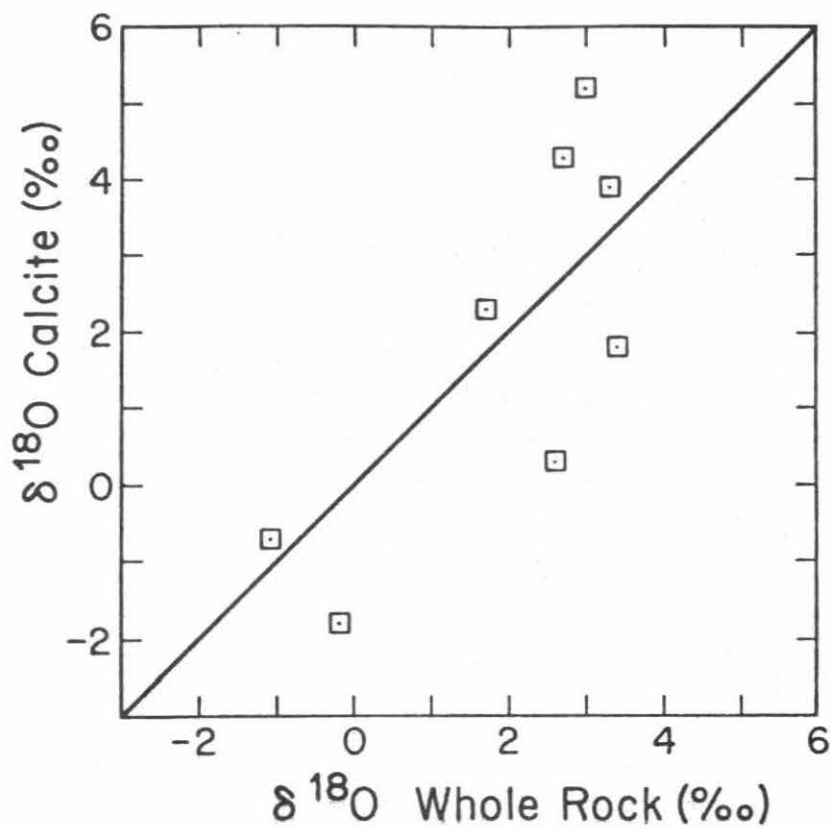


Figure 6-16. $\delta^{18}\text{O}$ values of coexisting calcites and whole-rocks from the Stony Mountain region, Colorado.

low- ^{18}O igneous rocks by utilizing the hydrogen and oxygen isotopic data in conjunction with mineralogical criteria for the temperature of hydrothermal exchange. The simplest case is that of a closed-system model, analogous to that employed by Sheppard et al., (1969), Wenner and Taylor (1973) and Taylor (1971; 1973).

Consider a closed meteoric water-rock system in which the water and rock undergo oxygen isotopic exchange. Thus we have

$$W\delta_W^i + R\delta_R^i = W\delta_W^f + R\delta_R^f$$

where δ_R^i , δ_W^i = initial $\delta^{18}\text{O}$ values of the whole rock and meteoric water, respectively

δ_R^f , δ_W^f = final $\delta^{18}\text{O}$ values of the whole rock and meteoric water, respectively.

Of those oxygens that undergo exchange,

W = fraction of water oxygen atoms

R = fraction of rock oxygen atoms

Thus

$$\frac{W}{R} = \frac{\delta_R^i - \delta_R^f}{\delta_W^f - \delta_W^i}$$

Arguments have already been presented which demonstrate that we know δ_R^i with some accuracy. It has been demonstrated from hydrogen isotopic analyses (Section 6-3) that the $\delta^{18}\text{O}$ of the pristine meteoric ground waters in the Western San Juans at the time of intrusion of the Stony Mountain complex was ≈ -14 .

However, for completeness, and because there could have been some 'oxygen isotope shift' in the waters prior to their entering the Stony Mtn. system, the water/rock ratios discussed below are calculated for δ_W^i values of -10 as well as -14. The δ_R^f is, of course, the value measured on the rock today. In order to calculate the water/rock ratios we now only need consider how to estimate δ_W^f .

If H_2O was the dominant oxygen-bearing fluid then, at equilibrium, the only variables that determine δ_W^f are δ_R^f , the types of minerals present, and temperature. Of course, we also must know the temperature dependence between δ_W^f and δ_R^f . How do we go about doing this?

It is evident from Table 6-1 and Figure 6-2 that for most of the rocks analyzed $\delta^{18}O_F$ closely approximates $\delta^{18}O_R$. In fact the mean difference between $\delta^{18}O_F$ and $\delta^{18}O_R$ for fourteen samples is less than 0.3 per mil. This is not surprising inasmuch as feldspar is the dominant mineral in these rocks. A reasonable approximation of δ_W^f can thus be made by assuming $\delta_R^f = \delta_F^f$ and by utilizing the equilibrium feldspar-water oxygen isotope geothermometer experimentally determined by O'Neil and Taylor (1967). However, because minerals other than feldspar are less susceptible to oxygen isotopic exchange and will therefore more closely approximate their original igneous $\delta^{18}O$ values, the final whole-rock $\delta^{18}O$ values will in general be somewhat heavier than that predicted on the basis

of the above approximation. One way to approximately take into account the effects of these more resistant phases is to use a slightly more calcic value for the An content of the feldspar than that actually present in the rock in question. An alternative possibility, the one used here, is simply to assume that, except for feldspar, the rest of the rock is inert.

The experimental feldspar-water fractionation curves have the expression

$$\delta_F^f - \delta_W^f \approx (2.91 - 0.76\beta) (10^6 T^{-2}) - 3.41 - 0.41\beta,$$

where β is the An content of the feldspar, and

$\delta_F^f - \delta_W^f \approx 10^3 \ln \alpha_{F-W}$. For example, for a rock with $\beta = 0.30$, $\delta_R^f = +5.0$, $\delta_R^i = +8.5$ and $\delta_W^i = -14$ then

$$\frac{W}{R} = \frac{+8.5 - 5}{5 - \frac{(2.68) 10^6}{T^2} - [-14 - 3.533]}$$

Assuming the validity of the simple closed-system model, the W/R ratios are minimum estimates because (1) the meteoric ground waters have been assumed not to undergo an appreciable ^{18}O shift prior to isotopic exchange with the surrounding country rocks and (2) isotopic exchange was certainly not 100% effective and thus some water must get through certain fracture conduits without equilibrating completely with the ad-

joining rocks. This closed-system model assumes that all the water entering the system equilibrates with the rocks at the final exchange temperature. However, another type of model could have the water make a single cycle through the rocks and then be removed from the system. This open-system model has been considered by Taylor (Springer-Verlag monograph, in preparation), and yields W/R ratios smaller than, but not unlike those, calculated in the closed-system case employed here. Except for very high W/R ratios, the open-system model at 300°C coincides very well with the closed-system model at 500°C. The relationship between the two models is given by $\left(\frac{W}{R}\right)_{\text{open system}} = \ln\left[\left(\frac{W}{R}\right)_{\text{closed system}} + 1\right]$.

Gabbros

Calculated W/R ratios for the Stony Mountain gabbroic rocks are plotted against temperature for a variety of both δ_W^i and δ_R^f values in Figure 6-17. The temperature range given (900° - 400°C) is based solely on inferences from the petrographic and mineralogical evidence. The gabbros, in general, are very fresh and even in the most highly altered sample at least 3/4 of the original igneous minerals are preserved. Pyroxenes and biotites are apparently largely unexchanged even though they show some evidence of alteration to uralite, epidote, chlorite, sericite and magnetite. On the other hand, the plagioclase has suffered marked ^{18}O exchange, in most cases

Figure 6-17. Plot of temperature vs W/R (atomic oxygen) for gabbroic rocks from Stony Mtn. Striped pattern encloses range of W/R ratios for $\delta_W^i = -14$ and -10 , and $\delta_R^f = +6, +4, +3, +2$, and $+1$. Heavily striped area is overlapping region. Curves are calculated on the basis of $\delta_R^i = +6.5$, for a rock system behaving as An_{50} plagioclase (see text). Circles represent W/R values calculated only for $\delta_W^i = -14$, and arbitrarily plotted at $\sim 500^\circ\text{C}$. The open circles are δ_R^f values, the smaller black dots are δ_F^f values from which 0.4 per mil has been subtracted (see Section 6.5), and the larger black dots are samples < 45 m from the inner diorite contact. Note the log scale for W/R.

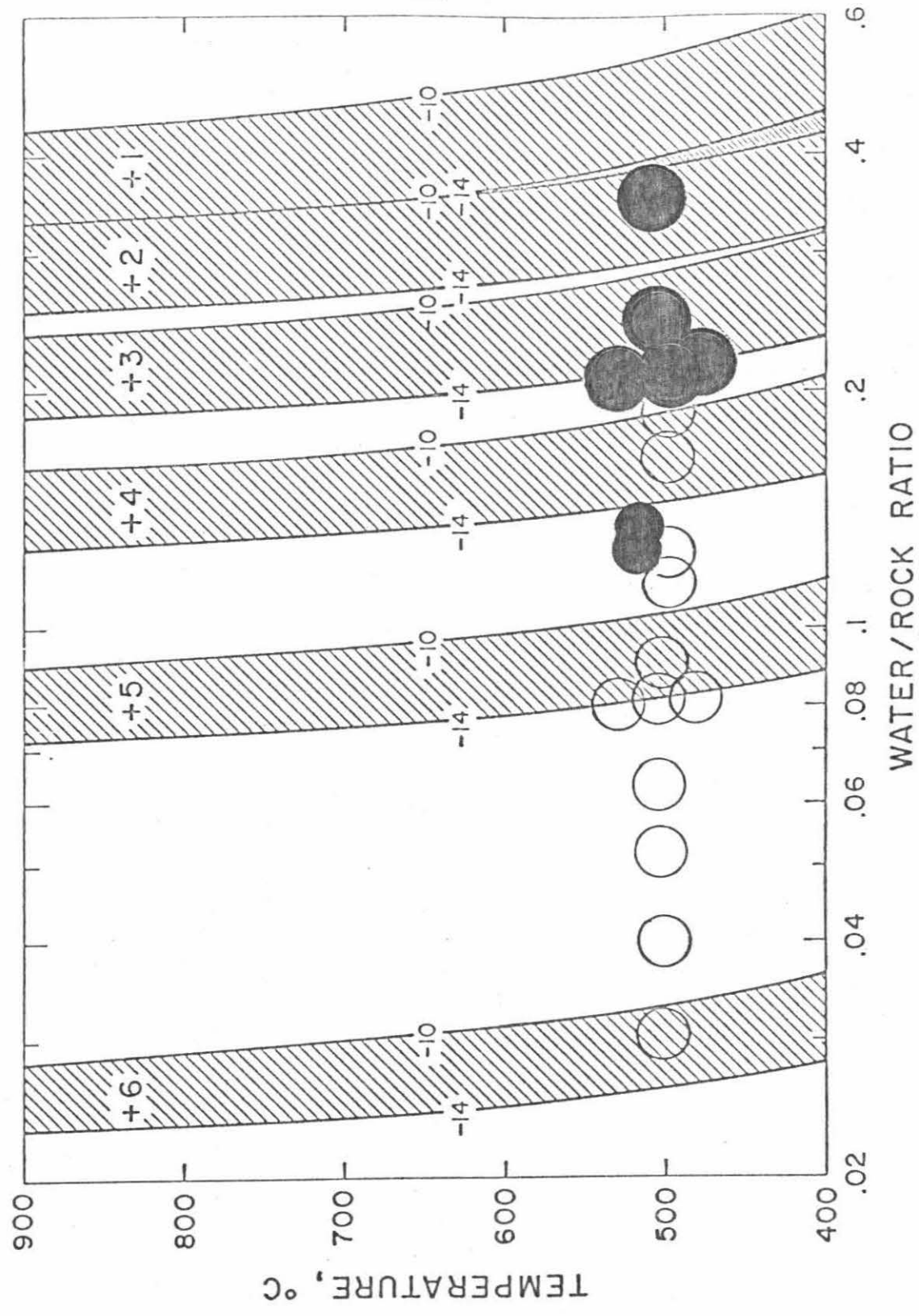


Figure 6-17

with little petrographic indication of alteration. Thus the mafic minerals are either inert remnants or not yet reacted, whereas the plagioclase is apparently stable during this alteration but undergoes oxygen exchange. In some respects these observations are analogous to those of Lawrence and Taylor (1972), who found that those parent minerals (in soil profiles) that were not in chemical equilibrium with the local ground waters did not undergo any significant $^{18}\text{O}/^{16}\text{O}$ exchange with those waters.

On the basis of their relatively fresh, unaltered appearance in thin section, it is likely that most of the hydrothermal ^{18}O exchange in the Stony Mtn. gabbros took place above approximately 400°C . Examples of other petrographically fresh, low- ^{18}O gabbros similar to those of Stony Mtn. can be seen in Mull, the Cuillin Center in Skye, and throughout most of the Skaergaard intrusion. Most of these examples also have fresh olivine, which implies an alteration $T \geq 500^{\circ}\text{C}$; low temperature hydrothermal alteration typically gives rise to hydrous phases dominated by chlorite, sericite, and clay minerals (e.g. the altered volcanics around hot springs in Yellowstone Park, Honda and Muffler, 1970, and the altered volcanics of the Reykjanes geothermal area, Iceland, Tomasson and Kristmannsdottir, 1972).

In the temperature range $400^{\circ} - 900^{\circ}\text{C}$ it is clear from Figure 6-17 that the calculated W/R ratios are almost inde-

pendent of temperature, fairly insensitive to δ_W^i , and mainly dependent on δ_R^f . The range of δ_R^f values for the gabbroic unit is from +5.9 to +1.4 (Table 6-1) with over 70% of the values falling between +3 to +5 per mil. If we limit our discussion to $\delta_W^i = -14$, the total range of integrated W/R ratios is 0.03 to 0.4 (Figure 6-17). Eliminating from consideration those samples within 45 m of the inner diorite contact, the W/R ratios are even further restricted, to 0.03 to 0.2. As will be discussed below, it is reasonable to exclude the above samples because they may have undergone oxygen isotope exchange in two stages; thus their integrated W/R ratios would be correspondingly higher. In the light of the above discussion, a very restricted range of W/R ratios is established for the main mass of gabbro exposed at Stony Mountain, namely 0.1 ± 0.1 .

The quartz monzonite associated with the gabbroic unit has lower $\delta^{18}O$ values than the main gabbroic mass; it exhibits an integrated W/R ratio on the order of 0.4. This could be due to (1) genuinely larger amounts of water circulating through the quartz monzonite than the gabbro, and/or (2) the effective W/R ratio being larger in the quartz monzonite than in the gabbro because the average grain size of the quartz monzonite is less than that of the gabbros (0.4 vs 1.2 mm; see Figure 6-10). Thus because of the finer grain size and larger surface area presented to the exchanging fluid, the

quartz monzonite might have undergone more efficient oxygen isotope exchange even though exposed to the same quantity of meteoric hydrothermal fluid and even though the quartz monzonite contains a higher content of quartz (which is difficult to exchange). This implies that the variation in W/R ratios in the gabbros themselves may be due to grain size variations. Because there is a correlation between average grain size and $\delta^{18}O_F$ in the gabbros (Figure 6-12) this means there must be a correlation between grain size and W/R ratios of these gabbros. This emphasizes the fact that this calculation gives us a time-integrated calculated W/R ratio, as opposed to the actual W/R ratio which would almost certainly be a larger number. A schematic diagram explaining these relationships is presented in Figure 6-18. Although the figure implies that for material with an infinitely fine grain size (and therefore infinitely reactive), the calculated W/R ratio is the same as the actual W/R ratio, this is true only for water that passes pervasively along grain boundaries. This is because the W/R can be still higher, inasmuch as large, throughgoing fractures can act as conduits for a large amount of water that is never in contact with the main mass of country rocks.

Outer diorite

Because we have assumed that the outer diorite had $\delta_R^i = +7.5$, the W/R ratios for this rock type will be given by

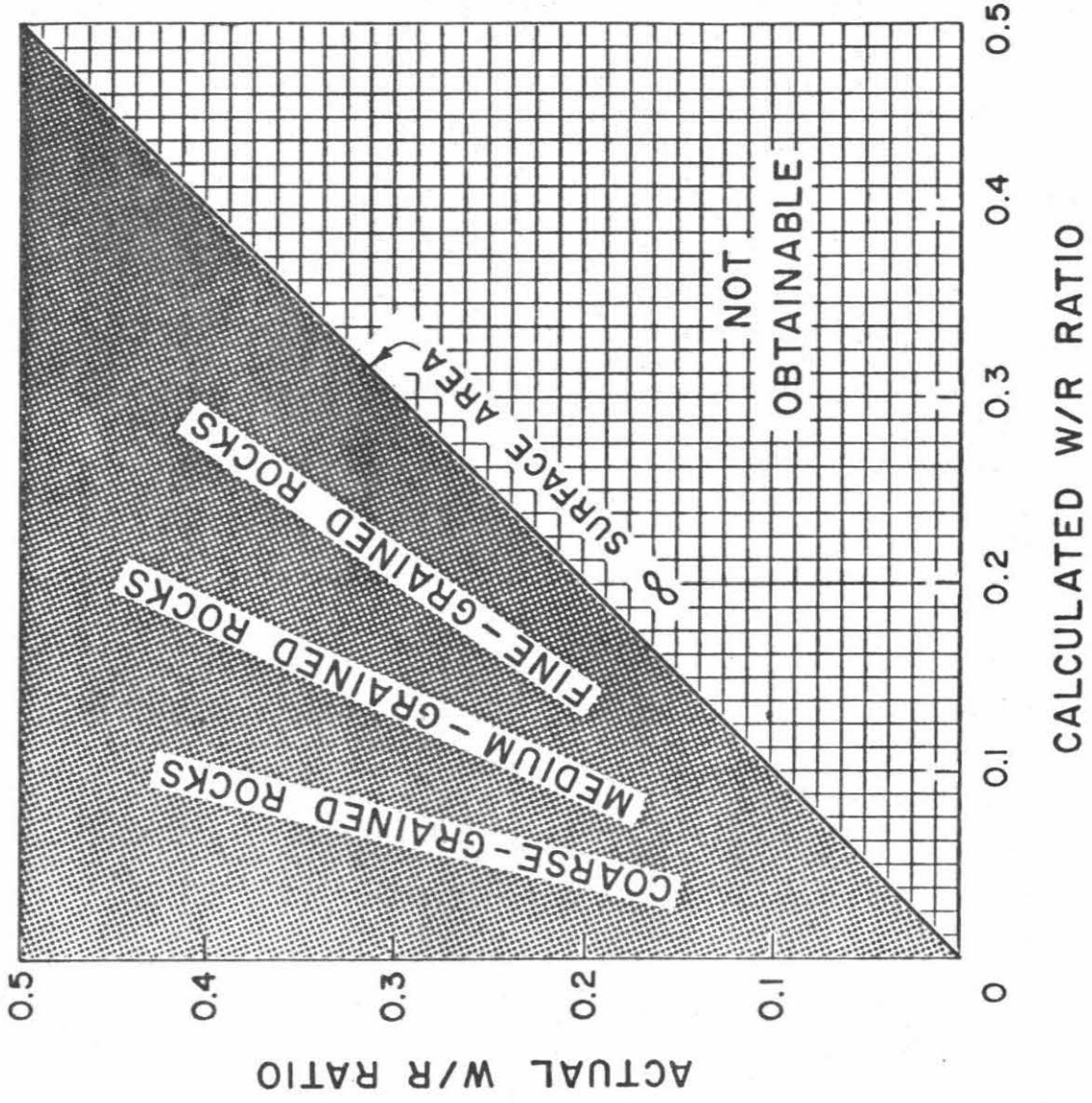


Figure 6-18. Schematic relationship for actual and calculated W/R ratios as a function of grain size.

appropriate extrapolation between Figure 6-17 and 6-19. This rock unit contains a significantly higher abundance of alteration minerals than does the gabbro, but even in the most exchanged sample (SM-89, $\delta^{18}O_R = -1.1$) there are a few remnant, well-preserved amphibole and pyroxene phenocrysts. In most cases the propylitic (greenschist) alteration had destroyed less than about half of the primary mineral assemblage. Thus the temperature range considered for the outer diorite is extended down to 300°C (see Figure 6-19), 100°C lower than considered for the gabbroic unit. Note again that temperature does not strongly influence the W/R values. For SM-89, a W/R ratio of about 1 is required. The other two samples with very low $^{18}O/^{16}O$ ratios are SM-3a and SM-41 (+1.6 and +2.2 respectively) and they indicate a W/R \approx 0.5; these samples are from the cigar-shaped intrusion that branches off from the main arcuate diorite unit. All the other δ_R^f values of the outer diorite (and associated hornblende monzonite) fall within the range +2.7 and +5.9, implying W/R \approx 0.1 to 0.3. In summary, with the sole exception of SM-89, all the outer diorite samples exhibit a narrow range of W/R \approx 0.3 \pm 0.2. The andesitic dike rocks exhibit a W/R range of about 0.3 to 0.6.

Tertiary volcanic rocks

As previously described, the volcanic rocks can be thought of as having experienced two periods of isotopic exchange that

possibly overlapped in time, firstly, as a volcanic pile overlying a magma chamber of batholithic dimensions and, secondly, due to the local effect of epizonal plutons such as the Stony Mountain complex. Figure 6-19 is a T vs W/R plot applicable to the Tertiary volcanic rocks, constructed for $\delta_R^i = +8.5$, for a whole-rock system behaving as An_{30} plagioclase. The temperature scale is restricted to the range $200^\circ - 600^\circ\text{C}$, because the volcanic rocks have, in general, attained propylitic mineral assemblages typical of the greenschist facies. The typical assemblage is quartz-sericite-chlorite-carbonate-opaques \pm epidote \pm uralite \pm albite. Biotite is invariably absent. A series of W/R estimates is given below, based on a $T \approx 300^\circ\text{C}$ (e.g. see Turner, 1968), but as can be seen from Figure 6-19, changing the temperature from 250° to 500°C will not significantly affect the results. Again, limiting our discussion to $\delta_W^i = -14$, the volcanic rocks define W/R ratios in the range of about 0.3 to 1.2. Two-thirds of the volcanics analyzed for $^{18}\text{O}/^{16}\text{O}$ fall within the range $+2.0 \pm 1$ per mil, which corresponds to W/R ratios of approximately 0.6 ± 0.15 . The rhyolite also falls within this range, while the breccia pipe ($\delta_R^f = +5.0$) suggests a $W/R \approx 0.2$.

It is interesting to note that the δ_R^i necessary for the volcanic rocks to have the same W/R ratio as the outer diorite is about $+4.0$ - identical to the regional average $\delta^{18}\text{O}$ in

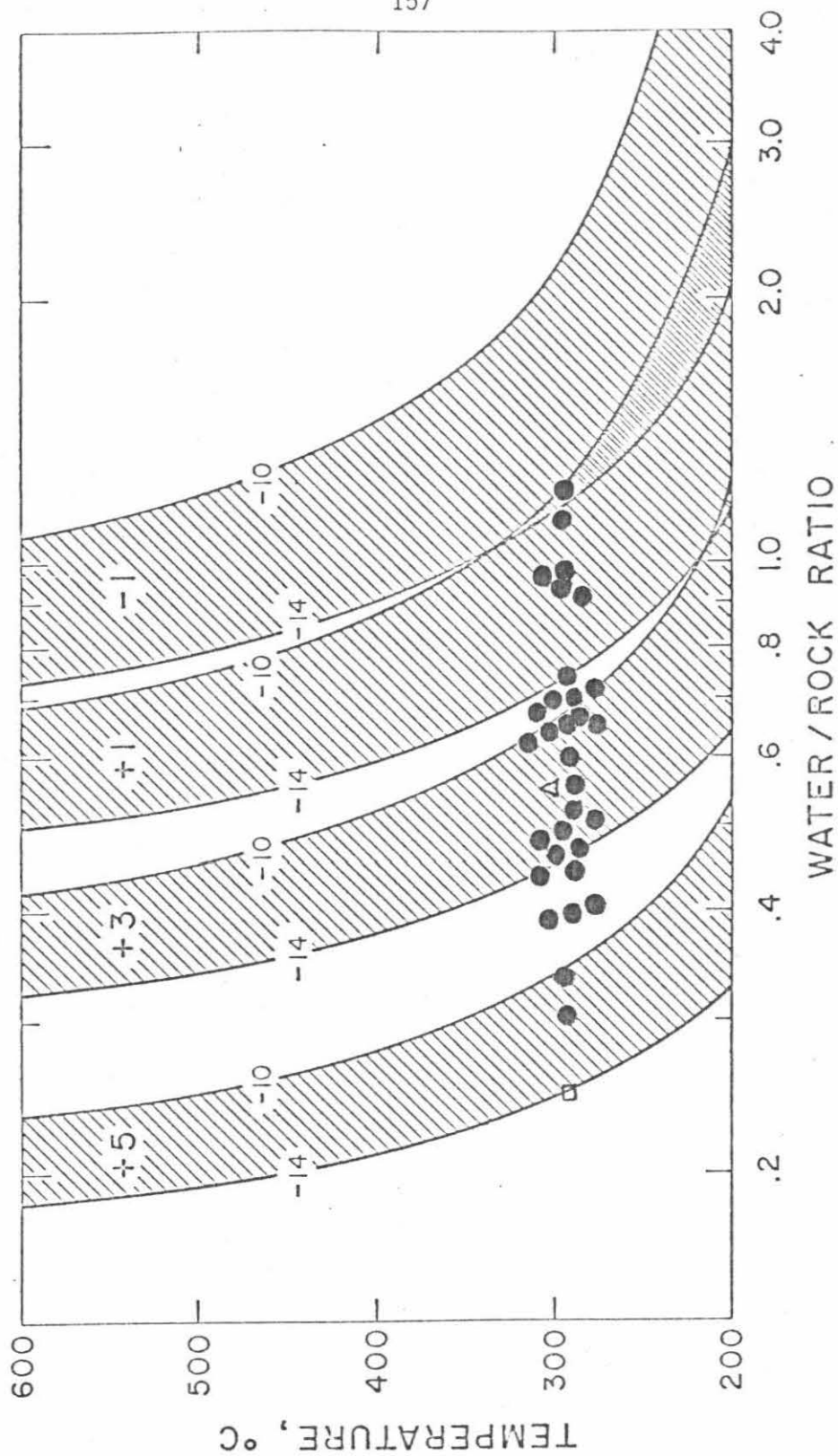


Figure 6-19.

Temperature vs W/R (atomic oxygen ratio) diagram for felsic rocks from the Stony Mtn. region. For explanation, see Figure 6-17. Curves are calculated on the basis of $\delta_1^{18}O = +8.5$ for rock systems behaving as An_{30} plagioclase. Black dots are volcanic rocks, open square is breccia pipe, and triangle is rhyolite, plotted arbitrarily at $\sim 300^\circ C$ and $\delta_1^{18}O = -14$.

the Silverton-Ouray area. This may be considered as an independent argument in favor of a two-stage process.

Thus a picture emerges whereby the volcanic rocks, the rhyolite, and the dikes exhibit the largest calculated W/R ratio (~ 0.6), followed by the outer diorite (~ 0.3) and then the gabbro (~ 0.15); this is also the order of increasing grain size. Once again it is emphasized that the actual W/R ratios are larger than the calculated values; the correlation between the grain size and W/R ratios for a given degree of $\delta^{18}\text{O}$ depletion clearly demonstrates this point.

Veins

As mentioned above, major fracture systems will allow bulk transfer of H_2O , almost all of which will not be in contact with the rocks through which it passes. Thus the true W/R ratios for vein systems are expected to be much larger than the W/R ratios calculated from $\delta_{\text{R}}^{\text{f}}$ in the plutonic rocks themselves. This implies that $\delta_{\text{W}}^{\text{f}}$ will be closer to $\delta_{\text{W}}^{\text{i}}$ in fracture flow systems than in systems where intergranular flow or diffusion of H_2O predominates. Note that the average calculated $\delta_{\text{W}}^{\text{f}}$ for H_2O that coexisted during deposition of four vein quartz samples (Section 6.6) is ~ -7 . Analyses of vein material may give greater insight into the true W/R and $\delta_{\text{W}}^{\text{i}}$ values than do analyses of the bulk rocks.

6.12 Low-¹⁸O magma hypothesis

Even after all the isotopic effects that can reasonably be ascribed to grain size, mineralogy and proximity to fractures are taken into account, a major enigma remains. Why does the central diorite intrusion have such a uniformly low-¹⁸O value? Conceivably, this might have come about if a major vein and fracture system passed through this zone of the Stony Mountain complex. However, the detailed quadrangle map of Burbank and Luedke (1969) does not show any particular concentration of veins in this area, nor was any observed by the present writer. The entire area appears to be equally highly veined. Note that the +3 $\delta^{18}\text{O}$ contour in Figure 6-2 centers directly on the inner diorite even though the +2 contour is apparently offset to the northeast because of biased sampling from that area.

If all the isotopic effects in the Stony Mountain complex are due solely to ¹⁸O exchange subsequent to crystallization (as in fact most seem to be), there is a major problem in explaining how the low-¹⁸O aqueous fluids were able to travel through the gabbro and outer diorite shells and only exchange appreciably with the central diorite core. This might offhand be explained on the basis of the fine grain size of the inner diorite, except for the following points: (1) the inner and outer diorites do not markedly differ in grain size, (2) the gabbro, which is relatively coarser-grained throughout, is also depleted in ¹⁸O near the central core; this obviously

cannot be explained by grain-size effects, and (3) the central diorite is relatively fresh and unaltered; its primary igneous texture, a pronounced 'pilotaxitic' flow-foliation, is perfectly preserved.

The only plausible way out of the above dilemma is to assume that the inner diorite was in fact emplaced as a low- ^{18}O magma. This could have come about through some process of mixing and exchange between meteoric H_2O and a silicate melt in a deeper magma chamber.

The hypothesis that low- ^{18}O magmas might be produced by interaction with meteoric H_2O was first entertained by Taylor (1968, p. 58, 61) to explain some of the ^{18}O -depleted igneous rocks of the Inner Hebrides, Scotland, and Skaergaard intrusion, Greenland. However, at that time the data did not warrant any firm conclusions on this matter.

The first tangible evidence for the existence of such low- ^{18}O magmas came from Forester and Taylor (1972) in discussing the Stony Mtn. inner diorite. Oxygen isotopic exchange between magma and meteoric water was also one of the possibilities mentioned by Muehlenbachs *et al.* (1972; 1974) to explain the abnormally low $^{18}\text{O}/^{16}\text{O}$ ratios in fresh, recent lava flows from Iceland. Friedman *et al.* (1974) postulated large-scale interaction between meteoric waters and magma for the Yellowstone Plateau volcanic lavas but did not suggest the mechanism for this interaction.

If the inner diorite is an example of a low- ^{18}O magma then we would predict that the $\Delta^{18}\text{O}$ -values in this rock should reflect normal igneous temperatures even though the $\delta^{18}\text{O}$ -values are abnormally low. This has been tested in SM-99b. This sample yields a $\Delta_{\text{F-M}} = 3.3$, equivalent to a quench equilibration temperature of about 860°C (Anderson *et al.*, 1971) assuming no subsolidus exchange. The estimated temperature error contributed solely by the analytical error (± 0.1 per mil) is $\pm 24^{\circ}\text{C}$. This plagioclase-magnetite equilibration temperature is reasonable for rocks of this composition (Piwinski, 1968; Piwinski and Wyllie, 1968), yet the $\delta^{18}\text{O}$ -values are depleted by about 5 per mil with respect to 'normal' igneous values. Further, a mass balance calculation, utilizing estimated modes for SM-99b, gives $\delta^{18}\text{O}_{\text{p}} \approx +2.2$. This gives a $\Delta_{\text{F-p}} = 0.9$, corresponding to a temperature of about 900°C (Figure 3, Anderson *et al.*, 1971) and compatible with the temperature estimated from $\Delta_{\text{F-M}}$. This internal consistency of the oxygen isotopic data, the reasonable temperature estimates, the well-preserved igneous textures, and the lack of hydrothermal alteration effects all lend support to the hypothesis that the inner diorite is the crystallization product of a low- ^{18}O magma. How then might it have been produced?

Consider an isotopically normal magma of andesitic composition occupying a shallow level chamber, for example, at a depth of about 3.7 km where the lithostatic pressure would

be 1 kb. Let us suppose that this is initially an anhydrous melt and that, in its present shallow level environment by some 'magical' means (unspecified as yet) it absorbs water from the permeable country rocks to the point of maximum saturation. Under these conditions ($P_{H_2O} = P_{Total}$) the maximum solubility of water in an andesitic melt at $1100^{\circ}C$ is about 4.5 weight per cent (Hamilton et al., 1964). There is no chemical analysis yet available for the inner diorite, but inasmuch as it is remarkably similar mineralogically and modally to fresh specimens of the outer diorite (Dings, 1941), the amount of oxygen in the inner diorite is calculated using a chemical analysis of the latter (Table 6-4; 46.64% oxygen). If the melt absorbed pristine meteoric water of $\delta^{18}O = -14$ from the highly fractured country rocks (weight % oxygen in water = 88.9), we have

$$\frac{\text{No. of gm of O in water}}{\text{No. of gm of O in rock}} = \frac{(4.5) (0.889)}{(95.5)(0.466)} = 0.09$$

This calculation is strictly in terms of oxygen, so the system would be composed of 8 atom % oxygen from the water and 92 atom % oxygen from the anhydrous melt. Hence, with $\delta_R^i = +7.5$ for the anhydrous inner diorite magma, we have

$$0.92 (+7.5) + 0.08 (-14) = \delta_R^f, \text{ and}$$

$$\delta_R^f = +5.3$$

Table 6-4

Calculated wt. % oxygen in the inner diorite, Stony Mtn.

	1	2	3
SiO ₂	60.71	53.26	32.33
Al ₂ O ₃	18.20	47.07	8.57
Fe ₂ O ₃	2.76	30.05	0.83
FeO	3.30	22.26	0.73
MgO	2.20	39.69	0.87
CaO	5.83	28.53	1.66
Na ₂ O	3.56	25.81	0.92
K ₂ O	2.78	16.98	0.47
TiO ₂	0.66	40.05	0.26
	100.00		46.64

1 Chemical analysis of outer diorite (Dings, 1941), recalculated on a CO₂- and H₂O-free basis.

2 Weight % oxygen in component oxide.

3 Weight % oxygen in component oxides of 1.

Thus it is impossible to lower the $\delta^{18}\text{O}$ value of the original magma by more than 2 per mil by simply saturating it with pristine meteoric waters. Inasmuch as this calculation assumes $P_{\text{Total}} = P_{\text{H}_2\text{O}}$, this is the maximum ^{18}O depletion that can be expected by such a process. In a system where the fluid is in hydrostatic equilibrium in a fissure system open to the surface, $P_{\text{Total}} \approx 3P_{\text{H}_2\text{O}}$ and the $\delta^{18}\text{O}$ value of the magma could then only be lowered by about 1 per mil. (if $P_{\text{H}_2\text{O}} \approx 0.3$ kb, only 2.3 wt % H_2O can be dissolved in an andesite magma, Hamilton et al., 1964).

An additional mechanism is thus required to lower the ^{18}O content of the inner diorite melt, as the $\delta^{18}\text{O}$ of this postulated magma was approximately +2.5. As suggested by Forester and Taylor (1972), one possible way is for the meteoric water to enter, bubble through, and leave the melt continuously until the required amount of isotopic exchange is met. A mass balance calculation requires exchanging about one out of every four oxygen atoms in the melt by oxygen from a large reservoir of meteoric water of $\delta^{18}\text{O} = -14$. This hypothetical bubbling process would be about 10^{10} times more rapid than one involving simple diffusion of water (in solution) through the melt (Burnham, 1967). Thus the formation of a separate aqueous phase in the magma will markedly expedite the isotopic exchange process.

The fundamental problem here is how H_2O could migrate into a magma from the hydrostatic convective circulation system established in the country rocks. The silicate melt is under a lithostatic pressure that is approximately a factor of three times higher than the hydrostatic pressure in the fissure system. Open channels could not be maintained in the immediate vicinity of the magma chamber without being injected with magma. If meteoric water is to become absorbed by the magma it must penetrate the country rocks immediately adjacent to the magma chamber by grain boundary diffusion.

The problem is even more acute when it is realized that any H_2O finally able to diffuse into the magma would have experienced an ^{18}O shift to higher $\delta^{18}O$ values than those characterized by the local, pristine meteoric waters. Table 6-5 illustrates the much larger amounts of water required to produce the Stony Mountain inner diorite melt ($\delta_R^i = +7.5$, $\delta_R^f = +2.5$) with various values of $\delta_W^i > -14$.

Because it is unlikely that we can account for even as much as a 2 per mil ^{18}O depletion by direct influx of meteoric H_2O into the magma, other processes must be considered. The most likely way to produce a low- ^{18}O melt is by oxygen isotopic exchange between the already hydrothermally altered, ^{18}O -depleted country rocks and magma. Exchange between the shell of hydrothermally altered volcanic rocks (e.g. San Juan Tuff) around the magma chamber and the liquid magma would be faci-

Table 6-5

Calculated*water/rock ratios necessary to produce low- ^{18}O inner diorite melt ($\delta_R^f = +2.5$) for various δ_W^i

δ_W^i	-12	-10	-8	-6	-4	-2	0	+2
W/R	0.3	0.4	0.5	0.6	0.8	1.1	2.0	10.0

* Calculated assuming $\delta_R^i = +7.5$ and $\delta_W^f = \delta_R^f = +2.5$.

litated by the high water content of the hydrothermally altered country rocks. The maximum amount of ^{18}O depletion this process can attain is that of the δ -value of the country rocks themselves. The efficiency of this exchange process therefore depends on the surface-to-volume ratio of the magma chamber. Note that this mechanism is not one of wholesale assimilation but merely communication and exchange between oxygen in the silicate melt and oxygen in the country rocks (probably mainly feldspars and hydrous phases). Volcanic country rocks with an average $\delta^{18}\text{O} = +1.0$ would have to contribute 75% of the oxygen in this exchange process to account for the low- ^{18}O inner diorite magma. If the magma had already been lowered by 2 per mil (perhaps by direct interaction with meteoric waters) and exchanged with country rocks with $\delta^{18}\text{O} \approx 0$, then approximately equal volumes of magma and rock would be involved.

Another possible exchange model could involve direct melting of hydrothermally altered, ^{18}O -depleted country rocks in the roof zone above the magma chamber. Again, these melted rocks could have $\delta^{18}\text{O}$ values as low as the average $\delta^{18}\text{O}$ values of the hydrothermally altered volcanic rocks from which they formed, providing they did not mix with 'normal' magma. The necessary heat may in whole or in part be supplied from another intrusion (Stony Mountain gabbro?), from supply of new magma in a volcanic conduit to the surface, from superheat,

and/or from the heat of crystallization of early-formed crystals. Muehlenbachs (1973) proposed that partial melting of hydrothermally altered basalts in Iceland might result in low- ^{18}O (and low D) siliceous magmas, some of which have $\delta^{18}\text{O}$ values as low as +2.8.

Another way in which a low- ^{18}O magma might be produced is by large-scale assimilation of low- ^{18}O rocks into the magma or by the sinking of low- ^{18}O xenoliths through the magma chamber (Taylor, 1974b). Complete solution of the country rock would not be expected because the calorimetric demands are too high but oxygen isotopic exchange would still occur. Shieh and Taylor (1969a) found that xenoliths apparently rapidly exchange ^{18}O with their host magmas in a plutonic environment.

It is likely that each of the above-mentioned mechanisms may be important; the total integrated effect may give rise to a low- ^{18}O magma such as the postulated Stony Mountain inner diorite with an ^{18}O depletion of about 5 per mil. It is in just such a geological environment whereby the mechanisms can be active, since repeated epizonal igneous intrusion, ring-fracture and ring-dike formation, block subsidence, dike swarms, large-scale stoping and intermittent breccia formation would be expected to be accompanied by such developments. On the other hand, the apparent lack of any such ^{18}O -depletion in the silicate melt that occupied the Skaergaard magma chamber

(Taylor and Forester, 1973) may be due to the fact that the Skaergaard magma was intruded as a single pulse of silicate liquid that subsequently underwent a relatively simple, quiescent sequence of fractional crystallization.

Chapter 7

THE SCOTTISH TERTIARY IGNEOUS PROVINCE

7.1 Introduction

The Scottish Tertiary Province is one of the classic areas of igneous petrology. It constitutes but a part of the larger province, now present as scattered remnants, that is termed North Atlantic, Thulean or Brito-Arctic. This larger province includes northeast Ireland, the Faeroe Islands, St. Kilda, the west and east coasts of Greenland, and the eastern coast of Baffin Island.

The Scottish Tertiary province is in general characterized by transitional plateau basalts (Ridley, 1971; Thompson et al., 1972) with a number of associated central intrusive complexes (e.g. Skye, Mull, Ardnamurchan and Arran). The rocks vary from ultramafic (e.g. Rhum) to granophyres. Basaltic dike swarms typically radiate out from the intrusive centers, but are concentrated along a NNW trend (Figures 7-1 and 7-2).

7.2 Isle of Skye, Scotland

The Tertiary geology of southern Skye was first mapped in detail by Harker (1904). The mapping was done at the turn of the century, and the results were published on one-inch maps, Sheets 70 and 71 of the Geological Survey of Great Britain, Ordnance Survey.

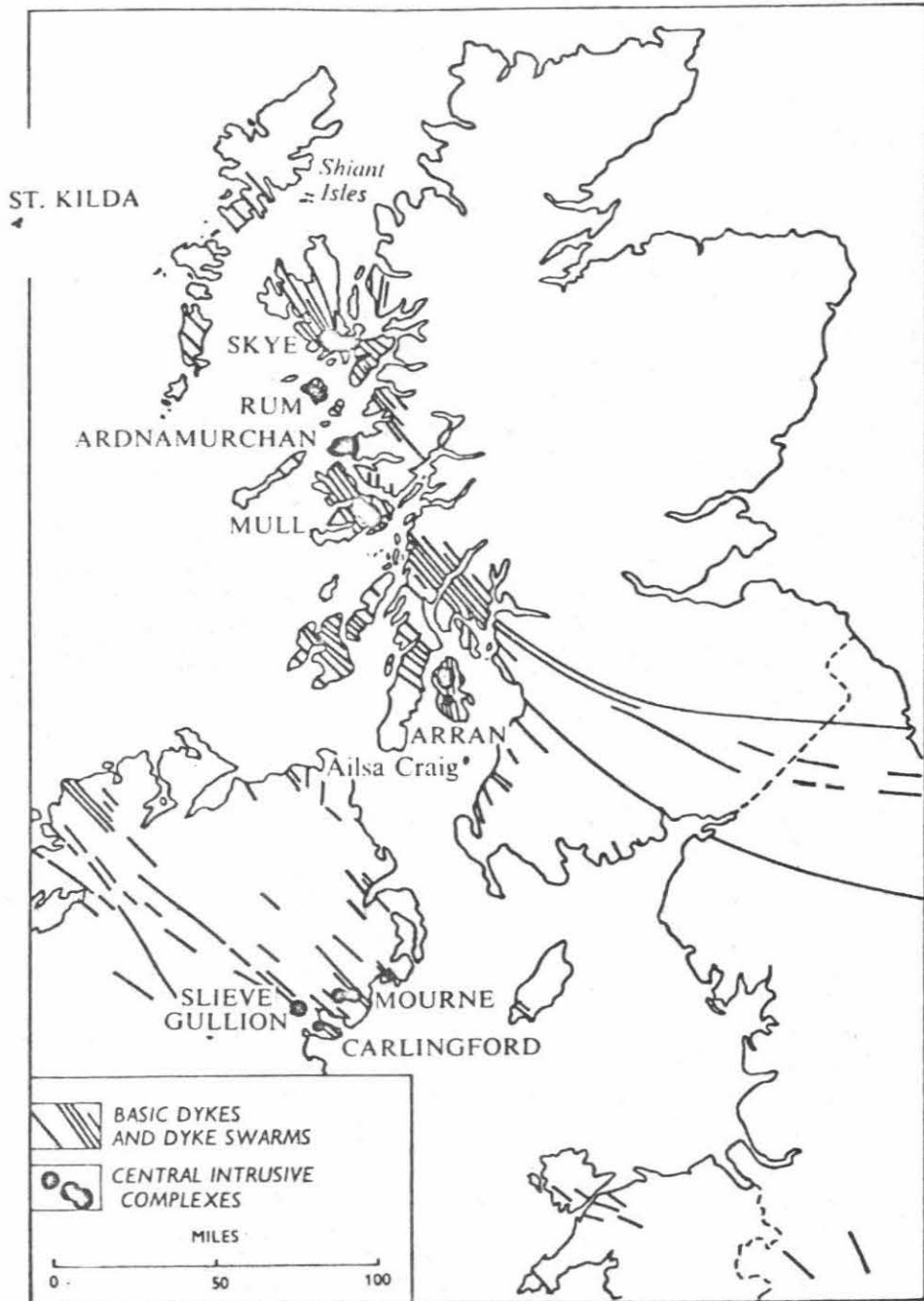


Figure 7-1. Tertiary dike swarms and major plutonic centers of Scotland, England, and northern Ireland (after Richey and Thomas, 1930).

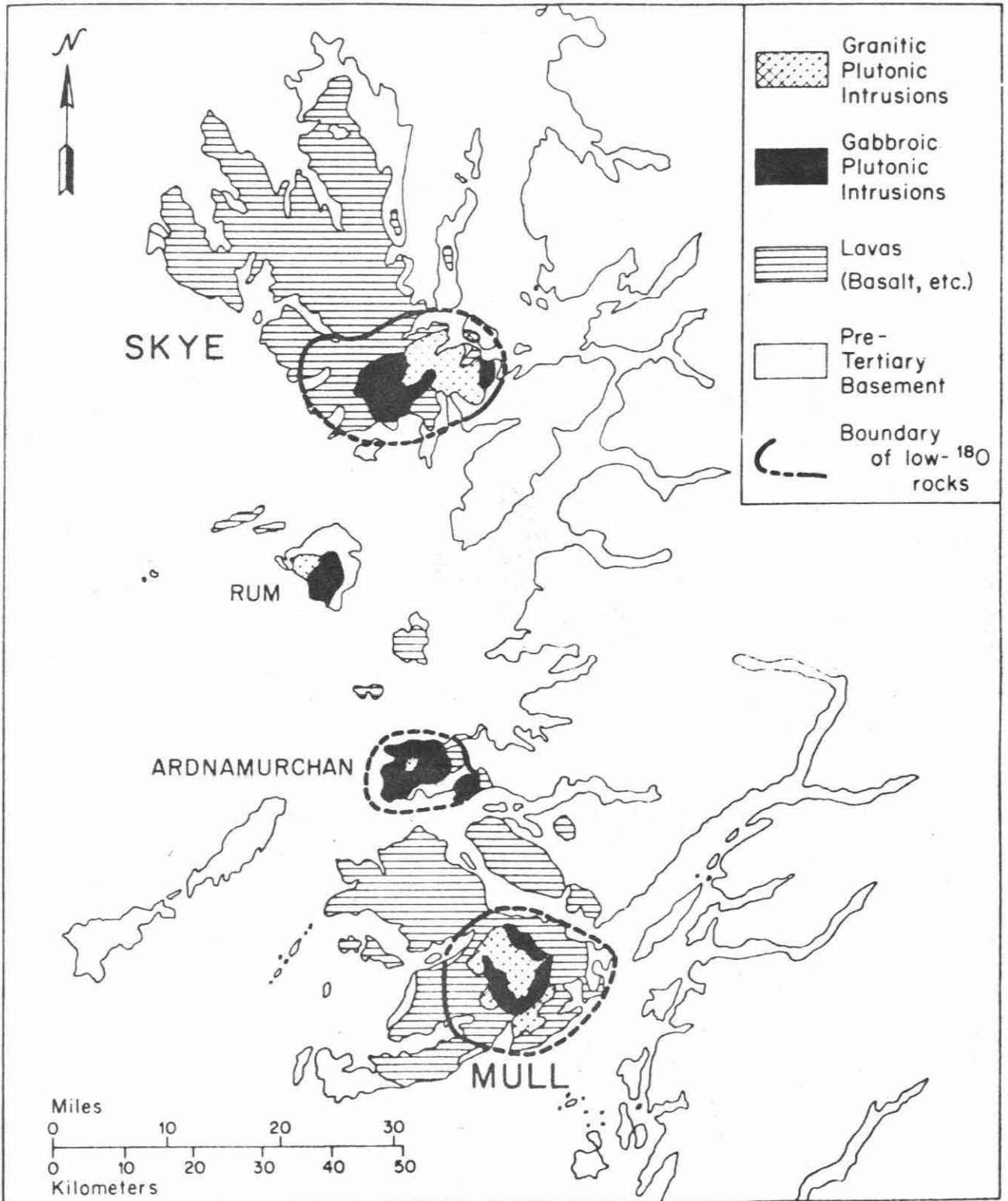


Figure 7-2. Simplified geologic map of the Inner Hebridian islands of western Scotland. The generalized outer boundaries of low 180 igneous rocks of the main volcanic centers are shown (after Taylor and Forester, 1971, and Taylor, 1974b).

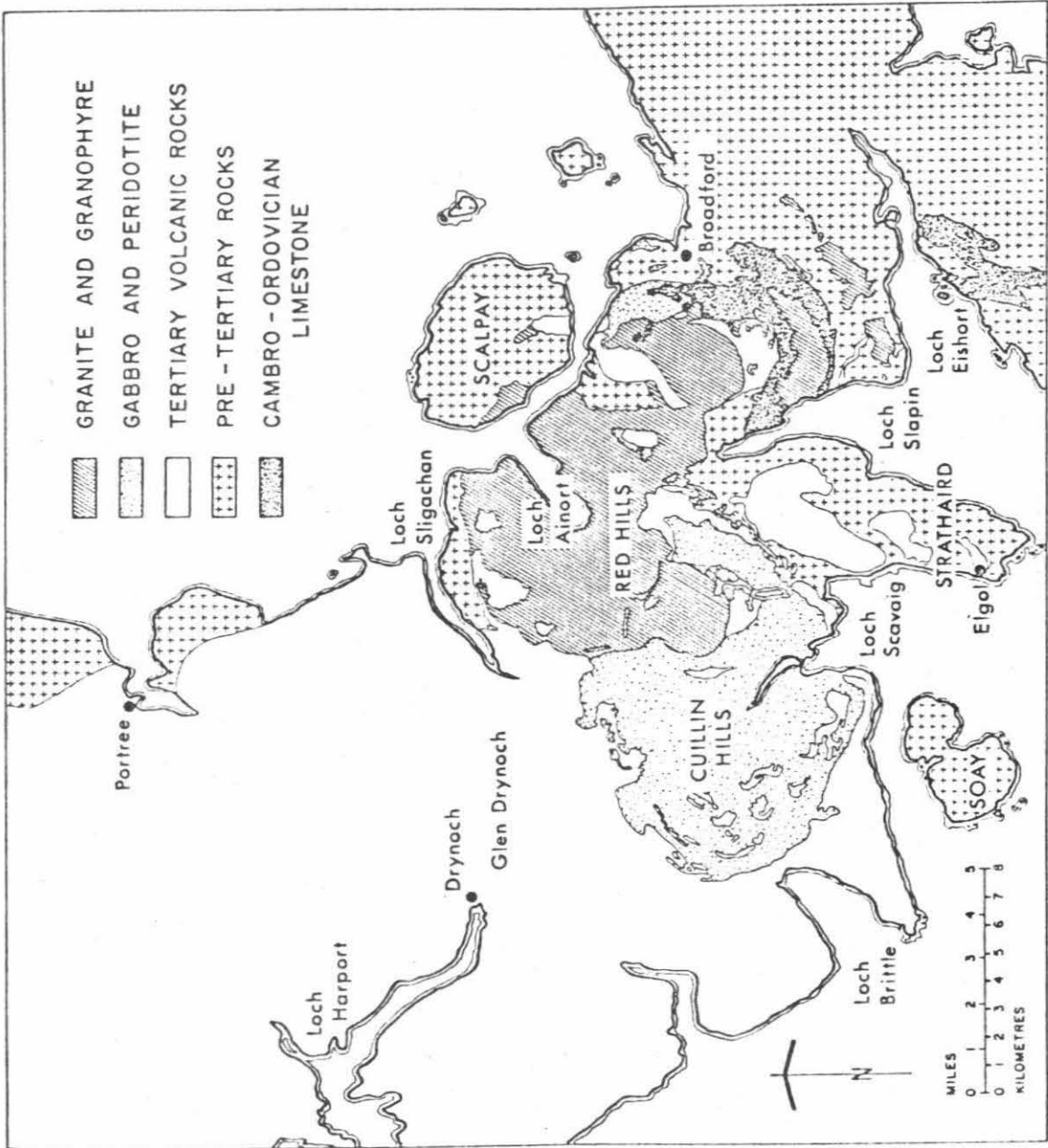


Figure 7-3. Generalized geologic map of southern Skye (modified after Harker, 1904).

Richey (1961) has given a summary account of the Tertiary igneous rocks of Skye (see Figure 7-3) and a more recent description has also been published by Stewart (1965). A large number of papers dealing with the specific localities on the Isle of Skye have appeared mainly in the 1960's. Some of the more important references are an account of the Cuillin layered intrusion by Wager and Brown (1967), a structural and petrographic analysis of the Creag Strollamus area by King (1953), detailed field and petrologic studies on the Western Red Hills by Bell (1966), Wager *et al.* (1965), and Thompson (1969), and metamorphism of the lavas on Strathaird peninsula by Almond (1964). These and other pertinent studies will be discussed in more detail below. Representative chemical analyses of the igneous rocks at Skye are given in Table 7-1. Many of these analyzed samples are from the same outcrops studied in the present work, or are from a nearby outcrop of the same rock unit.

7.3 Pre-Tertiary geology of Skye

Lewisian

Along the Sound of Sleat in southern Skye are exposed rocks of the Lewisian basement complex, a series of highly deformed and metamorphosed amphibolites and gneisses of Precambrian age. They are separated from the younger rocks to the west by the Moine Thrust.

Table 7-1

Chemical analyses of some Tertiary igneous rocks,
Isle of Skye

	1	2	3	4	5	6	7	8	9	10
SiO ₂	46.0	45.68	46.1	43.09	48.16	74.31	69.62	71.68	71.60	77.12
Al ₂ O ₃	13.7	14.66	22.8	7.51	16.55	11.71	13.91	12.55	13.30	11.11
Fe ₂ O ₃	3.6	2.88	2.39	0.52	3.07	1.63	1.18	2.29	1.81	1.72
FeO	7.1	9.67	4.10	7.14	8.14	1.67	3.01	2.40	2.64	0.71
MgO	10.2	9.82	8.99	33.48	6.94	0.04	0.46	0.24	0.12	0.06
CaO	11.1	9.37	12.81	5.75	10.08	0.61	1.73	0.92	0.93	0.11
Na ₂ O	2.4	2.14	1.23	0.65	3.29	4.11	4.27	4.28	4.21	3.55
K ₂ O	0.5	0.19	0.13	0.12	0.46	5.22	4.92	4.37	4.37	4.90
H ₂ O(+)	2.8	3.43	1.29	1.18	1.82	0.39	0.53	0.64	0.39	0.17
H ₂ O(-)	1.1	0.36			0.18	0.05	0.12	0.25	0.36	0.17
TiO ₂	1.65	1.65	0.38	0.16	0.88	0.36	0.49	0.38	0.40	0.15
P ₂ O ₅	0.05	0.07	0.03		0.13	0.03	0.14	0.03	0.05	tr
MnO	0.27	0.22	0.09	0.05	0.33	0.06	0.03	0.05	0.10	0.02
Total	100.47	100.14	100.47	100.04*	100.03	100.19	100.41	100.08	100.28	99.79
Q						29.6	21.0	27.4	27.02	37.5
Or	2.8	1.1	1.0	0.56	2.8	30.8	29.1	25.8	25.83	29.0
Ab	20.4	17.7	11.0	1.31	27.8	31.2	36.1	36.2	35.61	29.9
An	25.0	30.1	56.0	17.24	29.2		4.3	2.1	4.34	
C									0.06	
Ac						3.2				0.1
Wo	12.5	6.6	3.0	7.19	8.3	1.2	1.4	0.9		0.2
En Di	9.0	4.1	14.4	5.60	4.8	0.1	0.4	0.2		0.2
Fs	2.4	2.1	2.2	0.79	3.2	1.3	1.1	0.8		
En Hy	1.3	10.2			.8		0.8	0.4	0.30	
Fs	0.4	5.5			.4	0.9	2.7	1.2	2.88	
Mt	5.3	4.2	2.6	0.70	4.4	0.8	1.7	3.3	2.61	1.9
Ilm	3.2	3.2	0.6	0.30	1.7	0.7	0.9	0.7	0.76	0.3
Hm										0.4
Ap	0.1	.2			0.3	0.1	0.3	0.1	0.09	tr
Ne				2.42						
Water	3.9	3.8	1.3	1.2	2.0	0.4	0.7	0.9	0.76	0.3
Other	14.2 [†]	11.2 [†]	10.2 [†]	63.17 [†]	14.5 [†]					

Table 7-1 (Cont'd)

	11	12	13	14	15	16	17	18	19
SiO ₂	76.41	60.07	54.18	58.35	71.03	68.60	72.60	73.99	74.47
Al ₂ O ₃	11.71	14.22	13.74	11.62	12.86	13.51	12.98	13.02	11.32
Fe ₂ O ₃	1.68	3.71	1.88	3.31	0.69	1.59	1.88	0.76	2.06
FeO	0.77	6.65	10.79	7.32	3.61	3.83	2.08	1.60	2.22
MgO	0.17	1.39	2.42	3.40	0.50	0.63	0.47	0.31	0.78
CaO	0.42	4.35	6.34	4.73	1.54	1.89	1.38	1.22	1.69
Na ₂ O	3.62	4.02	3.46	3.50	4.31	4.07	3.55	3.43	2.79
K ₂ O	4.92	2.75	1.85	2.81	4.33	3.99	4.09	4.74	3.44
H ₂ O(+)	0.50	0.67	1.40	1.99	0.49	0.81	0.11	0.22	0.47
H ₂ O(-)	0.12	0.06	0.26	0.21	0.15	0.43	0.28	0.14	0.04
TiO ₂	0.14	1.53	1.97	2.12	0.42	0.61	0.48	0.32	0.67
P ₂ O ₅	0.04	0.60	1.30	0.91	0.11	0.15	0.06	0.05	0.06
MnO	0.002	0.26	0.30	0.25	0.06	0.16	0.07	0.02	0.06
Total	100.50	100.28	99.89	100.52	100.25**	100.27	100.03	99.82	100.07
Q	35.6	14.3	7.8	13.2	24.2	23.1	32.10	32.28	39.87
Or	29.1	16.3	10.9	16.6	25.6	23.6	24.16	27.80	20.30
Ab	30.6	34.0	29.3	29.6	36.5	34.4	30.00	28.82	23.57
An	1.2	12.6	16.5	7.7	3.0	6.8	6.48	6.11	7.98
C							0.35		0.06
Ac									
Wo	0.3	2.1	2.7	4.1	1.3	0.7			
En Di	0.2	0.7	0.8	2.1	0.3	0.2			
Fs		1.5	2.0	1.9	1.1	0.5			
En Hy	0.2	2.8	5.2	6.4	1.0	1.4	0.17	2.65	3.30
Fs		5.7	13.5	5.8	4.4	4.5	1.60		
Mt	2.1	5.4	2.7	4.8	1.0	2.3	2.73	0.93	2.99
Ilm	0.3	2.9	3.8	4.0	0.8	1.2	0.91	0.61	1.28
Hm	0.3								
Ap	0.1	1.3	3.1	2.1	0.3	0.4	0.12		0.13
Ne									
Water	0.6	0.7	1.7	2.2	0.6	1.2	0.4	0.4	0.5
Other					0.3 ^{††}			0.43	

* Cr₂O₃ = 0.39; ** CO₂ = 0.15; † Olivine; †† Calcite

1. Olivine basalt, basal lava group, Strathaird (Almond, 1964). Approximately 2 km south of SK-231.
2. Basalt, Creag Strollamus (King, 1953). 20 m west of SK-70.
3. Allivalite, Cuillin Hills (Hutchison, 1968). 3.2 km west of BM-37.
4. Peridotite, Cuillin Hills (Weedon, 1965). 1 km west of BM-37.
5. Gabbro, Creag Strollamus (King, 1953). 400 m northeast of SK-63.
6. Maol na Gainmhich Epigranite. (Wager et al., 1965). Same locality as SKY-7a,b.
7. Glamaig Epigranite (Wager et al., 1965). Approximately 2 km north of IGC-13.
8. Beinn Dearg Mhor Epigranite (Wager et al., 1965). Approximately 1.2 km west-southwest of SK-128.
9. Loch Ainort Epigranite (Bell, 1966). Same locality as BM-25.
10. Southern Porphyritic Epigranite (Thompson, 1969). 1 km east of IGC-6.
11. Southern Porphyritic Felsite (Wager et al., 1965). Same locality as IGC-13.
12. Marscoite (Wager et al., 1965). Same locality as IGC-13.
13. Ferrodiorite (Wager et al., 1965). Same locality as IGC-13.
14. Glamaigite (Wager et al., 1965). 1.7 km east of SK-503.
15. Marsco Epigranite (Thompson, 1969). 500 m south of ICG-6.
16. Meall Buidhe Epigranite (Wager et al., 1965). Same sample locality as SK-521.
17. Glas Gheinn Mhor Epigranite (Bell, 1966). Approximately 1.6 km south of SK-109.
18. Beinn an Dubhaich granite (Tilley, 1949). Same locality as SK-82.
19. Coire Uaigneich granophyre (Wager et al., 1953). 800 m southwest of SK-157.

Torridonian

In southeastern Skye, the late Precambrian Torridonian strata consist largely of about 7000 feet of essentially flat-lying sandstones, mudstones and shales (Diabaig Group) overlain by about 4500 feet of arkosic grits (Applecross Group). Elsewhere in northwest Scotland, the Torridonian is overlain unconformably by Lower Cambrian quartzites. Geochronological measurements by K/Ar and Rb/Sr whole-rock isochron methods on pebbles within the Torridonian sediments suggest a maximum depositional age of about 1100 m.y. (Moorbath et al., 1967). There is now evidence for an angular unconformity within the Torridonian (Lawson, 1965; Stewart, 1966; Gracie and Stewart, 1967). Significantly, Irving and Runcorn (1957) have found that the paleomagnetic pole positions of the Lower and Upper Torridonian differ by about 50° , and Runcorn (1964) suggested that the Lower Torridonian is much older than the Upper Torridonian. Moorbath (1969) reported a Rb-Sr whole-rock isochron age for the Lower Torridonian shales and siltstones of 935 ± 24 m.y., and that of the Upper Torridonian as 761 ± 17 m.y. (using $\lambda^{87}\text{Rb} = 1.47 \times 10^{-11} \text{yr}^{-1}$). Unfortunately, the proposed unconformity has not yet been identified in the Skye section.

Durness Limestone

The Cambro-Ordovician Durness Limestone in Skye is mainly dolomitic with layers or nodules of chert. Where affected by

the Tertiary intrusions, this unit is largely recrystallized and calcite is the principal carbonate. The limestones have been involved in a complicated thrusting event, and there is disagreement as to whether the limestone was thrust over the Torridonian in the vicinity of Creag Strollemus (Bailey, 1954), or vice versa (King, 1953).

Mesozoic

Sedimentary rocks of Mesozoic age crop out around the perimeter of the Tertiary lavas in Skye. The Triassic of central Skye consists of conglomerate, breccia, marl and sandstone. The rock fragments are commonly Torridonian sandstone or Cambro-Ordovician limestone (Richey, 1961). The Jurassic system is represented by about 1000 meters of marine and brackish water sediments, chiefly sandstone, shale, and limestone (Richey, 1961; Hudson, 1962).

7.4 The Tertiary igneous rocks of Skye

Introduction

The lavas of Skye (Plate 7-1a) cover approximately 1500 km². On the basis of sedimentary intercalations used as marker horizons, Anderson and Dunham (1966) determined the maximum thickness of lavas in North Skye to be about 2300 meters. The dominant Skye lavas vary from nepheline- to hypersthene-normative basalts (Thompson et al., 1972). The age of the igneous rocks of Skye is Eocene (Moorbath and

Welke, 1969; Moorbath and Bell, 1965) which is compatible with isotopic age measurements made on rocks from other parts of the Brito-Arctic province (Beckinsale, 1974; Purdy *et al.*, 1972; Tarling and Gale, 1968; Miller and Brown, 1965; Miller and Harland, 1963). Very briefly, the plutonic igneous complex of central Skye consists of three intrusive centers. The oldest center is the gabbroic complex known as the Cuillin Hills. This was followed by granophyres and granites of the Western Red Hills, and finally by granites, granophyres, and intrusive breccias of the Eastern Red Hills.

Cuillin gabbro complex

The mafic and ultramafic intrusive complex of the Cuillin Hills (Figure 7-4) and the Blaven (Blath Bheinn) Range (Plate 7-1b) is an oval shaped mass, approximately 13 km in the long (E-W) dimension. At least a 5 km-thick section of cumulates are present in this intrusion (Wager and Brown, 1967; see Plate 7-2). There are two separate intrusive masses that constitute the Cuillin Hills. The older unit, the Outer Gabbros, includes sheets of gabbro, intrusive tholeiites, and the Ring Eucrite (Weedon, 1961; Hutchison, 1966; Wager and Brown, 1967). The younger, main unit is a disrupted layered intrusion, ranging from dunite, peridotite and allivalites, to eucrites and gabbroic cumulates (Weedon, 1965; Wager and Brown, 1967). Contemporary as well as post-gabbro faulting has disrupted the layered sequence to some extent (Plate 7-3).

- Plate 7-1a. Looking north from Sconser Lodge across Loch Sligachan at tiered basaltic lava flows. Flows are generally about 2-10 m thick. Photo by H.P. Taylor.
- Plate 7-1b. View across Loch Slapin to east face of Blaven Range, Skye. The face shows the contact between the dark-gray Cuillin gabbros and the light-gray basalts. The Coire Uaigneich granophyre crops out at the base of the cliff near talus slopes in left center of photograph. The grassy slopes are underlain by Mesozoic sedimentary rocks; foreground is Cambro-Ordovician Durness Limestone.



Plate 7-1a



Plate 7-1b



Plate 7-2a. Layered Cuillin gabbro; strike 140° , dip 45° NE. At this locality (SK-219), average $\delta^{18}O_F = -6.5$ and $\delta^{18}O_P = -0.5$.



Plate 7-2b. Cuillin gabbro (SK-208) cut by thin leucocratic plagioclase-rich veinlets. Gabbro has $\delta^{18}O_F = +1.0$ and $\delta^{18}O_P = +2.0$



Plate 7-3. Dunite blocks (SK-270; $\delta^{18}O_{01} = +2.4$) in Cuillin gabbro. The silvery spots in the gabbro are caused by large poikilitic crystals of pyroxene. Photo by H.P. Taylor.

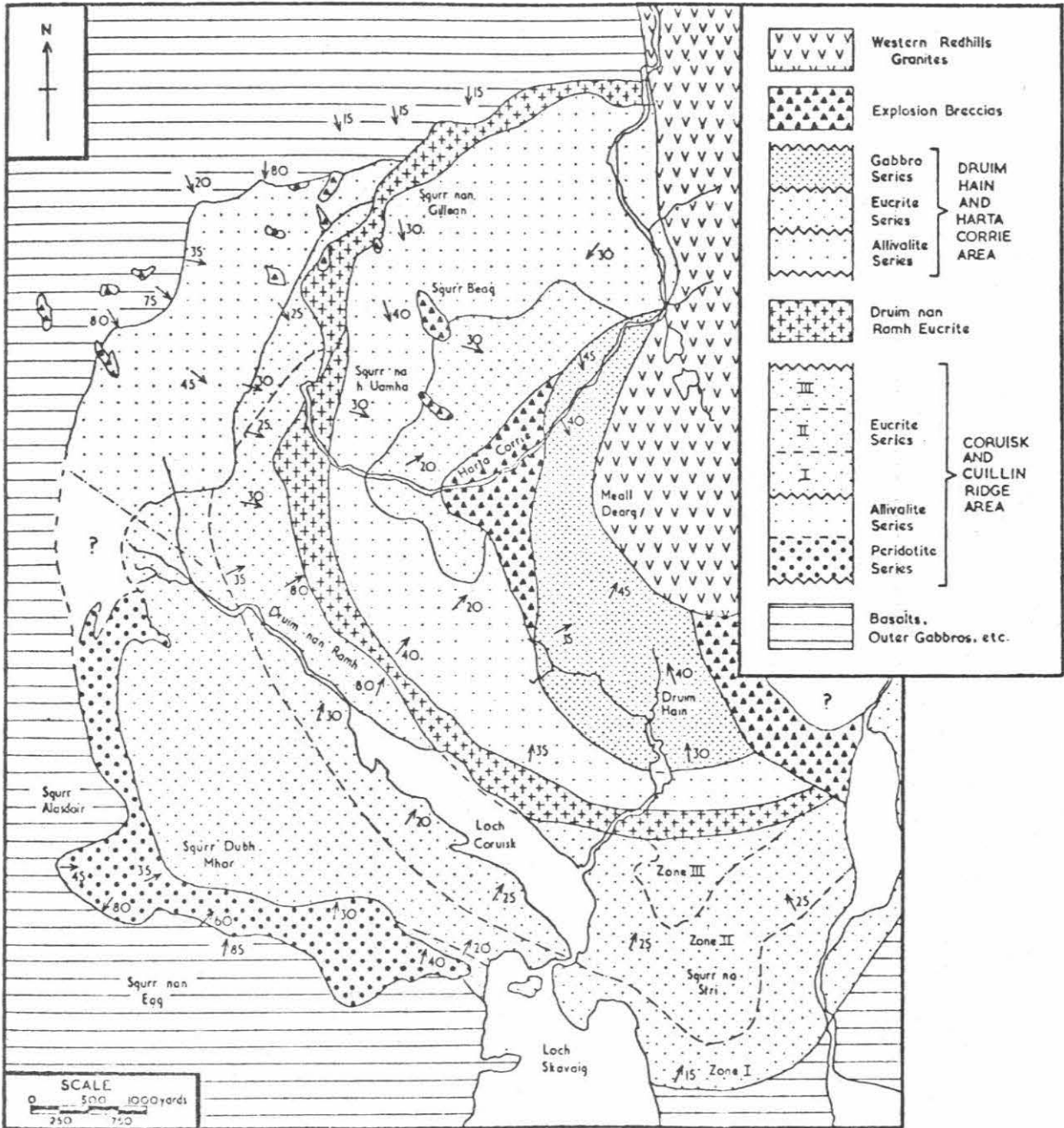


Figure 7-4. Geologic map of the Cuillin intrusion (after Wager and Brown, 1967).

The final stage of emplacement in the Cuillin complex is represented by the Loch na Creitheach volcanic vent. The vent is composed primarily of pyroclastic debris, mostly basalt (Jassim and Gass, 1970). The Cuillin complex was then truncated by the Western Red Hills granophyre along its north-eastern edge (see Figure 7-4).

Western Red Hills

The Western Red Hills complex (Figure 7-5) is emplaced into Tertiary basaltic lavas, the Cuillin gabbro and Mesozoic and Torridonian sediments. In places, for example on top of Glamaig, remnants of the roof of plateau lavas are still exposed.

The complex consists of about nine separate granitic and granophyric arcuate intrusions, with near-vertical, outward-dipping contacts. The mode of emplacement is thought to have been a combination of piecemeal stoping and ring-dike intrusion (Bell, 1966; Wager et al., 1965; Thompson, 1969). Wager et al. (1965) proposed the term "epigranite" for this type of high-level granite.

The first group of intrusions (Early epigranites, see Figure 7-5) are disposed about a NE-SW oval, centered in the vicinity of Loch Ainort. The second group of arcuate intrusions (Later Intrusions) seem to be centered about a slightly different focus, and cut across the earlier epigranites.

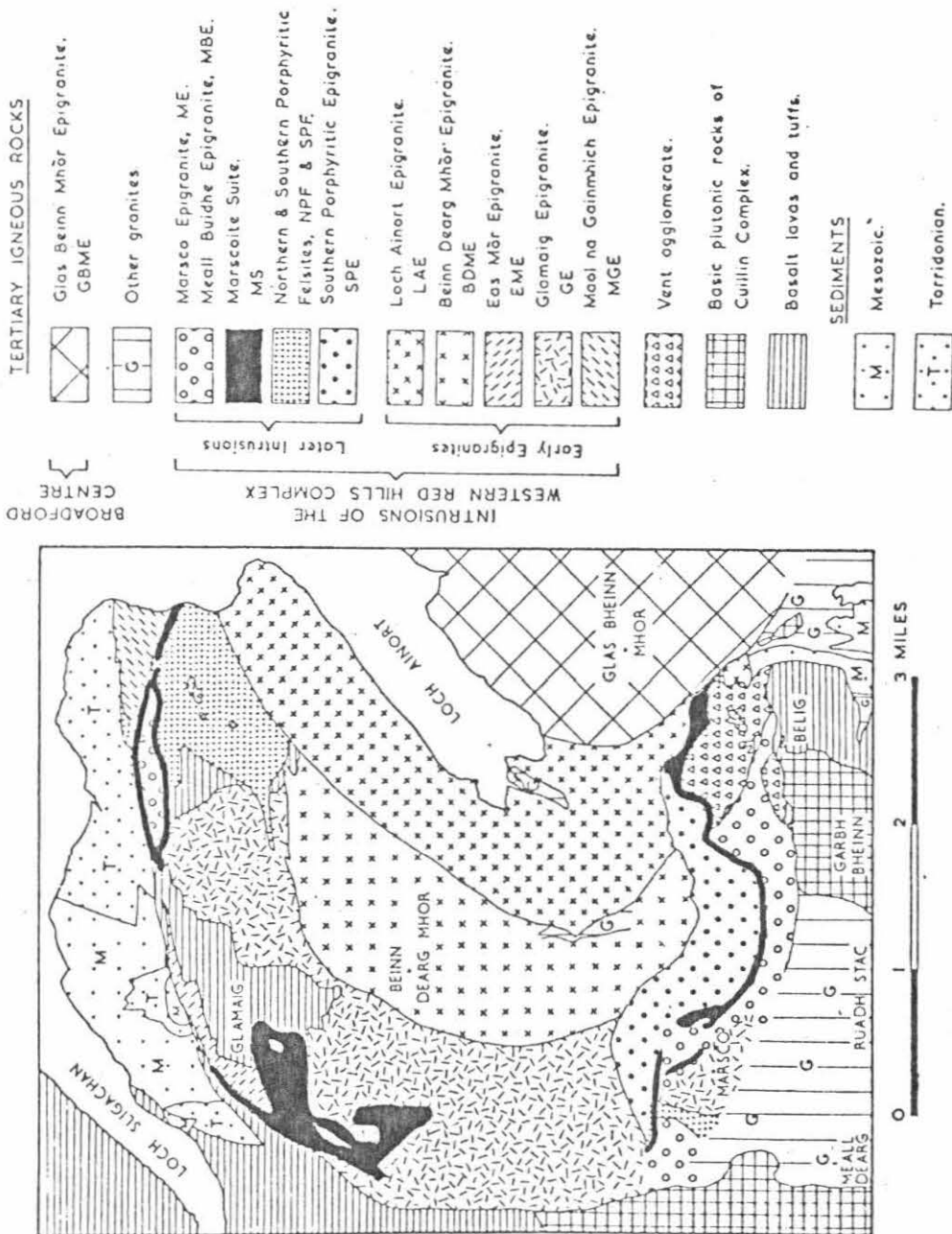


Figure 7-5. Geologic map of the Western Red Hills, Skye (after Wager et al., 1965, with corrections; see text). Note the abbreviations given here are the same as those used in the text.

Note that the apparent drafting error of Wager et al. (1965) in their Figure 1, interchanging the order of intrusion of the SPE with the NPF and the SPF, which has been perpetuated by all those who copied that figure (notably Moorbath and Bell, 1965, and Bell, 1966), has here been corrected. The SPE has been placed as the earliest of the Later Intrusions, as based on the field relationships. Note also that the positions of the GE and the MGE of Wager et al. (1965) have been switched in Figure 7-5. The age of the MGE relative to the GE has not been definitely established, although these are known to be the two oldest granitic intrusions in the Western Red Hills. The MGE is the outermost arcuate unit, and on this basis would conform to the pattern of intrusion of oldest to youngest as we moved inward towards the center. As will be discussed below, there also is a possible suggestion from the systematics of the $\delta^{18}\text{O}$ data that the MGE is older than the GE.

Quartz and feldspar generally comprise about 90% of the epigranitic rocks from Skye. The remaining minerals may include fayalite, ferrohedenbergite, alkali amphibole, biotite and opaque oxides. Alteration of the primary mafic minerals to chlorite, uralite, magnetite, epidote, serpentine, etc. can generally be observed in almost every epigranitic rock of the central intrusive complex. Such effects are occasionally so pervasive that only remnants or pseudomorphs of the primary mafic minerals remain. Practically all the granitic rocks

from the ring-dike complexes also contain highly turbid alkali feldspars (see Plate 8-2). These feldspars are almost invariably associated with granophyric textures. Mirolitic cavities are also characteristic of many of the granitic rocks from central Skye. All of the above-described mineralogical and textural features can logically be attributed to the meteoric-hydrothermal fluids responsible for the ^{18}O depletion (Taylor and Forester, 1971).

The following brief descriptions of the rocks that make up most of the Western Red Hills intrusive center are based largely on works by Wager et al. (1965), Thompson (1969) and Bell (1966). Chemical analyses for all of these rocks are given in Table 7-1.

The MGE is a hypersolvus granite with alkali amphibole. Coarse microperthite comprises approximately two-thirds of the rock. Granophyric intergrowths are restricted to the chilled contact rock. The GE is a medium grained amphibole- and biotite-bearing rock with mirolitic cavities, and the rock commonly contains a few per cent of small inclusions. Pink alkali feldspar mantles the sodic plagioclase grains; the latter mineral has an intermediate structural state. The BDME is a pyroxene granite, with phenocrysts of anorthoclase fringed by a granophyric intergrowth of quartz and alkali feldspar. The fayalite is largely altered to serpentine. The LAE is very similar to the BDME; possibly these were once one intrusion. Both intrusions have fayalite and sodic ferrohedenbergite.

The SPE is a miarolitic, leucocratic granophyre with phenocrysts of alkali feldspar and bipyramidal quartz in a granophyric base. The alkali feldspars show transitional optics. This epigranite is typically crushed and shattered. In places the pulverized material is in the form of mylonitic veins. The breccia may have been the result of explosions due to high P_{H_2O} during the later stages of solidification of part of the magma (Wager et al., 1965). The SPF contains quartz and alkali feldspar phenocrysts similar to those of the SPE, in a granophyric matrix. Note that these rocks are the richest in silica and poorest in iron and magnesium of the Skye felsic rocks (Table 7-1). The NPF is similar to the SPF, but contains more phenocrysts, in addition to blocks of vent agglomerate and small inclusions of basalt.

The MS includes marscoite, ferrodiorite, and in the northern area, glamaigite. Marscoite is somewhat chilled against the SPF, which was apparently still partially molten during the emplacement of the MS. The marscoite is characterized by xenocrysts of andesine, alkali feldspar, and quartz in a fine-grained groundmass of the same. This grades into the ferrodiorite, composed of andesine phenocrysts, pyroxene, hornblende and opaques. In some samples, the ferrodiorite also has quartz xenocrysts, and encloses masses of andesinite, granophyre, and gneiss (presumably Lewisian). The northern late intrusions have no associated ferrodiorite exposed. A

variant of the marscoite is present in the northern area, and is called glamaigite.

Harker (1904) recognized that the marscoite was a hybrid rock. The chemical compositions of the rocks, the proportions and the types of phenocrysts, and the close association in space and time of marscoite, ferrodiorite, and the SPF support the suggestion that the marscoite is a product of mechanical mixing of approximately 70% ferrodiorite and 30% SPF (Wager et al., 1965; Thompson, 1969).

The MBE contains up to 20% of oligoclase phenocrysts rimmed with turbid alkali feldspar, in a groundmass of alkali feldspar and quartz. Mafic minerals include hornblende, biotite, and pyroxene. The ME is typically non-porphyritic and miarolitic; otherwise it is similar to the MBE.

Eastern Red Hills

The country rocks into which the granites of the Eastern Red Hills (Plate 7-4) were emplaced are compositionally much more varied than elsewhere in central Skye. The country rocks include Mesozoic sediments, Durness limestone, Torridonian sandstone, and Tertiary basalts and agglomerates (Figure 7-6). The sequence of intrusion is not as well determined in the Eastern Red Hills as it is in the Western Red Hills, but possibly except for the BDG the order of intrusion of the granites seem to correlate fairly well with the type of relationship between age and geometry exhibited by the Early Epigranites of



Plate 7-4. View to the NE across Loch Slapin of Beinn Dearg Mhor (left) and Beinn Dearg Bheag, both of which constitute the southwestern half of the Beinn na Caillich granophyre of the Eastern Red Hills. The grassy slopes below Beinn Dearg Mhor are underlain by Mesozoic shales, whereas the outcrops across the Loch are of Cambro-Ordovician Durness Limestone.

the Western Red Hills. Namely, the sequence of intrusion appears to be from the outside of the complex inward to the center (i.e. GBME → BCroG → AFG → BCG). Thus the BCG would be one of the latest major granitic intrusions in Skye (Stewart, 1965; see Figure 7-6).

The principal intrusions of the Eastern Red Hills center in terms of their relative age relationships, are as follows (Stewart, 1965):

- | | | |
|----|---|-----------------------|
| a) | Olivine-gabbro sheets in basalts of Beinn na Cro and Creagan Dubh | Older than d. |
| b) | Broadford gabbro (olivine-free) | Older than e. |
| c) | Glas Bheinn Mhor-Dunan epigranite, GBME | ? |
| d) | Beinn na Cro granite, BCroG | Older than h, also g? |
| e) | Allt Fearna granite, AFG | Older than h, also g? |
| f) | Beinn an Dubhaich granite, BDG | Older than g? |
| g) | Kilchrist Hybrids | Older than h. |
| h) | Beinn na Caillich granophyre, BCG | |
| i) | Composite sills | Relative age unknown |

The GBME cuts the Western Red Hills granites. It contains plagioclase phenocrysts in a granophyric groundmass of quartz and alkali feldspar. Numerous partially digested xenoliths are present. It has been suggested that the BCroG, AFG, and BDG may be parts of the same arcuate body. The BDG, however, is in many respects unique: (a) it was emplaced into limestone country

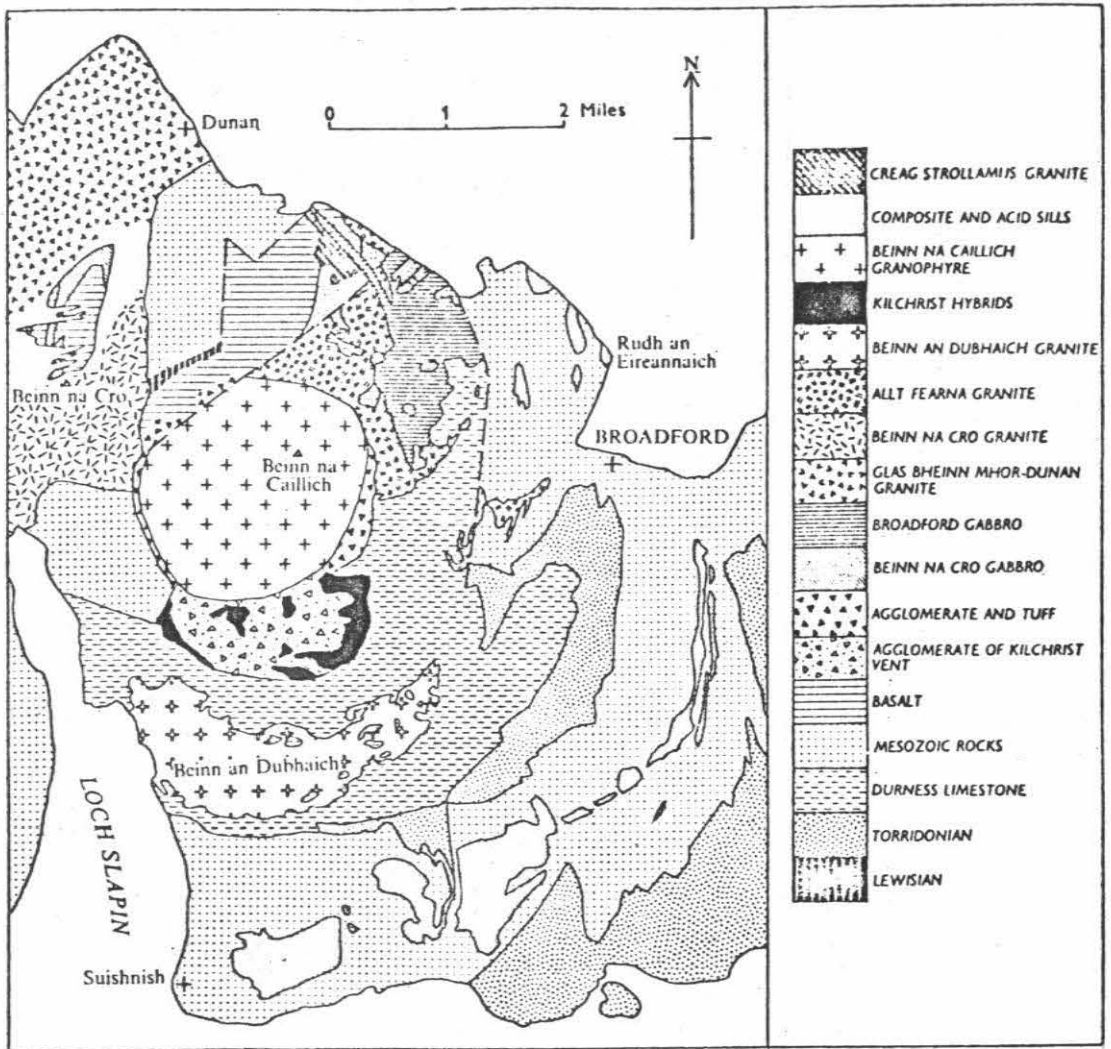


Figure 7-6. Geologic map of the Eastern Red Hills, Skye (after Stewart, 1965). Abbreviations used in the text for these rock units are given in Table 8-1.

rocks, (b) the inversion temperatures of quartz from the BDG are similar to those of quartz from rhyolites, (c) the feldspars exhibit intermediate optics (Tuttle and Keith, 1954), and (d) this granite has produced contact metamorphic skarns with boron- and fluorine-bearing minerals (Tilley, 1951; 1949).

Excellent examples of composite sills intruding Mesozoic sediments are to be found in an arcuate belt extending from Suishnish to Broadford. A felsic member almost always occurs between two mafic ones, and when evidence of their relative age is obtainable, the felsic rock is always found to be younger than its mafic margins. The Rudh' an Eireannaich (R an E) sill is a remarkable example of such a composite sill, with basaltic margins, felsic center, and hybrid zones indicative of mixing of two liquids (Buist, 1959).

Chapter 8

ISOTOPIC RESULTS: ISLE OF SKYE, SCOTLAND

8.1 Introduction

All the $\delta^{18}\text{O}$ and $\delta^{13}\text{C}$ values for the analyzed minerals and rocks from the Isle of Skye are given in Table 8-1, and presented in Figures 8-1, 8-2, and 8-3. The hydrogen isotopic analyses are presented in Table 8-2 and Figure 8-4. The $\delta^{18}\text{O}$ values in this study cover an enormous range (-7.1 to +21.4). This range is extended upward to +30 if we include the carbonates analyzed for $\delta^{18}\text{O}$ by Urey et al. (1951) in their work on the paleotemperatures of a Jurassic belemnite from Skye. Hydrogen isotopic variations are also very large, extending from -38 to -132.

The hydrogen isotopic data will be considered first, followed by a discussion of the $^{18}\text{O}/^{16}\text{O}$ systematics. To simplify the discussion of the data, each major geologic unit is examined in detail in a separate section. This study of southern Skye constitutes the most detailed oxygen isotopic program yet undertaken on a single igneous complex. Three hundred and seventy-six separate samples have been analyzed for their $^{18}\text{O}/^{16}\text{O}$ ratios. The major impetus for this program came from the preliminary work of Taylor (1968) and Taylor and Forester (1971); it was felt that a detailed study of the low- ^{18}O rocks of Skye would contribute markedly to our understanding of the detailed mechanism of meteoric water-rock interactions at high temperatures.

Figures 8-1 and 8-2 (in pocket).

$\delta^{18}\text{O}$ analyses of minerals and rocks of Skye. The geologic units can be identified with reference to Figures 7-4, 7-5, and 7-6. Black dots = sample localities; no symbol = whole rock; Q = quartz; q = Q phenocrysts; K = alkali feldspar; k = K phenocrysts; F = plagioclase; f = F phenocrysts; P = pyroxene; A = amphibole; Ol = olivine; C = calcite; D = dolomite; Ep = epidote; m = miarolitic; g = granophyric; c = calculated. Cuillin sample IGC-15 ($\delta^{18}\text{O}_F = -5.4$), near the contact with the Western Red Hills, is plotted in both Figures. The details of the contacts from the Western Red Hills, as well as the $\delta^{18}\text{O}$ data, have been omitted from Figure 8-1. The scales are the same in both Figures.

Figure 8-3. $\delta^{18}\text{O}$ analyses of minerals and rocks of Skye in the area not covered by Figures 8-1 and 8-2. Symbols as above.

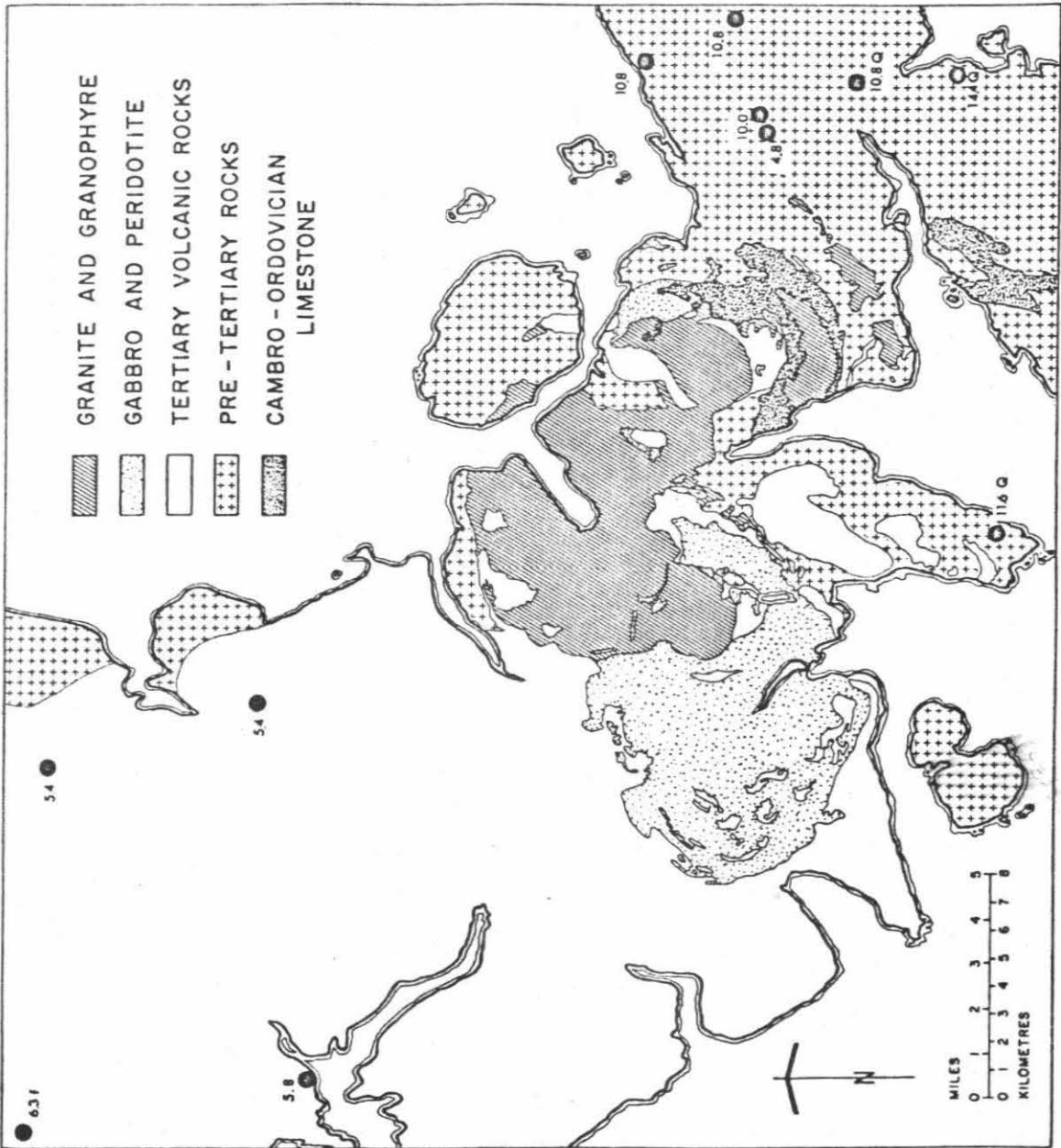


Figure 8-3

Table 8-1

$\delta^{18}\text{O}$ and $\delta^{13}\text{C}$ analyses of minerals and rocks
from the Isle of Skye, Scotland

Sample ¹ (SK-)	Mineral ²	$\delta^{18}\text{O}$ (‰)	Remarks ³
Basaltic volcanic rocks			
39	WR	-2.0	Seriz pheno of plag (1mm) in aphanitic gdmass of seriz plag, chl, mag, and ep. Amyg filled with chl, qtz, ep, and ct. Ep veinlet cuts rock.
60	WR	-3.4	
61	WR	-3.3	
62	WR	-3.4	
67	WR	-6.6	Highly amyg basalt.
70	WR	-6.0	
122	WR Ct	+1.9±0.0(2) +6.1	Amyg basalt Veinlet in basalt. ($\delta^{13}\text{C}=-6.5$)
143	WR	-1.4	
144	WR	-0.2	
153	WR	-4.4	Aphanitic mag-rich basalt, with seriz plag, mag, chl. ep, and px. Cut by veinlets filled with zeolites, ep, and white mica.
155	WR	-5.2	
159	WR	+5.4	Melanocratic basalt, 5.5km south of Portree.
161	f, clear f, green	+6.3 +6.3	'Big-feldspar' basaltic mugearite, 3km SW of Loch Greshornish, near Upperglen.
164	WR	+5.8	Clear, oscillatory zoned plag pheno (0.7mm) in intersertal aphanitic gdmass of plag, chlorophaeite, mag, and px. Chl pseudo after ol pheno.
165	WR	+4.7	Basalt with plag pheno.
166	WR	+4.8	Similar to SK-164, except slightly coarser grain size and more plag-rich.
168	WR	+0.4	Similar to SK-164, except interstices between plag v cloudy and sericite and mag-rich.
169	WR	+2.2±0.0(2)	Amyg basalt.

Table 8-1 (Cont'd)

Sample (SK-)	Mineral	$\delta^{18}\text{O}$ (‰)	Remarks
170	WR	+4.7	Highly amyg basalt.
231	WR	+3.0	
236C	WR*	+1.1	Slightly cloudy, seriz plag, chl after px and ol, mag-rich px, and ep. Amyg filled with chl and ct.
238A	WR	+3.8	
239A	WR	+1.6	Same as SK-168, except with ep- and ct-filled amyg.
239D	Ep	+1.7	Cryptocrystalline ep-rich veinlet cutting ep- and ct-rich basalt; similar to SK-239A.
240	WR	+2.1	
241B	WR*	+1.5	Reddish volcanic rock, with 3cm long amyg with ct and chl. 7m from SK-241A. Similar to SK-236C.
242	WR*	+2.5	Similar to SK-241B. Fractured basalt.
244	WR*	+3.1	Pilotaxitic; seriz plag, ol, and px all altered to chl, mag, ct, and hem.
245	WR*	+3.1	Ol pheno (0.8mm) now completely altered to ct, chl, and iddingsite, with cracks and rims totally sheathed in opaques. Clear to dusty zoned plag, fresh to altered px, mag, hem, ct, and apatite. Amyg with ct and chl.
281B	WR	-1.3	3m from contact with Cuillin gabbro. Fresh, equigranular (0.3mm) rock with diffusely zoned, clear to slightly dusty plag, dusty px, spinel, and apatite.
282	WR	-2.7	
500	WR	+3.1	
501A	WR	+0.6	
517	WR	-6.0	Aphanitic rock with feld, chl, opaques, sericite and ep. Cut by veinlets of ep and chl. Ep has hundreds of inclusions of some needle-like mineral.
518	WR	-7.1	Similar to SK-517.
519	WR	-5.6	
523	WR	+1.4	

Table 8-1 (Cont'd)

Sample (SK-)	Mineral	$\delta^{18}\text{O}$ (‰)	Remarks
524	WR	+2.3	
525	WR	+4.1	
526	WR	+3.6±0.2(2)	
527	WR	+5.7	
529	WR*	+4.3	
530	WR*	+3.3	
SKY-2	WR	-3.6	
SKY-17	WR	+5.4	
SM/67/45	WR	+5.8	
Volcanic rock samples exclusive of basalts			
31	WR	+0.7±0.1(3)	Tuffaceous agglomerate. Matrix of devitrified welded glass, qtz and feld, with strong flow banding, with pheno of embayed euhedral xls of qtz, K (0.5mm), and rock fragments (1mm).
33	WR	-0.3	Kilchrist vent agglomerate. Angular fragments ($\leq 1\text{cm}$) of altered basalt, quartzite, and carbonate, in a fg comminuted matrix rich in chl, ct and sericite.
30	WR*	+10.2	Quartzite fragment from Kilchrist vent agglomerate. Subangular fragments up to 30cm across.
30a	Ct	+1.4	Calcareous sandstone fragment, Kilchrist vent. ($\delta^{13}\text{C}=-3.5$).
32	WR	-2.4	Micro-adamellite. Aphanitic, gray-green.
34	WR	-0.6±0.1(2)	Quartzite fragment from Kilchrist vent.
54	WR	-1.6	Vent agglomerate.
222	WR	-5.1	5cm-thick felsic veinlet in volcanic agglomerate. Seriz, cloudy to turbid feld, ep, amph, opaques and apatite.
223	WR	-7.0±0.1(2)	Basaltic tuff. Altered fragments in an aphanitic gdmass rich in chl, opaques, ep, and feld needles.
224	WR	-6.3	Basaltic agglomerate.
247	WR	-3.2	Volcanic agglomerate. Dusty to cloudy feld (0.1mm) ep, opaques, and chl, with trachytic texture. Some vesicles with qtz and chl.

Table 8-1 (Cont'd)

Sample (SK-)	Mineral	$\delta^{18}\text{O}$ (‰)	Remarks
249A	WR	-0.7	Rhyolite. Fine flowbands, largely qtz-feld, with some lensoid areas with coarser (0.08mm), qtz-feld intergrowths.
251	WR*	-3.1	Volcanic breccia; most of the fragments are of basaltic volcanic rocks; some are gabbro.
Dikes, sills, and sheets (basaltic, unless noted otherwise)			
5	WR	+3.3	2m thick; cuts lmst. Sample 5cm from contact.
10	WR WR	-3.6 -3.8	Plag pheno (0.2mm) in pilotaxitic structure, wet in an altered aphanitic gdmass of feld, chl, ep, ct, and sericite. 4cm thick dike. Cuts BDG.
17	WR	+7.9	Clear plag pheno (0.4mm) in gdmass of clear to dusty plag, px, opaques, and chl. Dike cuts shales.
19	WR	+6.9	Gabbroic intrusion; subophitic, generally quite fresh. Clear to slightly cloudy, zoned plag (1.1mm) with chl along cracks; px fresh, but some showing incipient alteration to chl; opaques, and minor gphy intergrowths.
20	WR	+6.4	Gabbroic sheet at base of SK-22.
22	WR	+5.8	Felsite sheet; m. Pheno of embayed qtz (0.4mm), cloudy plag (1mm) and turbid K (1mm), in a partially gphy gdmass of qtz, seriz feld, biot, and opaques.
24	WR	+7.9	Similar to SK-19, except grain size $\sim 0.3\text{mm}$. 3m from contact with shales.
25	WR	+9.1	Contact with shales. Same as SK-24, except grain size $\sim 0.1\text{mm}$, and more chl.
28	WR	-0.6	Felsic portion of composite sill.
29	WR	-1.0	Mafic central portion of composite sill.
45	WR	$+4.6 \pm 0.2(2)$	Pre-BDG dike. Seriz plag; px altered to amph, and chl, opaques. Cut by veinlets rich in amph. 3cm from lmst contact.
46	WR	+1.1	Pre-BDG dike; 15 m from contact.

Table 8-1 (Cont'd)

Sample (SK-)	Mineral	$\delta^{18}\text{O}$ (‰)	Remarks
47	WR	+2.8	30m from contact.
82	WR	+7.5	1m from BDG contact. Dike is 1m thick and cuts 1mst.
83	WR	+8.4	Same dike as SM-82.
86	WR	+4.8±0.1(2)	Amyg basaltic dike cutting sandstone.
93	WR	+5.8	Cuts Lewisian (SK-99); center. Fresh plag and px in subophitic texture; chl after ol and in interstitial areas; mag; chl amyg.
94	WR	+6.0	Cuts Lewisian; contact. Same dike as SK-93.
100	WR	+7.0	Trachyte cutting Lewisian (NG 661 093).
102	WR	-0.5	Flow-banded pitchstone dike in basalt. Felsic spherulites, some with concentric structure, and dusty K and qtz (β -morphology) pheno (1mm) in devitrified felsic gdmass, some gphy textures.
106	WR	+0.1	35cm thick dike. Strike 130°, dip 55°W.
121	Ct	+3.8	Veinlet in dike cutting shales ($\delta^{13}\text{C}=-6.7$).
154	WR	-2.1	Dike cuts basalt; Strike 130°, dip 90°.
167	WR	+3.9±0.2(3)	Subophitic textured diabase, with clear, zoned plag, v fresh px (1mm), chl pseudo after ol (and some px), mag, and ct.
188	WR	-2.9	3m thick dike in 1mst; Strike 150°, dip 90°. Sample from center.
193	WR	+0.2	1m thick aphanitic dike cutting BDG; strike 140°, dip 90°. Sample from center. Clear to dusty, zoned plag, dusty px altering to chl; mag, ct, and sericite. Amyg with qtz, ct, and chl.
194	WR	-2.0	Same dike as SK-193; contact.
200	WR	+5.2	Gray, porphyritic sheet.
210	WR	-4.0	Cone sheet in Cuillin Hills.
211	WR	-1.8	Dike cutting SK-210.
213	WR	-3.1	Cuillin radial dike; strike 90°, dip 60°.

Table 8-1 (Cont'd)

Sample (SK-)	Mineral	$\delta^{18}\text{O}$ (‰)	Remarks
225	WR	-2.6	Felsic Cuillin dike. Glomeroporphyritic pheno of corroded β -morphology qtz and v cloudy to turbid feld (1.0mm), with minor gphy textures, in aphanitic gdmass of qtz and seriz feld.
232	WR	+4.3	Basaltic intrusion in lmst.
235A	WR*	+5.0	1m thick dike in shale; strike N, dip 78°E; similar to SK-235D.
235D	WR*	+3.3	01 pheno (2mm) now completely altered to talc, mag, and chl, in subophitic gdmass of clear to seriz, zoned plag (1mm) and fresh px; mag.
237B	WR	-5.0	2.2cm from contact with shales.
238B	WR	+2.6	Center of 1m thick dike; strike 8°, dip 90°.
241A	F WR	+2.5 +2.0±0.1(2)	1m thick dike cutting SK-241B; strike 145°, dip 90°. Fresh px and clear zoned plag, with intersertal mag and palagonite.
250	WR	-0.3	
258	WR	+1.1	1m thick dike cuts SKY-19; strike 160°, dip 85°W. Sample center.
265	WR	+2.9	Granitic dike; 8cm thick in Cuillin. Qtz (35%, 0.6mm), cloudy to turbid plag and K (60%), amph, chl, ep, sphene, and opaques.
266A	Q WR	+5.7 +4.8	3cm thick granitic dike, cuts Cuillin.
268B	Q WR	+2.2 +0.4	40cm thick biotite-bearing granitic dike, cuts gabbro; strike 175°, dip 90°.
285D	WR	+5.4±0.2(2)	Clear plag pheno (1.5mm), in subophitic textured clear fresh zoned plag and fresh px, with interstitial palagonite (?); mag. Sample from center of 3m thick dike (strike 135°, dip 90°) that cuts GBME.
292A	WR	+4.7	Pre-BDG dike with 1.5mm cloudy plag pheno in an aphanitic gdmass of seriz feld, biot, chl, and mag.
515C	q k WR	+3.8 -2.1 -1.4±0.2(2)	Felsic dike cutting sandstone. Pheno of β -morphology qtz (1.2mm) and cloudy K (2mm) in an aphanitic, partially gphy gdmass of qtz and K.
528	WR*	+4.1	

Table 8-1 (Cont'd)

Sample (SK-)	Mineral	$\delta^{18}\text{O}$ (‰)	Remarks
531A	WR	+4.2±0.0(2)	Center of 2m thick dike cutting GBME. Similar to SK-285D except more chl.
532B	WR	+5.9	Dike cutting GBME. Pheno of oscillatory zoned, clear to cloudy plag (1.3mm), px, and qtz, in an aphanitic gdmass of seriz feld, qtz, chl and mag.
533	WR	+2.2±0.0(2)	Center of 1m thick dike.
534C	WR	+5.4	Center of 2m thick dike cutting sandstone. Zoned plag, with myriads of needle-like inclusions, px, chl, biot, ct, sericite, and mag.
SKY 4	WR	+5.2	
SKY 5	F WR	+1.0 -2.1	
SKY 6	WR	-3.2	
SKY 8	WR	-2.3	
SKY 18	WR	+7.4	
SKY 19	WR	+1.3	
SKY 20	WR	+1.4	
SKY 21	WR	+1.4	
SKY 25	WR	+0.3	
SKY 27	WR	+0.1	
SKY 28	WR	+4.8	
SKY 30	WR	+5.5	
BM-10	WR	-2.7	
BM-53	WR	+2.1	
SM/67/35T	WR	+0.1	
SM/67/35M	WR	+1.4	
Cuillin complex			
208	F P	+1.0 +2.0	Laminated gabbro; clear, fresh plag (40%, 0.8mm) in mosaic texture; cpx (60%, 1mm) fresh to partly altered to chl; ol (tr) altered to talc; apatite. Thin fractures traverse the rock.

Table 8-1 (Cont'd)

Sample (SK-)	Mineral	$\delta^{18}\text{O}$ (‰)	Remarks
212	F (mg)	-1.4	Dusty plag (40%, 4mm), seriz along cracks; cpx (60% up to 4cm) quite fresh, but has opaque alteration along cracks. Minor chl. Cuspate grain boundaries.
	F (cg)	-3.0±0.1(2)	
	P (mg)	+3.2	
	P (cg)	+2.7±0.0(2)	
215	F	-3.6	Similar to SK-208 with mag. Seriz and chl most intense as we approach the thin fractures and veins. V well laminated.
217	F	-4.2	Well laminated gabbro. Plag (30%, 1mm) is clear, but cracked and veined by chl; cpx (50%, 1mm) as in SK-212; mag (20%, 1mm) as intercumulus phase, ol now mag, chl and talc. See Plate 8-1b.
	P	+2.7	
	M	-1.4	
219	F	-6.3	Passed max mag setting on Frantz (~50%). Passed intermed mag setting (~30%) Passed low mag setting (~10%) Passed v low mag setting (~10%) Average plag Extremely well laminated cumulate. Clear to v cloudy seriz plag, highly fractured and cracked; cpx altering to chl and ura-lite, esp along cracks and rims; mag and ep. Intensity of alteration increases as you approach main fractures that cut rock.
	F	-6.7	
	F	-6.9	
	F	-7.1	
	F	-6.5	
	P&A	-0.5	
226	F	-4.8	Passed through at high mag setting (~50%). Passed through at low mag setting (~50%). Extremely fine dusty gray zoned plag (2mm); ol (2mm), fresh except for minor talc & opaque alteration on rims and cracks; cpx as in SK-212. Main mafic alteration is adjacent to fractures that cut the rock.
	F	-5.6	
227	F	-0.1	
229	f	-3.2	Clear, fresh plag pheno (1cm) in mg matrix of clear to dusty plag; dusty px; ol mainly fresh, but some altered to talc, bowlingite and mag; sericite.
253B	f	+2.5	Cracked & cloudy plag pheno in m-cg sub-ophitic matrix of v fresh px, v cloudy, seriz plag; chl & mag.

Table 8-1 (Cont'd)

Sample (SK-)	Mineral	$\delta^{18}\text{O}$ (‰)	Remarks
260	F	+0.4	Well laminated gabbro; v fresh zoned plag (50%, 2mm), v fresh cpx (45%, 1mm), ol as in SK-229 (2.5mm). See Plate 8-1c.
	P	+0.7	
	Ol	+1.3	
263	F	+0.4	Laminated; equigranular, mosaic texture, probably recrystallized. Plag, v fresh, clear (60%, 0.2mm); cpx (30%, 0.2mm), v fresh; ol (10%, .2mm) generally fresh; some replaced by talc, chl, and mag. Rock is cut by thin veinlet of chl.
264D	F	-0.6	At contact with dike; zoned, fresh, clear plag (80%, 5mm), seriz along cracks, & some vfg ep in cracks where ep veinlets cut the rock; fresh px (15%, 2cm) somewhat cracked & veined by opaques; mag (2%, 1mm), ol, now largely chl, serp, talc, biot & opaques.
	P	+1.5	
266B	F	-0.3	Similar to SK-260, except with plag megacrysts; ol v fresh; mosaic texture.
269	F	+1.9	Clear, v fresh zoned plag, fresh cpx, & fresh ol with opaque rims; mag. Px poikilitically encloses other phases.
	P	+3.2	
270	Ol	+2.4±0.0(2)	Dunite block, 2m x 2m, in gabbro (see Plate 7-3). Fresh ol (\approx 2mm) in mosaic texture with trains of dust-like opaque inclusions; spinel. Thin veinlets (chl, talc?) cut rock.
273	F	-2.2	Similar to SK-226.
274	F	-1.3±0.2(2)	Slightly zoned, highly fractured & veined seriz plag (40%, 3mm); cpx (55%, 1.5cm) cracked, with dusty opaques along cleavages, & veined by chl; fresh ol, with minor talc, bowlingite & mag.
	P	+0.7±0.0(2)	
275	F	-1.8±0.2(2)	Similar to SK-260 with dusty rims on cpx; also layer of fg fresh gabbro similar to SK-263.
276	F	-2.7±0.2(3)	Same as SK-260, with v fresh ol.
280	F	-3.0	Extremely well laminated cumulate, similar to SK-226. All minerals unaltered except for dusty inclusions. Minerals elongated parallel to layers.

Table 8-1 (Cont'd)

Sample (SK-)	Mineral	$\delta^{18}\text{O}$ (‰)	Remarks
281A	F	-3.2	5m from basalt contact. Clear to inclusion-rich plag pheno (3mm), in f-mg mosaic texture of clear to faintly dusty plag, cpx, fresh ol, mag & biot.
	WR	-3.4	
H4058	F	-3.0	Passed through as max non-mag fraction.
	WR	-0.3	
H4601L	WR	+0.3	
IGC-15	F	-5.4	
SKY 24	F	-3.8	
	P	+1.6	
SKY 29	WR	-2.3	
BM 37	WR	+2.7	
Broadford gabbro			
51	F	-3.5	Densely fractured & veined rock; green pleoc amph (1.5mm) with patchy biref; highly altered seriz, cloudy to turbid plag, often with chl alteration along cleavages & cracks, & intense pinkish seriz plag on rims; mag, chl, ct, ep, talc (?), sphene, and apatite.
	A	-1.9	
	WR	-3.1	
57	WR	-4.2	Feldspar-rich vein cutting gabbro similar to SK-51. Patchy, clouded K, with minor gphy texture; ep.
SKY 16	WR	-2.7	
Granitic and granophyric rocks			
Maol na Gainmhich Epigranite (MGE)			
511B	Q	+5.2	V cloudy to turbid K (2.6mm); cracked qtz (1mm) with trains of dusty inclusions; mafics now largely chl; mag & ep. Ep veinlets cut rock. Where fractures cut rock, the minerals are crushed & fg. See Plate 8-2b). K corrected for 2% qtz.
	K	-6.7	
512A	q	+3.9	Pheno of cloudy K perthite (1.5mm) & qtz as above (1.6mm) in fg equigranular gdmass of same; amph, chl, & mag. Chl veinlets cut rock; k corrected for 2% qtz.
	k	-4.9	

Table 8-1 (Cont'd)

Sample (SK-)	Mineral	$\delta^{18}\text{O}$ (‰)	Remarks
512C	Q	+6.3	Cloudy to turbid perthitic K (1.1mm), some with gphy, & somewhat dusty qtz (0.9 mm); opaques. Some qtz up to 3 mm, & these were analyzed here. K corrected for 4% qtz.
	K	-5.7	
SKY-7a	Q	+5.6	K corrected for 1% qtz.
	K	-5.7	
SKY-7b	Q	+3.5	K corrected for 1% qtz.
	K	-5.3	
Glamaig Epigranite (GE)			
123	Q	+2.1	Seriz turbid plag & K (2.5mm), dusty & cracked qtz (0.4mm); some gphy textures; amph, biot, chl, opaques, apatite & ep; 5% fg inclusions are present (digested xenoliths). K corrected for 8% qtz.
	K	-4.7	
124	Q	+5.7	Similar to SK-123, with fresh amph; ep veinlets cut rock. K corrected for 5% qtz.
	K	-4.2	
	A	-5.2	
125	WR	-5.0	Similar to SK-123, expect rock is highly fractured & veined by ep and chl. Much of the rock shows signs of crushing & comminution.
126	WR	-5.9	Similar to above.
Beinn Dearg Mhor Epigranite (BDME)			
128	Q	+2.0	Fractured, dusty qtz (0.8mm) & turbid feld (3mm) surrounded by coarse gphy intergrowths. Cpx totally altered to opaques. Numerous fractures cut the rock, & rock is crushed along these surfaces. See Plate 8-2c. K corrected for 3% qtz.
	K	-6.0	
183	WR	-1.8	Similar to above; crushed rock.
503	Q	+4.0	Turbid K pheno (3mm), often in clusters of 2 or 3 with rims of gphy; also coarser isolated grains of fractured dusty qtz (1.2mm). Some v fresh cpx; amph, biot, opaques & apatite. K corrected for 6% qtz.
	K	-1.6	

Table 8-1 (Cont'd)

Sample (SK-)	Mineral	$\delta^{18}\text{O}$ (‰)	Remarks
Loch Ainort Epigranite (LAE)			
111a	mQ	+3.3	Similar to SK-128, except fractures not evident; m cavities in rock.
	mK	-4.1	
112	Q	+4.8	Similar to SK-128, with fayalite altered to serp; feld (2.5mm), qtz (2mm), sphene and amph. K corrected for 3% qtz.
	K	-2.2	
130	Q	+2.3	Large turbid zoned feld pheno (up to 1cm) some with clear to dusty cores with chl alteration along rims & cracks; surrounded by gphy intergrowths of turbid K & dusty qtz. Amph, cpx, chl, opaques, serp, sphene & ct; m cavities with qtz, ep, & feld.
	K (calc'd)	-4.8	
	WR	-2.3	
131	Q	+3.6	Similar to SK-130, with some oscillatory zoned pheno.
	K	-0.3	
171	Q	+4.1	Pheno similar to SK-130; set in an equigranular to gphy matrix of turbid K & dusty qtz. Cpx, amph, serp, chl, opaques, biot, & sphene; m cavities. K corrected for 6% qtz.
	K	-4.5	
505	Q	+3.2	Similar to SK-171 & SK-130 with relatively fresh cpx & amph, & ct. Shadowy inclusions. K corrected for 5% qtz.
	K	-0.5	
506	Q	+4.0	Highly fractured, sheared & brecciated qtz & turbid K in comminuted gdmass of same; chl.
	K (calc'd)	-1.4	
	WR	+0.4	
507	Q	+4.1	Similar to SK-130, with highly developed gphy textures. Mafic minerals totally altered. K corrected for 8% qtz.
	K	-2.0	
	mQ	+3.0	
	mQ	+2.6	
	mQ	+1.7	
	mK	-4.3	
SKY 9	Q	+2.9	
	F	-0.5	
BM-25	WR	+1.4	
Southern Porphyritic Epigranite (SPE)			
172	gQ	-0.6	Pheno of v cloudy to turbid K (2mm) & cracked embayed dusty β -morphology qtz (1mm) in a crushed & pluverized base of same, with some gphy; chl, white mica & opaques; k corrected for 8% qtz.
	q	+0.8	
	k	-4.7	

Table 8-1 (Cont'd)

Sample (SK-)	Mineral	$\delta^{18}\text{O}$ (‰)	Remarks
181	q	-2.6±0.0(2)	Pheno of turbid K (1.8mm) & cracked, dusty qtz (1.5mm) in a fg gphy gdmass. See Plate 8-2a. 3 cm from magnetite veinlet <3 mm from magnetite veinlet
	q; HF strip	-2.7	
	k	-3.5	
	WR	-3.1	
	WR	-3.0	
182	q	+3.5	Similar to SK-181, except qtz pheno (β -morphology; 2mm) not as cracked & gdmass shows spherulitic structures, as well as gphy ones.
	q; HF strip	+5.2	
	k	-3.1	
	WR	-1.7	
Southern Porphyritic Felsite (SPF)			
IGC-13	q	+4.0	Similar to SK-182. β -morphology qtz.
	k	+2.6	
Northern Porphyritic Felsite (NPF)			
SKY-13	WR	-3.5	
Marscoite Suite (MS)			
SKY-10	Q	+4.5	F corrected for 4% qtz.
	F	-6.1	
	WR	-4.2	
SKY-11	WR	-6.0	
SKY-14	Q	+4.9	
	F	+0.1	
SKY-15	WR	-3.0	
Meall Buidhe Epigranite (MBE)			
521	WR	+0.1	Patchy, clear to v cloudy plag pheno rimmed by turbid K, in a gdmass of turbid K, cracked, dusty qtz, fresh amph, ep, chl, opaques, cpx, apatite & sphene. Some gphy textures.
SKY-12	WR	-3.5	
Marsco Epigranite (ME)			
173	Q	+6.2±0.0(2)	Similar to SK-521, except equigranular; feld \approx 2.1 & qtz \approx 1.5mm; serp after fayalite; v fresh amph; m cavities. F corrected for 1% qtz.
	F	-0.8	

Table 8-1 (Cont'd)

Sample (SK-)	Mineral	$\delta^{18}O$ (‰)	Remarks
177	gQ	+6.0	Similar to SK-521 and SK-173, with better developed gphy textures around K - rimmed zoned plag. Equigranular (~2mm). Mafics slightly more altered than in SK-173. F corrected for 9% qtz.
	Q	+5.5	
	F	-3.5	
180	Q	+5.9	Similar to SK-177 with mafics slightly more altered, & more gphy textures. Feld (1mm) & dusty qtz (0.5mm); m cavities. F corrected for 7% qtz.
	F	+0.4	
IGC-6	Q	+6.4	Similar to SK-173, with fresh cpx & amph.
	K	+1.2	
Glas Bheinn Mhor Epigranite (GBME)			
109	Q	+2.3	Cloudy to turbid zoned plag pheno (2mm) in a m-fg turbid gphy base; amph, cpx, chl, biot, opaques, serp & apatite.
286	Q	+2.4	Clear to cloudy oscillatory zoned plag pheno (2.5mm) in a well developed gphy base; mafics more altered than in SK-109; some 1cm sized partially digested inclusions. Small m cavities with pyrite, qtz & feld.
	K (calc'd)	-1.6	
	WR	-0.2	
SKY-3	WR	+0.2	
SM/67/36	WR	-1.2	
Beinn na Cro Granite (BCroG)			
SKY-26	Q	+4.5	
	K	-0.7	
Allt Fearna Granite (AFG)			
52	Q	+3.7	Turbid K & dusty qtz. Rock is highly fractured with crushed fg qtz & feld along fractures; chl, opaques, sphene. Chl-rich veinlets cut the rock. K corrected for 2% qtz.
	K	-3.7	
74	Q	+4.9	Turbid K (2.2mm) & quite dusty cracked qtz (1mm), about 1/3 of which is in gphy intergrowths; chl, opaques. K corrected for 1% qtz.
	K	-3.8	

Table 8-1 (Cont'd)

Sample (SK-)	Mineral	$\delta^{18}O$ (‰)	Remarks
Beinn an Dubhaich Granite (BDG)			
9	WR	+5.3	Slightly clouded to turbid K, dusty qtz, & cloudy plag; amph, biot, chl, opaques & sericite. Minor gphy textures. Assuming $\delta^{18}O_Q = +7.3$, calc'd $\delta^{18}O_K = +4.2$.
11	Q K	+7.0 +0.9	Contact with dike SK-10. K corrected for 1% qtz. Cloudy K (1.2mm) & qtz (1.2mm); minor gphy textures. Chloritic amph.
12	Q K	+7.4 +4.2	Cloudy to turbid feld especially on rims, (1.4mm) & dusty qtz (1.3mm); some zoned plag, amph, chl, biot, opaques, sericite, sphene, & apatite. Coarse graphic texture.
13	WR	+5.7	Pheno of clear to cloudy K, qtz, & zoned plag (up to 5mm), in a variable-sized mfg gdmass of broken qtz, turbid feld & sericite. Chl, amph, biot, opaques, & apatite. Assuming $\delta^{18}O_Q = +7.3$, calc'd $\delta^{18}O_K = +4.7$
78	WR	+5.7	
189	Q K	+7.8 +5.8	Feld (2.1mm), usually clear in central parts, & cloudy to turbid on rims; dusty qtz (1.5mm), amph, biot, sphene, opaques, & apatite. Granitoid.
190	WR WR	+2.1 +2.5	Felsic dike, <2mm from BDG Felsic dike, 1cm from BDG Aphanitic K & qtz.
191	Q K	+7.2 -1.0	Cloudy K (0.5mm) & somewhat dusty qtz (0.3mm); equigranular. Amph, biot, opaques. K corrected for 1% qtz.
192	Q WR	+7.6±0.2(3) +1.9±0.1(2)	Qtz pod Felsite. Similar to SK-191, except slightly finer-grained (~0.3mm).
195	Q K	+6.9±0.0(2) +0.5±0.0(2)	Contact with dike SK-194 Cloudy to turbid K (0.7mm) & dusty qtz (0.6mm); altered mafics. Some clear feld cores. K corrected for 1% qtz.
196	q k Q (gdmass) WR	+7.1±0.0(2) +5.0±0.0(2) +7.4 +4.2±0.3(2)	Pheno of cloudy feld (1.2mm) & dusty qtz (1.2mm) in fg gdmass of same; amph, chl, opaques; k corrected for 3% qtz. Calc'd $\delta^{18}O_K$ in gdmass = +1.7; calc'd $\delta^{18}O$ gdmass = +4.0.

Table 8-1 (Cont'd)

Sample (SK-)	Mineral	$\delta^{18}\text{O}$ (‰)	Remarks
290	Q	+7.5±0.1(2)	<½cm from fracture; similar to SK-189.
	K	+2.7±0.1(3)	
SKY 22	Q	+7.3	
	K	+4.9	
	M	-0.1	
20813	Q	+7.0	
	K	+6.0	
	F	+6.3	
	WR	+6.2	
Beinn na Caillich Granophyre (BCG)			
36	Q	+3.4	Turbid feld (1.6mm) & dusty qtz (0.8mm) in a fg gphy base, with opaques & altered mafics; m cavities with qtz & feld.
	K	+0.9	
37	WR	+3.1	Same as SK-37b
37b	Q	+4.5	Similar to SK-36, except slightly coarser grained feld, & gphy textures not as prevalent. K corrected for 5% qtz.
	K	+0.8	
	mQ	+3.7	
	mK	-2.0	
38	WR	+0.9	Similar to SK-36, but with prevalent gphy textures, chl, & ct.
Creag Strollamus Granite (CSG)			
SKY 1	Q	+1.0	
	K	-3.1	
Coire Uaigneich Granophyre (CUG)			
147	WR	-1.3	Needles of inverted tridymite, in a fg gdmass of gphy, v cloudy feld & qtz; opx altered to chl, serp, & biot; opaques, ep & apatite.
157	WR	-2.5	Similar to SK-147, but rims of feld v dusty.
284	WR	+0.5	Similar to SK-147, but not as altered. Fresh opx is present; feld are clear to cloudy with v dusty rims; oscillatory zoned plag.
Jurassic sediments			
2	WR	-0.6±0.1(2)	Shale; aphanitic; opaque-rich; white micas.
16	WR	+12.4	Shale; fossiliferous beds; gritty in part.

Table 8-1 (Cont'd)

Sample (SK-)	Mineral	$\delta^{18}\text{O}$ (‰)	Remarks
120	WR	+7.4	Shale; calcareous; strike 35°, dip 35°W.
134	Q	+11.3	Sandstone, interbedded with lmst. Strike 10°, dip 40°W.
135	Q	+12.0	Sandstone
136	WR	+13.0	Sandstone, subhorizontal beds.
142	Q	+11.6	Sandstone
151	Ct	+5.7	Lmst, 5 cm from contact with basalts ($\delta^{13}\text{C}=+1.5$).
206	Q	+10.0	Sandstone at contact with Rudh' an Eireannaich sill
254	Ct	+15.1	Lmst, angular qtz, ct, white mica, opaques ($\delta^{13}\text{C}=-0.1$).
259	Ct	+9.0	Lmst, 2m below base of R an E sill. Subrounded qtz, ct, feld, chl. ($\delta^{13}\text{C}=-0.4$).
293	WR	0.0	Shale
Triassic sediments			
201	WR	+10.9	Conglomerate; quartzite fragment.

Table 8-1 (Cont'd)

Sample (SK-)	Mineral	$\delta^{13}\text{C}$ (‰)	$\delta^{18}\text{O}$ (‰)	Remarks
Cambro-Ordovician Durness Limestone				
4	Ct	-3.5	+19.0	Bedding strike 50°, dip 25°NW.
	D	-2.8	+21.4	
6	Ct	-3.1	+6.6	Cut by SK-5.
14	Ct	-1.7	+20.8	Bedding strike 135°, dip 90°.
42	Ct	-4.6	+0.5	Banded lmst skarn.
	D	-5.1	-0.6	
43	Ct	-4.9	+9.7	
44	Ct	-1.8	+15.9	
48	Ct	-1.5	+19.2	20m west of contact with dike.
49	Ct	-1.7	+11.9	Silicified lmst near BDG.
50	Ct	-1.8	+17.4	Bedding strike 40°, dip 50°S.
79	Ct	-3.2	+17.0	5m from SK-78 (BDG).
85	Ct	-4.0	+16.1	Skarn in quarry.
	D	-3.3	+19.1	
187	Ct	-1.0	+16.3	

Table 8-1 (Cont'd)

Sample (SK-)	Mineral	$\delta^{18}\text{O}$ (‰)	Remarks
Torridonian sandstone			
41	Q WR	+3.6 +2.8	Fractured sandstone.
63	Q	-3.9	Highly fractured & veined sandstone.
77	WR	+1.5	Fractured rock.
87	WR	+10.0	1m from SK-8b (dike).
88	Q	+10.8	Sandstone, intercalated with shaly beds, strike 30° , dip 30°W . Subangular qtz, ct, white mica, feld, chl, & opaques.
90	Q	+14.4	Similar to SK-88.
116	WR	-6.2	Highly fractured & veined rock.
203	WR	+10.8	
283	Q	+6.3	Qtz in a dusty to cloudy feldspathic matrix.
288	WR	+2.0	Dusty, fractured qtz, clear to cloudy feld, chl, ep and opaques.
512F	Q	+4.9	Qtz, cloudy feld, chl, biot, white mica, sphene, opaques. Rock is highly fractured & veined.
514A	Q	+3.7	Similar to SK-512F.
515B	Q	+6.6	
516A	WR	-3.2	
534D	WR	+10.8	
Lewisian Gneiss			
91	WR	+6.0	Crenulated feldspathic mica schist; foliation strike 90° , dip 48°S . (NG 679 115).
92	WR	+7.6	mg quartzofeldspathic bands alternating with fg qtz, feld, & ep. Biot, chl, sphene, opaques. (NG 665 084).
98	Q	+9.4 \pm 0.1(2)	Vein in Lewisian (NG 654 059).
99	WR	+6.6	mg actinolite-biot-qtz-feld-ep-chl-opaque schist. (NG 654 059).

1. All sample numbers without letter prefix are SK- .
2. Abbreviations are Ep = epidote; f = plagioclase phenocrysts; Ol = olivine; m = miarolitic; g = granophyric; other symbols as in Table 6-1.
3. Abbreviations are amyg = amygdaloidal, amygdules; ep = epidote; gphy = granophyric; NG = national grid reference for Ordnance Survey 1 in to 1 mile maps; Serp = serpentine, biref = birefringence; lmst = limestone; pseudo = pseudomorphic; other symbols as in Table 6-1. For descriptions of SKY1-30, see Taylor and Forester (1971); for descriptions of 20813, H4058, H4601L, BM-10, 37 & 53, see Moorbath and Bell (1965); for descriptions of SM/67/36, SM/67/35T, SM/67/35M, and SM/67/45, see Moorbath and Welke (1969). IGC samples are from Ian Campbell collection at Caltech.

8.2 Hydrogen isotope systematics

As in other areas where $\delta^{18}\text{O}$ analyses indicate that the rocks have been strongly perturbed by heated meteoric waters during cooling and crystallization, D/H analyses totally confirm this contamination effect. Hydrogen isotope analyses have been carried out on sericites, amphiboles, chlorites, biotites and epidote from the Tertiary igneous rocks of Skye, as well as on several whole-rock samples from the Torridonian and Lewisian.

The hydrogen isotope systematics exhibited by the igneous rocks at Skye are similar to those displayed by the rocks in the Stony Mountain complex, Colorado (see Section 6.3). Sericites are found to concentrate deuterium relative to the hydrous mafic silicates, but each phase is drastically depleted in δD with respect to 'normal' igneous rocks (on the order of 50 per mil, Figure 8-4). The sericites are exceedingly uniform in δD , with values of -104, -106 and -107. The chlorites have an average $\delta\text{D} = -127$ and are indistinguishable from the Tertiary amphiboles which average -124 (excluding SK-532B). Possible reasons why the chlorite samples have less deuterium than expected on the basis of the D/H data of Taylor and Epstein (1966) have already been stated above in Section 6.3.

Hydrogen yields from these samples indicate that the feldspars are turbid and in thin sections they appear at first glance to be largely altered to sericite. However, they maintain

Table 8-2

Hydrogen isotopic analyses from Isle of Skye, Scotland

SAMPLE (SK-1)	MINERAL ¹	ROCK UNIT	δD^2 (per mil)	REMARKS ³
239D	Ep	Basalt	-38±0 (2)	
22	S	Felsite sheet	-104	
74	S	Allt Fearna Granite	-106	
225	S	Felsite dike	-107	
51	A	Broadford gabbro	-123	
99	A	Lewisian	-74	
189	A	Beinn an Dubhaich Granite	-120	
124	A	Glamaig Epigranite	-128±1 (2)	
219	A	Cuillin gabbro	-119	
173	A	Marsco Epigranite	-127	
177	A	Marsco Epigranite	-121±1 (2)	
521	A	Meall Buidhe Epigranite	-127	
532B	A+C	Basaltic dike	-105	50%A, 50%C
99	B	Lewisian	-72	
268B	B	Granitic dike	-118	
236C	C	Basalt	-122	
253B	C	Cuillin gabbro	-126	
243B	C	Basalt	-132	C amygdules
288	C+W	Torridonian sandstone	-101	70%C, 30%W. Trace of Ep.
90	W+C	Torridonian sandstone	-95	90%W, 10%C
88	W+C	Torridonian sandstone	-63	85%W, 15%C
89	W	Torridonian sandstone	-66	

1. S = sericite; A = amphibole; C = chlorite; W = white mica; Ep = epidote.
2. Analytical error is average deviation from the mean. Numbers in parentheses indicate number of separate analyses.
3. Complete descriptions given in Table 8-1. Mineral percentages give the estimated % contribution of each mineral to the measured δD value.

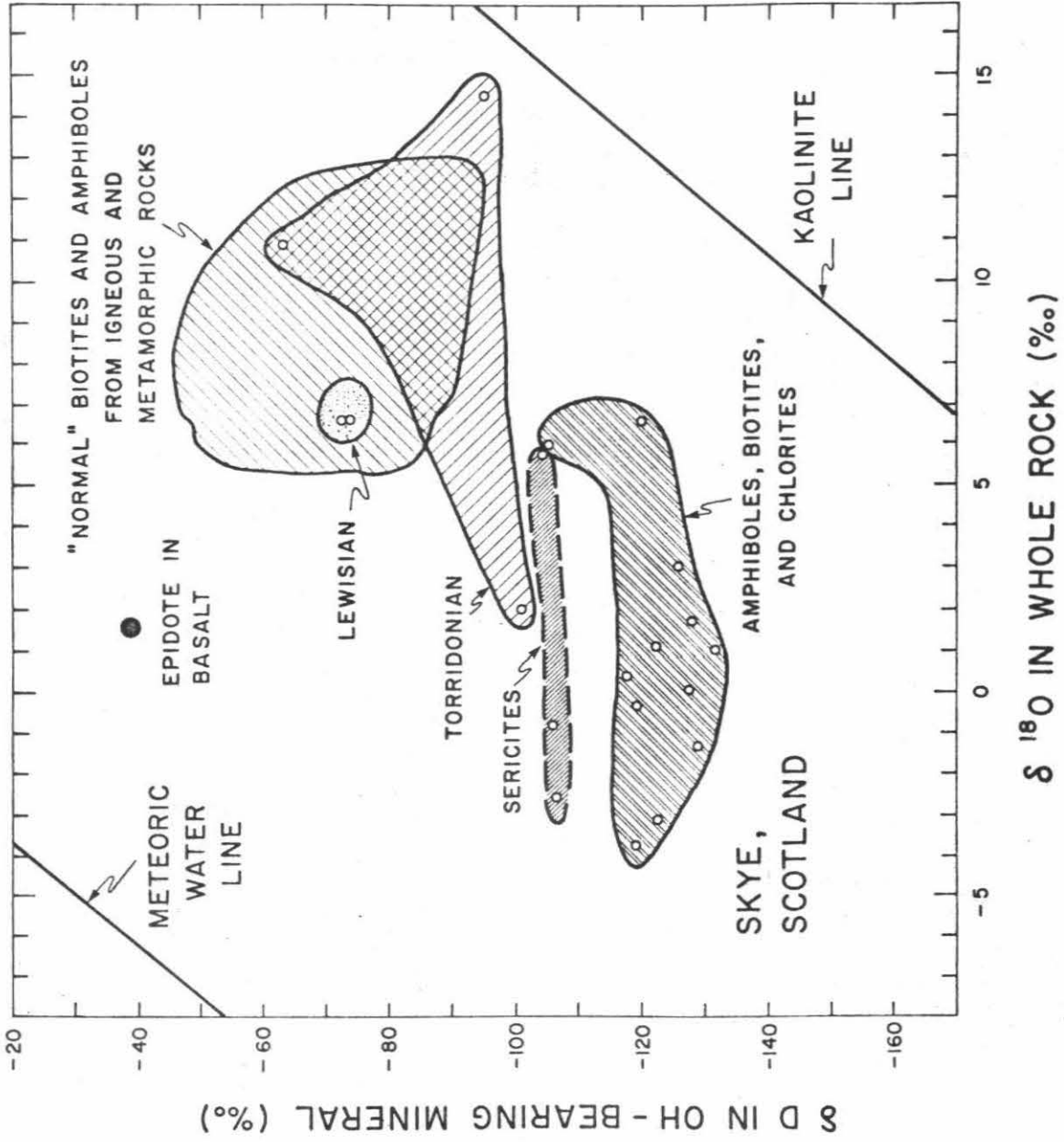


Figure 8-4. δD vs $\delta^{18}O$ diagram for hydroxyl-bearing minerals from Skye.

their feldspar optics and, as confirmed by the hydrogen yield data, the very fine-grained sericite makes up but a minor part of the feldspar.

The Tertiary amphiboles range from -105 to -128. Note that the sample with the most positive δD value in this group (-105) also has a 'normal' $\delta^{18}O_R = +5.9$. This is one of a series of basaltic dikes cutting the GBME on the southwest side of Loch Ainort that have normal $\delta^{18}O$ (+5.2,+5.4,+4.2; see Fig. 8-2). Here then is evidence that some late-stage igneous activity occurred at Skye well after the emplacement of the major plutons that were responsible for the maintenance of the large meteoric-hydrothermal convection systems. The hydrothermal activity in the vicinity of the GBME must have nearly ceased at the time of intrusion of these fine-grained dikes; otherwise they would have exchanged with the meteoric-hydrothermal fluids and the adjacent low- ^{18}O granophyric country rocks and thereby attained $\delta^{18}O$ values on the order of zero. The $\delta D = -105$ may represent a partial hydrogen isotopic exchange with the GBME.

Another interesting sample is SK-189, with a $\delta D_A = -120$. This BDG sample has the most 'normal' $\delta^{18}O$ -values for coexisting quartz and alkali feldspar of any of the rocks from the BDG, and in fact is the most pristine (i.e. unaltered) granite yet analyzed from Skye in terms of oxygen isotopes. In terms of D/H however, it is indistinguishable from rocks that have undergone drastic ^{18}O depletion. This is not unexpected of course because Δ_{Q-K} is indeed slightly larger than normal, suggesting some ^{18}O

exchange of the alkali feldspar; note that if the oxygen isotopic compositions have been affected at all, one would expect that the original hydrogen isotopic record would be totally wiped out.

Data from the Torridonian are more difficult to interpret, because they represent Precambrian clastic and authigenic material as well as, in some instances, newly formed minerals. SK-288 is the only such sample close to the central intrusive complex, and it has clearly undergone significant oxygen isotope exchange ($\delta^{18}O_R = +2.0$). Its position on the δD vs $\delta^{18}O$ plot (Figure 8-4) is similar to that of the Tertiary rocks whose dominant hydrous phase is sericite.

Both SK-88 (sandstone) and SK-89 (shale) have similar δD values (-63 and -66) that are much higher than any of the Tertiary samples except the epidote from SK-239D. These samples are a good 8 km from the central intrusive center of Skye and appear to be well outside the area of hydrothermal alteration (see also Figure 8-9). Although the NNW-trending dike swarm has affected the region, the δD values in these rocks cannot have been very much modified from their original values. However, SK-90 is even further removed from the Tertiary plutonic complexes, approximately 12 km distant, yet it has a $\delta D = -95$, or about 30 per mil lower than SK-88 or SK-89. The dominant hydrous phase in all three cases is white mica, but note that SK-90 is from a distinctly different group within the Torridonian succession. The SK-90 sample plots very close to the

kaolinite line, and it conceivably could have undergone exchange with meteoric waters at very low temperatures.

Coexisting biotite and amphibole from a Lewisian schist (SK-99) have identical δD values of -73 ± 1 . Thus, in terms of both oxygen and hydrogen isotopes, these samples are totally unaffected by the Tertiary events on Skye. This is not surprising, inasmuch as these samples are from outcrops more than 16 km away from the plutonic centers of Skye. Note that, on the δD vs $\delta^{18}O$ plot (Figure 8-4), they fall within the area of 'normal' isotopic values shown by igneous and metamorphic rocks.

The most enigmatic sample is SK-239D, an epidote with $\delta D = -38$ and $\delta^{18}O = +1.7$. The epidote is even more enriched in deuterium than biotites and amphiboles from 'normal' igneous and metamorphic rocks (see Figure 8-4). It is possible for the H_2O of a hydrothermal fluid to become enriched in deuterium if it undergoes some reduction to H_2 or CH_4 . For example, at $300^\circ C$, the equilibrium fractionation between H_2O and H_2 is approximately 500 (Bottinga, 1969). However, a strongly reducing environment is not in accord with the presence of epidote, which is characterized by trivalent iron. It should be noted that the H_2 contents in these hydrothermal fluids throughout the Skye area must have been very low. For example, under oxygen fugacities equivalent to the quartz-fayalite-magnetite buffer, at $P_{gas} = 500$ bars and $T = 727^\circ C$, the fugacity ratio $f_{H_2}/f_{H_2O} = 0.02$. At $527^\circ C$, the ratio is still 0.02, and at $527^\circ C$ under conditions of the nickel-nickel oxide buffer, this ratio is 4.7×10^{-3} .

(Eugster and Skippen, 1967). These H_2 contents are too small to have caused appreciable changes in the δD of the H_2O . At about $500^\circ C$, with $H_2/H_2O = 0.02$ and $\delta D_{H_2O}^i = -90$, the δD of the H_2O in the final fluid will be increased only by 8 per mil, in spite of the large H_2O-H_2 equilibrium fractionation of about 300 (Bottinga, 1969).

It is perhaps also possible that ocean water was involved in the hydrothermal alteration of certain basalts and thus responsible for the deposition of some of the epidote at Skye. However, no other samples at Skye have been found with δD values as anomalously close to ocean water as this, and there is no indication from the geology that submarine igneous activity occurred here. It should be further noted that a chlorite sample from a basalt only 1 km distant from SK-239D has a $\delta D = -122$.

A major problem in explaining this δD value lies in the fact that the hydrogen isotopic behavior of epidote is not known. No experimental work has been done on the D/H fractionations of this phase, and very few analyses have been reported. Epidote-rich samples from the Boulder batholith, Montana tend to be richer in D than analogous epidote-poor samples (Sheppard and Taylor, 1974). Epidote amygdules from hydrothermally altered basalt surrounding the Skaergaard intrusion, East Greenland, have been analyzed by Taylor and Forester (1973), and they turn out to be only about 20 per mil richer in deuterium than the chlorite amygdules. Epidote from the Lake Superior

Keweenaw Lavas, Michigan, have $\delta D \approx -45$ to -60 , similar to the coexisting prehnite and analcite (Forester and Taylor, unpublished data). Therefore, although there is some evidence from other localities that suggests at equilibrium epidote tends to concentrate D relative to many other OH-bearing minerals, there is at present no adequate explanation for the striking D enrichment shown by sample SK-239D.

If we utilize a reasonable fractionation factor for the amphibole-water system using the data of Suzuki and Epstein (1974), we can estimate that the Eocene meteoric waters in Skye had $\delta D \approx -95$ or -90 . Similarly, the sericite data suggest a δD value of the hydrothermal fluids at Skye to have been approximately -90 or -85 . Using the well-established relationship between δD and $\delta^{18}O$ in pristine meteoric waters (Craig, 1963), this gives $\delta^{18}O = -12$ to -13 for the early Tertiary meteoric waters on Skye. Because of the characteristic positive " ^{18}O shift" shown by geothermal waters, this would represent the probable minimum value for the meteoric-hydrothermal waters at Skye; therefore all of the oxygen isotope effects discussed below must have been produced by waters with $\delta^{18}O > -12$ to -13 .

8.3 Lewisian gneiss

The only two localities on the Isle of Skye where the Lewisian basement gneiss crops out are (1) east of Beinn na Cro (see Figure 7-5) and (2) bordering the Sound of Sleat. All the Lewisian samples analyzed in this study are from the

latter area. Three samples of these metamorphic rocks have $\delta^{18}\text{O}$ values of +6.0, +6.6, and +7.6. A 3 m-thick quartz vein within the Lewisian (SK-98) has a $\delta^{18}\text{O} = +9.4$. These samples are all more than 16 km from the central intrusive complex, at a distance where even the basalts would not have been affected (see Figure 8-9). It is also clear from the hydrogen isotopic analyses (Section 8.2) that these Lewisian samples have not exchanged with Tertiary meteoric waters. Furthermore, the dike rocks cutting the Lewisian all have normal $\delta^{18}\text{O}_R$ values (SK-93, 94 and 100 are +5.8, +6.0, and +7.0 respectively).

The Lewisian samples are lower in ^{18}O than most analyzed schists and gneisses throughout the world; the latter typically have $\delta^{18}\text{O}_R$ values between +10 and +18 (Garlick and Epstein, 1967; Devereux, 1968; Shieh and Taylor, 1969a; Schwarcz et al., 1970; Turi and Taylor, 1971). However, most of these higher- ^{18}O rocks are pelitic or semi-pelitic in composition. High-grade metamorphic rocks (e.g. granulites and some metamorphic eclogites, Taylor, 1969; Wilson et al., 1970; Wilson, 1971; Vogel and Garlick, 1970; Javoy and Allegre, 1967; Schwarcz and Clayton, 1965) approach the $^{18}\text{O}/^{16}\text{O}$ ratios of igneous rocks. The Lewisian represents a polymetamorphic terrane that has undergone an early granulite-facies metamorphism, at least two separate amphibolite facies metamorphic events, as well as mylonitization and faulting events (Bowes, 1969; Lambert and Holland, 1972; Moorbath and Park, 1971). Thus, very early in

its evolution, the Lewisian samples may have attained oxygen isotopic compositions approaching those of igneous rocks. The samples are essentially gabbroic or dioritic in composition, so they also could have started out with igneous $\delta^{18}\text{O}$ values. Thus, in spite of their relatively low $\delta^{18}\text{O}$ values, the Lewisian metamorphic rocks are best interpreted as not having been affected at all by the Tertiary meteoric-hydrothermal events.

8.4 Torridonian sedimentary rocks

The Precambrian Torridonian rocks of Skye have been variously affected by the Tertiary meteoric-hydrothermal activity; the effects are largely a function of distance from the central intrusive complex. This is illustrated in Figure 8-5, where $\delta^{18}\text{O}_Q$ is plotted against distance from the nearest major intrusive body. As will be seen below, the relationship shown here is similar to the relationship exhibited by the other country rocks at Skye, namely the Jurassic shales and the basaltic lavas. In this case, however, we are dealing with the relatively resistant mineral quartz, and thus the effects extend outward only about 1 km. If we plot $\delta^{18}\text{O}$ vs distance, we have a similar trend, except that the low- ^{18}O effects extend outward for about 4 km because the $\delta^{18}\text{O}_R$ values are substantially lower than $\delta^{18}\text{O}_Q$ (see Table 8-1 and Figure 9-3). These differences between the whole-rock and quartz graphs are a result of the lower resistance to oxygen isotope exchange

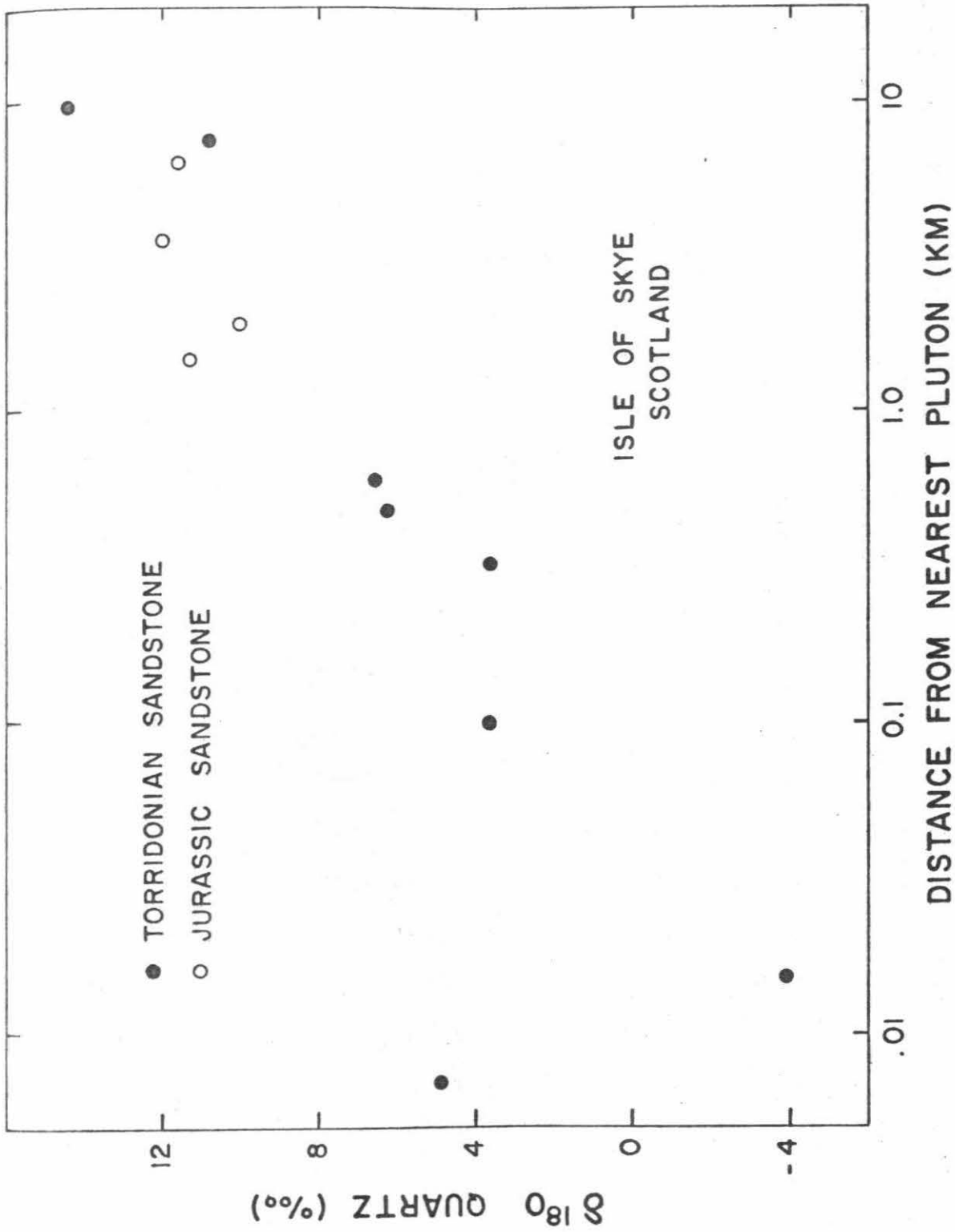


Figure 8-5. Semilogarithmic plot of $\delta^{18}O_Q$ from Torridonian and Jurassic sandstones vs distance from nearest Tertiary pluton.

of the other minerals present in the Torridonian sediments, namely feldspars, clay minerals, carbonates, and rock fragments.

The most significant aspect of the isotopic data from the Torridonian rocks is that the meteoric-hydrothermal convection systems must have penetrated downward at least to the level of the lowermost section of flat-lying sedimentary rocks present in the Skye area. This means that, at a minimum, the convective circulation went down essentially to the unconformity with the basement Lewisian gneiss.

The Torridonian sandstone sample SK-63 ($\delta^{18}O = -3.9$) represents the most ^{18}O -depleted quartz sample yet analyzed from the Scottish Tertiary Province, except for that of the Grigadale granophyre in Ardnamurchan (-6.0). SK-63 is from the Creag Strollamus area of Skye (King, 1953), a complex region where highly fractured and 'granitized' Torridonian is spatially associated with Tertiary volcanic rocks, the Broadford gabbro, and granitic intrusions. Inasmuch as 'normal', unaltered Torridonian sandstone has $\delta^{18}O_Q \geq +10.8$, the quartz in SK-63 must have been lowered in ^{18}O by about 14 to 15 per mil! The Torridonian here is so intimately invaded and affected by granite, that King (1953) regarded the granites as having formed by the in situ granitization of Torridonian. The particular geologic occurrence of this sample, especially its highly sheared and fragmented nature and its intimate association with igneous intrusions, apparently aided the oxygen isotopic exchange process.

8.5 Cambro-Ordovician Durness limestone

The Durness limestone, as previously mentioned, forms a uniquely important rock unit involved in the Tertiary igneous complex. Normal sedimentary carbonate rocks have well-defined $\delta^{18}\text{O}$ values of about +18 to +25 and $\delta^{13}\text{C}$ values of about -1 to +1 (Keith and Weber, 1964; Degens and Epstein, 1962). The calcite samples of the Durness limestone analyzed in this study deviate strongly from these 'normal' values; they range from +0.5 to +20.8 ($\delta^{18}\text{O}$), and -4.9 to -1.0 ($\delta^{13}\text{C}$), while the dolomites vary from -0.6 to +21.4 ($\delta^{18}\text{O}$) and -2.8 to -5.1 ($\delta^{13}\text{C}$) (see Figure 8-6).

Except for the most ^{18}O -depleted sample, the dolomites have heavier $\delta^{13}\text{C}$ and $\delta^{18}\text{O}$ values than coexisting calcites in the same sample. This is the expected relationship both from an equilibrium standpoint, and the fact that dolomites are more resistant to isotopic exchange with H_2O than are calcites. Isotopic disequilibrium between dolomite and calcite is particularly apparent in skarn sample SK-42. This is probably analogous to the type of isotopic disequilibrium observed in almost all coexisting silicate minerals in the Skye intrusive complex (see below). One way in which the disequilibrium in these carbonates could have come about is as follows. Assume that the carbonates equilibrated at approximately 400°C with $\delta^{18}\text{O}_{\text{H}_2\text{O}} \approx -5$, producing dolomite with $\delta^{18}\text{O} \approx -0.6$, the present-day value. If the temperature of the hydrothermal fluid then

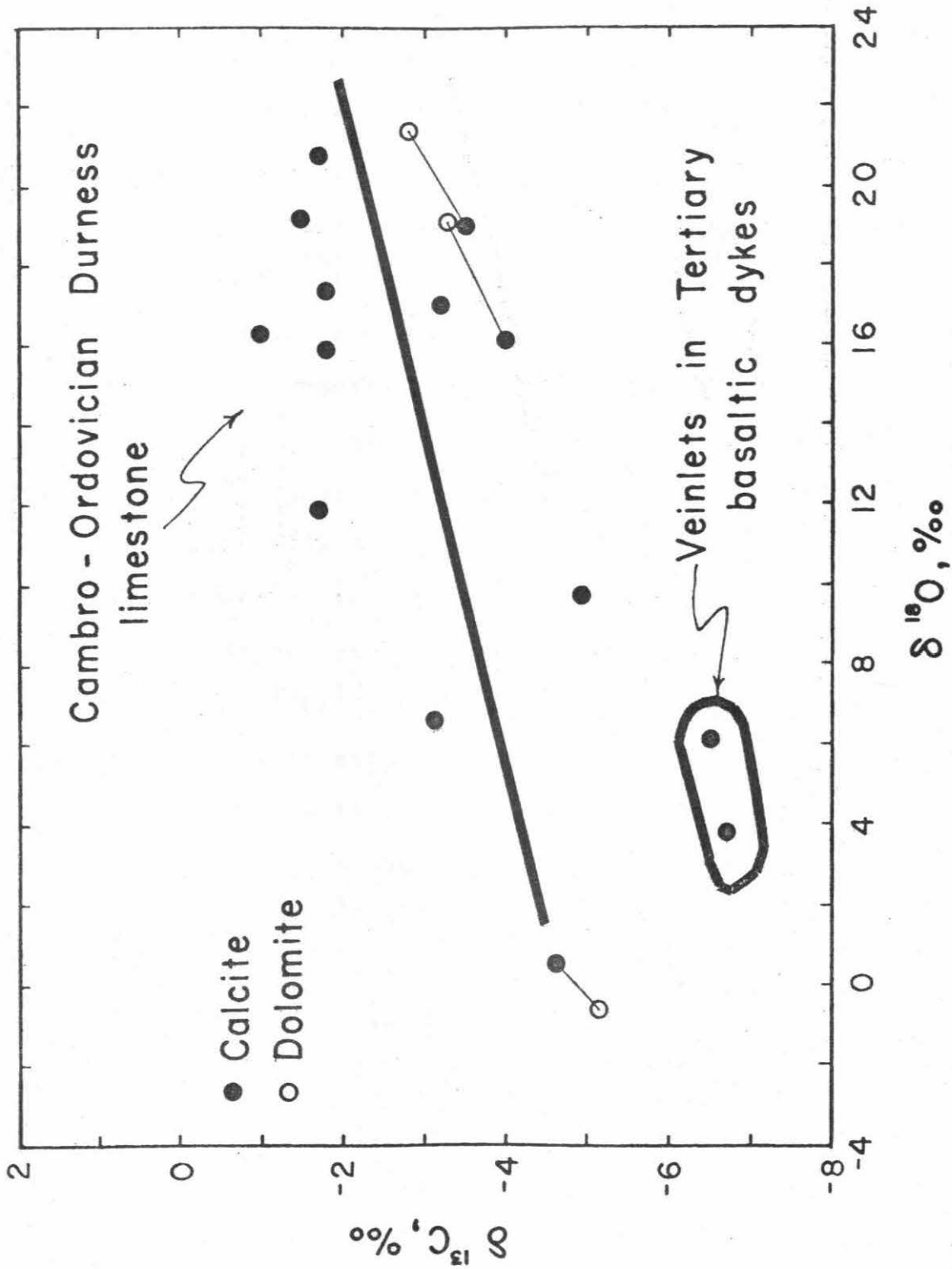


Figure 8-6. $\delta^{13}\text{C} - \delta^{18}\text{O}$ plot for carbonates from Skye. The least squares straight line (slope = 0.12) is also shown.

decreased by about 100°C, or the isotopic composition of the water increased to about -4, then the calcite may have undergone retrograde reequilibration to the new equilibrium value ($\delta^{18}\text{O} = +0.5$, its present-day value) while the more resistant dolomite may have maintained its original recrystallized isotopic composition.

Note that there is a positive correlation shown in Figure 8-6 between $\delta^{13}\text{C}$ and $\delta^{18}\text{O}$. The slope of the best-fit line through these Durness carbonate data-points is 0.12. If we assume that CO_2 was the dominant oxygen-bearing fluid evolved during decarbonation and skarn formation from these dolomites, then the isotopic changes in the carbonates may have approximately followed a Rayleigh-type distillation with $R = R_0 f^{\alpha-1}$, or $\delta - \delta_0 = 10^3 (\alpha - 1) \ln f$, where f represents the fraction of CO_2 remaining at any stage of the process. This type of equation would apply to both $^{18}\text{O}/^{16}\text{O}$ and $^{13}\text{C}/^{12}\text{C}$ ratios. If the reactions over the whole of the Durness limestone occurred, on the average, at approximately 350°C, we find that at equilibrium, $\alpha^{13}\text{C}_{\text{Ct-CO}_2} = 0.9976$ and $\alpha^{18}\text{O}_{\text{Ct-CO}_2} = 0.9900$ (Bottinga, 1968). Thus the evolution of CO_2 on a $\delta^{13}\text{C}-\delta^{18}\text{O}$ diagram will be represented by a line of slope $(\alpha^{13}\text{C}-1) / (\alpha^{18}\text{O}-1)$ or 0.24. This slope is significantly different than that defined by the isotopic data of the Cambro-Ordovician Durness Limestone. It is however similar to the slopes defined by contact metamorphic marbles and skarns of (a) the Trenton limestone in the vicinity of the Mount Royal pluton, Montreal (Deines and Gold, 1969; slope ≈ 0.28),

and (b) the Birch Creek aureole near Inyo batholith, California (Shieh and Taylor, 1969b; slope ≈ 0.25). Thus this equilibrium Rayleigh-type model affords a qualitative explanation for the distribution of points on a $\delta^{13}\text{C} - \delta^{18}\text{O}$ plot for the two above-mentioned contact metamorphic zones, but cannot quantitatively explain the Durness carbonate data unless the α values are modified by kinetic factors or other non-equilibrium effects.

It should also be noted that if H_2O was an additional phase in the fluid, then because of ^{18}O exchange between the H_2O and CO_2 , the effect on our Rayleigh distillation model would be to increase the slope of the line, and thus an even greater discrepancy would exist between the calculated and actual slopes. This emphasizes the fact that another process may have operated in the evolution of the recrystallized Durness limestone. The constraint is that the process would have to yield a lower slope than that defined by our Rayleigh model. Such a process, namely exchange with low- ^{18}O hydrothermal waters, is abundantly evident elsewhere in Skye, and therefore it is logical that it also operated in the Durness limestone at least to some extent. In fact, meteoric waters must have penetrated the limestone unit in order to reach the BDG (see below).

The effect of isotopic exchange with the groundwaters would be to lower the $\delta^{18}\text{O}$ values of the carbonates; those skarn samples that have been most strongly metamorphosed apparently have also undergone the most ^{18}O exchange with heated

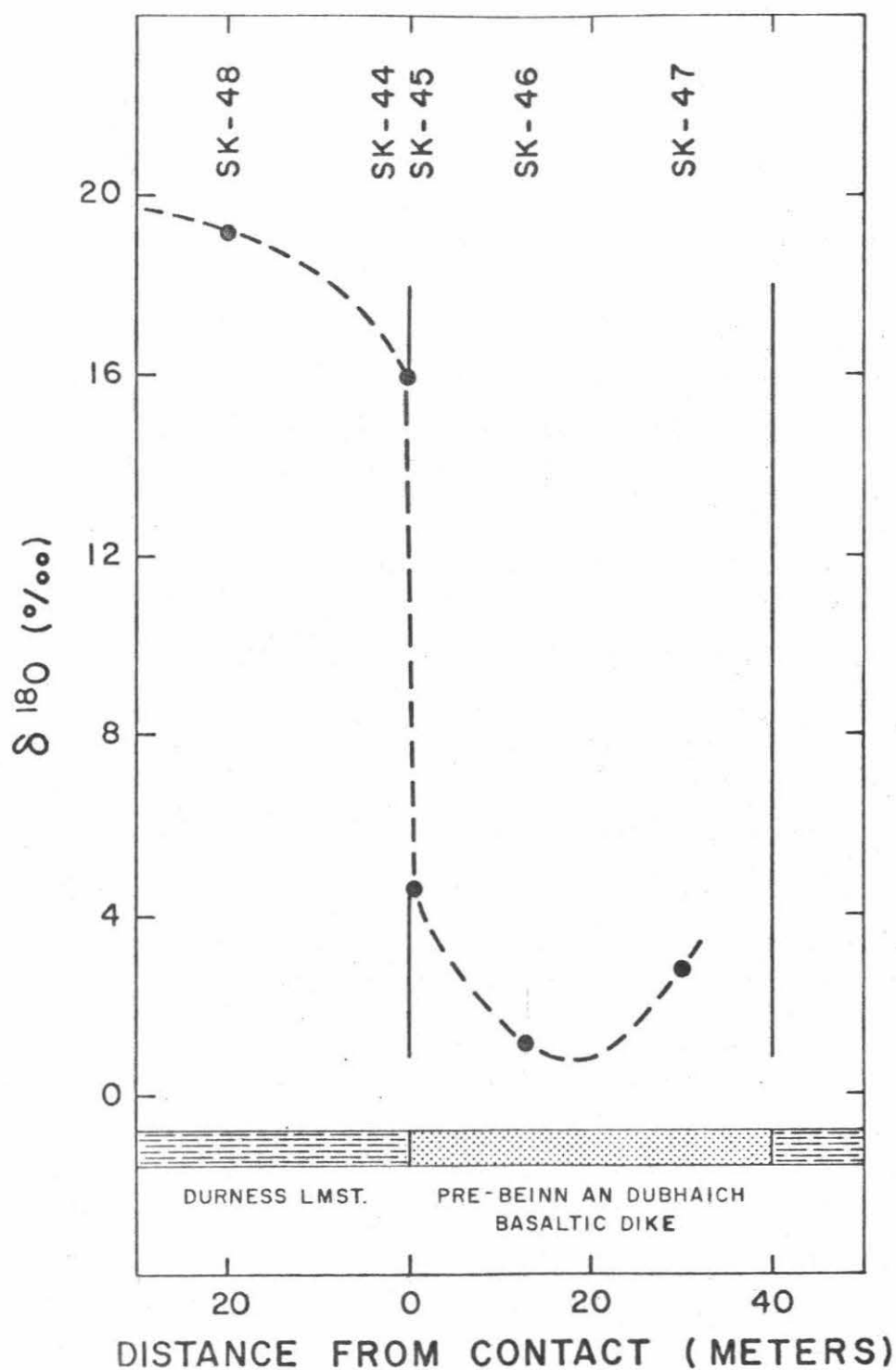


Figure 8-7. Plot of $\delta^{18}O$ vs distance for whole-rock samples in the immediate vicinity of a composite, pre-BDG dike that intrudes the Durness limestone.

meteoric waters. The latter process would have little if any effect on the $\delta^{13}\text{C}$ values, inasmuch as the carbon reservoir is essentially the carbonate unit itself. Hence, it appears that two processes have acted simultaneously during the recrystallization of the Durness limestone - (1) evolution of CO_2 following a normal Rayleigh-type distillation pattern, and (2) exchange with heated meteoric ground waters.

Two calcite veinlets from the Tertiary basaltic dikes of Skye are also plotted in Figure 8-6. Note that their $\delta^{13}\text{C}$ values (-6.7; -6.5) are compatible with an igneous origin for the carbon (Deines and Gold, 1973; Deines, 1970; Taylor *et al.*, 1967) while the $\delta^{18}\text{O}$ values could be accounted for by crystallization between 150° and 200°C from H_2O with $\delta^{18}\text{O} \approx -6$.

There are some interesting isotopic relationships exhibited at the contacts between the limestones and the intrusive dikes. A 40 m thick complex composite dike which cuts the Durness limestone, but is truncated by the BDG, was sampled in detail (Figure 8-7). The $\delta^{18}\text{O}$ gradient at the contact is approximately 20 per mil/m over a distance of about 0.5 m. The fairly symmetric distribution of $\delta^{18}\text{O}$ values across the dike suggests that this multiple dike occupies a major pre-BDG fracture which allowed easy access to the meteoric-hydrothermal fluids. Continued fracturing and magma injection led to strong ^{18}O depletion of the main part of the dike ($\delta^{18}\text{O}_R \approx +1$), but interaction between the margins of the dike and the isotopically heavy Durness limestone contact rocks increased the $\delta^{18}\text{O}$ values near the

contact to about +4 or +5. There is also a possibility, however, that these basaltic dikes may have originally been intruded, at least in part, as low- ^{18}O magmas.

8.6 Mesozoic sediments

The Mesozoic sedimentary rocks have been variously affected by the Tertiary plutonic centers of Skye. Similar to the relationship shown by the Torridonian, there is an excellent correlation between $\delta^{18}\text{O}_R$ of the Jurassic shales and their proximity to the nearest major intrusion (Figure 8-8). The $\delta^{18}\text{O}_R$ of the shales vary from +12.4 to -0.6. These isotopic effects extend outward at least 1.3 km from the intrusive contacts, if we assume these shales originally had normal $\delta^{18}\text{O}$ values of about +14 to +19 (Silverman, 1951; Taylor and Epstein, 1962b; Savin and Epstein, 1970). Thus some of these shale samples probably have been lowered in ^{18}O by more than 14 per mil.

The light-colored Middle Jurassic sandstones of Skye (Morton, 1965) have exceedingly uniform oxygen isotope ratios, typical of sedimentary sandstones elsewhere in the world (Savin and Epstein, 1970). Three sandstone samples from the Strathaird Peninsula have $\delta^{18}\text{O}_Q = +11.3$, +11.6 and +12.0 (see Figure 8-5), while another has $\delta^{18}\text{O}_R = +13.0$. A sample collected from the contact of the Rudh an Eireannaich (R an E) sill near Broadford has $\delta^{18}\text{O}_Q = +10.0$; its $\delta^{18}\text{O}$ value may have been lowered by the R an E sill.

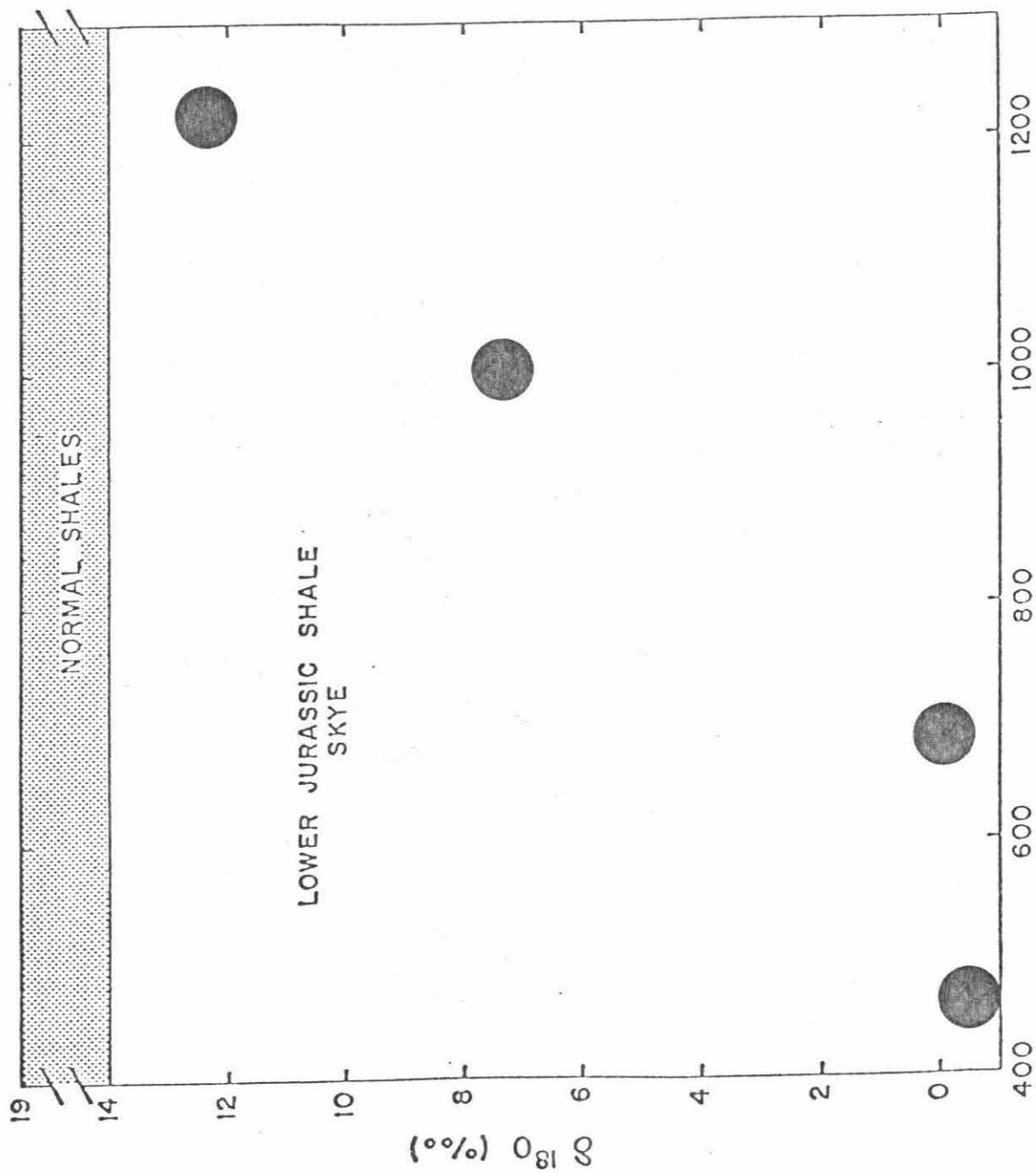


Figure 8-8. Plot of $\delta^{18}O$ vs distance for samples of Jurassic shale from Skye.

The carbonates of the Great Estuarine Series (Hudson, 1962) have been the subject of a stable isotope study by Tan (1969). While the majority of the carbonates have 'normal' $\delta^{18}\text{O}$ values of +25 to +30, those in the vicinity of the Tertiary igneous intrusions show significant ^{18}O -depletion. For example, the calcites from limestone, marlstone, and calcareous shale on the shore north of Elgol on Strathaird Peninsula have $\delta^{18}\text{O} = +22.5$ to $+12.3$, whereas $\delta^{18}\text{O}_{\text{dol}}$ varies from $+27.8$ to $+18.5$ (Tan, 1969; Tan and Hudson, 1971). These values are with respect to SMOW, and have been recalculated from Tan's data which are given in terms of PDB.

Isotopic effects similar to those found by Tan and Hudson were also found in the present study (Table 8-1). In particular, SK-151 has $\delta^{18}\text{O}_{\text{Ct}} = +5.7$, and is the most ^{18}O -depleted Mesozoic carbonate yet analyzed from Skye. It was collected 5 cm from the contact with the overlying Eocene basalts, and is only 0.25 km from the contact of the gabbro pluton in the Blaven Range. Note that this sample is also more ^{18}O -depleted than any of the regionally metamorphosed marbles of Sheppard and Schwarcz (1970) or contact metamorphosed marbles described by Shieh and Taylor (1969b).

In general, the minor intrusive bodies that invade the Mesozoic sedimentary rocks are little affected by the interaction of heated meteoric groundwaters. In part, this is due to the fact that they are intrusions of small volume, and so the meteoric-hydrothermal effects that they produce are equally

small. Another reason is that the Mesozoic country rocks are not as permeable as the basalts. In fact, shales are notoriously impermeable to ground water flow. All things considered, it is not surprising to have $\delta^{18}O_R = +7.9$ (SK-24) for a gabbroic dike cutting shales, with the contact gabbro having $\delta^{18}O_R = +9.1$ (SK-25). Here is an apparent example of ^{18}O -enrichment due to contamination or isotopic exchange with the country rock shales; similar effects in larger intrusions have been described by Turi and Taylor (1971a, b) and Shieh and Taylor (1969a). Note also the near-normal $\delta^{18}O$ values of the dikes and composite sill near Rudha Suisnish (SK-19, 20, 22), Elgol (SKY-28), and those further north (SK-200; 232).

Not all of the minor intrusions are as little affected. Samples from a composite sill south of Broadford (SK-28 and 29) have $\delta^{18}O_R = -0.6$ and -1.0 respectively. A dike north of Strollamus has $\delta^{18}O_R = +0.1$, while five samples from the R and E sill range from $+0.1$ to $+1.4$ and average $+1.3$ (Taylor and Forester, 1971). A 1 m-thick dike that cuts the R and E sill (Buist, 1959) has $\delta^{18}O_R = +1.1$ (SK-258). Hence, although most of the ^{18}O depletion has taken place where basaltic lavas are the dominant country rocks, near the central intrusions the less permeable Mesozoic rocks also were strongly affected by the circulative hydrothermal systems in the early Tertiary.

The only Triassic rock analyzed is a quartzite fragment from a conglomerate (SK-201) with $\delta^{18}O = +10.9$. This value is compatible with the suggestion based on geologic observations

that the majority of fragments in this Triassic conglomerate were derived from the Torridonian (Richey, 1961).

8.7 Basaltic country rocks and dikes

All sample localities representing basalts, vent agglomerates, tuffs, and those basaltic dikes that are pre-Red Hills in age are plotted in Figure 8-9. The $\delta^{18}\text{O}$ contours in this figure are based on whole-rock $\delta^{18}\text{O}$ values measured on 111 samples of these rock types. The reason that the late-stage basaltic dike rocks which cut the Red Hills granites are excluded is that we want to monitor the isotopic effects produced by hydrothermal activity at the times of major plutonic activity. As discussed in Section 8.2, some very late stage igneous events occurred after cessation of the major hydrothermal systems associated with the main plutonic masses. Thus in Figure 8-9 we are comparing rocks of similar mineralogy and grain size with respect to the major Eocene episode(s) of hydrothermal alteration.

Normal, fresh, unaltered basaltic rocks have $\delta^{18}\text{O}$ values that typically fall in the range +5.5 to +6.5 (Taylor, 1968; Anderson et al., 1971; Garlick, 1966). Thus all the sample points that lie above (outside) the $\delta = +5$ contour on Figure 8-9 have essentially 'normal' $\delta^{18}\text{O}$ values. All these 'normal' samples were collected well away from the central intrusive complexes. The $\delta^{18}\text{O}_R$ values are extremely systematic, decreasing inward toward the center of the plutonic complex.

Figure 8-9. Contours of whole-rock $\delta^{18}\text{O}$ values for pre-Red Hills basalts, basaltic dikes, and agglomerates. $\delta^{18}\text{O}$ contours at +5, +3.5, +2, -3, and -5 are based on 111 data points. The black dots are sample localities. The area within the +5 contour is approximately 500 km².

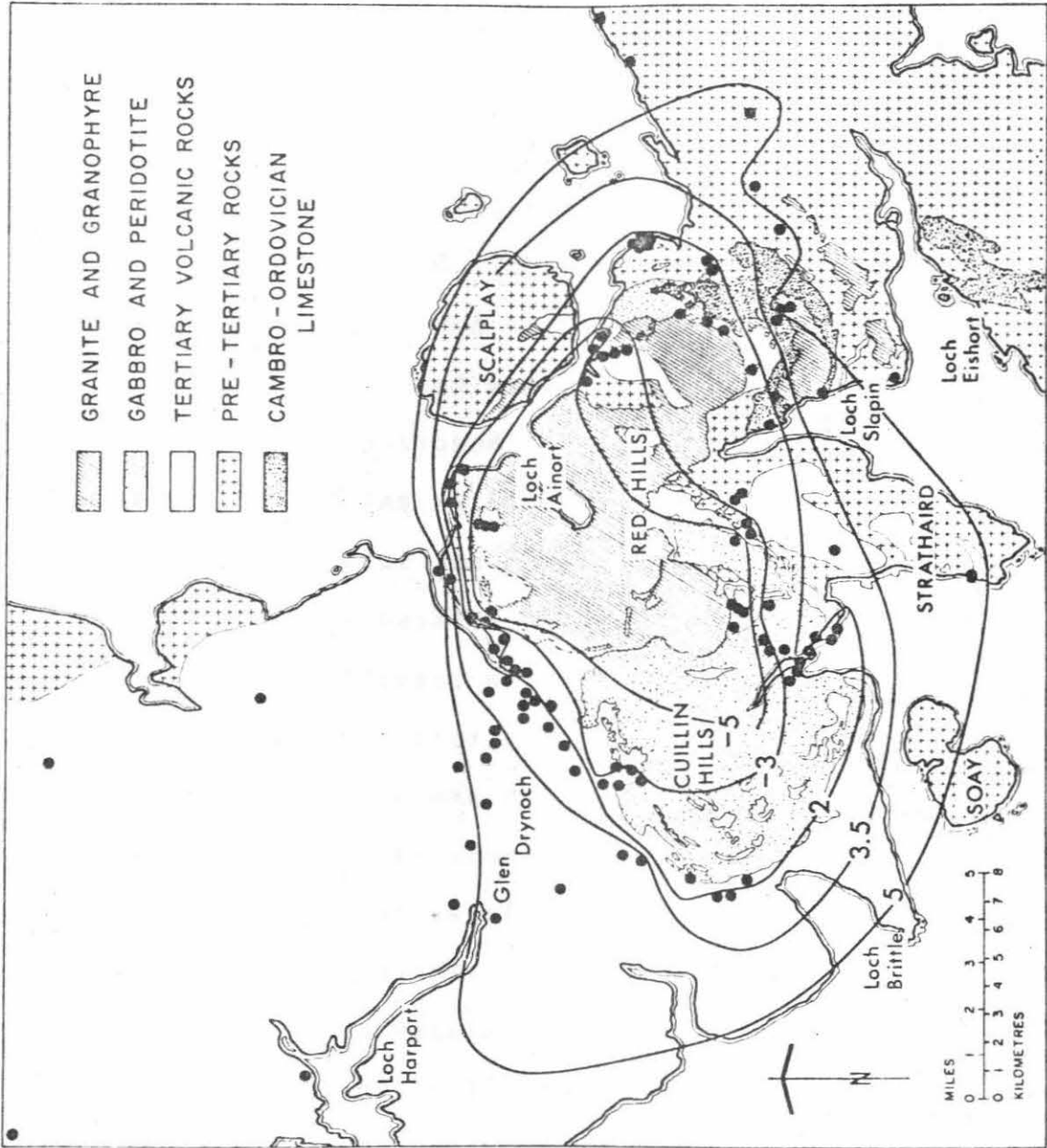


Figure 8-9

The samples inside the $\delta = -5$ contour must all have been depleted in ^{18}O by at least 10 per mil.

This radial inward depletion in ^{18}O is undoubtedly caused in part by increasing temperatures towards the intrusive centers. Therefore, although it is an oversimplification, it is instructive to consider the following model. Let us assume that the W/R ratio was constant throughout the area of Figure 8-9 during hydrothermal activity, with a uniform value of 1.5. Assuming $\delta_R^f = \delta_F(\text{An}_{50})$, and utilizing the ^{18}O fractionation curve between feldspar and water (O'Neil and Taylor, 1967), temperatures can be assigned to each of the $\delta^{18}\text{O}$ contours (Table 8-3). Thus for samples within the $\delta = -5$ contour we obtain $T > 650^\circ\text{C}$; $T \approx 200\text{-}300^\circ\text{C}$ at the margins of the plutonic complex; and $T < 85^\circ\text{C}$ for the basalts outside of the $\delta = +5$ contour. Notice for three different W/R ratios indicated in Table 8-3, the calculated temperatures are not strongly dependent on the W/R ratio in the region where $\delta^{18}\text{O}_R > 0$. For example, at $\delta_R^f = +3$, the calculated temperatures are 130° , 120° and 115° , respectively, for W/R ratios of 1.0, 1.5 and 2.0. The hypothetical temperature gradients range from about $35^\circ\text{C}/\text{km}$ to $350^\circ\text{C}/\text{km}$ and average approximately $70^\circ\text{C}/\text{km}$.

As pointed out by Taylor and Forester (1971) and Taylor (1971), there are two reasons why the outer basalts would not be drastically altered from their original primary values: (1) the meteoric waters coincidentally have approximately $\delta^{18}\text{O}$ values required for isotopic equilibrium between An_{50} plagioclase

Table 8-3

Calculated temperatures* of oxygen isotope exchange between H₂O and basaltic country rocks and dikes, assuming constant water/rock ratios

Temperature, °C

δ_R^f	W/R = 1.0	W/R = 1.5	W/R = 2.0
+6	70°	70°	70°
+5	85°	85°	85°
+4	105°	100°	100°
+3	130°	120°	115°
+2	160°	145°	135°
0	240°	200°	180°
-3	565°	360°	295°
-4	980°	470°	360°
-5	∞	655°	450°
-6	∞	1130°	595°
-7	∞	∞	895°

* Assuming $\delta_R^f = \delta_F(\text{An}_{50})$, utilizing the following equation:

$$\frac{W}{R} = \frac{+6.6 - \delta_R^f}{\delta_R^f - [\Delta - 12]}$$

where +6.5 = δ_R^i , -12 = δ_W^i (see Section 8.2), and

$$\Delta = 2.53 (10^6 T^{-2}) - 3.61; T \text{ is in } ^\circ\text{K (O'Neil and Taylor,}$$

1967)

($\delta^{18}O_F \approx +6.5$) and water at low temperatures, and (2) because of the low temperatures prevailing at distances well away from the heat source (intrusive), the water-rock interactions would involve much lower isotopic exchange rates.

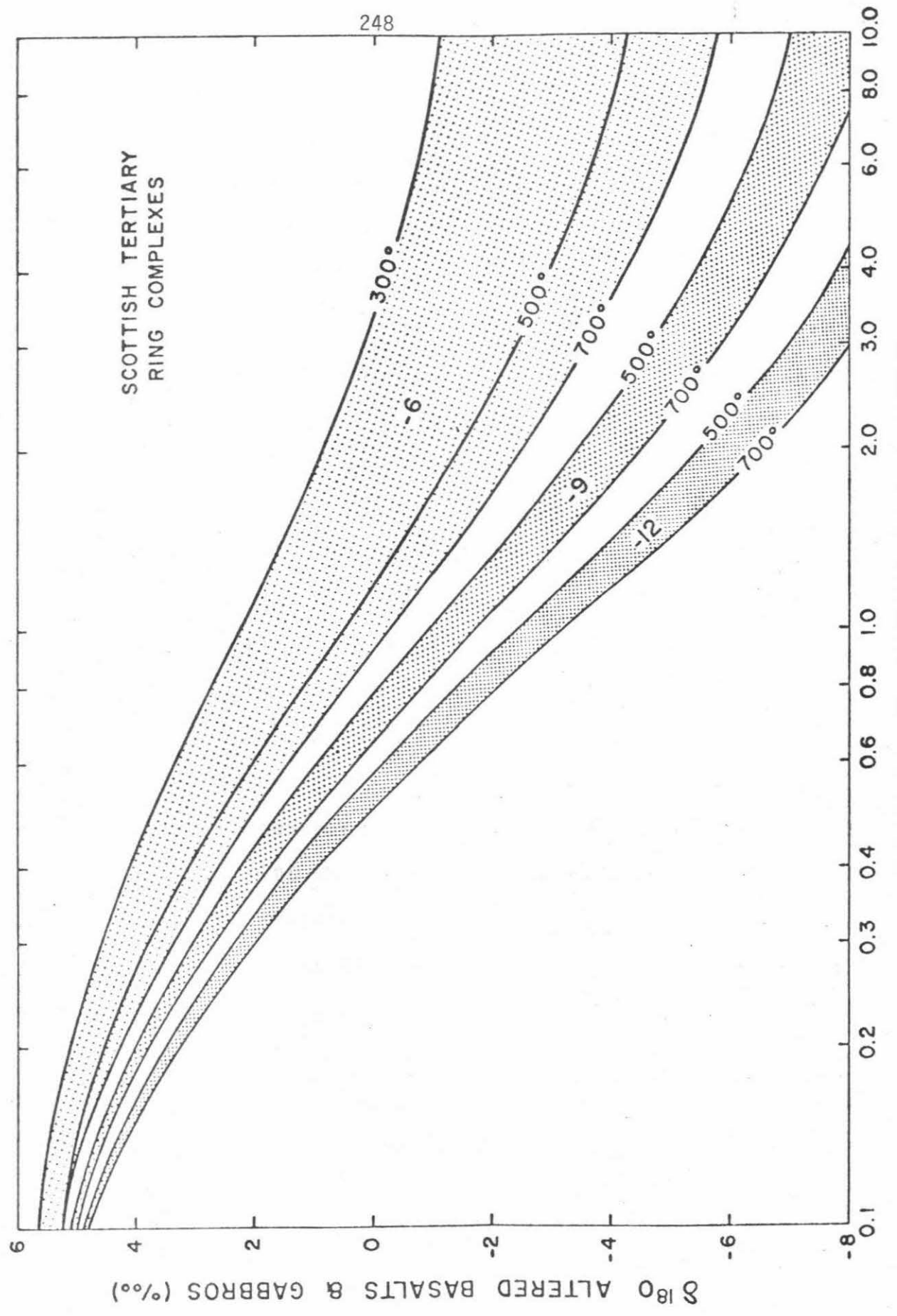
Our assumption of a constant W/R value is obviously not entirely realistic. The W/R value probably increases as we approach the margins of the intrusives, because the flow of water is radially inward, and the rock volume decreases radially inward as the square of the distance (assuming cylindrical geometry). Thus, if W/R = 0.1 at a distance of 10 km from the intrusive center, at 1 km the W/R would be 10. Increase of the W/R ratios in the vicinity of the heat source is also evident from the flow pattern analyses of Wooding (1957) and Elder (1965; 1967), and from measurements in modern geothermal systems. On the other hand, the isotopic composition of the water also changes as isotopic exchange takes place between the water and the mineral phases in the rocks through which it passes. This process acts in a direction that counterbalances that of underestimating the W/R ratios, thus partially correcting the inherent errors in our simplified model.

Water/rock ratios

Figure 8-10 is a δ_R^f vs W/R diagram constructed for basaltic rock types (An₅₀ plagioclase; see Section 6.11 for details). In the light of the considerations dealt with in Section 8.2, it is not necessary to consider $\delta_W^i < -12$.

Figure 8-10. $\delta^{18}\text{O}$ vs W/R diagram for basaltic and gabbroic rocks from northwest Scotland. Calculated curves based on $\delta_{\text{R}}^{\text{i}} = +6.5$ for system behaving as An_{50} plagioclase. Although not plotted in the diagram, it should be noted that the 300°C isotherm for $\delta_{\text{H}_2\text{O}}^{\text{i}} = -9$ coincides very closely to that of the 500°C line for $\delta_{\text{H}_2\text{O}}^{\text{i}} = -6$; similarly, the 300°C line for $\delta_{\text{H}_2\text{O}}^{\text{i}} = -12$ corresponds almost exactly to the 500°C isotherm for $\delta_{\text{H}_2\text{O}}^{\text{i}} = -9$.

SCOTTISH TERTIARY
RING COMPLEXES



WATER / ROCK (ATOMIC OXYGEN RATIO)

Figure 8-10

Basalts SK-223 ($\delta^{18}\text{O} = -7.0$) and SK-518 ($\delta^{18}\text{O} = -7.1$) are the most ^{18}O -depleted whole-rock samples analyzed from Skye. Reference to Figure 8-10 indicates that it is impossible to explain these ^{18}O values with $\delta_{\text{H}_2\text{O}}^i \geq -6$. Even for $\delta_{\text{H}_2\text{O}}^i = -9$, extremely high W/R ratios ($\gg 10$) are required for temperatures lower than about 500°C . All basaltic whole-rock samples with $\delta^{18}\text{O} \leq -3$ require minimum W/R ratios of at least 1. The data from the Tertiary volcanic rocks of Skye thus require that a wide range of water-rock ratios, from essentially zero up to values greater than 2 or 3, are needed to characterize this province. The average estimated water/rock ratio for these hydrothermally altered basalts is at least 0.5.

The $\delta = +5$ contour represents the approximate outermost limit of meteoric-hydrothermal alteration in southern Skye. Essentially all the rocks within this area ($\sim 500 \text{ km}^2$) are significantly depleted in ^{18}O . If the effects originally extended over a vertical distance of about 3 km (see Figure 4-5), this implies that some 1500 km^3 of rock have undergone appreciable ^{18}O -depletion, and therefore an approximately equal volume of water has passed through the rocks. This is an enormous amount of water, but can easily be accounted for by normal amounts of rainfall. For example, with a catch basin area of 2000 km^2 and assuming that only 10% of an annual rainfall of 75 cm is added to the deep circulation system, it would require 10^4 y. to supply the needed amounts of H_2O . It is certain that the intrusive igneous activity at Skye extended over a much longer period than

this. Beckinsale (1974), for example, suggested that the igneous activity in Mull lasted for about 10 m.y. Therefore even though large amounts of rock have been affected and large amounts of H_2O are necessary, the quantities are well within reason.

The problem remains, then, to account for the quantities of heat energy necessary to drive the convection system. If the hydrothermally altered rocks have been produced by an average rise in temperature of the basaltic country rocks from about $50^\circ C$ to $300^\circ C$, then with a specific heat of $0.26 \text{ cal/gm}/^\circ C$, 65 cal/gm of heat must be added to this alteration zone. With $W/R \approx 0.6$, 0.33 gm of H_2O must be heated along with every gm of rock, demanding an additional 85 cal/gm . Thus the hydrothermally altered country rocks require approximately 150 cal/gm . Now consider a silicate melt crystallizing and cooling from 1000° to $300^\circ C$. The maximum heat that can be liberated in this exothermic process, including the latent heat of crystallization, is about 280 cal/gm . Exothermic hydration reactions (see Section 4.2) may account for an additional 35 cal/gm . Thus a cylindrical stock of magma only contains enough energy to produce a hydrothermally altered aureole about 0.7 stock diameters wide (see Taylor, 1971; 1974b). This calculated value is very close to what is actually observed in Skye (Figure 8-9). Note that Bott and Tuson (1973) have interpreted their gravity survey as indicating that about 3500 km^3 of material ($\rho = 3.01 \text{ g cm}^{-3}$) underlie the plutonic centers of Skye to a depth of about 14 km .

8.8 Cuillin gabbro complex

General statement

All the $\delta^{18}\text{O}$ values for the Cuillin rocks are presented in Table 8-1; the oxygen isotope data on coexisting minerals in all the gabbroic rocks from Skye are plotted on Figure 8-11.

On the basis of a few analyzed specimens from the Cuillin Hills, Taylor and Forester (1971) suggested that the $\delta^{18}\text{O}$ values increase as one moves toward the interior of the complex. The present study substantiates that preliminary conclusion (see Figures 8-12 and 8-13). The new data, however, make it clear that the entire Cuillin layered complex, as well as the dike rocks which cut it, are abnormally low in ^{18}O . The general inward enrichment in ^{18}O in the complex is presumably a result of the fact that the interior samples are (1) a progressively greater distance away from the contact with the permeable plateau basalts through which the meteoric ground waters migrated, and (2) a progressively greater distance away from the later intrusive bodies (i.e. the Western Red Hills granites and explosion vents, which set up their own meteoric-hydrothermal convective systems). The effects of these later events are superimposed upon the Cuillin gabbros, which were the country rocks into which the granites were intruded (see below).

Plagioclase

Plagioclase feldspar $\delta^{18}\text{O}$ values range from +2.5 to -7.1 (29 samples; see Table 8-1). The $\delta^{18}\text{O}_F$ values are plotted and

Figure 8-11. $\delta^{18}\text{O}$ analyses of coexisting minerals from all gabbroic rocks of Skye, Scotland, arranged in order of decreasing $\delta^{18}\text{O}_F$. Also shown are the ^{18}O values for coexisting minerals in a hypothetical original gabbro with a 'normal' (i.e. unexchanged) $^{18}\text{O}/^{16}\text{O}$ ratio, as well as the $\delta^{18}\text{O}$ values of minerals that would have crystallized from a hypothetical low- ^{18}O gabbroic melt that may have existed in the Skye area (see text). Samples with prefix SKY are from Taylor and Forester (1971); mg = medium grained; vcg = very coarse grained; all samples are from the Cuillin Hills except SK-51, which is from the Broadford gabbro.

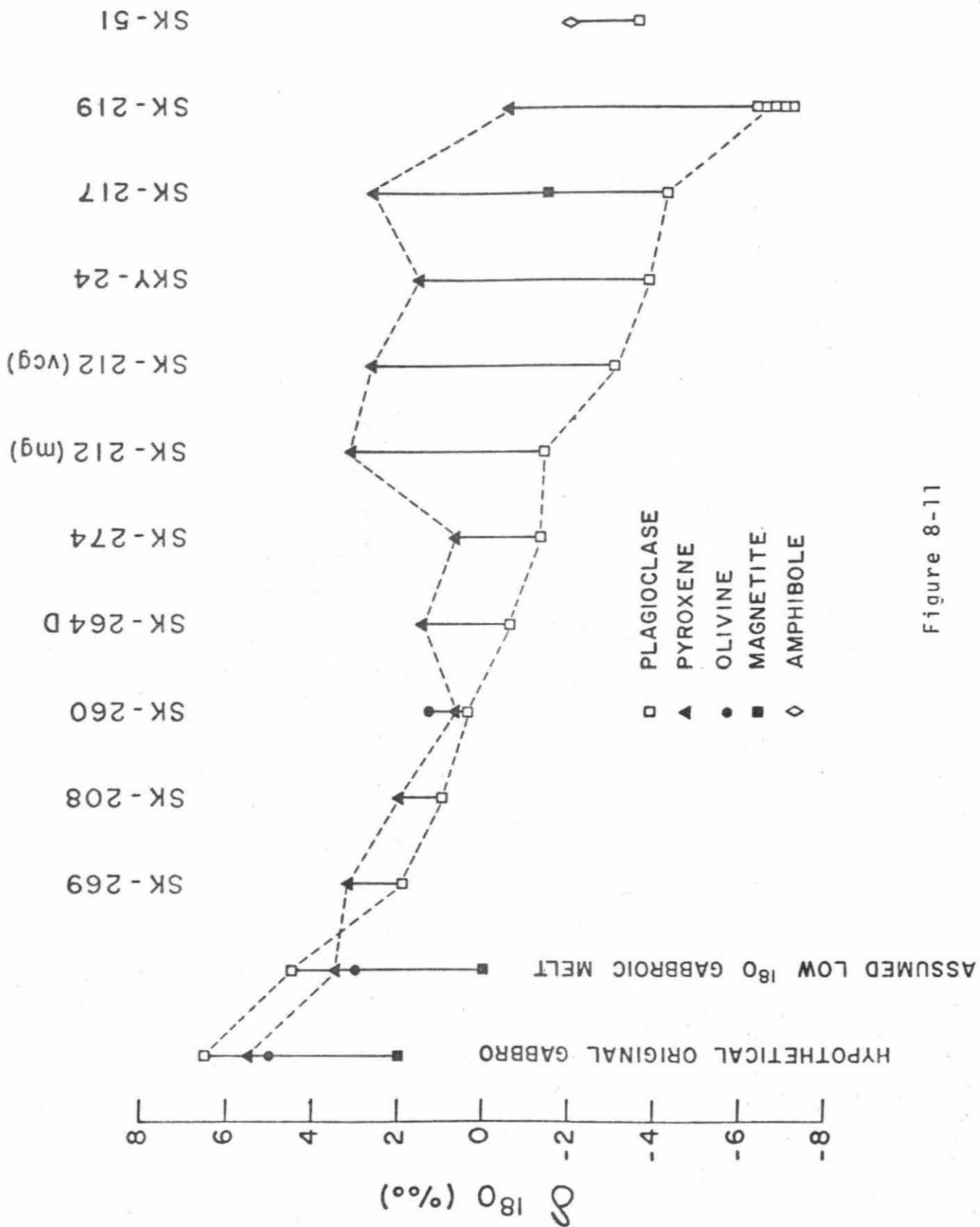


Figure 8-11

contoured on Figure 8-12. Where several plagioclase separates of differing magnetic susceptibility were analyzed, the weighted average was used (see Chapter 3); thus only 23 analyses are plotted on Figure 8-12. All samples falling within the central contour have $\delta^{18}\text{O}_F > 0$. The most pertinent features shown in Figure 8-12 are the following: (1) the most positive $\delta^{18}\text{O}_F$ values define an ovoid central core in the Cuillin complex, in the vicinity of Loch Coruisk; (2) the most ^{18}O -depleted plagioclases are in close proximity to either the earlier plateau basalts or to the later granites and the volcanic vent, and (3) the $\delta^{18}\text{O}_F$ contours cut across the various primary igneous stratigraphic units of the Cuillin layered series.

We would a priori predict on the basis of the meteoric-hydrothermal model that, for the intrusion of an epizonal pluton into basaltic country rocks, the least affected rocks would be those in the core region of the intrusion; $\delta^{18}\text{O}_{\text{H}_2\text{O}}$ would tend to increase as water-rock interaction and isotopic exchange went on, and thus the initial isotopic contrast between the water and rock would diminish both with time and with distance of penetration into the central core of the intrusion. The distribution of ^{18}O contours was originally probably fairly symmetric just after emplacement and cooling of the Cuillin complex. The pattern was then modified by later periods of oxygen isotope exchange that occurred during and just after intrusion of the vent agglomerate and Western Red

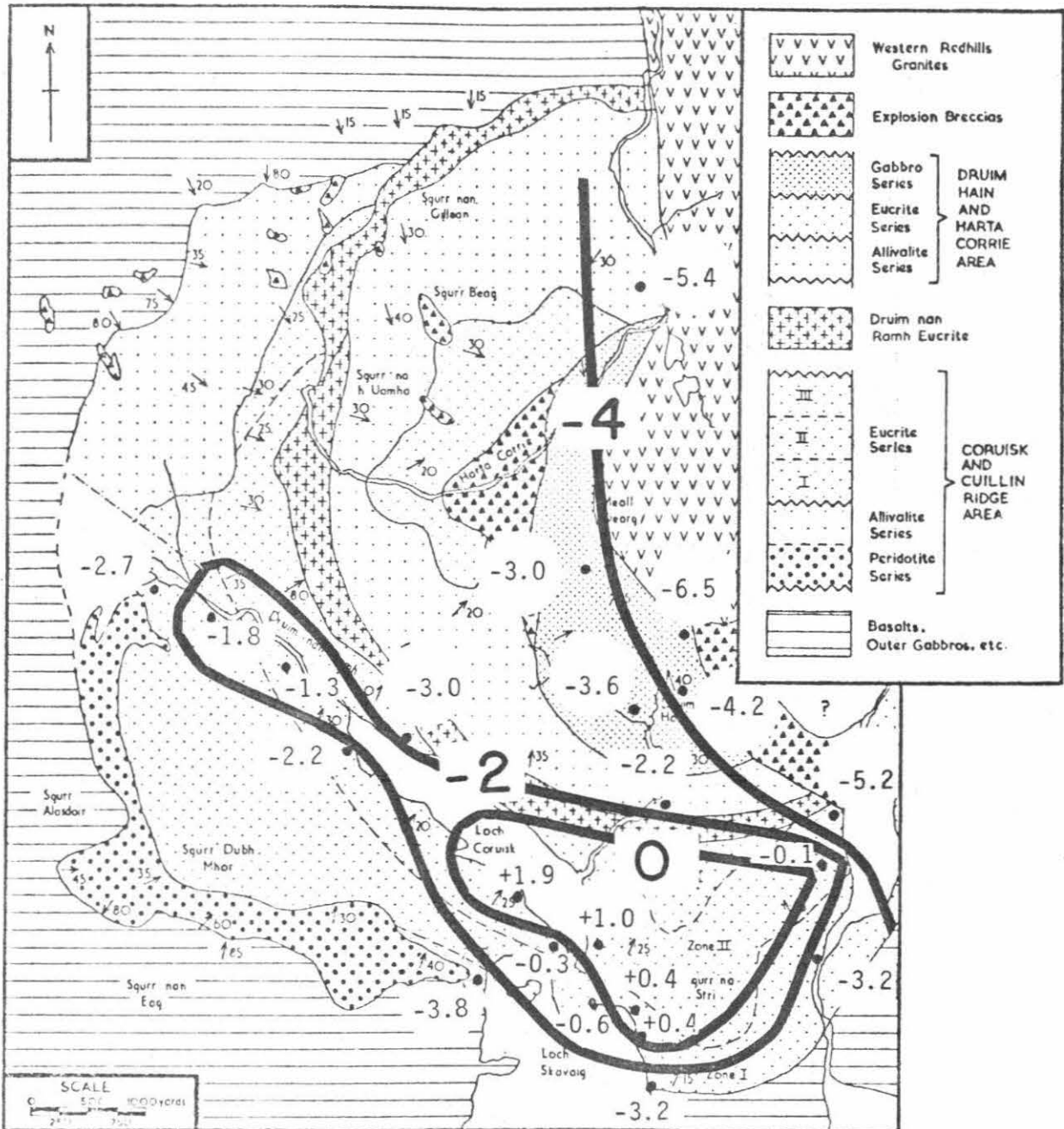


Figure 8-12. Plot of $\delta^{18}O$ values of plagioclase in the Cuillin intrusion, Skye, showing approximate contours at $\delta^{18}O_F = 0, -2, \text{ and } -4$.

Hills granitic complex; this produced the final pattern shown on Figure 8-12. Note that the $\delta^{18}\text{O}_F = -4$ contour closely parallels the contacts between the gabbros and the Western Red Hills granites and explosion breccias (Figure 8-11).

The fact that the $\delta^{18}\text{O}_F$ contours cut across the primary igneous structural subdivisions (and cryptic compositional variations of the minerals) in the Cuillins gabbros indicates that these $\delta^{18}\text{O}$ variations were largely imposed subsequent to crystallization. Thus it is clear from the plagioclase data alone that this mineral has been exchanged in the solid state throughout a major part of the Cuillin layered intrusion. As pointed out below, some ^{18}O exchange could have occurred with the gabbroic melt itself, but stringent limitations can be placed on the maximum amount of ^{18}O exchange that could have taken place prior to crystallization of the silicate liquid. It is clear from the ^{18}O data on coexisting plagioclase and pyroxene that subsolidus exchange of oxygen isotopes was dominant. Normal Δ_{F-P} values from gabbroic rocks are about +1.0 (e.g. Taylor, 1968). In the Cuillin gabbros these Δ -values are invariably negative. Thus all of the plagioclases must have been lowered in ^{18}O to some extent in the solid state. Some of the plagioclases have been lowered to a remarkable degree, by 13 to 14 per mil. As in prior studies, it is clear from the data presented in Figure 8-11 that of the several minerals in the gabbros, feldspar is by far the most susceptible to oxygen isotope exchange. There is no correlation between grain size

and $\delta^{18}\text{O}$ for the plagioclase. In fact, several samples exhibiting a wide variation in grain size were collected at locality SK-212; the medium-grained plagioclase turned out to have a slightly more 'normal' $\delta^{18}\text{O}$ (-1.4) than the plagioclase of the pegmatitic gabbro ($\delta^{18}\text{O}_F = -3.0$). The same grain-size relationship holds for the $\delta^{18}\text{O}$ of the coexisting pyroxene (see Figure 8-11). A reasonable explanation for this is that the pegmatitic gabbro is probably a recrystallized rock formed by interaction with a high-temperature aqueous solution. The recrystallization may have occurred simultaneously with oxygen isotope exchange in the presence of the meteoric-hydrothermal fluid phase, and thus the coarser-grain size may have been produced by the meteoric-hydrothermal activity.

Four different plagioclase separates were analyzed from SK-219 (average $\delta^{18}\text{O}_F = -6.5$). In order of increasing magnetic susceptibility, the $\delta^{18}\text{O}_F$ values are -6.3, -6.7, -6.9, and -7.1, respectively. The ^{18}O variation is outside analytical error. Each magnetic separate gave identical oxygen yields consistent with the mineral separate being pure calcic plagioclase, although the more magnetic samples do contain more of the dust-like, opaque inclusions (presumably magnetite). The heterogeneous oxygen isotope distribution in the SK-219 plagioclase is yet another indication of isotopic disequilibrium and subsolidus exchange. It is interesting that the lowest- ^{18}O plagioclase contains the greatest abundance of opaque inclusions, suggesting that the dusty, cloudy appearance of the

plagioclase was itself produced by subsolidus hydrothermal exchange. These same conclusions apply to SK-226, where two different magnetic separates of plagioclase have $\delta^{18}\text{O} = -4.8$ and -5.6 .

The most ^{18}O -depleted plagioclase samples should most closely approach the isotopic composition of the original, unexchanged meteoric ground waters, because at equilibrium $\Delta_{\text{F-H}_2\text{O}}$ is positive at all temperatures below about 600°C (O'Neil and Taylor, 1967). It has already been demonstrated from the hydrogen isotope data (Section 8.2) that $\delta_{\text{H}_2\text{O}}^{\text{i}}$ was about -12 , but the ^{18}O data from SK-219 demonstrate independently that $\delta_{\text{H}_2\text{O}}^{\text{i}}$ must have been lower than -7 . In fact, $\delta_{\text{H}_2\text{O}}^{\text{i}}$ surely was much lower than -7 , because of the typical positive ' ^{18}O shift' shown by all geothermal waters, and because it otherwise requires almost an infinite amount of water to explain the low $\delta^{18}\text{O}$ values of some of the Cuillin plagioclases (see Figure 8-10). Even today, Skye does not receive this amount of rain, although there are many Scots who would refute this. To reasonably explain $\delta^{18}\text{O}_{\text{F}}$ values as low as -7.1 with a $\delta_{\text{H}_2\text{O}}^{\text{i}}$ value of -12 would require that $W/R > 2.3$ at temperatures of 700°C or lower (refer to Figure 8-10). If $\delta_{\text{H}_2\text{O}}^{\text{i}} = -9$, the $W/R > 4.8$ for all temperatures lower than 700°C , and $W/R > 10.0$ for all temperatures lower than 500°C . The range of W/R values necessary to explain the Cuillin plagioclases, utilizing the most probably correct value of $\delta_{\text{W}}^{\text{i}} = -12$ and $T \approx 700^\circ\text{C}$, is $W/R \approx 0.3$ to 5.0 . At temperatures significantly lower than 700°C , much larger W/R values would be required.

Pyroxene

The $\delta^{18}O_p$ values are plotted and contoured in Figure 8-13. Fewer data are available than for plagioclase, so the overall shapes and trends of the contours in Figure 8-13 was drawn with some artistic license to roughly conform with the ones shown in Figure 8-12. Nonetheless it is clear that there is an inward increase in $\delta^{18}O_p$ in the gabbro body even though the $\delta^{18}O$ variation for pyroxene is not nearly as large as for plagioclase (only from +3.2 to -0.5). The pertinent features of Figure 8-13 are exactly those of Figure 8-12: (1) a central core contains the highest $^{18}O/^{16}O$ ratios, (2) the lowest $^{18}O/^{16}O$ ratios are found close to the original margins of the Cuillin complex or to contacts with younger rock units, and (3) the $\delta^{18}O_p$ contours clearly transect the stratigraphic subdivisions in the igneous layering shown by the Cuillin gabbros. Note that amphibolitization of the pyroxenes is only apparent near the Western Red Hills contact and coincides with the very low $\delta^{18}O_F$ values.

The fact that a similar pattern of $\delta^{18}O$ values holds for the pyroxenes as well as the plagioclases indicates that the same basic processes affected both of these minerals. The fact that the variation in $\delta^{18}O_p$ is smaller than the variation of $\delta^{18}O_F$ reaffirms and supports our earlier contention that plagioclase is more susceptible to oxygen isotope exchange than pyroxene. If the original igneous plagioclase had $\delta^{18}O_F = +6.5$ in the Cuillin gabbro, then we would expect the original pyroxene

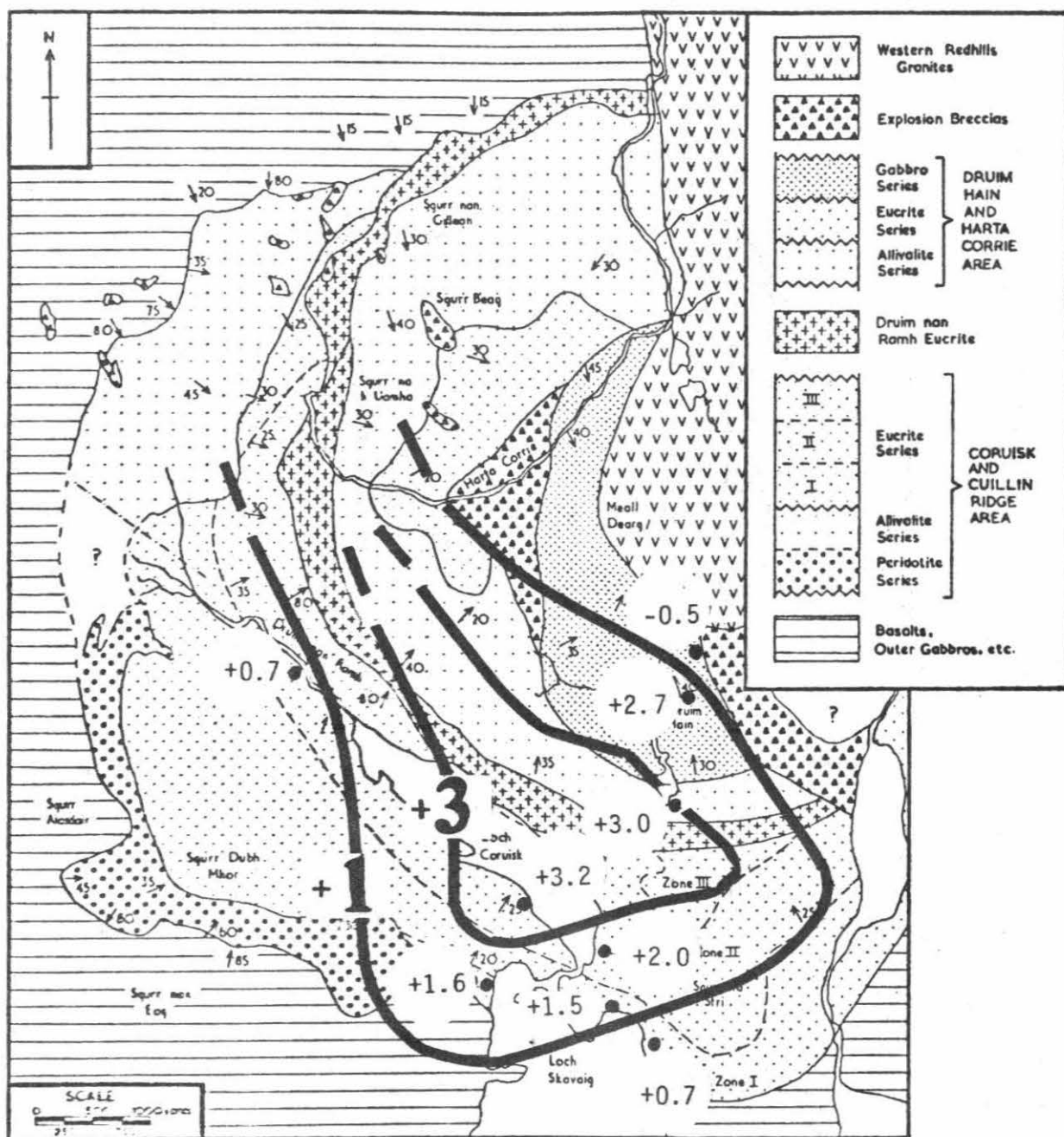


Figure 8-13. Plot of $\delta^{18}\text{O}$ values of clinopyroxene in the Cuillin intrusion, Skye, showing approximate contours at $\delta^{18}\text{O}_p = +3$ and $+1$.

to have $\delta^{18}O_p = +5.5$ (see Figure 8-11). Inasmuch as the typical Cuillin pyroxenes now have $\delta^{18}O \approx +3$, and if we assume that the Cuillin complex was derived from an isotopically homogenous magma, the maximum amount of ^{18}O lowering that could have occurred in the melt was about 2.5 per mil.

Plagioclase-pyroxene fractionations

Combining the data of Figures 8-12 and 8-13, we obtain Δ_{F-p} values contoured in Figure 8-14. The pattern is, by necessity, similar to that of Figures 8-12 and 8-13, with the most 'normal' fractionations concentrated in a core region in the Cuillin gabbro. Normal Δ_{F-p} values for gabbroic rocks are about +1.0 (see Figure 8-11), but all of the Cuillin Δ_{F-p} values are negative. Some values are as low as -6.9, emphasizing that the pyroxene is much less susceptible to oxygen isotope exchange than the plagioclase. It has never before been shown that an entire intrusion has a Δ -value reversed from the normal equilibrium fractionations, but nowhere in the entire Cuillin complex do you find plagioclase heavier in ^{18}O than the coexisting pyroxene. This is in marked contrast to the situation at Stony Mountain, Colorado and is largely the result of the longer and vastly more complex history of hydrothermal activity at Skye, as well as because of the larger W/R ratios.

Magnetite

Magnetite is an uncommon phase in the Cuillin layered series. It occurs as a cumulus phase in Zones I and III of the Eucrite Series, but is most abundant in the Gabbro Series (Figure 7-4). The only analyzed magnetite is from the latter horizon, where 1 mm grains of cumulus magnetite make up about 20% of the gabbro (SK-217; Plate 8-1b). Compared to other plagioclase-pyroxene-magnetite assemblages in gabbroic igneous rocks (Taylor, 1968), the plagioclase has been lowered in $\delta^{18}\text{O}$ by 10.7 per mil, the pyroxene by 2.7 per mil, and the magnetite by approximately 3.4 per mil (Figure 8-11). We would conclude from this sample alone that magnetite shows about the same susceptibility to oxygen isotope exchange as pyroxene, because the pyroxene and magnetite grains in this rock are about equal in size. From $\delta^{18}\text{O}$ values of coexisting phases from the Stony Mountain, Colorado, it was also suggested that pyroxene and magnetite had similar susceptibilities to oxygen isotope exchange. However, this was qualified by the fact that the magnetite of the Stony Mountain complex was of several origins, and may not necessarily represent single-stage isotopic exchange from its primary value. The magnetite of SK-217 demonstrates that, at the very maximum, we can only have had about a 3.4 per mil $\delta^{18}\text{O}$ lowering in the silicate melt from which SK-217 crystallized.

Olivine

The main mass of layered peridotites and dunites in the Cuillin Hills is represented by the ultramafic rocks of Sgurr Dugh (Weedon, 1965). After solidification, these ultramafic cumulates were invaded by a tholeiitic gabbro magma and were broken into blocks which were deposited along with the eucrite cumulates. One of these dunite blocks, SK-270 (Plate 7-3), is composed of fresh, unserpentinized olivine (Fo_{87} , Weedon, 1965) with minor chrome-spinel. Apart from the zones where this rock has undergone granulation and crushing, the minerals are remarkably well preserved, and secondary alteration products are rare. The olivine in SK-270 has a $\delta^{18}O = +2.4$. Inasmuch as olivines in typical basalts and dunites have relatively constant $\delta^{18}O_{01} \approx +5.0$ (Reuter et al., 1965; Taylor and Epstein, 1962b; Anderson et al., 1971), SK-270 has been depleted in ^{18}O by about 2.6 per mil, and the olivine of SK-260 has been lowered by about 3.7 per mil. The SK-270 data indicate that no more than about a 2.6 per mil lowering of the pristine $\delta^{18}O$ value of the Cuillin magma could have taken place. Note that in SK-260, the plagioclase has undergone considerably more ^{18}O -depletion (6.1 per mil) than the coexisting olivine, while the pyroxene has experienced only a slightly larger depletion (4.8 per mil) than the olivine. Because of the coarser grain size of the olivine (Table 8-1) this suggests that olivine probably has about the same resistance to oxygen isotope exchange as pyroxene.

Summary

It thus appears that if a homogeneous, low- ^{18}O Cuillin magma ever existed, the ^{18}O data on pyroxene, olivine and magnetite from a wide variety of Cuillin rocks all indicate approximately the same amount of maximum $\delta^{18}\text{O}$ lowering for this silicate melt. These numbers are 2.3, 2.6, and 3.4 per mil, respectively. These similarities, as well as the striking uniformity of the $\delta^{18}\text{O}_p$ values, suggest that the Cuillin gabbroic magma may indeed have been a low- ^{18}O melt, depleted by about 2 to 3 per mil relative to 'normal' basalts (see Assumed Low- ^{18}O Gabbroic Melt in Figure 8-11). It is, of course, possible that the entire $\delta^{18}\text{O}$ depletion in the Cuillin olivines and pyroxenes occurred after crystallization at subsolidus temperatures. Inasmuch as olivine is well preserved almost everywhere in the layered Cuillin intrusion, this would imply that all of the ^{18}O exchange must have taken place at temperatures above the stability field of serpentine (i.e. above approximately 500°C (Tuttle and Bowen, 1949). It also would imply that after the high-temperature exchange had occurred, the olivine-bearing rocks must all have become isolated from any further interaction with the meteoric-hydrothermal fluids. There is no obvious reason why this should have happened, and it thus seems more reasonable that $\delta^{18}\text{O}_{01}$ in the Cuillin gabbros represent primary igneous values. Note that Muehlenbachs et al (1974) have reported that some fresh Icelandic basalts have ^{18}O depletions up to 3.8 per mil.

An interesting point should be considered in regard to the depth of circulation of the hydrothermal fluids. The stratigraphic thickness of the Cuillin layered intrusion (ignoring the outer gabbros) is at least 5 km (Wager and Brown, Chap. XV, Fig. 224). Because of the evidence for faulting, arcuate fracturing and magma chamber collapse, the layered gabbros have a somewhat complex structure. Let us, however, assume that the gabbro layering was essentially sub-horizontal directly following crystallization. The amount of cover above the layered complex can then be estimated from the data of Brown (1963) on the Coire Uaigneich granophyre. This granophyre was emplaced directly after the Cuillins intrusion, and Brown (1963) concluded that the overlying plateau basalts at the time were about 1 km thick. Hence, it is suggested that large quantities of convecting meteoric ground waters reached depths on the order of at least 6 km. This depth is comparable to the suggested depths of meteoric-hydrothermal alteration at the Skaergaard intrusion (Taylor and Forester, 1974), in the Western Cascades (Taylor, 1971, Figure 9) and at Wairakei, New Zealand (see Figures 4-3 and 4-4, Chapter 4).

8.9 Broadford gabbro

The age relationship of the Broadford gabbro with respect to other intrusions in southern Skye is not well known, except that it is definitely older than the AFG (Stewart, 1965). The gabbro is olivine-free, and commonly shows signs of shearing

and fragmentation with the development of actinolite and chlorite as alteration minerals. The Creag Strollamus area in which the Broadford gabbro occurs is one of extreme structural and petrographic complexity. As pointed out by King (1953) this area "represents in miniature all the formational and structural elements of the plutonic region of Skye".

The $\delta^{18}\text{O}_R$ values of the gabbros have been lowered by almost 10 per mil (Table 8-1). Actinolitic amphibole after pyroxene has $\delta^{18}\text{O} = -1.9$, while coexisting plagioclase has $\delta^{18}\text{O} = -3.5$ (Figure 8-11), again confirming that feldspars are the most susceptible to oxygen isotope exchange. Note that all of the Cuillin gabbros show much less mineralogical evidence of hydrothermal alteration than those at Broadford. The Broadford gabbro has apparently suffered oxygen isotopic exchange down to much lower temperatures than did the Cuillin gabbros. The former typically has abundant uralite, while the latter underwent partial amphibolitization of the pyroxenes only in those rocks adjacent to the Western Red Hills granites. The reason for this difference probably lies in the fact that the Broadford gabbro is close to, and has been affected by the many granitic intrusions of Eastern Red Hills, whereas the Cuillin complex in general is relatively far removed from the subsequent intrusive plutonic centers.

As discussed previously, the basaltic and Torridonian country rocks are also highly depleted in ^{18}O in the Broadford area. One of the most striking characteristics of the low- ^{18}O

rocks in the Creag Strollamus area is their highly veined, fractured, faulted and fragmented nature. There is little doubt that this mechanical disaggregation, and the lengthy and complex plutonic igneous activity in this area were responsible for the low $^{18}\text{O}/^{16}\text{O}$ ratios exhibited by these rocks.

8.10 Coire Uaigneich granophyre

The age of the Coire Uaigneich granophyre is pre-Red Hills granites but post-Cuillin gabbros. It forms a narrow strip of outcrops between the Blaven Range and the basalts, and its relative age was established by recognizing that the cone sheets that cut the Cuillin complex but not the Red Hills granites also intrude this granophyric mass (Richey, 1932). This rock is unusual among the granophyres at Skye in that (a) it is hypersthene-bearing, (b) inverted tridymite crystals are present, indicating a $T_{\text{melt}} \geq 900^{\circ}\text{C}$, (c) it has a very high normative quartz content (39.87%; see Table 7-1), similar to that of the Torridonian arkose of Skye, and (d) its Rb-Sr 'isochron' demonstrates it has not had a simple closed-system evolution (Long, 1964). Wager *et al* (1953) suggested, and Brown (1963) provided experimental evidence, that this granophyre may well be a melting product of the Torridonian sandstone.

The CUG has an average whole-rock $\delta^{18}\text{O} = -1$. Modifying the basic model of Brown (1963), let us assume that the Torridonian in contact with the Cuillin intrusion is partially

- Plate 8-1a. Stony Mountain gabbro, SM-101. Clear to dusty plagioclase ($\delta^{18}O = +5.2$), fresh biotite (center of photograph, $\delta^{18}O = +5.5$) and pyroxene ($\delta^{18}O = +5.5$), magnetite ($\delta^{18}O = +2.0$), and apatite. Width of field = 2.5 mm. Plane polarized light.
- Plate 8-1b. Cuillin gabbro, SK-217. Well laminated rock, with fairly clear plagioclase ($\delta^{18}O = -4.2$), cracked and veined by chlorite; clinopyroxene ($\delta^{18}O = +2.7$) is very fresh except for some dusty magnetite along cracks; and magnetite ($\delta^{18}O = -1.4$). Width of field = 2.5 mm. Plane polarized light.
- Plate 8-1c. Cuillin gabbro, SK-260. Well laminated rock, with fresh plagioclase ($\delta^{18}O = +0.4$) and very fresh clinopyroxene ($\delta^{18}O = +0.7$). Width of field = 2.5 mm. Plane polarized light.

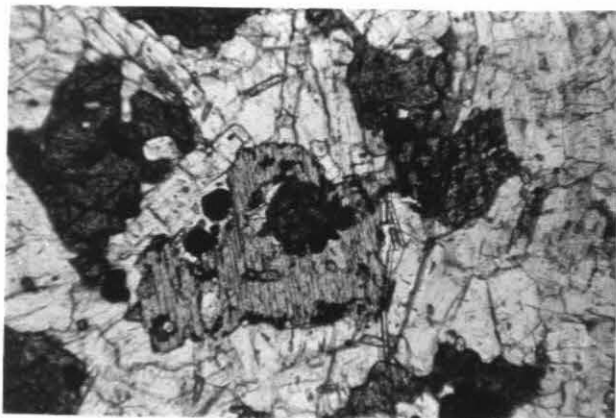


Plate 8-1a

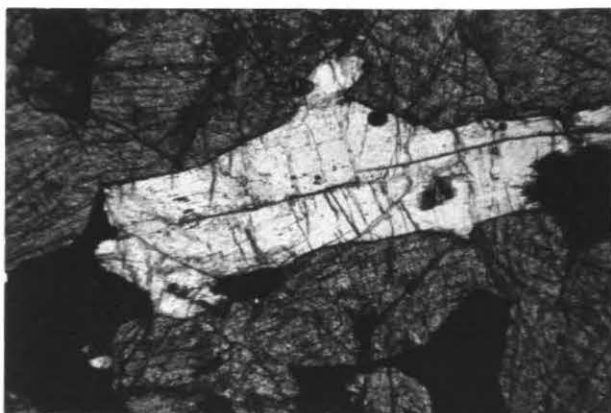


Plate 8-1b



Plate 8-1c

- Plate 8-2a. Southern Porphyritic Epigranite, SK-181. Phenocrysts of β -morphology quartz ($\delta^{18}\text{O} = -2.6$) and turbid alkali feldspar ($\delta^{18}\text{O} = -3.5$) in a granophyric matrix. Note the cracked and dusty nature of the quartz. Width of field = 2.5 mm. Plane polarized light.
- Plate 8-2b. Maol na Gainmhich Epigranite, SK-511B. Quartz ($\delta^{18}\text{O} = +5.2$, center of photograph) contains trains of dust-like inclusions; alkali feldspar ($\delta^{18}\text{O} = -6.7$) is cloudy to turbid, especially around the rims of some of the grains. Width of field = 2.5 mm. Plane polarized light.
- Plate 8-2c. Beinn Dearg Mhor Epigranite, SK-128. Turbid alkali feldspar ($\delta^{18}\text{O} = -6.0$) surrounded by coarse granophyric intergrowths of turbid alkali feldspar and quartz. The quartz in the intergrowth is optically continuous. Width of field = 2.5 mm. Plane polarized light.

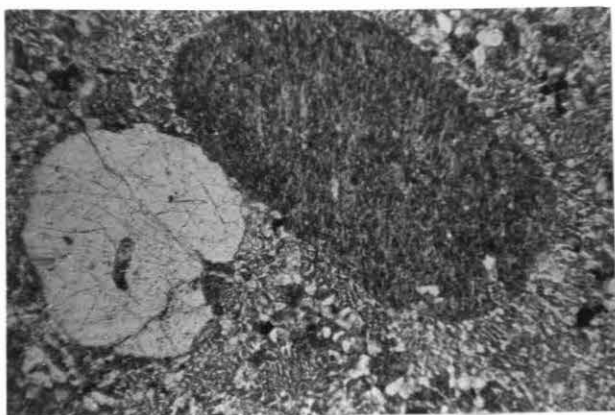


Plate 8-2a



Plate 8-2b

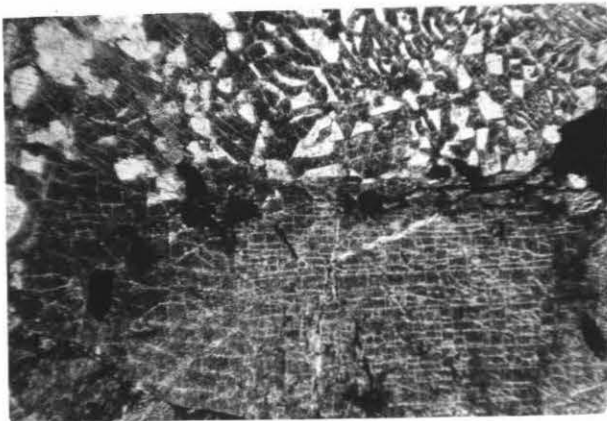


Plate 8-2c

melted in the presence of meteoric ground waters, at about 300 bars P_{H_2O} and $970^\circ C$ (see Figure 3, Brown, 1963). This would lead to about 2 wt % H_2O in the melt. Using $\delta_W^i = -12$, $\delta_R^i = +10.8$ (e.g. Torridonian samples SK-534D; SK-203), a mass balance calculation indicates $\delta_R^f = +9.8$. Hence only about 1/12 of the observed ^{18}O depletion of the CUG can be explained by direct influx of low- ^{18}O H_2O during the generation of the melt. The remaining 11 per mil of ^{18}O depletion must have been produced either by later hydrothermal alteration, or else the CUG melt was formed by partial fusion of Torridonian sandstones that had already been lowered in ^{18}O by 10 or 12 per mil prior to melting. If this happened, the CUG could well have been originally intruded as a low- ^{18}O melt. Note that some Torridonian samples have been lowered even more than this (e.g. SK-63 in the Creag Strollamus area and SK-116 and SK-516A north of Meall Buidhe). If we assume that the CUG was a low- ^{18}O magma, the ^{18}O data independently confirm Brown's model. Here is a possible example where meteoric waters were responsible for generating a melt, because dry melting of a rock of this normative composition requires an unrealistically high $T \approx 1200^\circ C$ (Brown, 1963).

8.11 Western Red Hills

Of the nine arcuate intrusions of the Western Red Hills center (Figure 7-5), eight have been extensively sampled. The earlier granite intrusions in general have lower $\delta^{18}O$ values

(particularly in K feldspar) than do the later intrusions. Quartz ranges from +6.4 to -2.7, and alkali feldspar varies from +2.6 to -6.7 (Table 8-1, and Figures 8-1 and 8-15). The average Δ_{Q-K} value is remarkably large, namely 6.9.

The earliest of these granites, the MGE, exhibits a very restricted range of $\delta^{18}O_K$ values (-4.9 to -6.7) and exceptionally large nonequilibrium Δ_{Q-K} values (see Figure 8-15). SK-512c has the largest Δ_{Q-K} (12.0) reported in the literature, and the average Δ_{Q-K} value for the MGE is 10.6. The GE also has extremely large Δ_{Q-K} values (6.8 and 9.9) and $\delta^{18}O_R$ values as low as -5.9. The amphibole (hastingsite) of SK-124 has a $\delta^{18}O$ value (-5.2) that is lower than that of the coexisting K-feldspar (-4.2). In this respect this sample is similar to the feldspar-amphibole pairs from Oregon (Taylor, 1971), but the amphibole from SK-124 is the most ^{18}O -depleted amphibole analyzed to date. Two quartz samples from the BDME have $\delta^{18}O = +2.0$ and $+4.0$, with Δ_{Q-K} values of 8.0 (SK-128) and 5.6 (SK-503), respectively.

The LAE was studied in detail in order to test the variability of $\delta^{18}O_Q$ and $\delta^{18}O_K$ within a single epigranite intrusion. The range of $\delta^{18}O$ in the LAE was found to be similar to that found in other intrusions that have not been sampled so extensively. The $\delta^{18}O_Q$ values range from +1.7 to +4.8, while $\delta^{18}O_K$ vary from -0.3 to -4.8. Note that the $\delta^{18}O_Q$, $\delta^{18}O_K$, and Δ_{Q-K} values of the euhedral minerals in the miarolitic cavities fall essentially within the same range of values as the host-

Figure 8-15. Plot of $\delta^{18}\text{O}$ values of coexisting minerals from the Western and Eastern Red Hills of Skye. Numbers are the $\Delta_{\text{Q-K}}$ values. Also shown are $\delta^{18}\text{O}$ analyses of miarolitic (m) and granophyric (g) minerals. The abbreviations used for these granitic intrusions are the same as given in Table 8-1.

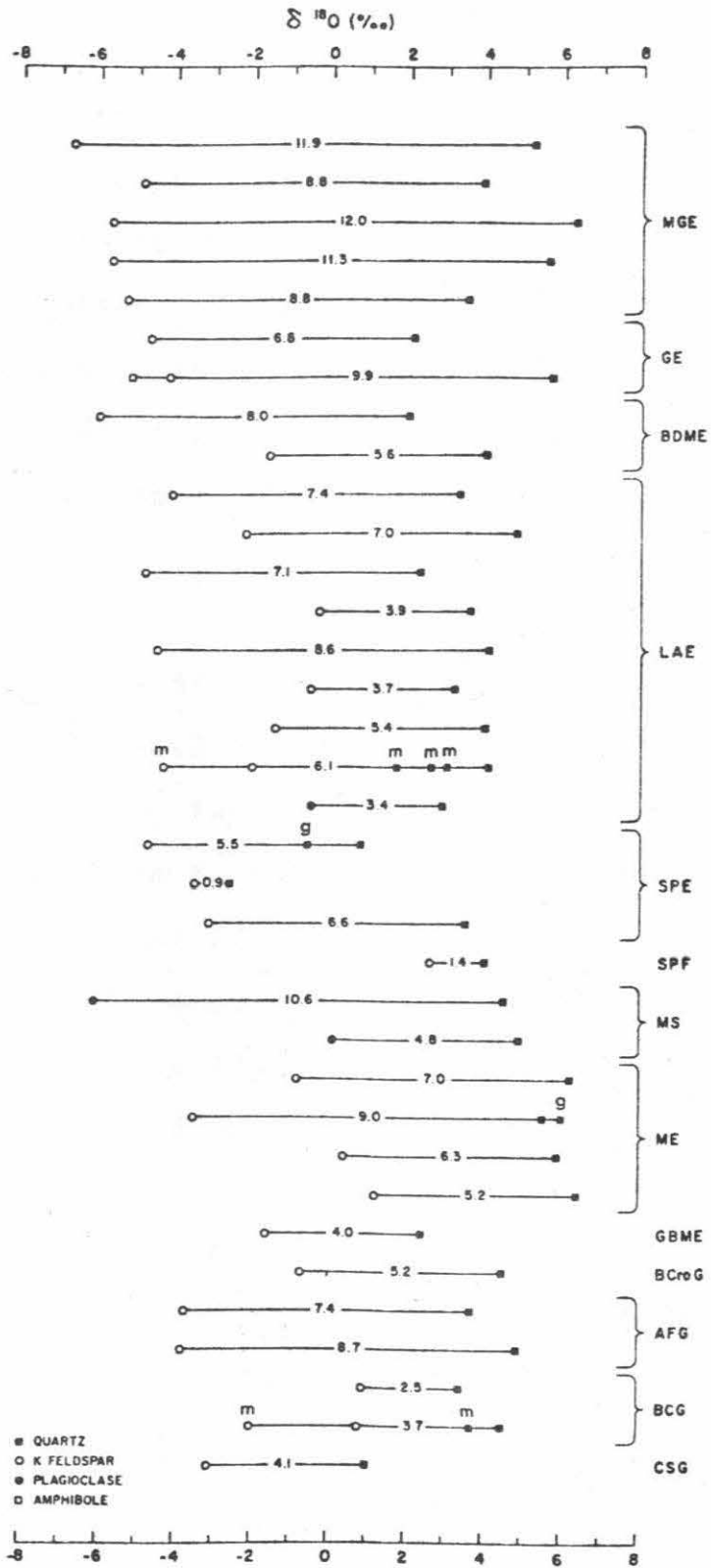


Figure 8-15

rock phases (Table 8-1; Figure 8-15). Different samples of miarolitic quartz from cavities within the same hand specimen (SK-507) vary in $\delta^{18}\text{O}$ (+1.7, +2.6 and +3.0). These cavities are prima facie evidence of the presence of a gas phase, and the ^{18}O data and other mineralogical characteristics make it clear that this gas phase was largely H_2O . Unfortunately, the same post-consolidation processes that have affected the host-rock minerals have also affected the miarolitic minerals, as indicated by the large $\Delta_{\text{Q-K}}$ values of the latter.

Perhaps the most intriguing $^{18}\text{O}/^{16}\text{O}$ ratios are those of the SPE. Firstly, the SPE exhibits an exceptionally large spread in $\delta^{18}\text{O}_{\text{Q}}$ from +5.2 to -2.6. Secondly, the β -morphology quartz of SK-181 has by far the lowest $\delta^{18}\text{O}$ value (-2.6) of any quartz yet analyzed from the Red Hills. Thirdly, this same sample has a normal $\Delta_{\text{Q-K}} = 0.9$, approximately the expected equilibrium value at magmatic temperatures. On the other hand, two other samples of the SPE have $\Delta_{\text{Q-K}}$ values of 5.5 and 6.6. Both HF and F_2 stripping experiments were done on the SPE samples in an attempt to better understand these provocative oxygen isotope analyses. These will be discussed in detail below.

The SPF, a rock very similar to the SPE, has $\delta^{18}\text{O}_{\text{Q}} = +4.0$. Moreover, it has a near-normal $\Delta_{\text{Q-K}}$ value of 1.4. The MS exhibits widely divergent $\Delta_{\text{Q-K}}$ values (10.6 and 4.8), with the two quartz $\delta^{18}\text{O}$ values being very similar (+4.5 and +4.9). The $\delta^{18}\text{O}_{\text{R}}$ values extend down as low as -6.0.

Four samples from the ME are remarkably similar isotopically. The $\delta^{18}\text{O}$ of quartz varies from +6.4 to +5.9, while in feldspar the range is from +1.2 to -3.5. Note that the granophyric quartz in SK-117 is very similar in ^{18}O to the coarser-grained equigranular quartz in the same hand specimen (+6.0 vs +5.5). It is significant to note that in the Western Red Hills the rock unit that is characterized by greatest uniformity of $\delta^{18}\text{O}$ values of the mineral phases and has the highest $\delta^{18}\text{O}_\text{Q}$ values is the last (youngest) intrusion, namely the ME.

We will now apply the meteoric-hydrothermal convective model in an attempt to explain the first-order features shown by the isotopic data, namely the fact that much larger ^{18}O depletions (particularly in feldspar) are seen in the earlier granites than in the later intrusions. Upon intrusion of each pluton, a hydrothermal convective system will be established or else an older, preexisting system will be modified. Oxygen isotopic exchange will take place in the nearby country rocks as well as in the fractured, now crystallized, cooling pluton. If after sufficient cooling, a subsequent event further fractures the country rocks, intrusion of another arcuate pluton may occur, and this will commonly be intruded along an arc interior to the previous pluton. This new pluton will also set up a meteoric water convective system and cause ^{18}O depletion of the surrounding country rocks, including the earlier intrusive, as well as undergoing ^{18}O exchange itself. Thus each pluton will set up its own convective hydrothermal system

that will affect all earlier (older) intrusions. Other things being equal, we would predict that according to this model, the older intrusives would be more affected (having experienced a number of overlapping hydrothermal alteration events and hence more oxygen isotope exchange) than the younger intrusions which have only experienced relatively few events. Another factor that may be important is that the older intrusions on the outside of the complex are directly adjacent to the volcanic country rocks, which in general are more permeable to ground water movement than the later plutonic intrusions. Also, as time goes on, the meteoric-hydrothermal systems tend to be self-sealing because the older fractures (e.g. in the volcanic country rocks) will be filled with vein minerals that are deposited from the circulating solutions. All of these effects are cumulative and all indicate that the older, outermost ring intrusions should show the greatest ^{18}O depletions.

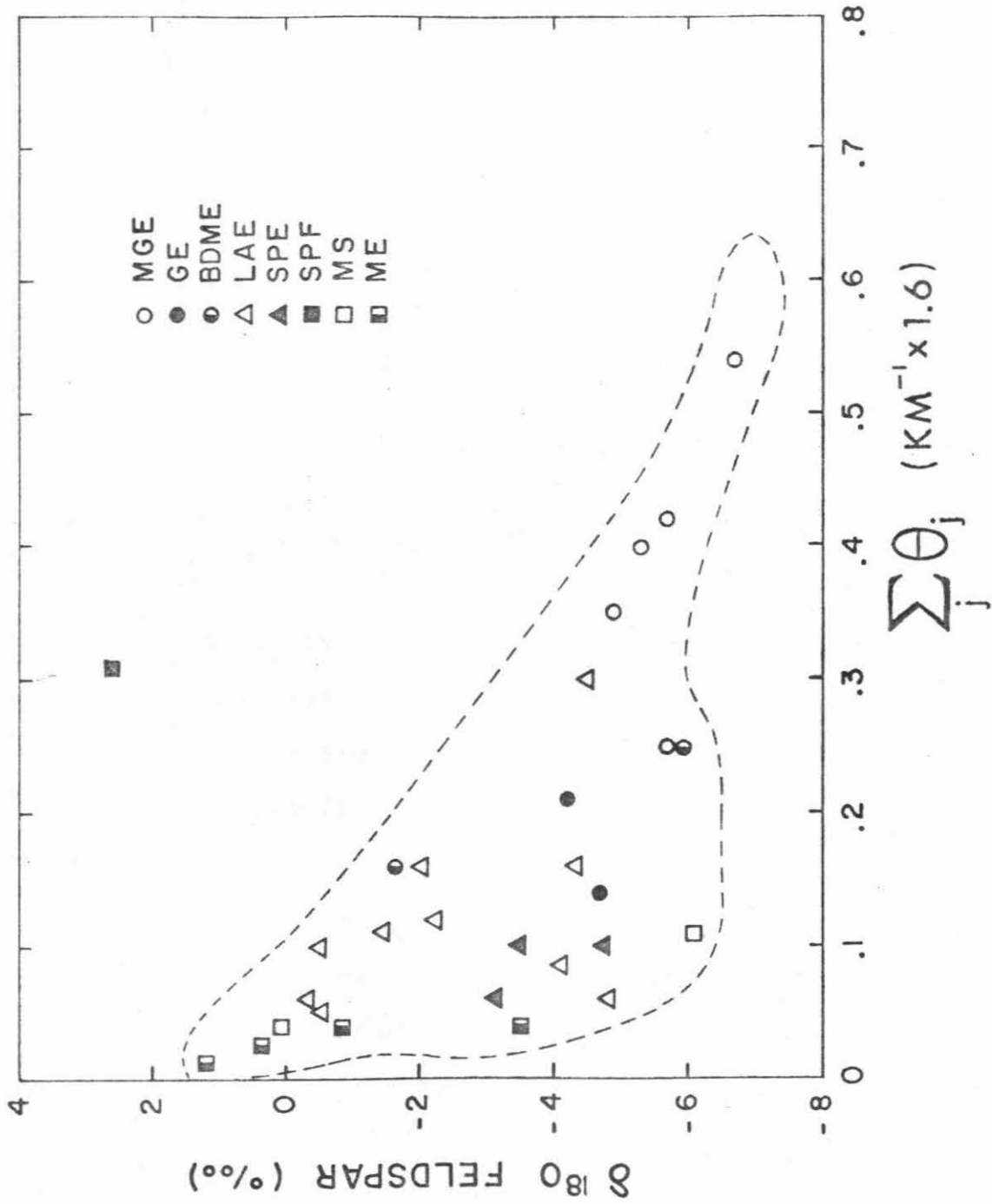
Some of the variables that would affect this model are the following: (a) The closer a country rock sample is to the heat source, the higher the temperature of the exchange reaction will be, and thus the more closely will it reflect the value of $\delta_{\text{H}_2\text{O}}$. This will lead to greater ^{18}O depletions. Added to this is the fact that the higher temperatures promote more rapid isotopic exchange. (b) The larger the volume of the intrusion (heat source), the greater will be the $\delta^{18}\text{O}$ change in a sample at a given distance away from the contact, other things being equal. This is because the hydrothermal

system will be larger and will persist for a longer time.

(c) The susceptibility to oxygen isotope exchange will be dependent on mineralogy and grain size. Quartz-rich rocks and coarser-grained rocks will in general be less affected.

In order to make a semi-quantitative test of the above model, only $\delta^{18}O_K$ (actually 25 samples are K feldspar, and three are plagioclase) has been used in the following calculations. Alkali feldspar is the mineral most susceptible to oxygen isotope exchange and would best monitor the exchange process. Most of these rocks are of essentially identical mineralogy, as they are all granitic in composition and quartz and feldspar constitute about 90% of each rock. Also, grain size does not vary substantially, and in any event as will be shown below, there is a general lack of correlation between $\delta^{18}O_K$ and grain size (except for the BDG of the Eastern Red Hills; see Section 8.13).

A function that will be a rough measure of the oxygen isotope-distance relationships in our model is designated $\Sigma_j \theta_j$. This function is defined as being inversely proportional to D , the distance (in km) from a given sample locality to the contact of the intrusive body that has produced the particular meteoric-hydrothermal system, and also it is defined as being directly proportional to the volume of the intrusion. Since these Red Hills intrusions apparently have near-vertical contacts, their respective outcrop areas will be an appropriate measure of their volumes. The area function is taken to be the



fraction of the invading pluton's area with respect to the area of the whole granitic intrusive complex at the time of intrusion. Thus the area fraction is a varying function of time, equal to

$$\frac{a_j}{\sum_{i \leq j} a_i}$$

where a_j is the area of the particular (jth) intrusion producing the meteoric-hydrothermal system, and $\sum_{i \leq j} a_i$ denotes the cumulative area of all intrusions up to the time that the jth intrusion is emplaced. Thus, we define

$$\theta_j = \frac{1}{D_j} \left(\frac{a_j}{\sum_{i \leq j} a_i} \right) \text{ (in km}^{-1}\text{)}$$

For every alkali feldspar analyzed from a given pluton, a θ_j value can be calculated for each subsequent intrusion; this is calculated by measuring the shortest distance D (in km) from the sample to the intrusive contact. We can then sum all of these contributions from each intrusion, and obtain a function $\sum_j \theta_j$.

The isotopic exchange function $\sum_j \theta_j$ is plotted against feldspar $\delta^{18}O$ in Figure 8-16. Except for one point, there is a fairly good correlation between $\delta^{18}O_K$ and $\sum_j \theta_j$, indicating that to a first approximation, the model is a reasonable one. The only point falling well off the trend is a sample from the SPF (IGC-13). The probable reason why it has an anomalously high $\sum_j \theta_j$ value (0.2) for a $\delta^{18}O_K = +2.6$ is because IGC-13 is

very close (only ~ 80 m) to the MS and ME; the contribution of these intrusions to $\sum_j \theta_j$ is thus inordinately large. The SPF has only been affected by the MS, ME, and GBME, the first two being of small volume and the last of which is very distant. In fact, the MS was probably intruded almost contemporaneously with the SPF. Wager et al. (1965) point out that "the marscoite has the appearance of having been pushed into the SPF while the latter was still a viscous liquid". Also, the sample is located at the far edge of the Western Red Hills complex and therefore has only experienced the edge effects of the sinuous MS and arcuate ME intrusions, in spite of the fact that the full volumes of these intrusions are applied to the generation of the $\sum_j \theta_j$ function.

Let us now examine the oxygen isotopic data from the Western Red Hills in more detail. Figure 8-17 is a plot of $\delta^{18}O_Q$ in the eight intrusions vs their order of emplacement. Inasmuch as quartz is the most resistant rock-forming mineral to oxygen isotope exchange, its $\delta^{18}O$ value should best reflect the $^{18}O/^{16}O$ ratio of the original magma from which it crystallized. If each intrusion had a homogeneous $^{18}O/^{16}O$ ratio when emplaced as a liquid, then the most positive $\delta^{18}O_Q$ value would most closely reflect the isotopic composition of the primary igneous quartz prior to hydrothermal alteration. In Figure 8-17 a line is drawn connecting the most ^{18}O -rich quartz samples from each intrusion. 'Normal' granitic rocks of this type elsewhere in the world typically have $\delta^{18}O_Q \approx +8.5 \pm 0.5$; this 'normal' value is also indicated on this figure.

Figure 8-17. $\delta^{18}\text{O}_\text{Q}$ vs age of intrusion for the Western Red Hills, Skye. All individual $\delta^{18}\text{O}_\text{Q}$ analyses are shown for each intrusion, and a line joins the maximum $\delta^{18}\text{O}_\text{Q}$ value for each sequence (see text). Normal epigranite quartz is assumed to have $\delta^{18}\text{O}_\text{Q} = +8.5$.

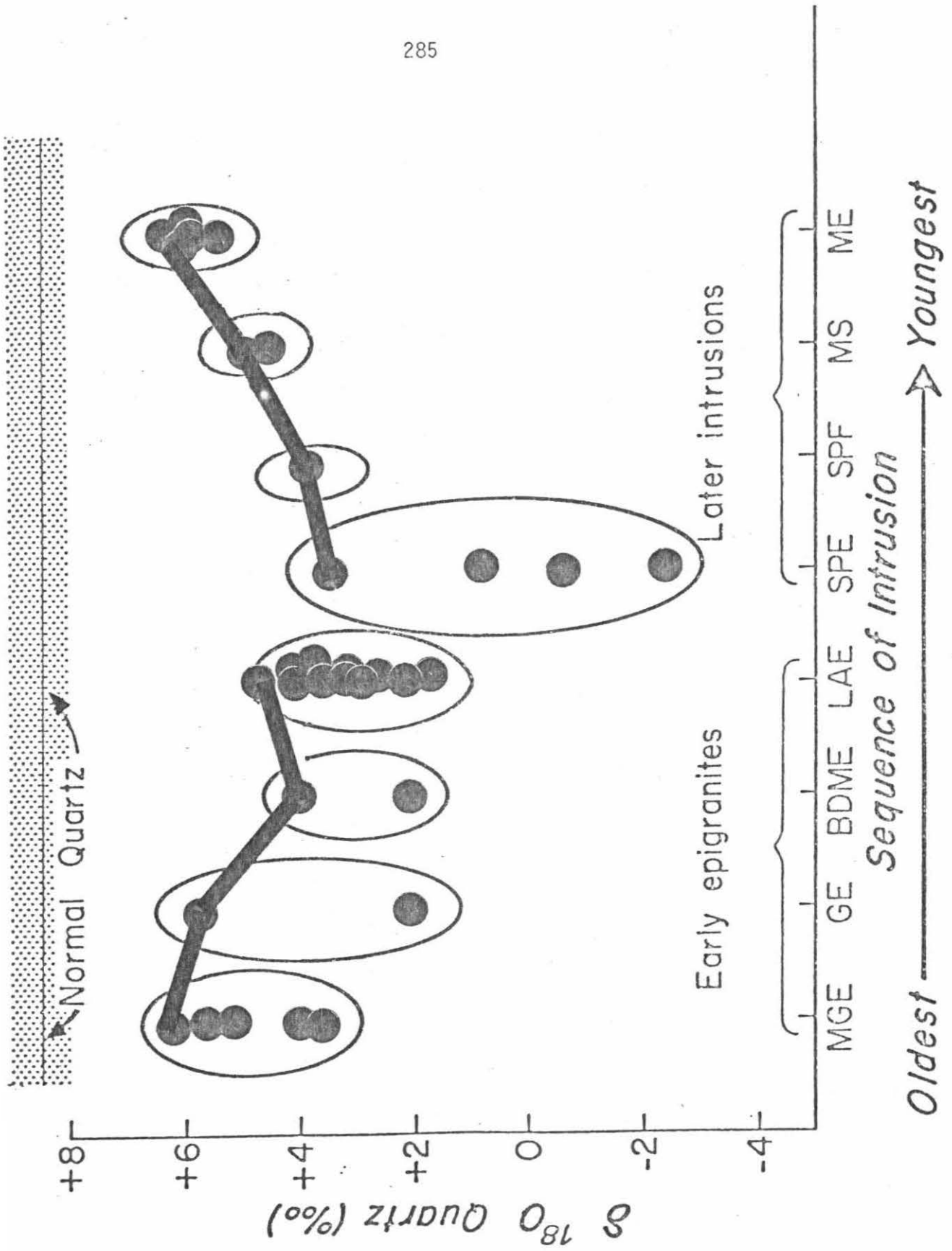


Figure 8-17

Although the total effect is only about 3 per mil, the pattern that emerges from this plot is that $\delta^{18}O_Q$ decreases with time during emplacement of the Early Epigranites, but appears to increase with decreasing age in the Later Intrusions. These provocative trends might conceivably be attributed to chance except that (a) the trends in both the Early Epigranites and the Later Intrusions are substantially monotonic functions of time and (b) the break in sign of the slope of the trend occurs, in time, between the Early Epigranites and the Later Intrusions, which is also a geological and petrological discontinuity. It is unlikely that both (a) and (b) can be attributed to coincidence and these trends therefore may be real and significant. This conclusion is further emphasized by the fact that there is no correlation between grain size and $\delta^{18}O_Q$ in the Western Red Hills intrusions (see Figure 8-18), possibly suggesting that the major $\delta^{18}O$ lowering of the quartz is a primary igneous feature.

How might we interpret the trends of Figure 8-17? As described above in discussing our convective isotope exchange model, other things being equal, we would expect the older intrusions to be more affected by the hydrothermal exchange than the younger intrusions. Thus, if all the granite magmas originally had similar $\delta^{18}O$ values, we might a priori expect a positive slope on this diagram, as is actually shown by the Later Intrusions. The most reasonable explanation why the Early Epigranites exhibit a negative slope is that these intru-

sions, to differing degrees, represent emplacement of low- ^{18}O magmas.

Assuming that 'normal' granite quartz has $\delta^{18}\text{O} = +8.5$, the maximum $\delta^{18}\text{O}$ lowering that the MGE, GE, BDME and LAE silicate melts could have experienced relative to 'normal' granite magmas is 2.2, 2.8, 4.5 and 3.7 per mil, respectively. A general $\delta^{18}\text{O}$ -lowering of the magmas with time might perhaps be expected if meteoric water continuously exchanged with a shallow magmatic reservoir; the youngest magmas would be the most affected because they were exposed to exchange for the longest time. Also, if the melts were formed by partial melting of pre-existing rocks, as suggested by the Pb isotope data (see below), the younger magmas might be derived from rocks that had undergone progressively greater ^{18}O depletion as the meteoric-hydrothermal activity built up to its maximum. Details of the possible mechanisms that may give rise to low- ^{18}O melts have already been discussed in Section 6.12 and need not be repeated here. However, it should be emphasized that the Western Red Hills, characterized by multiple intrusions, repeated fracturing, and ring-dike emplacement, constitute an ideal geologic situation to allow long-continued access of meteoric ground waters to a magma chamber. The most likely mechanisms to produce the types of low- ^{18}O melts envisioned above would be (1) partial melting of the rocks overlying a magma chamber in the zone of meteoric-hydrothermal exchange, and assimilation processes involving direct melting, or (2)

direct exchange between the granitic melt and the ^{18}O -depleted country rock. Partial melting would be facilitated by the water-rich environment in the country rocks; any magmas produced by partial melting in such terranes almost certainly must be low- ^{18}O magmas.

Note that if the Early Epigranites represent a sequence of magmatic differentiates from a common melt, we would expect to see some systematic chemical trends between these intrusions. These are not evident (see Table 7-1), which might suggest the following: (a) The oxygen isotope exchange process may have significantly altered the primary chemical compositions of the granophyric rocks. (b) An additional process has operated to modify both the elemental and isotopic chemistry of the granitic rocks, such as assimilation of low- ^{18}O , hydrothermally altered country rocks. Alternatively, and perhaps more likely, these intrusions may represent partial melting products of the underlying basement gneiss. If the granitic rocks are indeed products of partially melted, inhomogeneous Lewisian gneiss, then we would not expect a continuous variation in major element chemistry between the Early Epigranites, especially if differing amounts of partial melting occurred.

Applying an approach similar to that used on the Stony Mountain inner diorite, we can calculate the amount of ^{18}O depletion involved in melting the Lewisian basement. If melting occurs at a depth of about 7 km with the fluid in

hydrostatic equilibrium, the maximum solubility of H_2O in a granitic melt would be about 3.5 wt % (Burnham and Jahns, 1962; Hamilton et al., 1964). Using $\delta^{18}O = +6.7$ for the Lewisian (see Table 8-1), $\delta_{H_2O}^i = -12$ and $\delta_{H_2O}^f = \delta_R^f$, the final melt would have a $\delta^{18}O = +5.5$. Quartz crystallizing from the melt would have a $\delta^{18}O \approx +6.5$ - i.e. not much higher than that of the most ^{18}O -rich quartz from the epigranites of the Western Red Hills, and in fact, of all granitic rocks from southern Skye except the BDG. This model did not require any prior ^{18}O depletion of the Lewisian gneiss, so it demonstrates that with the addition of only a minor amount of meteoric-hydrothermal alteration of the gneiss, the partial melting model advocated by Bell, 1966 and Thompson, 1969 can readily account for the envisaged low- ^{18}O granitic magmas.

Whereas $\delta^{18}O_Q$ may closely reflect the oxygen isotope ratio of the original Western Red Hills magmas, $\delta^{18}O_K$ (Figure 8-19) best reflects the total time-integrated effect of the meteoric-hydrothermal alteration process that operated on the solidified intrusives. The Early Epigranites show a general trend of increasing $\delta^{18}O_K$ with decreasing age. Again, this is the trend that would a priori be predicted for feldspars that have been affected by overlapping meteoric-hydrothermal systems and have exchanged dominantly at subsolidus temperatures. Restricting ourselves for the moment to the Early Epigranites, we can develop a self-consistent model to explain the $^{18}O/^{16}O$ systematics of both quartz and alkali feldspar in these granophyric rocks.

The model utilizes 'normal' initial values of $\delta^{18}O_Q = +8.5$ and $\delta^{18}O_K = +7.5$, the maximum $\delta^{18}O_Q$ values measured (Figure 8-17) and the average $\delta^{18}O_K$ values (to minimize local variations; see Figure 8-19), along with the following constraints: (1) the $\delta^{18}O$ depletions of the magmas increase with time; (2) the degree of ^{18}O exchange at subsolidus temperatures decreases with time and (3) prior to subsolidus exchange the $\delta^{18}O$ depletions of the primary igneous quartz are, of course, exactly the same as for the primary igneous alkali feldspars. The final model for the Early Epigranites is shown in Figure 8-20.

The low- ^{18}O magma field in Figure 8-20 is constrained by the $\delta^{18}O_Q$ values, as well as the constraints mentioned above. Thus the ^{18}O depletions in the magmas appear to vary from about 1.5 per mil in the early MGE to 3 per mil in the later LAE. The $\delta^{18}O$ lowering of the LAE melt must have been at least 2 per mil, otherwise the field of subsolidus exchange would enlarge towards the younger intrusions, contrary to constraint (2). Post-crystallization oxygen isotopic exchange in the quartz may be about 3.0 per mil for both the MGE and the LAE, while alkali feldspar has clearly been depleted in ^{18}O by at least 13.2 to 7.0 per mil. No matter how one varies the basic model, there is no escaping the conclusion that the alkali feldspars have suffered extreme ^{18}O depletion with respect to quartz, almost wholly during post-crystallization exchange. For the Early Epigranites, the two processes (post-crystallization oxygen isotopic exchange and ^{18}O depletion

of the silicate melt) appear to contribute approximately equally to the final, measured ^{18}O depletion of the quartz, whereas for alkali feldspar the dominant process is clearly subsolidus exchange. In terms of $\delta^{18}\text{O}_R$, at least 80% of the total ^{18}O depletion is due to oxygen isotopic exchange at subsolidus temperatures.

A similar analysis can be done for the Later Intrusions. If we ignore the deviation of the single data point from the SPF (for reasons already given in Section 8.11), the Later Intrusions are characterized by a maximum $\delta^{18}\text{O}$ lowering of the melts of only up to 2 per mil. The positive slope for quartz in Figure 8-17 severely restricts the low- ^{18}O magma field and again emphasizes the dominance of post-crystallization oxygen isotopic exchange in these granophyric rocks.

Nevertheless, Figure 8-17 displays another striking characteristic to which we have alluded. This is the large variation of $\delta^{18}\text{O}_Q$ in the SPE (+3.5 to -2.6). This range is more than 50% greater than that displayed by any other intrusion in the entire Red Hills area. In addition, the SPE has the lowest $\delta^{18}\text{O}_Q$ values yet analyzed from the granophyric rocks of Skye. This is all the more remarkable when it is realized that these quartz crystals are among the coarsest in grain size of all Red Hills intrusions (see Figure 8-18).

The most obvious explanation of the oxygen isotope data is that the SPE represents an extreme example of a low- ^{18}O magma. To test this hypothesis, the following experiments

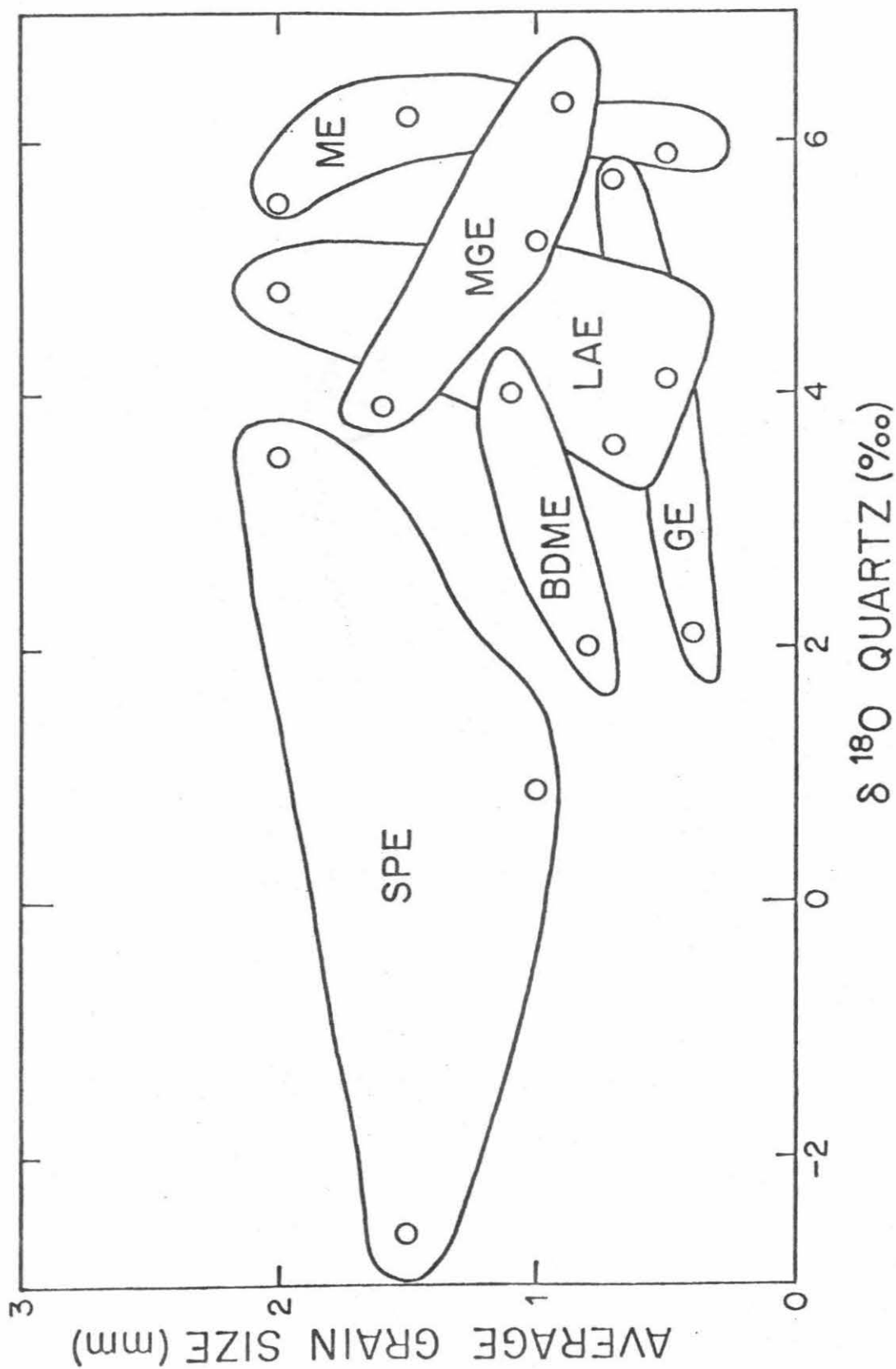


Figure 8-18. Plot of average grain size vs $\delta^{18}\text{O}_Q$ for quartz samples from the Western Red Hills, Skye.

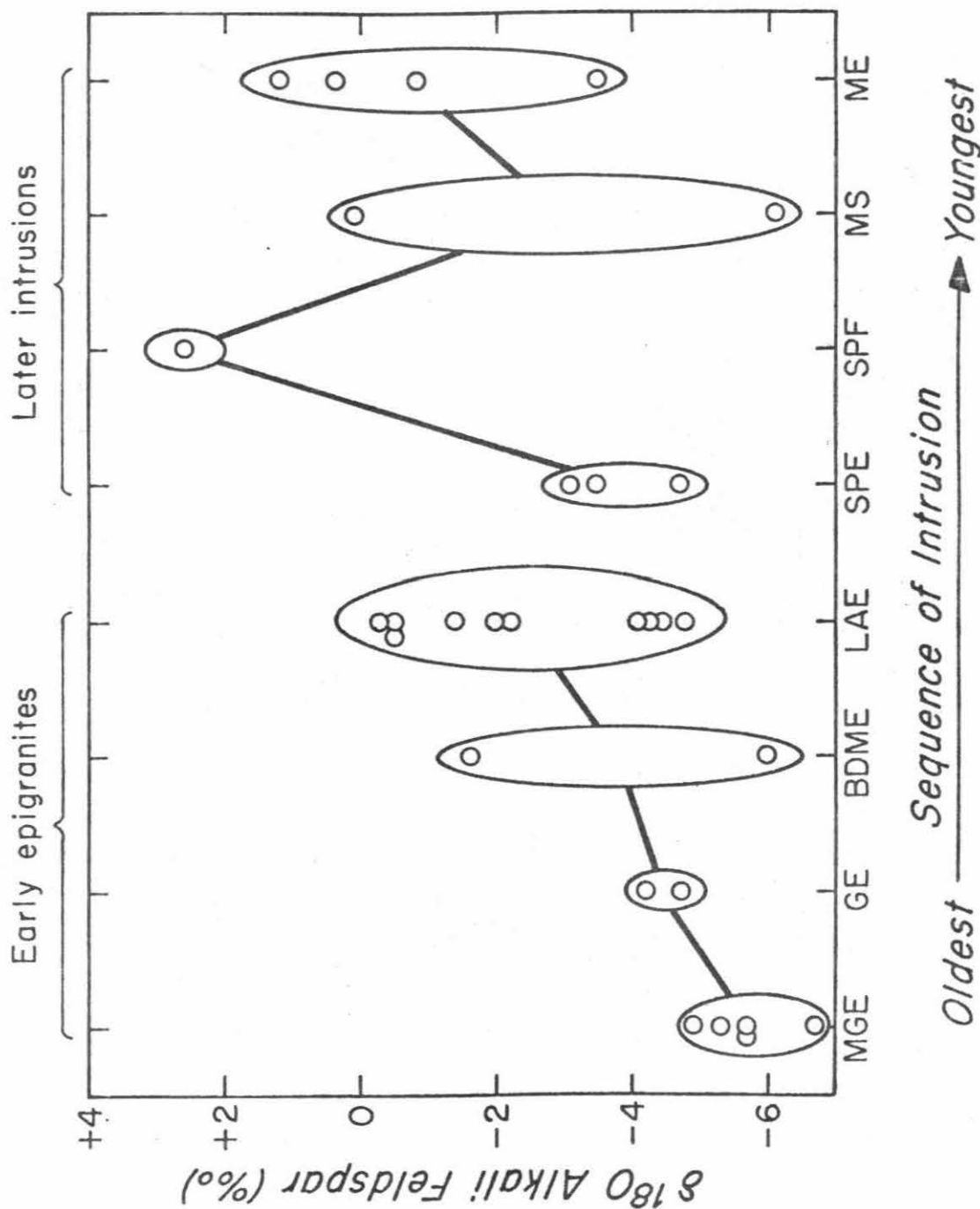


Figure 8-19. $\delta^{18}O_K$ vs age of intrusion for the Western Red Hills, Skye. The line joins the average $\delta^{18}O_K$ value for each sequence (see text).

Figure 8-20. A model for the Early Epigranites of the Western Red Hills, Skye, comparing the amounts of ^{18}O depletion attributed to subsolidus exchange with ^{18}O depletion of the magma (see text). The ^{18}O depletion of magma field is limited by the maximum measured $\delta^{18}\text{O}_Q$, assuming $\delta^{18}\text{O}_Q^i = +8.5$ (and $\delta^{18}\text{O}_K^i = +7.5$). All $\delta^{18}\text{O}_Q$ values are shown, whereas only $\delta^{18}\text{O}_K$ values $\leq \delta^{18}\text{O}_K$ (average) are plotted.

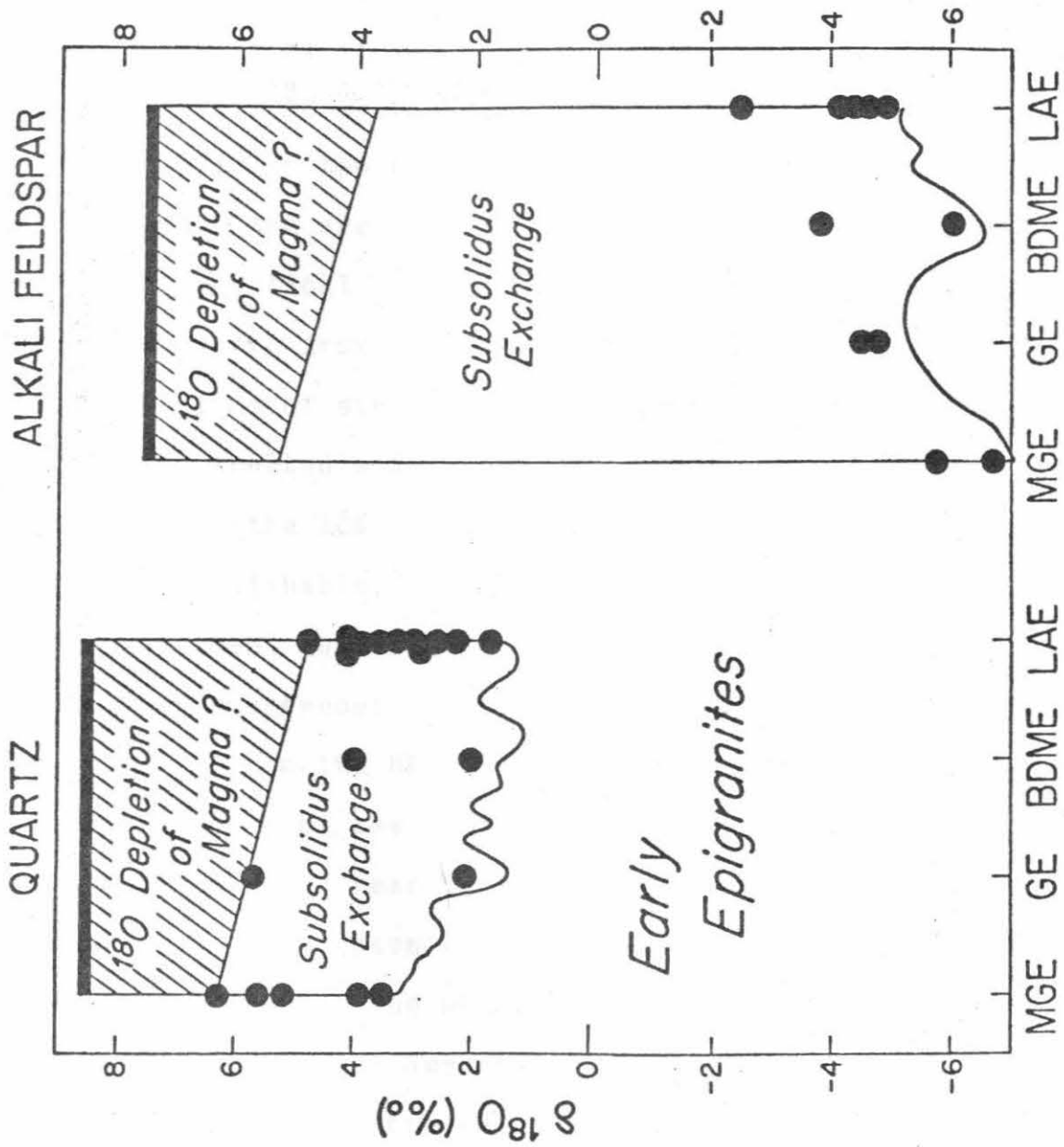


Figure 8-20

were made. A hand-picked separate of individual euhedral quartz phenocrysts was prepared from the most ^{18}O -rich SPE sample (SK-182; $\delta^{18}\text{O}_\text{Q} = +3.5$). This sample (not crushed or ground in any way) was subjected to HF stripping until 82.3% of the original 103.4 mg of sample had been removed. The residual quartz had a $\delta^{18}\text{O} = +5.2$. This indicates some oxygen isotopic inhomogeneity in the quartz. A mass balance calculation indicates that the average $\delta^{18}\text{O}$ of the dissolved quartz was +3.1. An identical experiment was tried on the most ^{18}O -depleted quartz from the SPE, SK-181. In this case however, after 102.1 mg of single-crystal quartz phenocrysts ($\delta^{18}\text{O} = -2.6$) were treated with a 48% HF solution at room temperature for six hrs, the 20% residual quartz was analyzed and found to be indistinguishable from the original sample ($\delta^{18}\text{O} = -2.7$). This experiment suggests that the quartz from SK-181 is isotopically homogeneous, but it should be noted that the residual quartz from the HF stripping experiment did not represent the inner cores of the original quartz crystals. Instead, these grains after reaction exhibited a marked dendritic appearance. The reason for this is that the quartz crystals contain fractures along which the HF has caused preferential dissolution of SiO_2 . Nevertheless, we would expect that if these fractures were present during hydrothermal alteration, the greatest amount of ^{18}O exchange would have taken place there, and no such effect was found. This suggests that the quartz grains in SK-181 were relatively inert during the

meteoric-hydrothermal alteration. In order to attempt to settle this question, another experiment was carried out on SK-181.

A 103.6 mg sample of single-crystal quartz phenocrysts from SK-181 was subjected to a F_2 stripping experiment, similar to the fluorination stripping experiments described by Epstein and Taylor (1971) on the lunar fines and breccias. The results are given in Table 8-3 and plotted in Figure 8-21. For each of the 12 fractions, the sample was reacted with an excess of F_2 at successively higher temperatures for about 30 minutes, except for the last fraction which was reacted overnight. The first three fluorination fractions (A, B, and C, Table 8-3) yielded almost no oxygen (estimated to be less than $1\mu\text{mole}$). This was undoubtedly because of the small reaction time and low reaction temperature, less than 210°C . These cuts are therefore not plotted in Figure 8-21, as the isotopic analyses are very uncertain and probably not meaningful.

The most striking characteristic displayed in Figure 8-21 is the oxygen isotopic uniformity of nearly every fraction analyzed during the F_2 stripping experiment. As expected, the weighted average $\delta^{18}\text{O}$ value for the quartz is -2.6 . The fluorine stripping experiment demonstrates that the quartz crystals are essentially isotopically homogeneous throughout, whether we are talking about the rims, the cores or along fractures. These data are very difficult to reconcile with the hypothesis

Table 8-3

$\delta^{18}\text{O}$ data obtained by successive fluorination stripping experiment on quartz phenocrysts of SPE (SK-181)

Sample	$\mu\text{moles O}_2$	Cumulative $\mu\text{moles O}_2$	Cumulative % O_2 extracted	$\delta^{18}\text{O}$ per mil
SK-181 Quartz Phenocrysts (103.6 mg)				
A. 30 min/80°C	~ 1	~ 1	0.06	+1.9
B. 30 min/155°C	~ 1	~ 2	0.1	-3.4
C. 30 min/210°C	~ 1	~ 3	0.2	-4.8
D. 30 min/270°C	~ 5	8	0.5	-2.3
E. 30 min/380°C	36	44	2.6	-4.5
F. 30 min/420°C	84	128	7.6	-2.6
G. 30 min/450°C	308	436	25.8	-2.6
H. 30 min/450°C	440	876	51.8	-2.6
I. 30 min/480°C	615	1491	88.2	-2.4
J. 15 min/440°C	50	1541	91.1	-1.7
K. 30 min/440°C	65	1606	95.0	-2.4
L. 16 hrs/560°C	85	1691	100.0	-2.7

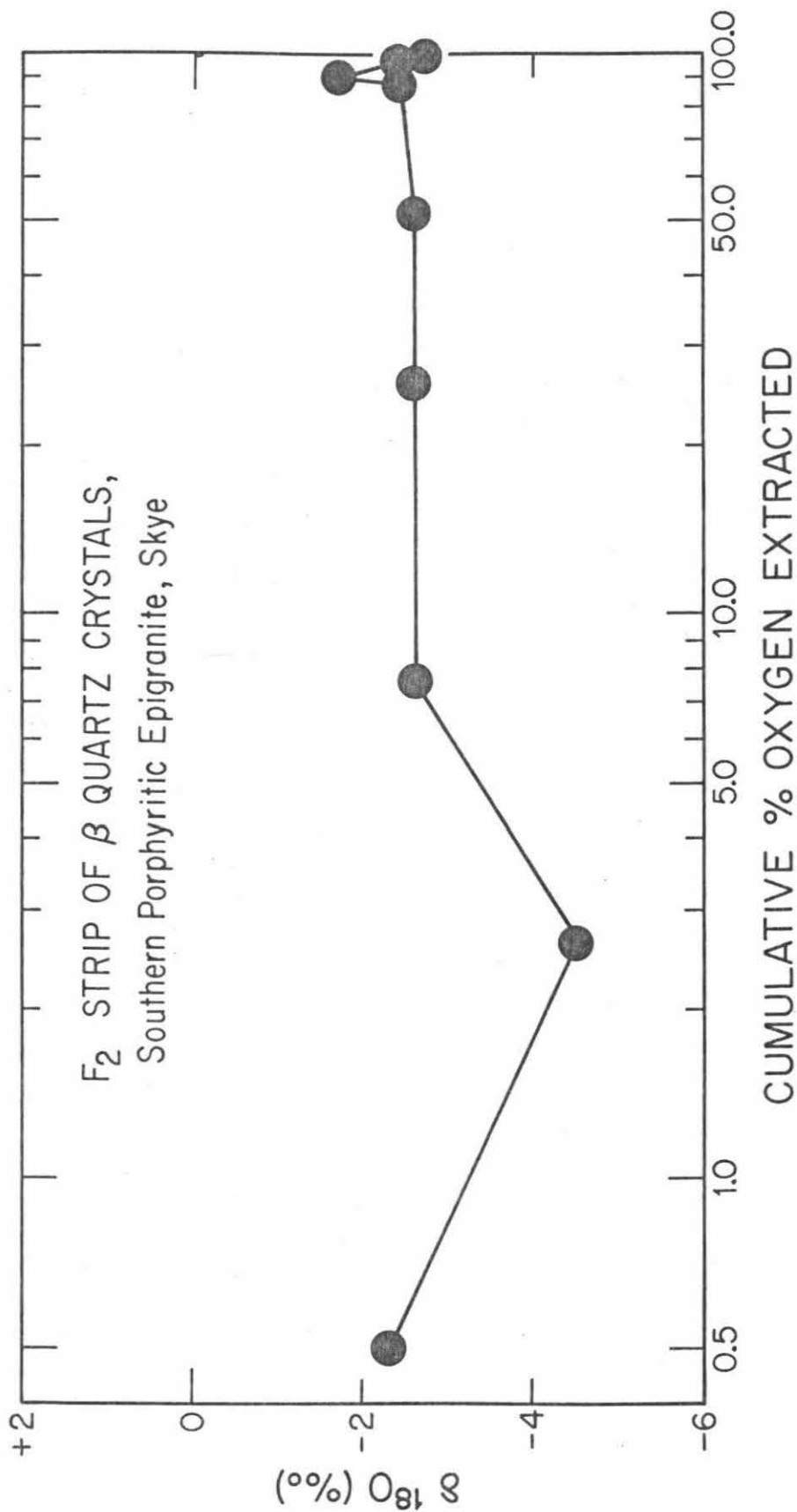


Figure 8-21. Graph showing the $\delta^{18}\text{O}$ variation of oxygen extracted by fluorination experiment on euhedral single-crystals of β -morphology quartz from SK-181 (see text). The data are tabulated in Table 8-3.

that the quartz, having originally crystallized with a 'normal' $\delta^{18}\text{O}$ value, subsequently underwent massive oxygen isotope exchange during hydrothermal alteration, completely homogenizing the $^{18}\text{O}/^{16}\text{O}$ of the quartz and still perfectly preserving the euhedral hexagonal bipyramids that are indicative of β -quartz crystals. We are forced to the conclusion that the oxygen isotopic homogeneity is a primary characteristic imposed on the quartz at the time of its crystallization, and hence it must have formed from a low- ^{18}O melt. The argument is solidly re-enforced by noting that SK-181 has essentially a 'normal' $\Delta_{\text{Q-K}} = 0.8$ (Table 8-1), compatible with near-equilibrium crystallization at magmatic temperatures. Aside from the possibly related SPF and a few BDG samples, this is the only epigranitic rock from Skye with a near-normal $\Delta_{\text{Q-K}}$ value!

If the SPE was generated as an extreme low- ^{18}O magma, why then is there such a large variation in $\delta^{18}\text{O}_{\text{Q}}$ in this rock type? The answer may be related to the manner in which the SPE melt was generated. The SPE most likely represents a melt generated largely from hydrothermally altered Torridonian arkose (Thompson, 1969). The source rock itself was probably originally isotopically non-homogeneous and therefore the melting process probably gave rise to a melt (or melts) that was also inhomogeneous in terms of $\delta^{18}\text{O}$. Note that the hydrothermally altered Torridonian sandstones on Skye do in fact show a wide range in $\delta^{18}\text{O}$ (see Section 8.4). As described in Section 7.4, the SPE and SPF are the most SiO_2 -rich and the

most MgO- and FeO-poor of all the felsic rocks from the Isle of Skye, and this includes the CUG. It therefore must have been an extremely viscous magma, too viscous in fact to homogenize itself isotopically by convection currents in the silicate liquid. The SPE is one of the smaller intrusive bodies of the Red Hills Complex so it would be easier to develop a low- ^{18}O melt of this magnitude. These arguments apply equally well to the SPF which may represent a less extreme low- ^{18}O magma. Note also that the SPF (IGC-13; Table 8-1) has a $\Delta_{\text{Q-K}} = 1.4$. Further, the $\delta^{18}\text{O}_{\text{Q}}$ values of the Marscoite Suite are not unlike that of the SPF and thus the isotopic evidence is in accord with the Wager et al. (1965) hypothesis on the origin of this hybrid rock.

8.12 Eastern Red Hills

All the $\delta^{18}\text{O}$ data for the Eastern Red Hills Complex are given in Table 8-1, while all the coexisting mineral data from these epigranitic intrusions (except for the BDG) are plotted in Figure 8-15. Conclusions in this section are less firm than for the Western Red Hills, mainly because the relative age relationships between the various granitic and granophyric bodies are not as well known (see Section 7.4). The tentative sequence of intrusion is plotted as a function of coexisting $\delta^{18}\text{O}_{\text{K}}$ and $\delta^{18}\text{O}_{\text{Q}}$ in Figure 8-15. Disregarding the BDG for the moment, the Eastern Red Hills show a spread of $\delta^{18}\text{O}_{\text{Q}}$ values (+4.9 to +1.0) similar to that in the Western Red Hills but the alkali feldspars

show a much wider variation in the Western Red Hills than the Eastern Red Hills.

In general, the maximum $\delta^{18}\text{O}_\text{Q}$ from each intrusion appears to increase with time from GBME to AFG (and BDG), but then decreases with time to CSG (Figure 8-15). The alkali feldspars do not seem to exhibit any well developed trend. What might cause $\delta^{18}\text{O}_\text{Q}$ to start decreasing after the intrusion of the BDG? Examination of Figure 7-5 indicates that this break coincides with the intrusion of the basaltic agglomerates of the large Kilchrist vent (Geikie, 1897) and associated intrusive ignimbrite (Ray, 1960; 1972). It is also interesting to note that the same $\delta^{18}\text{O}_\text{Q}$ trend of the Early Epigranites of the Western Red Hills was preceded by the intrusion of vent breccias north of Bellig (Bell, 1966) and the Loch na Creitheach vent (Jassim and Gass, 1970) north of Camasunary.

Sudden cauldron subsidence and penetration of magma into country rocks permeated with meteoric water is an ideal situation for locally generating enormous water pressures. This would be expected to produce repeated explosive activity and accompanying formation of breccia pipes and explosion vents filled with volcanic agglomerate (Taylor and Forester, 1971). Thus, not only would the process that formed volcanic vents provide easier access for meteoric waters to the magma chamber below, but the explosive activity itself was very likely caused by the presence of meteoric waters. In this regard, note that the Loch na Creitheach agglomerates and tuffs represent some

of the most ^{18}O -depleted rocks in the world. The average $\delta^{18}\text{O}_R$ from five separate volcanic vents in Skye is -2.7. These intrusions may themselves represent low- ^{18}O magmas.

Beinn an Dubhaich Granite (BDG)

The Beinn an Dubhaich granite (BDG) of the Eastern Red Hills of Skye is unique in that it was emplaced entirely into carbonate country rocks. The Cambro-Ordovician Durness Limestones have been extensively recrystallized, the original dolomite being mainly converted to calcite, with the formation of complex skarn zones near the BDG contact. Boron and fluorine bearing minerals are notable (Tilley, 1951). The BDG, intruded into the core of an arcuate anticline of Durness Limestone, contains numerous bodies of limestone that have not been structurally disturbed by its emplacement. Harker (1904) provided strong evidence for this by showing that pre-BDG dikes are aligned in both the limestone country rock and the limestone enclosed by the granite.

Because of its anomalous position at Skye, both in terms of type of country rock and its essentially 'normal' $\delta^{18}\text{O}$ values (Taylor, 1968; Taylor and Forester, 1971), the BDG was studied in some detail in the present work. The analyses include 11 quartz samples, 9 alkali feldspar, 6 whole rocks, 1 plagioclase and 1 magnetite separate (Table 8-1). Seven $\delta^{18}\text{O}_R$ values for dikes related to the BDG were also obtained. The $\delta^{18}\text{O}_Q$ values for the BDG are similar to those of 'normal' igneous quartz, whereas the $\delta^{18}\text{O}_K$ values cover a wide range,

+6.0 to -1.0. Most of the low $\delta^{18}\text{O}_K$ values are from fine-grained samples; these are very rare in the BDG, but several were studied to examine the $\delta^{18}\text{O}$ -grain size effect in greater detail.

The results of the quartz and alkali feldspar analyses are plotted in Figure 8-22 as a function of grain size. The most pertinent features shown by the isotopic data in this diagram are (a) $\delta^{18}\text{O}_Q$ is independent of grain size and restricted to the range +7.8 to +6.9, (b) $\delta^{18}\text{O}_K$ is strongly dependent on grain size, and (c) for a given grain size, $\delta^{18}\text{O}_K$ is lower for samples near joints, fractures and dikes than for samples of massive granite. The grain-size relationships apply not only from specimen to specimen, but also within a single rock sample. For example, SK-196 is a porphyritic BDG sample, and $\delta^{18}\text{O}_Q$ is similar in both the groundmass and phenocrysts, while $\delta^{18}\text{O}_K$ differs markedly in these two sites. Thus, the isotopic data clearly indicate that the BDG has undergone post-crystallization oxygen isotope exchange with meteoric-hydrothermal solutions. The W/R ratio was very low, however, except near fractures. This is consistent with the geologic features of the BDG. The BDG is well removed from all younger intrusions in the area, notably the intrusions of the Eastern Red Hills. Thus it may have been affected by only a single-stage hydrothermal episode. Also, the Durness Limestone may have been less permeable to ground waters than the plateau basalt country rocks. Another important effect is that the limestone probably acted as a high- ^{18}O "buffer", making ^{18}O -

depletion difficult. As first pointed out by Taylor and Forester (1971), such carbonate country rocks would provide a localized, easily exchanged, ^{18}O -rich reservoir that would probably produce much more ^{18}O -rich ground waters than would be observed throughout the rest of the Skye intrusive complex.

The carbonate rocks would have become even less permeable to H_2O if, during contact metamorphism and hydrothermal alteration, they in part deformed plastically or by recrystallization rather than by fracturing. At the physical conditions under which the BDG cooled and crystallized, the strength of dolomite is much less than that of basalt or granite (Griggs, Turner and Heard, 1960). The carbonate would deform by cohesive flow (Paterson, 1958); on a microscopic scale; this involves recrystallization and intra-crystalline gliding rather than cataclasis. In fact, any fractures that do form are likely to be 'sealed' in the presence of hydrothermal fluids, since the carbonates are much more easily recrystallized than silicate rocks, and also after the stress is removed, healing of fractures is likely to begin (Robertson, 1960).

It is significant that each of the three samples collected at the contact with fractures or dikes have $\delta^{18}\text{O}_k$ values indicative of more ^{18}O depletion than those of the main trend (Figure 8-22). The implication here is that these samples have been in contact with more water than those further removed from these channelways. Much higher W/R ratios must have been localized along the fractures, analogous to the situation that

produced the ^{18}O -depleted sample SM-89 from the Stony Mountain stock in Colorado.

8.13 Water/rock ratios in the Skye epigranites

We can treat the granitic rocks of Skye as we did the gabbroic rocks, with respect to estimating W/R ratios from $\delta^{18}\text{O}_R$ values. Thus Figure 8-23 has been constructed using parameters $\delta_R^i = +8.0$ for a system behaving as An_0 (see norms in Table 7-1). For simplicity, only -12 and -9 are considered for values of $\delta^{18}\text{O}_{\text{H}_2\text{O}}^i$.

Excluding the BDG, $\delta^{18}\text{O}_R$ values for the granitic rocks of Skye range from +3.1 (BCG, SK-37) to -5.9 (GE, SK-126). Whole-rock $\delta^{18}\text{O}$ values are either measured, or calculated from both the quartz and alkali feldspar $\delta^{18}\text{O}$ analyses. The mean $\delta^{18}\text{O}_R \approx -1$. Two-thirds of the rocks fall within the range -1 to -2. Using petrographic criteria and reasoning similar to that in Section 6.11, a reasonable average integrated temperature would be in the order of 400-500°C. Thus most of the granitic rocks from Skye can be seen to have experienced integrated W/R ratios of approximately 1.3 ± 0.5 . Recall also that all regions that have experienced significant ^{18}O depletion have average W/R ≈ 1 . Locally however, W/R ratios may approach very large values, e.g. SK-126, with $\delta^{18}\text{O}_R = -5.9$, represents a W/R > 5.0 (see Figure 8-23). Although there is close agreement to the W/R ≈ 1 to 2 predicted by the calculations carried through in Chapter 4, these granitic rocks invariably have

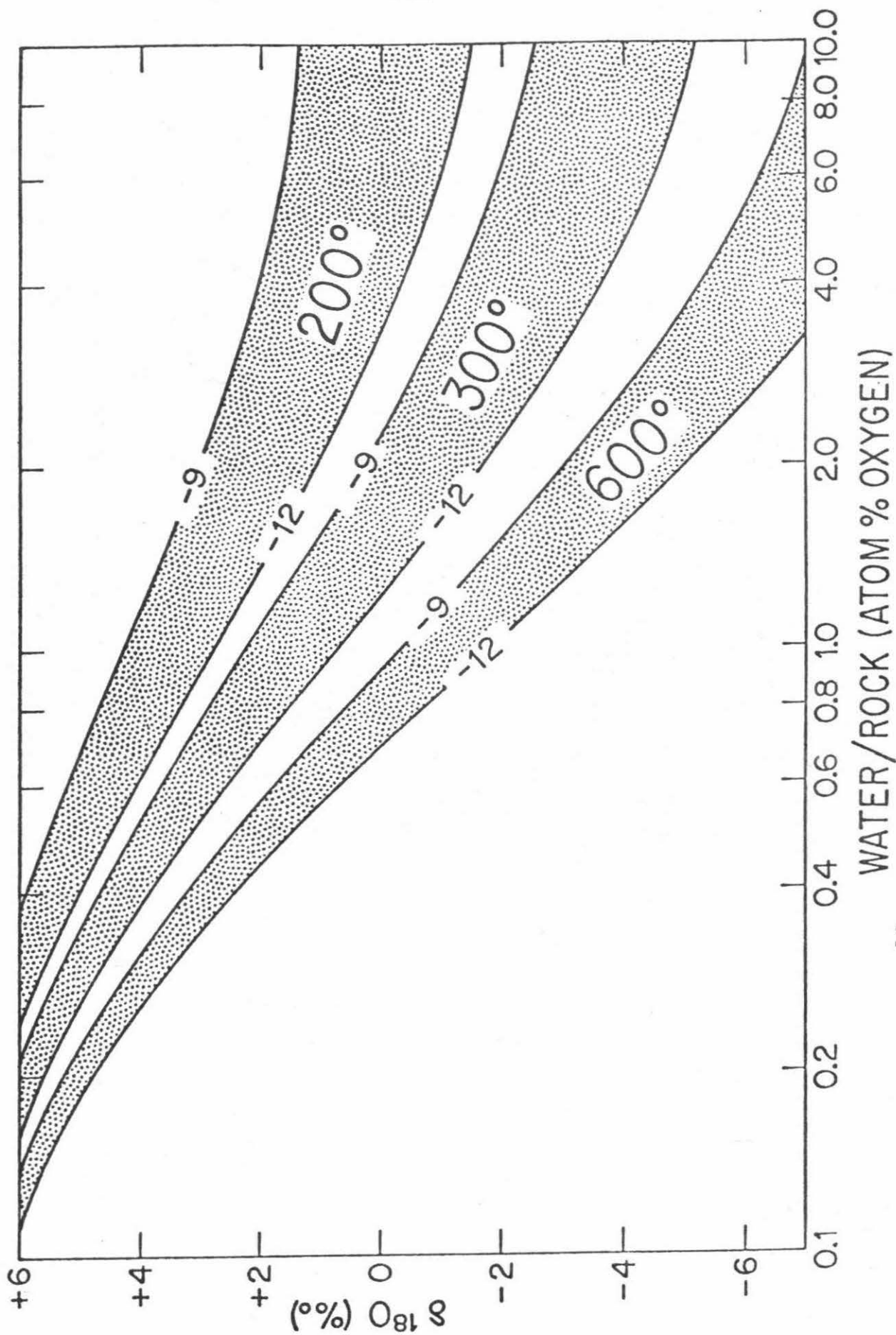


Figure 8-23. $\delta^{18}\text{O}$ vs W/R diagram for granitic rocks of Skye, Scotland.

Calculated curves are based on $\delta_{\text{R}}^{\text{j}} = +8.0$ for a system behaving as An_0 .

larger W/R values. It is conceivable that a large part of this discrepancy may be due to the granitic magmas having been generated as low- ^{18}O melts.

The BDG has an average $\delta^{18}\text{O}_R \approx +6.0$. Even if we take into consideration that $\delta_{\text{H}_2\text{O}}^i$ may have been greater than -9, this defines a W/R $\ll 1$. The alkali feldspar data clearly illustrate that the H_2O that did interact with the BDG was relatively low in ^{18}O , and therefore high W/R ratios along with high $\delta^{18}\text{O}_{\text{H}_2\text{O}}$ (by exchange with limestone) is impossible. Low W/R ratios are therefore demanded for the BDG, and this demands a fairly impermeable country rock. Only very locally, along fractures, did the W/R ratios approach unity.

8.14 Lead and strontium isotopic studies in Skye

The significance of the oxygen isotope data relative to Pb and Sr data from Skye have been discussed by Taylor and Forester (1971) as follows:

"Hamilton (1966) and Moorbath and Welke (1969) made the important discovery that the Pb isotopic compositions of the granitic rocks from Skye were similar to, and therefore largely inherited from, the underlying Lewisian gneisses. Moorbath and Welke (1969) clearly demonstrated that the Pb in all the analyzed igneous rocks from Skye is a mixture of a modern 'Tertiary' lead and a Precambrian lead (~ 3000 m.yrs. old) that has an isotopic composition identical to the average lead in the Lewisian Basement. In particular, the Skye granitic igneous rocks were found to contain mostly Precambrian lead, while the Cuillin gabbros largely contain 'Tertiary' lead.

In the light of the large-scale oxygen isotope exchange that has occurred in Skye, it is of interest to see if any relationship exists between the $^{18}\text{O}/^{16}\text{O}$ and lead isotope ratios. Many of the same igneous

bodies analyzed by Moorbath and Welke (1969) were also analyzed for ^{18}O in the present study, and some analyses were on exactly the same specimens. The relationships are shown in Figure 8-24 where we plot $^{206}\text{Pb}/^{204}\text{Pb}$ ratios against ppm total Pb for the Skye samples of Moorbath and Welke. The $\delta^{18}\text{O}$ values are also shown on this diagram. As can be seen, there is no direct correlation between $\delta^{18}\text{O}$ and the $^{206}\text{Pb}/^{204}\text{Pb}$ ratios.

The samples plotted on Figure 8-24 however, can be divided into two groups on the basis of their $\delta^{18}\text{O}$ values. We have already established above that all the basaltic lavas more than 6 km distant from the central intrusive complex at Skye have essentially 'normal' $\delta^{18}\text{O}$ values. Such samples are designated 'outer dolerites and basaltic lavas' on Figure 8-24. The rest of the samples plotted on Figure 8-24 come from the vicinity of the central intrusive complex, where the rocks all have been strongly exchanged with meteoric-hydrothermal solutions. In contrast to the normal- ^{18}O plateau lavas, the latter rocks show a pronounced correlation between lead content and lead isotope ratio (a $^{207}\text{Pb}/^{204}\text{Pb}$ plot would show a similar relationship). A least squares line drawn through these data points is shown on Figure 8-24; the correlation coefficient is -0.9.

Moorbath and Welke (1969) noted the correlation between Pb content and Pb isotopic composition and they interpreted this as simply indicating that the greater the amount of Precambrian Lewisian lead assimilated by the magmas, the greater total amount of lead in the magmas. This may be a valid argument, but note that many of the outer dolerites and plateau basalt lavas are also strongly contaminated with 'Lewisian' lead and yet do not show this increase in total lead content. Also, in general, it is apparently as common to find Pb contamination of basaltic igneous rocks in continental areas as to find contamination of andesitic or rhyolitic rocks (Doe, 1970). Therefore, although it is certainly plausible that the lead isotope relationships shown in Figure 8-24, all may have been entirely produced by contamination, assimilation, and partial melting of Lewisian gneisses by gabbroic magmas, as

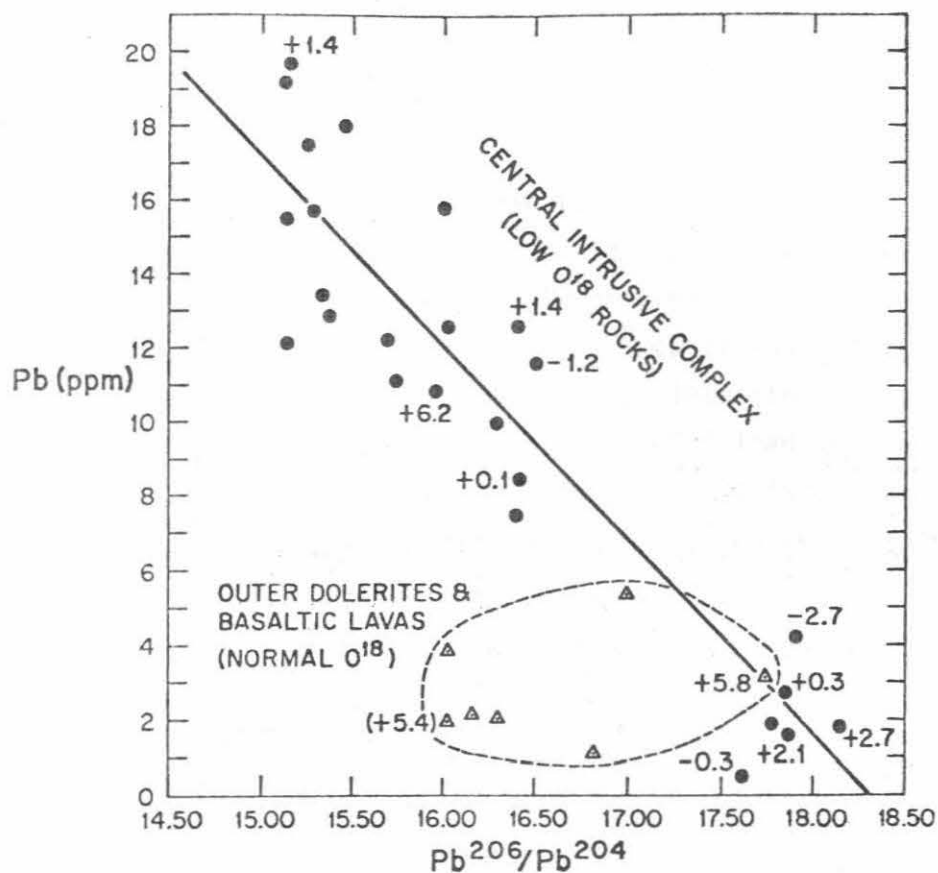


Figure 8-24. Plot of $^{206}Pb/^{204}Pb$ ratio vs Pb content for several igneous rocks from Skye (after Moorbath & Welke, 1969). The whole rock $\delta^{18}O$ values obtained on these same specimens are shown on the diagram. The value in parentheses was obtained on a nearby specimen, not the one actually analyzed for $^{206}Pb/^{204}Pb$. The heavy diagonal line is a least squares line drawn through the dark-circled data-points only. The only Pb data-point not plotted is that for the felsite of the outlying Cnoc Carnach sill. After Taylor and Forester (1971).

proposed by Moorbath and Welke (1969), the $\delta^{18}\text{O}$ data of the present study suggest another possibility as well.

If the hydrothermal solutions responsible for the profound oxygen isotope effects in Skye were all essentially pure H_2O , then obviously this exchange could have no effect on any chemical constituents in the rocks (including Pb). However, at high temperatures alkali chlorides partition strongly into any aqueous gas phase that coexists with igneous rocks or magmas (Burnham, 1967). The strong feldspathization and albitization found in the Scottish Tertiary intrusions indicate that the meteoric hydrothermal solutions at least locally contained appreciable Na and K. Such fluids therefore have the potential of dissolving appreciable lead (the Salton Sea, California brine, for example, contains 104 ppm of lead, White, 1965). Inasmuch as most of the lead in igneous rocks is in the feldspar (particularly K-feldspar) and, as shown, the oxygen in this mineral is invariably exchanged throughout the central intrusive complex at Skye, there is no doubt that the hydrothermal solutions would have exchanged lead with the feldspars as well.

Therefore, the mixing of lead isotopes demonstrated by Moorbath and Welke (1969) could have come about in part during the hydrothermal alteration after emplacement of the igneous rocks at their present level. The hydrothermal process would cause a vast mixing and homogenization of the young leads of the volcanics and the Mesozoic sediments with the Precambrian leads of the granitic rocks and the basement. All rocks would be affected, but those with very small amounts of initial lead would obviously be affected the most (i.e. the gabbros and peridotites). If the solutions contained even as much as 0.5 ppm of lead they could have caused an appreciable change in the $^{206}\text{Pb}/^{204}\text{Pb}$ ratio of the Cuillin gabbros and peridotites, which have lead contents of only 0.5 to 2.7 ppm (Figure 8-24).

The proposed mechanism would explain the following: (1) The outer dolerites and plateau basalts show a different Pb isotope behavior on Figure 8-24 than do the central intrusive igneous rocks because they have not been hydrothermally exchanged and thus retain their

original magmatic Pb isotope ratios. These rocks were definitely contaminated with Lewisian lead at the magmatic stage. (2) The gabbroic magmas of the Cuillin may originally have been contaminated with Lewisian Pb in the same way as the plateau basalts, but these ratios have since been modified by exchange with hydrothermal solutions carrying younger, more radiogenic leads. (3) Most of the granitic igneous rocks contain such high Pb concentrations (commonly 15 to 20 ppm) that their Pb isotope ratios could have been modified only slightly by the hydrothermal alteration. With decreasing initial Pb contents the rocks would be progressively more contaminated with the hydrothermal lead, thus producing the correlation shown on Figure 8-24. (4) The hydrothermal exchange process could have been responsible for homogenization of lead isotopes, particularly on a small scale. An example might be the Rudh' an Eireanneach composite sill in which the felsic and mafic portions both have similar lead isotopic compositions (Moorbath and Welke, 1969). We must re-emphasize that the hydrothermal alteration event definitely cannot be responsible for the 'old' Pb isotope ratios in the Skye granites. These granitic magmas must already have been contaminated with Precambrian lead at the time they were intruded.

Moorbath and Bell (1965) have obtained a large amount of Sr isotope data on the Skye igneous rocks. They concluded that the Skye granites could not have been formed by differentiation from the magmas which formed the nearby gabbros and basalts because the initial $^{87}\text{Sr}/^{86}\text{Sr}$ ratios of these rocks are totally different. Their arguments are well-reasoned and may indeed be valid. However, if the hydrothermal solutions responsible for the massive ^{18}O exchange in the Skye igneous complex contained even as little as 10 ppm Sr, some of these arguments might need revision. Although it is an extreme case, note that the Na-Ca-Cl brine at the Salton Sea contains about 740 ppm Sr (White, 1965).

A very rough correlation exists between initial $^{87}\text{Sr}/^{86}\text{Sr}$ ratio and Sr content in the Skye igneous rocks. For example, the porphyritic

felsite in the Meall a'Mhaoil area north of Lock Ainort analyzed by Moorbath and Bell (1965) has by far the highest initial $^{87}\text{Sr}/^{86}\text{Sr}$ ratio in Skye, 0.7213, as well as by far the lowest Sr content, 9.9 to 21.4 ppm. A number of granite, marscoite, and ferrodiorite samples have 0.711 to 0.715 and 79 to 257 ppm, respectively, whereas the gabbroic and basaltic rocks have 0.704 to 0.708 and 102 to 446 ppm. In the Mealla Mhaoil area there is a good correlation between amount and isotopic composition of Sr. The highest Sr content (457 ppm) occurs in a quartz diorite dike intruding the Maol na Gainmhich epigranite, and this dike has an initial $^{87}\text{Sr}/^{86}\text{Sr}$ of 0.7076 (Moorbath and Bell, 1965). All the Sr isotope data in this part of Skye conceivably could be explained as follows: (1) All the rocks in the area started with an initial $^{87}\text{Sr}/^{86}\text{Sr}$ of about 0.705-0.706. (2) The hydrothermal solutions that passed through the rocks contained perhaps 20-30 ppm of Sr with an isotope ratio of 0.721 or slightly higher. (3) The Sr isotope ratios of the quartz diorite were almost unaffected, those of the marscoites were strongly affected, and those of the porphyritic felsite were totally replaced; all these effects resulting from the relative amounts of Sr in each rock and in the hydrothermal solutions. This model would explain the uniform initial $^{87}\text{Sr}/^{86}\text{Sr}$ of the porphyritic felsite without making it necessary to conclude that the original felsite magma had a homogeneous ratio of 0.721, as suggested by Moorbath and Bell (1965).

None of the arguments presented above necessarily invalidates any of the conclusions of Moorbath and Bell (1965) or Moorbath and Welke (1969). If the hydrothermal solutions had very low Pb and Sr contents then all their arguments stand firm. However, it must be pointed out that the massive hydrothermal exchange that has occurred in Skye could also have appreciably affected the trace element geochemistry in these rocks and therefore one must be careful about utilizing such data to make firm conclusions as to the gneiss of the Skye granites."

Chapter 9

OTHER SCOTTISH TERTIARY PLUTONIC CENTERS AND MISCELLANEOUS LOCALITIES

9.1 Isle of MullGeneral geology

The classic Mull Memoir (Bailey et al., 1924) was one of the first papers to treat such concepts as magma type and magma series. These concepts led Kennedy (1931; 1933) to consider tholeiitic and olivine-basalt magmas as independent magma types and it is thus at Mull where serious petrogenetic thought on the origin of basaltic magmas began. A thickness of about 2 km of basaltic lavas still remain on the Isle of Mull, the most complete Tertiary lava succession in northwest Scotland (Figure 9-1). The alkali olivine basalts ('Plateau magma type') largely lie in the peripheral part of the island, while the overlying tholeiitic and high-alumina basalts ('nonporphyritic central magma type' and 'porphyritic central type' of the classic literature) are mainly confined to the central part of the complex, the old basaltic caldera. The earliest intrusive activity was concentrated along the margins of the caldera. Subsequently, the area around Beinn Chaisgidle (early caldera in Figure 9-1) became the center for intrusion. Finally, the center of igneous activity moved to the northwest, around Loch Ba, where the latest ring-dike intruded along the margins of a complete ring fault, surrounding a block which has subsided at least 1 km (the late caldera in Figure 9-1).

Table 9-1

$\delta^{18}\text{O}$ values of rocks and minerals from Mull, Arran, Ardnamurchan and various other localities

Sample # (M1-)	Mineral	$\delta^{18}\text{O}$ (‰)	Description
<u>Mull</u>			
16	WR*	+2.5	Greenish basalt; 1 km south of Salen.
17	WR	+4.7	Basalt. Seriz, zoned & cracked glomero-porphyrific plag pheno, with chl along cracks, in subophitic textured gdmass of seriz plag, fresh px, chl after ol, opaques, interstitial opaque-rich devitrified glass; pumpellyite.
18	WR	-3.5	Basalt; about 1 km east of Salen.
22	WR	+4.4	Basalt with pyrite.
	WR*	+4.5	
23	WR	+0.3	Basalt with pyrite.
24	f	+3.2	'Big-feldspar' basalt, near Loch Spelve.
25	WR	+0.1	Greenish mg subophitic gabbro, with cracked & seriz plag, fresh Ti-augite, chl (after ol) opaques & ep.
26	WR	-0.6	Basalt; north end of Loch Spelve.
37	WR	-3.0	Screen of basalt between ring-dikes, Allt Molach. Felted gdmass of cloudy plag, with pheno of plag, now largely altered to chl, ct & seriz; also frag of quartzofeldspathic material.
38	WR	-3.4	Highly granitized version of above. Seriz-feld pheno in a feld-rich matrix, with some gphy textures & chl.
47	WR	-3.0	Amyg basalt, near head of Loch na Keal.
49	WR	+0.6	Basalt.
50	WR	+3.7	Basalt.
51	WR	+4.5	Basaltic (dolerite) sheet.
52	WR	+5.6	Amyg basalt with ct.
	WR*	+5.6	

Table 9-1 (Cont'd)

Sample (M1-)	Mineral	$\delta^{18}O$ (‰)	Description
53	WR	+4.6	Basalt. Fresh pheno of ol; with alteration to opaques, chl & iddingsite along cracks & margins; in a fg ophitic gdmass of fresh Ti-augite, plag, opaques & chl.
54	WR	-6.5	Screen of basalt between Knock granophyre & Beinn a Ghraig granophyre. Aphanitic & fractured with feld, clinozoisite, opaques, px & chl.
81	WR	-5.4	Basalt. Seriz, plag, px altered largely to chl & opaques; zeolite.
118	WR	+1.5	Mugearite, head of Loch Scridain. Pheno of altered mafics (ol?), opaques & zoned plag in a pilotaxitic gdmass of cloudy plag, chl & opaques. Chl & opaque-rich alteration zones along fractures.
119	WR	+0.6	Ophitic basalt with fresh px & dusty plag. The grain boundaries between the px are preferentially altered to chl & opaques.
120	WR	+9.1	Basalt.
122	WR	+7.3	Basalt, fg, with plag, dusty px, opaques & altered ol.
125	Q K	+9.2 +8.5	Ross of Mull biotite granite, cg.
131	WR	-2.9	Ring-dike of mg felsic quartz-gabbro. Allt Molach. Cloudy plag with turbid rims; fresh px; accicular mafics altered to chl, ep & opaques; mag; interstitial qtz; apatite.
133	WR	-2.7	Late basic cone sheet cutting M1-131.
153	WR	-1.1	Fg felsic portion (5 m thick) of composite dike cutting ring-dikes in Allt Molach. Dusty to cloudy feld, qtz, chl, ct, actinolite.
155	WR	-2.7	Rhyolite dike, with flow banding, cutting basalt. Seriz feld pheno (with some ep) in a reddish, mosaic-fractured, cryptocrystalline (glassy?), partly devitrified matrix.

Table 9-1 (Cont'd)

Sample (M1-)	Mineral	$\delta^{18}O$ (‰)	Description
156	WR	-2.4	Felsic ring-dike. Zoned plag pheno with cloudy rims, in an equigranular gdmass of feld, qtz, opaques, chl, amph, ep, & apatite. Minor gphy; some small fg felsic fragments.
183	WR*	-6.1	Chl-rich basalt, near Derrynaculan granophyre.
184	WR	-3.4	Basalt, 1 km west of M1-183.
Mu11 1	WR	+2.2	
Mu11 2	WR	0.0	
Mu11 3	WR	-1.1	
Mu11 4	WR	-3.9	
Mu11 6	WR	-2.9	
Mu11 7	WR	-3.9	
Mu11 9	WR	-3.5	
Mu11 10	F	-1.6	
	P	-1.2	
Mu11 11	WR	-5.7	
Mu11 12	WR	+0.9	
Mu11 13	WR	-0.1	
Mu11 14	F	-4.9	
	P	-0.9	
Mu11 15	WR	+1.1	
Mu11 16	Q	+3.3	
	K	-0.8	
Mu11 17	WR	+6.1	
Mu11 18	WR	+5.2	
Mu11 19	Q	+2.6	
	WR	+3.4 (mg)	
	WR	+3.2 (fg)	
Mu11 20	WR	-0.7	

Samples Mu11 1 - Mu11 20 are from Taylor and Forester (1971)

Table 9-1 (Cont'd)

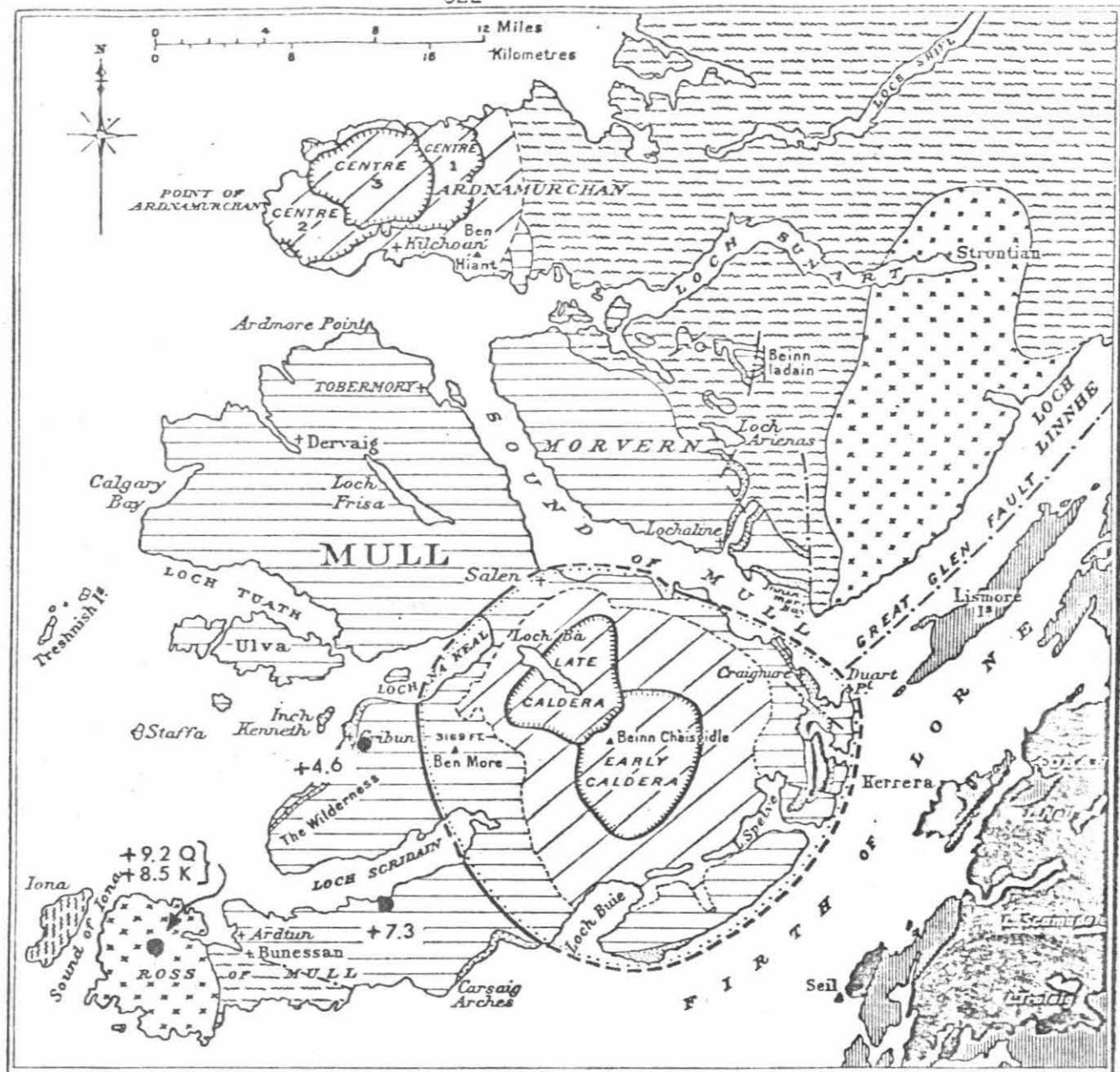
Sample	Mineral	$\delta^{18}\text{O}$ (‰)	Description
<u>Arran</u>			
AR-GE1	Q	+9.1	Outer granite, cg; 30 m from outer contact, Gleann Easan Biorach. NG 947491. K corrected for 5% qtz.
	K	-1.9	
NGS-3	Q	+9.2±0.0(2)	As above, 12 m from Hutton's contact, North Glen Sannox. NG 985468. K corrected for 5% qtz.
	K	+4.9	
NGS-5	WR	-3.7	Dalradian schist at Hutton's contact, NG 985468. Now a fg hornfels.
GS-1	WR	+8.9	Inner granite, equigranular fg. Between Glen Sannox and Leac an Tobair, near the margin of the inner granite. NG 969437.
AR-CB1	WR	+2.0	Crushed outer granite at mylonitized fault contact with Old Red Sandstone, Corrie Burn. NG 012417.
<u>Ardnamurchan</u>			
Ar-13	WR	+0.1	Biotite quartz monzonite, center 3, 0.5 km south of Achnaha.
<u>Little Chief Porphyry, California</u>			
LCP-130D	WR	+7.1	Near northern margin of north phase of stock (see McDowell, 1967).
	k	+6.4	
	B	+3.5	
LCP-149c	f	+7.5	
LCP-269	f	+8.1	Near south margin of north phase of stock.
LCP-DV152	WR(gdmass)	+8.1	
	f	+7.6	
LCP-297	WR	+0.1	Pyritic, fine-grained hypabyssal rock.
LCP-266F	k(core)	+3.7	
	f(rim)	+1.7	
LCP-124c	WR	+5.5	Near NE margin of north phase of stock.
<u>Clark County, Nevada</u>			
YAG-19B	K	+5.7	Keyhole Canyon granite pluton, 35°42'0", 114°55'0" (see Armstrong, 1970).
YAG-19A	B	+4.6	Railroad Pass adamellite pluton, 35°58'0", 114°55'0". Biotite has $\delta\text{D} = -102$.

Table 9-1 (Cont'd)

Sample	Mineral	$\delta^{18}\text{O}$ (‰)	Description
<u>Coryell Syenite, B.C.</u>			
F8-285	K	+5.0	Near Rossland, B.C. Tertiary pluton invading Lower Jurassic Rossland Formation volcanics (see Little, 1960).
<u>Miscellaneous samples</u>			
LOS-6a	k	+7.2	West margin of Little Olga granodiorite porphyry stock, Winston Mining District, Montana (Earl, 1964).
LOS-7	WR	+5.6	Late Cretaceous andesitic volcanic, at contact with Little Olga stock, west margin.
LOS-11a	k	+7.5	North margin of Little Olga stock.
I-46	WR	+6.3	Syenite, Vallee de Papenoo, Tahiti-nui (McBirney and Aoki, 1968).
BC-MB2	F	+6.2	Olivine gabbro plug of Miocene age, Mt. Begbie, B.C. (Farquharson, 1973).
C1163	WR	+7.5	Altered diorite, Viti Levu, Fiji. $17^{\circ}52'24''$, $177^{\circ}18'18''$ (Houtz, 1959).
Y-34	k	+9.7	Pink porphyritic biotite granite, Wolf Creek Area, St. Elias Range, Yukon (Sharp, 1943).

Figure 9-1. General geologic map of Mull-Morven area (from Guide to the Geological Model of Ardnamurchan, Mem. Geol. Surv., 1935). Black dots are sample localities from area not covered in Figure 9-2. Q = quartz; K = alkali feldspar; no symbol = whole rock $\delta^{18}O$.

Figure 9-2. Generalized geologic map of the eastern part of the Isle of Mull (after Bailey et al., 1924), showing the $\delta^{18}O$ data and localities (black dots). Also included are data from Taylor and Forester (1971) and Beckinsale (1974). F = plagioclase; P = pyroxene; others as in Figure 9-1.



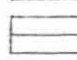
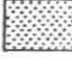


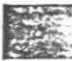
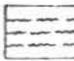

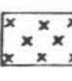



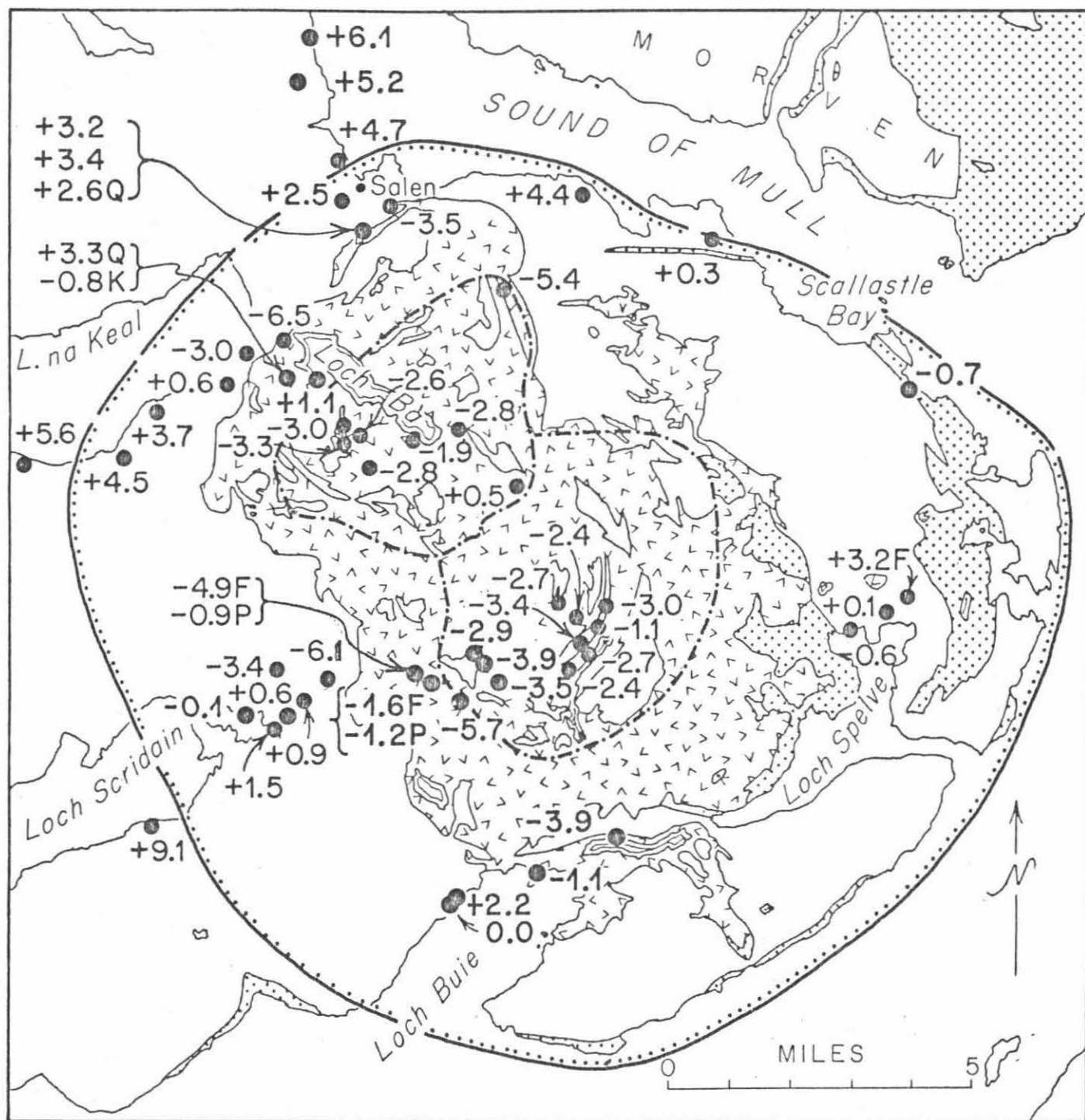
- | | | | | | |
|--|--|---|--|---|----------------------------|
|  | Tertiary Basalt Lavas outside Central Intrusive Complexes |  | Mesozoic Sediments (including Upper Carboniferous at Innimore Bay) |  | Dalradian Schists |
|  | Tertiary Igneous Rocks, etc. of Central Intrusive Complexes (boundary approximate) |  | Lower Old Red Sandstone Lavas and Sediments |  | Moine Schists and Gneisses |
|  | Margins of Subsidence-Calderas (Mull) and Plutonic-Vent Complexes (Ardnamurchan) |  | Granites of Caledonian Suite |  | Lewisian Gneiss |
|  | Limit of Pneumatolysis around Central Mull | | |  | Fault |

Figure 9-1



Tertiary
ring dike
intrusions



Tertiary
volcanic
rocks



Pre-Tertiary
rocks

--- Margins of main calderas Limit of pneumatolysis

Figure 9-2

A glance at the geological map of Mull (Sheet 44 of the Geological Survey of Great Britain) indicates the symmetrical nature of the intrusive complex of central Mull. The axis of symmetry, which trends NW-SE (see Figure 9-1) is the same direction along which the center of activity shifted with time. The intrusions associated with the early and late calderas include a myriad of arcuate cone sheets and ring dikes, explosion vents, gabbros and granophyres. The early cone sheets themselves have an aggregate thickness of about 1 km, made up of about 1000 individual intrusions. Other recent summaries of the geology of Mull are given by Richey (1961) and Stewart (1965).

Isotopic results

All $\delta^{18}\text{O}$ analyses from Mull are given in Table 9-1 and plotted in Figure 9-1 and 9-2. In addition, seven analyses of the Glen Cannel granophyre from Beckinsale (1974) and 23 analyses from Taylor and Forester (1971) are also included in Figure 9-2.

In spite of the geologic complexity of the Mull intrusive center, the $\delta^{18}\text{O}$ values of the igneous rocks present a fairly simple pattern. The rocks within the two calderas shown in Figure 9-2 are remarkably uniform, with a mean $\delta^{18}\text{O}_R = -2.7$ and an average deviation from the mean of only ± 0.6 per mil. There are some systematic variations with age, however. The earliest intrusives, including the early cone sheets, the Ben Buie gabbro (Mull-14), and the ring intrusive around Beinn Chaisgidle (e.g. Mull-6, 7; M1-131, 156) are characterized by

the lowest $\delta^{18}\text{O}$ values, with $\delta^{18}\text{O}_R \approx -3$. The Glen Cannel granophyre represents the first intrusive event of the later stage Loch Ba center, and it has an average $\delta^{18}\text{O}_R = -2.3$ (Beckinsale, 1974). The Beinn a Ghraig granophyre (Mull-16) post-dates the late cone sheets and has a $\delta^{18}\text{O}_R = +0.6$ (calculated by material-balance, see Table 9-1). Finally, the latest intrusion in the area, the Loch Ba ring dike (Mull-15), has $\delta^{18}\text{O}_R = +1.1$. This overall pattern of increasing $\delta^{18}\text{O}_R$ with decreasing age is analogous to the pattern shown by the later granitic intrusions in the Western Red Hills, Skye, and by Centers 2 and 3 in Ardnamurchan; the explanations given previously may also apply here (Section 8.12 of this work; Taylor and Forester, 1971).

Among the intrusive igneous rocks at Mull, the lowest $\delta^{18}\text{O}_R$ values are found along the borders of the caldera ring fractures; at the SW edge of the peripheral fracture zone of the early caldera, $\delta^{18}\text{O}_R = -2.9$ to -5.7 . These extremely low $\delta^{18}\text{O}$ values can probably be attributed to high contact metamorphic temperatures, and to the higher water/rock ratios that would accompany the fracturing associated with major cauldron subsidence; the latter would be expected to provide good access routes for the upward-moving waters that form part of the hydrothermal convection system (Taylor and Forester, 1971). The plutonic igneous rocks lying in the margins of the intrusive complex well away from the caldera ring fractures have $\delta^{18}\text{O}_R = -1.1$ to $+3.4$ (Figure 9-2).

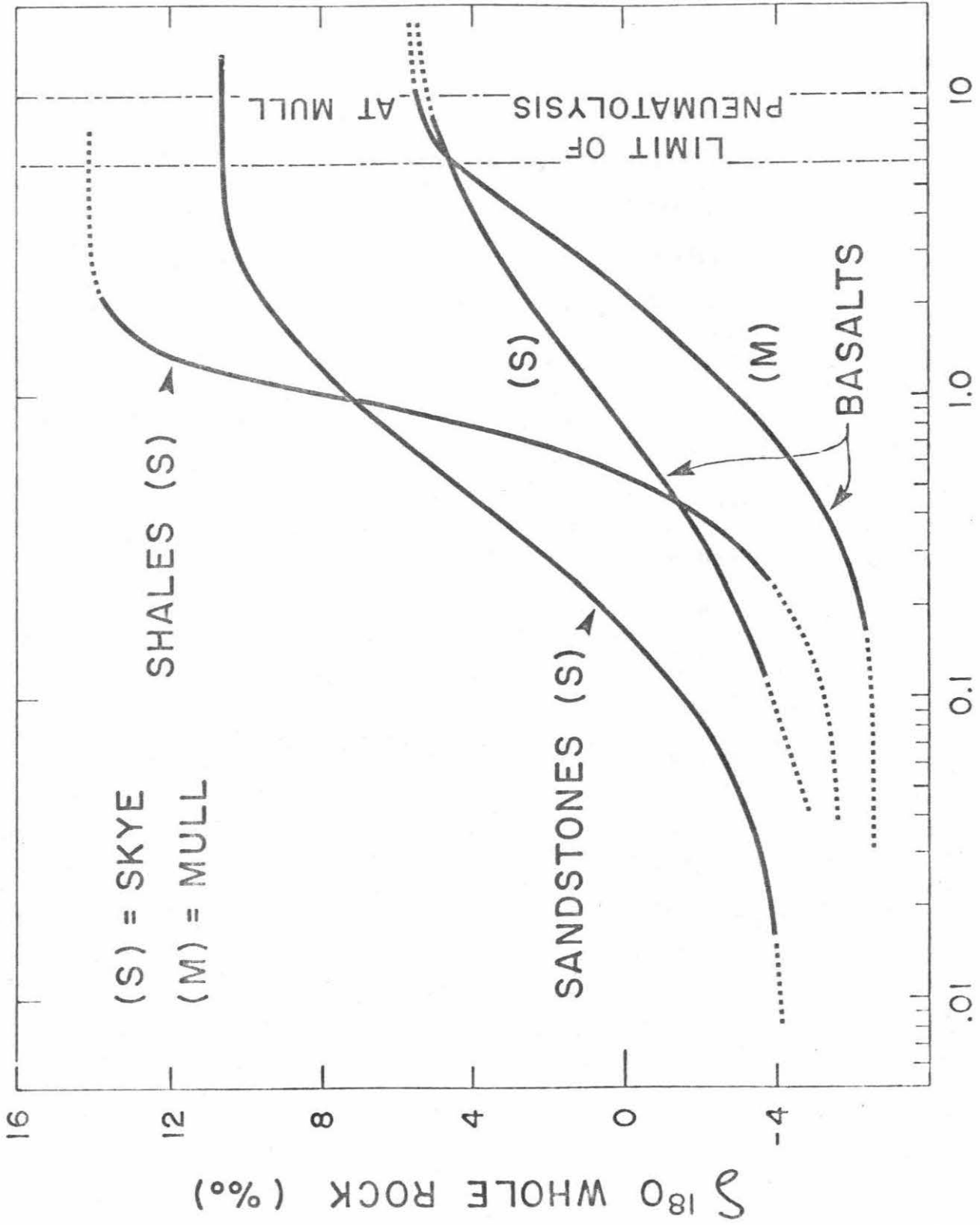
The most ^{18}O depleted rocks at Mull are the fine-grained volcanic rocks that lie closest to the central intrusive complex. Whole-rock $\delta^{18}\text{O}$ values as low as -5.4, -6.1 and -6.5 are observed. The most ^{18}O -depleted sample (M1-54) lies right at the periphery of the complex and is from a screen of basalt between the Knock granophyre and the Beinn a Ghraig granophyre. Overall, the plateau basalts at Mull range in $\delta^{18}\text{O}$ from -6.5 to +9.1, and they exhibit extremely systematic isotopic variations. The $\delta^{18}\text{O}_R$ values decrease radially inward as one approaches the central intrusive complex, in a manner analogous to that observed at Skye (see Section 8.7 and Figure 8-9). Note that the limit of pneumatolysis, shown on the map of Figure 9-2 and drawn on the basis of the mineralogical character of the plateau basalt lavas (Bailey *et al.*, 1924), coincides fairly well with an approximate $\delta^{18}\text{O}$ boundary between 'normal' and ^{18}O -depleted volcanic rocks. Recent mapping of the amygdule minerals in Mull (Walker, 1970) shows that the outer edge of the epidote zone corresponds almost precisely with the limit of pneumatolysis; just outside it lies the prehnite zone, almost coincident with the above-mentioned $\delta^{18}\text{O}$ boundary.

The prehnite and epidote zones occur in an area of the lava succession characterized by steeper dips (compared with the outer area of gentle dips in western and northern Mull), and constitute an aureole of striking regularity lying about 5 to 10 km from the central intrusive complex. These zones may therefore mark the approximate outer limit of the upward-moving

portion of the major meteoric-hydrothermal convection system(s). Note that all of the plateau basalts beyond the pneumatolysis limit have $\delta^{18}O_R \geq +4.7$. As mentioned in Section 8.7, at relatively low temperatures, the $\delta^{18}O$ values of the outer plateau basalts would not be drastically altered from their primary values of about +6.0. This is because of lower reaction rates, and also because the meteoric waters already have the $\delta^{18}O$ values required for isotopic equilibrium between plagioclase (An_{50}) and H_2O at low temperatures (e.g. $\delta^{18}O_F = +6.5$, then at $75^\circ C$, $\delta^{18}O_{H_2O} = -10.7$). There is only one basaltic country rock sample (M1-120, $\delta^{18}O_R = +9.1$) whose $\delta^{18}O_R$ has apparently been substantially increased by low temperature exchange (or weathering?).

Figure 9-3 shows generalized $\delta^{18}O_R$ profiles of sandstones, shales, and basalts from Skye, as well as the basalts from Mull, as a function of distance from the intrusive complex. Note that, where the country rocks are basalts, the $\delta^{18}O$ effects extend outward for about 8 km at both Mull and Skye, even though the Mull intrusive center is smaller than the Skye center. The profiles shown in Figure 9-3 are also distinctly different at the two centers; the steeper profile at Mull is possibly a result of the fact that the Mull intrusive center represents hundreds of individual, separate, sub-volcanic intrusive events, whereas at Skye there were clearly some large magma chambers that persisted over a considerable length of time (e.g. the Cuillin gabbro). Thus larger amounts of magma may have passed upward

Figure 9-3. Semilogarithmic plot of $\delta^{18}O_R$ vs distance from the central intrusive complex (for discussion, see text). The curves represent generalized, average profiles. The limit of pneumatolysis on the Isle of Mull (after Bailey et al., 1924) is also shown.



DISTANCE FROM CENTRAL INTRUSIVE COMPLEX (KM)

Figure 9-3

through the Mull center than in Skye, and the meteoric-hydrothermal effects would be correspondingly enhanced by the greater amount of heat energy available per unit area. Another factor to be considered is that at Mull the country rocks are entirely made up of permeable lavas. At Skye, in areas where the country rocks are made up of much less permeable shales, the $\delta^{18}\text{O}$ effects extend outward to only about 2 km. The sandstones, being somewhat more permeable than the shales and composed largely of quartz, feldspar, and carbonate, show measurable ^{18}O depletions outward for about 4 km (Figure 9-3).

It is interesting to note that all the profiles in Figure 9-3 apparently converge inward to a $\delta^{18}\text{O}_R \approx -4$ to -6 . This is not an unexpected result, inasmuch as at equilibrium all the rock types tend to approach the $\delta^{18}\text{O}_{\text{H}_2\text{O}}$ value of the exchanged meteoric water at sufficiently high temperatures. However, even at equilibrium the quartz-rich rocks will always be somewhat richer in ^{18}O than the basaltic rocks (Taylor and Epstein, 1962).

Note that the Ross of Mull granite pluton, 25 km W of the Mull center, with a K-Ar age of 420 my (Beckinsale and Obradovich, 1973) has 'normal' $\delta^{18}\text{O}_Q$ and $\delta^{18}\text{O}_K$ values of +9.2 and +8.5, respectively (Figure 9-1). Obviously, this intrusion has not been affected at all by the Tertiary meteoric-hydrothermal activity. As it was intruded into relatively impermeable Precambrian schist and gneiss, it is logical that there was no

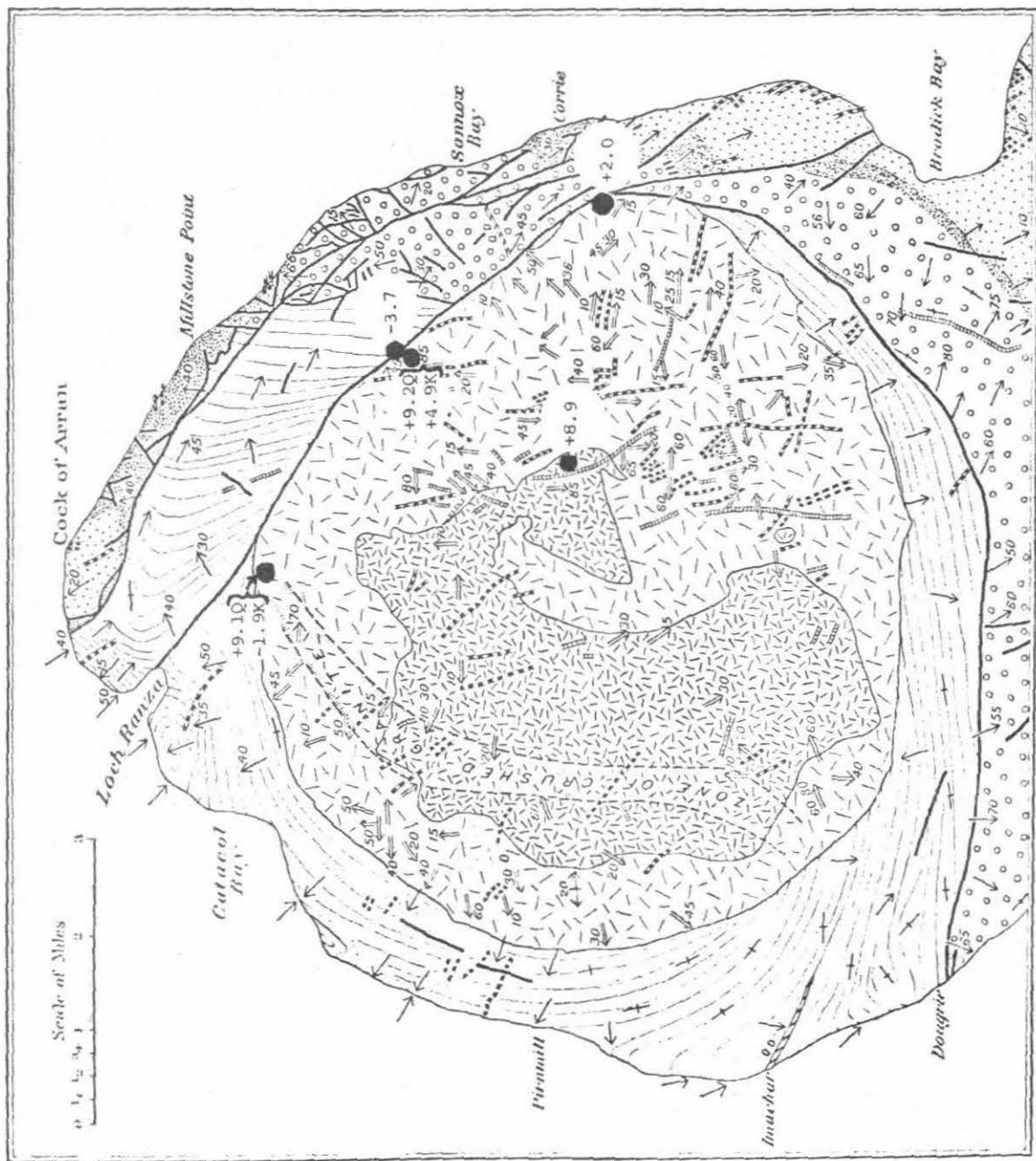
measurable involvement with heated ground waters during Silurian time, either.

9.2 Northern Granite Complex, Arran

The first detailed mapping of the island of Arran was carried out by Gunn (1903). Tyrrell (1928) incorporated much of Gunn's work in his memoir. More recent studies include brief reviews by Richey (1961) and Stewart (1965) and detailed studies by King (1954), Tomkeieff and Longstaff (1961) and MacGregor (1965).

There are two Tertiary central complexes on Arran - the Central Ring Complex and the earlier northern granite. The northern granite complex is about 13 km in diameter, and is composed of an outer coarse-grained biotite granite and a central and later fine-grained biotite granite. The country rocks around the granitic mass have been uplifted and tilted by the act of emplacement, so that they now strike approximately parallel to the granite margins. Portions of this contact are represented by a fault (Figure 9-4).

Only seven $\delta^{18}\text{O}$ values have been obtained from the Northern granite complex of Arran (Table 9-1; Figure 9-4). It is abundantly clear however that the outer granite has suffered extreme ^{18}O depletion and this must have taken place almost entirely at subsolidus temperatures. This is because sample AR-GE1 has a normal $\delta^{18}\text{O}_\text{Q} = +9.1$, but the coexisting alkali feldspar has $\delta^{18}\text{O} = -1.9$. Note that the $\Delta_{\text{Q-K}}$ value of 11.0 is



- | | |
|--|--|
| | |
| | |
| | |
| | |
| | |
- Dip, amount in degrees.
 Vertical of Schists & Later Strata.
 Anticline.
 Slabby Jointing in Granite.

Figure 9-4. Geologic map of northern Arran (after Tyrrell, 1928), showing the $\delta^{18}O$ data and localities (black dots). Notation as in Figure 9-1.

one of the largest from the Scottish Tertiary volcanic districts. Note also that AR-CB1 has the identical whole rock $\delta^{18}\text{O}$ value (+2.0) of that calculated for AR-GE1; it is probable that the alkali feldspar in AR-CB1 is similarly highly depleted in ^{18}O . Both samples are from the margins of the outer granite and near the contact with surrounding country rocks. All of the ^{18}O -depleted samples were collected in the vicinity of a major fault that may have acted as a channelway for meteoric-hydrothermal fluids. These samples demonstrate that solutions penetrated into the basement crystalline complex, although any important oxygen isotopic effects may be confined to the vicinity of major fractures (see Figure 9-4).

The inner granite, although finer grained than the outer granite, has a 'normal' whole rock $\delta^{18}\text{O} = +8.9$. It is virtually impossible for this specimen to have suffered any significant ^{18}O depletion. This inner granite becomes very fine grained at the contacts of the older outer granite (Flett, 1942), and yet is not at all depleted in ^{18}O . More sampling is obviously necessary to demonstrate whether or not the core of the Arran complex is anywhere depleted in ^{18}O .

The contact specimen NGS-5 has a $\delta^{18}\text{O} = -3.7$. This sample of Dalradian has the lowest $\delta^{18}\text{O}$ value of any metapelite yet reported, and must have been depleted by at least 10 per mil. The combination of close proximity to the fault contact

and the recrystallized, fine grained nature of this sample has certainly been favorable for oxygen isotopic exchange.

9.3 Miscellaneous localities

Little Chief Granite porphyry stock, California

The Little Chief Granite stock of Tertiary age is located in the central Panamint Range near Death Valley, California. It has been the subject of a detailed study by McDowell (1967, 1974) and McDowell and Albee (1966a and b).

The stock, predominantly of granite or quartz monzonite, is a composite intrusion with a south phase and a later north phase (Figure 9-5). It is bounded on the north, south and west by vertical faults which define a rectangular "trapdoor" of sedimentary rocks. The country rocks in the area include Precambrian crystalline rocks (Silver et al., 1961; Lanphere et al., 1964; Wasserburg et al., 1959), the later Precambrian Pahrump Group, and Cambrian sedimentary formations.

Only seven samples from the Little Chief stock have been analyzed in this study, with a total of 11 $\delta^{18}\text{O}$ analyses (Table 9-1). The results are plotted on Figure 9-5. LCP-124c has a $\delta^{18}\text{O} = +5.5$, which is significantly lower than the other samples from the north phase of the stock. The feldspar phenocrysts of LCP-266F have $\delta^{18}\text{O} = +3.7$, while the white outer rims of plagioclase have $\delta^{18}\text{O} = +1.7$. The most ^{18}O -depleted sample ($\delta^{18}\text{O} = +0.1$) is a pyritic, fine-grained hypabyssal rock probably related to the intense dike swarm at the eastern side of

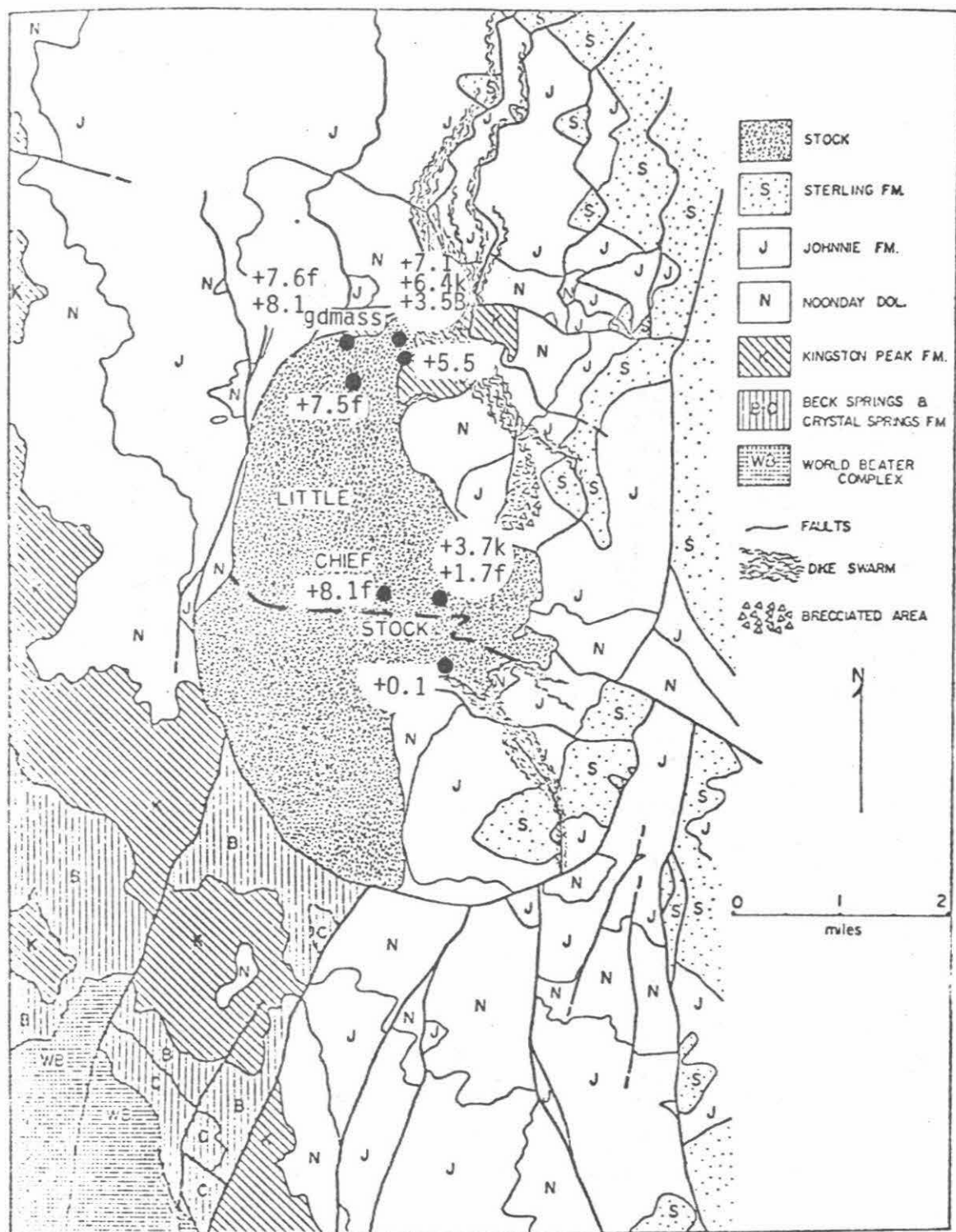


Figure 9-5. Generalized geologic map of the Little Chief stock area (after McDowell, 1967), showing the $\delta^{18}\text{O}$ data and sample localities (black dots). B = biotite; f, k = plagioclase and alkali feldspar phenocrysts, respectively; gdmass = groundmass.

the intrusion. Note that almost all of these samples are situated near the margins of the stock.

Although the data are meager, the most likely explanation for the abnormally low $^{18}\text{O}/^{16}\text{O}$ ratios of some of the samples is that these rocks underwent oxygen isotope exchange with heated, low- ^{18}O meteoric ground waters. This has apparently occurred in spite of the unfavorable, relatively impermeable nature of the country rock, probably because it is an example of an epizonal body whose emplacement was associated with major fault development.

Clark County, Nevada

Both samples analyzed (Table 9-1) are from Tertiary intrusive rocks in the vicinity of the Nevada-Arizona border (Armstrong, 1970). The $\delta^{18}\text{O}_K = +5.7$ is somewhat lower than expected for orthoclase in a 'normal' granite. The biotite from YAG-19A has a $\delta D = -102$, which is abnormally depleted in deuterium with respect to 'normal' igneous biotites (see Figure 6-6). These few analyses suggest small amounts of meteoric water may have exchanged with these Tertiary igneous rocks.

Coryell Syenite, British Columbia

This sample, from the Tertiary syenite that intrudes the Lower Jurassic volcanics near Rosslund, B.C. (Little, 1960) has a $\delta^{18}\text{O}_K = +5.0$. This sample is thus slightly depleted in ^{18}O , most likely as a result of exchange with hydrothermal-meteoric waters.

Miscellaneous samples

All these samples have essentially 'normal' $\delta^{18}\text{O}$ values, and there is no oxygen isotopic indication of interaction with meteoric-hydrothermal fluids (Table 9-1).

BIBLIOGRAPHY

- Albee, A.L., 1962, Relationships between the mineral association, chemical composition and physical properties of the chlorite series, Amer. Mineral., 47, p. 851-870.
- Almond, D.C., 1964, Metamorphism of Tertiary lavas in Strathaird, Skye, Trans. R. Soc. Edinb., 65, p. 413-434.
- Anderson, A.T., 1967, The dimensions of oxygen isotopic equilibrium attainment during prograde metamorphism, Jour. Geol., 75, p. 323-332.
- Anderson, A.T., Jr., R.N. Clayton, and T.K. Mayeda, 1971, Oxygen isotope thermometry of mafic igneous rocks, Jour. Geol., 79, p. 715-729.
- Anderson, F.W., and K.C. Dunham, 1966, The geology of Northern Skye, Mem. Geol. Surv. Gt. Britain.
- Armstrong, R.L., 1970, Geochronology of Tertiary igneous rocks, eastern Basin and Range Province, western Utah, eastern Nevada, and vicinity, U.S.A., Geochim. Cosmochim. Acta, 34, p. 203-232.
- Armstrong, R.L., 1969, K-Ar dating of laccolithic centers of the Colorado Plateau and vicinity, Geol. Soc. Am. Bull., 80, p. 2081-2086.
- Bailey, E.B., 1954, Contact of Tertiary lavas with Torridonian near Broadford, Skye, Geol. Mag., 91, p. 105-115.
- Bailey, E.B., C.T. Clough, W.B. Wright, J.E. Richey, and G.V. Wilson, 1924, The Tertiary and post-Tertiary geology of Mull, Loch Aline, and Oban, Mem. Geol. Surv. Scotland.
- Banwell, C.J., 1963a, Thermal energy from the earth's crust, Introduction and Part I, N.Z. Jour. Geol. Geophys., 6, p. 52-69.
- Banwell, C.J., 1963b, Oxygen and hydrogen isotopes in New Zealand thermal areas, in Nuclear Geology on Geothermal Areas, Spoleto, Italy, p. 95-138.
- Banwell, C.J., 1961, Geothermal drillholes - physical investigations: U.N. Conf. on New Sources of Energy, Paper G53.
- Barker, F., 1969, Precambrian geology of the Needle Mountains, southwestern Colorado, U.S.G.S. Prof. Paper 644-A.
- Beckinsale, R.D., 1974, Rb-Sr and K-Ar age determinations, and oxygen isotope data for the Glen Cannel granophyre, Isle of Mull, Argyllshire, Scotland, Earth Planet. Sci. Letters, 22, p. 267-274.
- Beckinsale, R.D., and J.D. Obradovich, 1973, Potassium-argon ages for minerals from the Ross of Mull, Argyllshire, Scotland, Scot. Jour. Geol., 9, p. 147-156.

- Bell, J.D. 1966, Granites and associated rocks of the Eastern part of the Western Red Hills Complex, Isle of Skye, Trans. R. Soc. Edinb., 66, p. 307-343.
- Bethke, P.M., R.O. Rye, and P.B. Barton, Jr., 1973, Hydrogen, oxygen, and sulfur isotopic compositions of ore fluids in the Creede district, Mineral Co., Colorado: Geol. Soc. America Annual Meeting, Abstracts with Programs, p. 549.
- Biehler, S., R.L. Kovach, and C.R. Allen, 1964, Geophysical framework of northern end of Gulf of California structural province, in van Andel, T.H., and Shor, G.G., Jr., Editors, Marine Geology of the Gulf of California - A Symposium, Amer. Assoc. Petroleum Geol. Mem. 3, p. 126-143.
- Bigeleisen, J., and M.G. Mayer, 1947, Calculation of equilibrium constants for isotopic exchange reactions, Jour. Chem. Phys., 15, p. 261.
- Bott, M.H.P., and J. Tuson, 1973, Deep structure beneath the Tertiary volcanic regions of Skye, Mull, and Ardnamurchan, northwest Scotland, Nature, Phys. Sci., 242, p. 114-116.
- Bottinga, Y., 1969, Calculated fractionation factors for carbon and hydrogen isotope exchange in the system calcite-carbon dioxide-graphite-methane-hydrogen-water vapor, Geochim. Cosmochim. Acta, 33, p. 49-64.
- Bottinga, Y., 1968, Calculation of fractionation factors for carbon and oxygen isotopic exchange in the system calcite-carbon dioxide-water, Jour. Phys. Chem., 72, p. 800-808.
- Bottinga, Y., and H. Craig, 1968, High temperature liquid-vapor fractionation factors for $H_2O-H_2O^{18}$ (abs): Amer. Geophys. Union Trans., 49, p. 356.
- Bottinga, Y., and M. Javoy, 1973, Comments on oxygen isotope geothermometry, Earth Planet. Sci. Letters, 20, p. 250-265.
- Bowen, N.L., 1928, The Evolution of the Igneous Rocks, Dover Publications, New York.
- Bowes, D.R., 1969, The Lewisian of northwest highlands of Scotland, in North Atlantic; geology and continental drift, Amer. Assoc. Petroleum Geol. Mem. 12, p. 575-594.
- Brown, G.M., 1969, The Tertiary igneous geology of the Isle of Skye, The Geologists Assoc., Guide No. 13, London.
- Brown, G.M., 1963, Melting relations of Tertiary granitic rocks in Skye and Rhum, Mineral. Mag., 33, p. 533-562.

- Buist, D.S., 1959, The composite sill of Rudh' an Eiveannaich, Skye, Geol. Mag., 96, p. 247-252.
- Burbank, W.S., 1941, Structural control of ore deposition in the Red Mountain, Sneffels, and Telluride districts of the San Juan Mountains, Colorado, Colo. Sci. Soc. Proc., 14, p. 141-261.
- Burbank, W.S., 1933, Vein systems of Arrastre Basin and regional geologic structure in the Silverton and Telluride quadrangles, Colorado, Colo. Sci. Soc. Proc., 13, p. 135-214.
- Burbank, W.S., and R.G. Luedke, 1969, Geology and ore deposits of the Eureka and adjoining districts, San Juan Mountains, Colorado: U.S. Geol. Survey Prof. Paper 535.
- Burbank, W.S., and R.G. Luedke, 1966, Geologic map of the Telluride quadrangle, southwestern Colorado, U.S. Geol. Survey Geol. Quad, Map GQ-504.
- Burnham, C.W., 1967, Hydrothermal fluids at the magmatic stage, in Barnes, H.L., (editor), Geochemistry of Hydrothermal Ore Deposits, Holt, Rinehart, and Winston, New York, p. 34-76.
- Burnham, C.W., and R.H. Jahns, 1962, A method for determining the solubility of water in silicate melts, Amer. Jour. Sci., 260, p. 721-745.
- Cathles, L.M., and D. Norton, 1974, Pluton driven ground water convection, Amer. Geophys. Union Trans. (abs.), 55, p. 488.
- Clayton, R.N., I. Friedman, D.L. Graf, T.K. Mayeda, W.F. Meents, and N.F. Shimp, 1966, The origin of saline formation waters: I. Isotopic composition, Jour. Geophys. Res., 71, p. 3869-3882.
- Clayton, R.N., J.R. Goldsmith, K.J. Johnson, and R.C. Newton, 1972a, Pressure effect on stable isotope fractionation, Amer. Geophys. Union Trans. (abs.), 53, p. 555.
- Clayton, R.N., L.J.P. Muffler, and D.E. White, 1968a, Oxygen isotope study of calcite and silicates of the River Ranch No. 1 Well, Salton Sea geothermal field, California: Amer. Jour. Sci., 266, p. 968-979.
- Clayton, R.N., B.F. Jones, and R.A. Berner, 1968b, Isotope studies of dolomite formation under sedimentary conditions, Geochim. Cosmochim. Acta., 32, p. 415-432.
- Clayton, R.N. and T.K. Mayeda, 1963, The use of bromine pentafluoride in the extraction of oxygen from oxides and silicates for isotopic analysis, Geochim. Cosmochim. Acta, 27, p. 43-52.
- Clayton, R.N., J.R. O'Neil, and T.K. Mayeda, 1972b, Oxygen isotope exchange between quartz and water: Jour. Geophys. Res., 77, p. 3057-3067.

- Conway, C.M., and H.P. Taylor, Jr., 1969, $^{18}\text{O}/^{16}\text{O}$ and $^{13}\text{C}/^{12}\text{C}$ ratios of co-existing minerals in the Oka and Magnet Cove carbonatite bodies, Jour. Geol., 77, p. 618-626.
- Coplen, T.B., 1973, Isotopic composition of calcite and water from the Dunes - DWR #1 geothermal test corehole, Imperial Valley, California, Amer. Geophys. Union Trans. (abs.), 54, p. 488.
- Coplen, T.B., and B.B. Hanshaw, 1973, Ultrafiltration by a compacted clay membrane - I., Oxygen and hydrogen isotopic fractionation, Geochim. Cosmochim. Acta, 37, p. 2295-2310.
- Craig, H., 1966, Isotopic composition and origin of the Red Sea and Salton Sea geothermal brines, Science, 154, p. 1544-1548.
- Craig, H., 1963, The isotopic geochemistry of water and carbon in geothermal areas in Tongiorgi, E., ed., Nuclear geology on geothermal areas, Spoleto, Pisa, Consiglio Nazionale della Ricerche, Laboratorio de Geologia Nucleare, p. 17-53.
- Craig, H., 1961, Isotopic variations in meteoric waters, Science, 133, p. 1702-1703.
- Craig, H., 1957, Isotopic standards for carbon and oxygen and correction factors for mass spectrometric analysis of carbon dioxide, Geochim. Cosmochim. Acta, 12, p. 133-149.
- Craig, H., G. Boato, and D.E. White, 1956, Isotopic geochemistry of thermal waters, Proc. 2nd Conf. on Nuclear Processes in Geologic Settings, Nat'l Research Council, Nuclear Sci. Ser. Rept., 19, p. 29-38.
- Craig, H., L. Gordon, and Y. Horibe, 1963, Isotopic exchange effects in the evaporation of water, Jour. Geophys. Res., 68, p. 5079-5087.
- Cross, W., 1899, Igneous rocks of the Telluride district, Colo., Colo. Sci. Soc. Proc., 5, p. 225-234.
- Cross, W., E. Howe, and F.L. Ransome, 1905, Description of the Silverton quadrangle, Colo., U.S. Geol. Surv. Geol. Atlas, Folio 120.
- Cross, W., and C.W. Purington, 1899, Description of the Telluride quadrangle, Colo., U.S. Geol. Survey Geol. Atlas, Folio 57.
- Cumberlidge, J.T., and V.A. Saull, 1959, Some experiments on surface and strain energy in minerals, Bull. Geol. Soc. Amer., (abs.), A26.
- Dansgaard, W., 1964, Stable isotopes in precipitation, Tellus, 16, p. 436-468.
- Degens, E.T., and S. Epstein, 1962, Relation between $^{18}\text{O}/^{16}\text{O}$ ratios in co-existing carbonates, cherts, and diatomites, Bull. Amer. Assoc. Petrol. Geol., 46, p. 534-542.

- Degens, E.T., J.M. Hunt, J.H. Reuter, and W.E. Reed, 1964, Data on the distribution of amino acids and oxygen isotopes in petroleum brine waters of various geologic ages, Sedimentology, 3, p. 199-225.
- Deines, P., 1970, The carbon and oxygen isotopic composition of carbonates from the Oka carbonatite complex, Quebec, Canada, Geochim. Cosmochim. Acta, 34, p. 1199-1225.
- Deines, P., and D.P. Gold, 1973, The isotopic composition of carbonatite and kimberlite carbonates and their bearing on the isotopic composition of deep-seated carbon, Geochim. Cosmochim. Acta, 37, p. 1790-1733.
- Deines, P., and D.P. Gold, 1969, The change in carbon and oxygen isotopic composition during contact metamorphism of Trenton limestone by the Mount Royal pluton, Geochim. Cosmochim. Acta, 33, p. 421-424.
- Devereux, I., 1968, Oxygen isotope ratios of minerals from the regionally metamorphosed schists of Otago, New Zealand, N.Z. Jour. Sci., 11, p. 526-548.
- Dings, M., 1941, Geology of the Stony Mountain stock, San Juan Mountains, Colorado, Bull. Geol. Soc. Amer., 53, p. 695-720.
- Doe, B.R., 1970, Lead Isotopes, Springer-Verlag, Berlin, Heidelberg.
- Donaldson, I.G., 1962, Temperature gradients in the upper layers of the earth's crust due to convective water flow, Jour. Geophys. Res., 67, p. 3449-3460.
- Dowgiallo, J., and E. Tongiorgi, 1972, The isotopic composition of oxygen and hydrogen in some brines from the Mesozoic in northwest Poland: Geothermics, 1, p. 67-69.
- Earll, F.N., 1964, Economic geology and geochemical study of Winston Mining district, Broadwater County, Montana, Montana Bureau Mines Bull., 41.
- Elder, J.W., 1967, Steady free convection in a porous medium heated from below, Jour. Fluid Mech., 27, p. 29-48.
- Elder, J.W., 1965, Physical processes in geothermal areas, in Terrestrial Heat Flow, Geophys. Mon. 8, NAS-NRD No. 1288, Amer. Geophys. Union, p. 211-239.
- Ellis, A.J., 1967, The chemistry of some explored geothermal systems, in Barnes, H.L., (editor), Geochemistry of Hydrothermal Ore Deposits, Holt, Rinehart, and Winston, New York, p. 465-514.
- Epstein, S., D. Graf and E.T. Degens, 1963, Oxygen isotope studies on the origin of dolomites, in Isotopic and Cosmic Chemistry, Craig et al., ed., North Holland Publishing Company, Amsterdam.

- Epstein, S., and T. Mayeda, 1953, The variation in O^{18} content of water from natural sources, Geochim. Cosmochim. Acta, 4, p. 213.
- Epstein, S., and H.P. Taylor, Jr., 1971, O^{18}/O^{16} , Si^{30}/Si^{28} , D/H, and C^{13}/C^{12} ratios in lunar samples, Proc. Second Lunar Sci. Conf., M.I.T. Press, 2, p. 1421-1441.
- Eslinger, E.V., and S.M. Savin, 1973, Mineralogy and oxygen isotope geochemistry of the hydrothermally altered rocks of the Ohaki-Broadlands, New Zealand geothermal area, Amer. Jour. Sci., 273, p. 240-267.
- Eugster, H.P., and G.B. Skippen, 1967, Igneous and metamorphic reactions involving gas equilibria: in Abelson, P.H., ed., Researches in Geochemistry, New York, John Wiley, 2, p. 492-520.
- Farquharson, R.B., 1973, The petrology of late Tertiary dolerite plugs in the South Caribou Region, British Columbia, Can. Jour. Earth Sci., 10, p. 205-225.
- Flett, W.R., 1942, The contact between the granites of North Arran, Trans. Geol. Soc. Glasg., 20, p. 180-204.
- Forester, R.W., and H.P. Taylor, Jr., 1972, Oxygen and hydrogen isotope data on the interaction of meteoric ground waters with a gabbro-diorite stock, San Juan Mountains, Colorado, Internat. Geol. Cong., 24th, Montreal 1972, sec. 10, Geochemistry, p. 254-263.
- Fornaseri, M., and B. Turi, 1969, Carbon and oxygen isotopic composition of carbonates in lavas and ejectites from the Alban Hills, Italy, Contr. Mineral. Petrol., 23, p. 244-256.
- Friedman, I., 1953, Deuterium content of natural water and other substances, Geochim. Cosmochim. Acta, 4, p. 89-103.
- Friedman, I., P.W. Lipman, J.D. Obradovich, J.D. Gleason, and R.L. Christiansen, 1974, Meteoric water in magmas, Science, 184, p. 1069-1072.
- Friedman, I., A.C. Redfield, B. Schoen, and J. Harris, 1964, The variation in the deuterium content of natural waters in the hydrologic cycle, Rev. Geophys., 2, p. 177-224.
- Garlick, G.D., 1966, Oxygen isotope fractionation in igneous rocks, Earth Planet. Sci. Letters, 1, p. 361-368.
- Garlick, G.D., 1964, Oxygen isotope ratios in coexisting minerals of regionally metamorphosed rocks, Ph.D. Thesis, California Institute of Technology.
- Garlick, G.D., and S. Epstein, 1967, Oxygen isotope ratios in coexisting minerals of regionally metamorphosed rocks, Geochim. Cosmochim. Acta, 31, p. 181-214.

- Garlick, G.D., and S. Epstein, 1966, The isotopic composition of oxygen and carbon in hydrothermal minerals at Butte, Montana, Econ. Geol., 61, p. 1325-1335.
- Garlick, G.D., I.D. MacGregor, and D.E. Vogel, 1971, Oxygen isotope ratios in eclogites from kimberlites, Science, 172, p. 1025-1027.
- Geikie, A., 1897, The Ancient Volcanoes of Great Britain, London.
- Godfrey, J.D., 1962, The deuterium content of hydrous minerals from the east-central Sierra Nevada and Yosemite National Park, Geochim. Cosmochim. Acta, 26, p. 1215-1245.
- Gracie, A.J., and A.D. Stewart, 1967, Torridonian sediments at Enarol Bay, Ross-shire, Scott. Jour. Geol., 3, p. 181-194.
- Graf, D.L., I. Friedman, and W.F. Meents, 1965, The origin of saline formation waters, 2, Isotopic fractionation by shale micropore systems, Ill. State Geol. Surv., Circ. 393.
- Griggs, D.T., F.J. Turner, and H.C. Heard, 1960, Deformation of rocks at 500°C to 800°C, Geol. Soc. Amer. Mem., 79, p. 39-104.
- Grindley, G.W., 1961, Taupo geological map of New Zealand, 1st ed, Wellington, N.Z. Dept. Sci. Indus. Res., sheet N94.
- Guide to the Geological Model of Ardnamurchan, 1935, Mem. Geol. Surv.
- Gunn, W., 1903, The geology of North Arran, South Bute and the Cumbraes, Mem. Geol. Surv. Gt. Britain.
- Hall, W.E., I. Friedman, 1969, Oxygen and carbon isotopic composition of ore and rock of selected Mississippi Valley deposits, U.S. Geol. Surv. Prof. Paper 650-C, p. C140-C148.
- Hall, W.E., I. Friedman, and J.T. Nash, 1973, Fluid inclusion and light stable isotope study of the Climax molybdenum deposits, Colorado, Geol. Soc. Amer. Annual Meeting, Abstracts with Programs, p. 649-650.
- Hamilton, D.L., C.W. Burnham, and E.F. Osborn, 1964, The solubility of water and effects of oxygen fugacity and water content on crystallization in mafic magmas, Jour. Petrol., 5, p. 21-39.
- Hamilton, E.I., 1966, The isotopic composition of lead in igneous rocks - I, The origin of some Tertiary granites, Earth Planet. Sci. Letters, 1, p. 30-37.
- Harker, A., 1904, The Tertiary igneous rocks of Skye, Mem. Geol. Surv. Gt. Britain.
- Helgeson, H.C., 1968, Geologic and thermodynamic characteristics of the Salton Sea geothermal system, Amer. Jour. Sci., 266, p. 129-166.

- Helgeson, H.C., 1967, Solution chemistry and metamorphism, in Abelson, P.H., editor, Researches in Geochemistry, 2, John Wiley & Sons, New York, p. 362-404.
- Hemley, J.J., 1959, Some mineralogical equilibria in the system $K_2O-Al_2O_3-SiO_2-H_2O$, Amer. Jour. Sci., 257, p. 241-270.
- Heyl, A.V., G.P. Landis, and R.E. Zartman, 1973, Isotopic evidence for the origin of Mississippi Valley-type mineral deposits: a review, Geol. Soc. America Annual Meeting, Abstracts with Programs, 5, p. 668-669.
- Hitchon, B., and I. Friedman, 1969, Geochemistry and origin of formation waters in the western Canada sedimentary basin - I, Stable isotopes of hydrogen and oxygen, Geochim. Cosmochim. Acta, 33, p. 1321-1349.
- Hitchon, B., and H.R. Krouse, 1972, Hydrogeochemistry of the surface waters of the Mackenzie River drainage basin, Canada, III, Stable isotopes of oxygen, carbon, and sulfur, Geochim. Cosmochim. Acta, 36, p. 1337-1358.
- Hoering, T.C., 1961, The physical chemistry of isotopic substances, Annual Report of the Director of the Geophys. Lab., p. 201.
- Honda, S., and L.J.P. Muffler, 1970, Hydrothermal alteration in core from research drill hole Y-1, Upper Geyser Basin, Yellowstone National Park, Wyoming, Amer. Mineral., 55, p. 1714-1737.
- Houtz, R.E., 1959, Regional geology of Lomawai-Momi, Nandronga, Viti Levu, Bull. Geol. Surv. Fiji, 3.
- Hudson, J.D., 1962, The stratigraphy of the Great Estuarine Series (Middle Jurassic) of the Inner Hebrides, Trans. Edinb. Geol. Soc., 19, p. 139-165.
- Hutchinson, R., 1968, Origin of the white allivalite, western Cuillin, Isle of Skye, Geol. Mag., 105, p. 338-347.
- Hutchinson, R., 1966, Intrusive tholeiites of the western Cuillin, Isle of Skye, Geol. Mag., 103, p. 352-363.
- Irving, E., and S.K. Runcorn, 1957, Analysis of the paleomagnetism of the Torridonian sandstone series of northwest Scotland, Phil. Trans. R. Soc. A250, p. 83-99.
- Jassim, S.Z., and I.G. Gass, 1970, The Loch na Creitheach volcanic vent, Isle of Skye, Scott. Jour. Geol., 6, p. 285-294.
- Javoy, M., and C.J. Allegre, 1967, Etude de la composition $^{18}O/^{16}O$ de quelques eclogites: consequences petrologiques et geophysiques, Bull. Soc. Geol. France, 9, p. 800-808.
- Keith, M.L., and J.N. Weber, 1964, Carbon and oxygen isotopic composition of selected limestones and fossils, Geochim. Cosmochim. Acta, 28, p. 1787-1816.

- Kennedy, W.Q., 1933, Trends of differentiation in basaltic magmas, Amer. Jour. Sci., 25, p. 239-256.
- Kennedy, W.Q., 1931, The parent magma of the British Tertiary province, Summary of Progress, Geol. Surv. Gt. Britain, p. 61-73.
- Kharaka, Y.K., F.A.F. Berry, and I. Friedman, 1973, Isotopic composition of oilfield brines from Kettleman North Dome, California, and their geologic implications, Geochim. Cosmochim. Acta, 37, p. 1899-1903.
- King, B.C., 1954, The Ard Bheinn area of the central igneous complex of Arran, Quart. Jour. Geol. Soc. London, 110, p. 323-354.
- King, B.C., 1953, Structure and igneous activity in the Creag Strollamus area of Skye, Trans. R. Soc. Edinb., 62, p. 357-402.
- Kovach, R.L., C.R. Allen, and F. Press, 1962, Geophysical investigations in the Colorado delta region, Jour. Geophys. Res., 67, p. 2845-2871.
- Kracek, F.C., and K.J. Neuvonen, 1952, Thermochemistry of plagioclase and alkali feldspars, Amer. Jour. Sci., Bowen Volume, p. 293-318.
- Lambert, R. St. J., and J.G. Holland, 1972, A geochronological study of the Lewisian from Loch Laxford to Durness, Sutherland, N.W. Scotland, Quart. Jour. Geol. Soc. London, 128, p. 3-19.
- Landis, G.P., R.O. Rye, and F.J. Sawkins, 1972, Geologic, fluid inclusion, and stable isotope studies of the Pasto Bueno tungsten-base metal deposit, Northern Peru (abs.), Geol. Soc. Amer. Annual Meeting, Minneapolis, Abstracts with Programs, p. 572-573.
- Lanphere, M.A. G.J. Wasserberg, A.L. Albee, and G.R. Tilton, 1964, Redistribution of strontium and rubidium isotopes during metamorphism, World Beater Complex, Panamint Range, California, in Isotopic and Cosmic Chemistry, Amsterdam, North-Holland Pub. Co., chap. 20, p. 269-320.
- Lapwood, E.R., 1948, Convection of a fluid in a porous medium, Proc. Cambridge Phil. Soc., 44, p. 508-521.
- Larsen, E.S., Jr., and W. Cross, 1956, Geology and petrology of the San Juan region, southwestern Colorado, U.S. Geol. Surv. Prof. Paper 258.
- Lawrence, J.R., and H.P. Taylor Jr., 1972, Hydrogen and oxygen isotope systematics in weathering profiles, Geochim. Cosmochim. Acta, 36, p. 1377-1393.
- Lawrence, J.R., and H.P. Taylor Jr., 1971, Deuterium and oxygen-correlation: Clay minerals and hydroxides in Quaternary soils compared to meteoric waters. Geochim. Cosmochim. Acta, 35, p. 993-1003.
- Lawson, A.C., 1914, Ore deposition in and near intrusive rocks by meteoric waters, Univ. Calif. Publ. Bull., 8, p. 219-242.

- Lawson, D.E., 1965, Lithofacies and correlation within the Lower Torridonian, Nature, 207, p. 706-708.
- Lipman, P.W., T.A. Steven, R.G. Luedke, and W.S. Burbank, 1973, Revised volcanic history of the San Juan, Uncompahgre, Silverton, and Lake City calderas in the western San Juan Mountains, Colorado, Jour. Res. U.S. Geol. Surv., 1, p. 627-642.
- Lipman, P.W., T.A. Steven, and H.H. Mehnert, 1970, Volcanic history of the San Juan Mountains, Colorado, as indicated by potassium-argon dating, Geol. Soc. America Bull., 81, p. 2329-2352.
- Little, H.W., 1960, Nelson Map Area, West Half, British Columbia, Geol. Surv. Canada Mem. 308.
- Long, L.E., 1964, Preliminary Rb-Sr investigation of Tertiary granite and granophyre from Skye, Geochim. Cosmochim. Acta, 28, p. 1870-1873.
- Luedke, R.G., and W.S. Burbank, 1968, Volcanism and cauldron development in the Western San Juan Mountains, Colorado. In Epis, R.C. (Editor), Cenozoic volcanism in the southern Rocky Mountains. Colorado School Mines Quart., 63, p. 175-208.
- Luedke, R.G., and W.S. Burbank, 1963, Tertiary volcanic stratigraphy in the western San Juan Mountains, Colorado, U.S. Geol. Surv. Prof. Paper 474-C, p. C39-C44.
- Luedke, R.G., and W.S. Burbank, 1962, eology of the Ouray quadrangle, southwestern Colorado, U.S. Geol. Surv. Geol. Quad. Map GQ-152.
- MacGregor, M., 1965, Excursion guide to the geology of Arran, Geol. Soc. Glasg.
- Matsuhisa, Y., H. Honma, O. Matsubaya, and H. Sakai, 1972, Oxygen isotopic study of the Cretaceous granitic rocks in Japan, Contr. Mineral. Petrol. 37, p. 65-74.
- Matsuhisa, Y, O. Matsubaya, and H. Sakai, 1973, Oxygen isotope variations in magmatic differentiation processes of the volcanic rocks in Japan, Contr. Mineral. Petrol., 39, p. 277-288.
- Mayor, J.N., and F.S. Fisher, 1972, Middle Tertiary replacement ore bodies and associated veins in the northwest San Juan Mountains, Colorado, Econ. Geol., 67, p. 214-230.
- McBirney, A.R., and K. Aoki, 1968, Petrology of the island of Tahiti, in Coats, R.R., R.L. Hay, and C.A. Anderson, Editors, Studies in volcanology, Geol. Soc. Amer. Mem. 116.
- McCrea, J.M., 1950, On the isotopic chemistry of carbonates and a paleo-temperature scale, Jour. Chem. Phys., 18, p. 849-857.

- McDowell, S.D., 1974, Emplacement of the Little Chief Stock, Panamint Range, California, Geol. Soc. Amer. Bull., 85, p. 1535-1546.
- McDowell, S.D., 1967, The intrusive history of the Little Chief granite porphyry stock, central Panamint Range, California, Ph.D. Thesis, California Institute of Technology.
- McDowell, S.D., and A.L. Albee, 1966a, Emplacement of the Little Chief granite porphyry stock, central Panamint Range west of Death Valley, California (abs.), Geol. Soc. Amer. Spec. Paper 87, p. 216.
- McDowell, S.D., and A.L. Albee, 1966b, Crystallization history of the Little Chief granite porphyry, California, based on electron microprobe analyses of the feldspars (abs.), Geol. Soc. Amer. Spec. Paper 87, p. 106.
- McKinney, C.R., J.M. McCrea, S. Epstein, H.A. Allen, and H.C. Urey, 1950, Improvements in mass spectrometers for the measurement of small differences in isotope abundance ratios, Rev. Sci. Inst., 21, p. 724-730.
- Mehnert, H.H., P.W. Lipman, and T.A. Steven, 1973a, Age of the Lake City caldera and related Sunshine Peak Tuff, western San Juan Mountains, Colorado, Isochron West, p. 31-33.
- Mehnert, H.H., P.W. Lipman, and T.A. Steven, 1973b, Age of mineralization at Summitville, Colorado, as indicated by K-Ar dating of alunite, Econ. Geol., 68, p. 399-401.
- Miller, J.A., and P.E. Brown, 1965, Potassium-argon age studies in Scotland, Geol. Mag., 102, p. 106-134
- Miller, J.A., and W.B. Harland, 1963, Ages of some Tertiary intrusive rocks in Arran, Min. Mag., 33, p. 521-523.
- Moorbath, S., 1969, Evidence for the age of deposition of the Torridonian sediments of northwest Scotland, Scott. Jour. Geol., 5, p. 154-170.
- Moorbath, S., and J.D. Bell, 1965, Strontium isotope abundance studies and Rb-Sr age determinations on Tertiary igneous rocks from the Isle of Skye, Northwest Scotland, Jour. Petrol., 6, p. 37-66.
- Moorbath, S., and R.G. Park, 1971, The Lewisian chronology of the southern region of the Scottish mainland, Scott. Jour. Geol., 8, p. 51-74.
- Moorbath, S., A.D. Stewart, D.E. Lawson, and G.E. Williams, 1967, Geochronological studies on the Torridonian sediments of northwest Scotland, Scott. Jour. Geol., 3, p. 389-412.
- Moorbath, S., and H. Welke, 1969, Lead isotope studies on igneous rocks from the Isle of Skye, northwest Scotland, Earth Planet. Sci. Letters, 5, p. 217-230.
- Morton, N., 1965, The Berreraig sandstone series (middle Jurassic) of Skye and Raasay, Scott. Jour. Geol., 1, p. 189-216.

- Muehlenbachs, K., 1973, The oxygen isotope geochemistry of acidic rocks from Iceland, Amer. Geophys. Union Trans. (abs.), 54, p. 499-500.
- Muehlenbachs, K., A.T. Anderson, Jr., and G.E. Sigvaldason, 1974, Low- O^{18} basalts from Iceland, Geochim. Cosmochim. Acta, 38, p. 577-588.
- Muehlenbachs, K., A.T. Anderson, Jr., and G.E. Sigvaldason, 1972, The origins of O^{18} -poor volcanic rocks from Iceland, Amer. Geophys. Union Trans. (abs.), 53, p. 566.
- Muehlenbachs, K., and R.N. Clayton, 1972, Oxygen isotope studies of fresh and weathered submarine basalts, Can. Jour. Earth Sci., 9, p. 172-184.
- Muffer, L.J.P., and D.E. White, 1969, Active metamorphism of Upper Cenozoic sediments in the Salton Sea geothermal field and the Salton Trough, southeastern California, Geol. Soc. Amer. Bull., 80, p. 157-182.
- Nier, A.O., 1947, A mass spectrometer for isotope and gas analysis, Rev. Sci. Inst., 18, p. 398-411.
- Ohmoto, H., Y. Kajiwara, and J. Date, 1970, The Kuroko ores in Japan; products of sea water? Geol. Soc. Amer. Annual Meeting, Abstracts with Programs, p. 640-641.
- Ohmoto, H., and R.O. Rye, 1970, The Bluebell Mine, British Columbia. I. Mineralogy, paragenesis, fluid inclusions, and the isotopes of hydrogen, oxygen, and carbon, Econ. Geol., 65, p. 417-437.
- O'Neil, J.R., R.N. Clayton, and T. Mayeda, 1969, Oxygen isotope fractionation in divalent metal carbonates, Jour. Chem. Phys., 51, p. 5547-5558.
- O'Neil, J.R., and M.L. Silberman, 1973, Stable isotope relations in epithermal Au-Ag deposits, Western U.S.A., Geol. Soc. Amer. Annual Meeting, Dallas, Abstracts with Programs, p. 758.
- O'Neil, J.R., M.L. Silberman, B.P. Fabbi, and C.W. Chesterman, 1973, Stable isotope and chemical relations during mineralization in the Bodie Mining District, Mono County, California, Econ. Geol., 68, p. 765-784.
- O'Neil, J.R., and H.P. Taylor, Jr., 1969, Oxygen isotope fractionation between muscovite and water, Jour. Geophys. Res., 74, p. 6012-6022.
- O'Neil, J.R., and H.P. Taylor, Jr., 1967, The oxygen isotope and cation exchange chemistry of feldspars, Amer. Mineral., 52, p. 1414-1437.
- Palmason, G., 1967, On heat flow in Iceland in relation to the mid-Atlantic ridge, in Bjornsson, S., Editor, Iceland and mid-ocean ridges, Soc. Sci. Islandica, 38, p. 111-127.
- Paterson, M.S., 1958, Experimental deformation and faulting in Wombeyan marble, Geol. Soc. Amer. Bull., 69, p. 465-476.

- Pinckney, O.M., and R.O. Rye, 1972, Variation of O^{18}/O^{16} , C^{13}/C^{12} , texture and mineralogy in altered limestone in the Hill Mine, Cave-in-District, Illinois, Econ. Geol., 67, p. 1-18.
- Piwinskii, A.J., 1968, Experimental studies of igneous rock series: Central Sierra Nevada Batholith, California, Jour. Geol., 76, p. 548-570.
- Piwinskii, A.J., and P.J. Wyllie, 1968, Experimental studies of igneous rock series: a zoned pluton in the Wallowa Batholith, Oregon, Jour. Geol., 76, p. 205-234.
- Purdy, J.W., A.E. Musset, S.R. Charlton, M.J. Eckford, and H.N. English, 1972, The British Tertiary Igneous Province: Potassium-argon ages of the Antrim basalts, Geophys. Jour. R. Astr. Soc., 27, p. 327-335.
- Ray, P.S., 1972, A rhyolitic injection-breccia in tuff near Allt Slapin, Strath, Skye, Scotland, Geol. Mag., 109, p. 427-434.
- Ray, P.S., 1960, Ignimbrite in the Kilchrist vent, Skye, Geol. Mag., 97, p. 229-239.
- Reuter, J.H., S. Epstein, and H.P. Taylor, Jr., 1965, O^{18}/O^{16} ratios of some chondritic meteorites and terrestrial ultramafic rocks: Geochim. Cosmochim. Acta, 29, p. 481-488.
- Richey, J.E., 1961, British Regional Geology. Scotland: The Tertiary Volcanic Districts. (3rd Ed., revised by A.G. MacGregor and F.W. Anderson). H.M. Geol. Surv.
- Richey, J.E., 1932, Tertiary ring structures in Britain, Trans. Geol. Soc. Glasg., 19, p. 42-140.
- Richey, J.E., and H.H. Thomas, 1930, The Geology of Ardnamurchan, north-west Mull and Coll., Mem. Geol. Surv. Scotland.
- Ridley, I., 1971, The petrology of some volcanic rocks from the British Tertiary province: The islands of Rhum, Eigg, Canna, and Muck, Contr. Mineral. Petrol., 32, p. 251-266.
- Robertson, E.C., 1960, Creep of Solenhofen limestone under moderate hydrostatic pressure, in Griggs, D.T., ed., Rock deformation - a symposium, Geol. Soc. Amer. Mem., 79, p. 227-244.
- Robinson, B.W., and J.P.N. Badham, 1974, Stable isotope geochemistry and the origin of the Great Bear Lake silver deposits, Northwest Territories, Canada, Can. Jour. Earth Sci., 11, p. 698-711.
- Robinson, B.W., and H. Ohmoto, 1973, Mineralogy, fluid inclusions, and stable isotopes of the Echo Bay U-Ni-Ag-Cu deposits, Northwest Territories, Canada, Econ. Geol., 68, p. 635-656.
- Runcorn, S.K., 1964, Paleomagnetic results from Precambrian sedimentary rocks in the western United States, Geol. Soc. Amer. Bull., 75, p. 687-704.

- Savin, S.M., and S. Epstein, 1970a, The oxygen and hydrogen isotope geochemistry of ocean sediments and shales, Geochim. Cosmochim. Acta, 34, p. 43-64.
- Savin, S.M., and S. Epstein, 1970b, The oxygen isotopic compositions of coarse grained sedimentary rocks and minerals, Geochim. Cosmochim. Acta, 34, p. 323-329.
- Schwarcz, H.P., and R.N. Clayton, 1965, Oxygen isotopic studies of amphibolites, Can. Jour. Earth Sci., 2, p. 72-84.
- Schwarcz, H.P., R.N. Clayton, and T. Mayeda, 1970, Oxygen isotopic studies of calcareous and pelitic metamorphic rocks, New England, Geol. Sci. Amer. Bull., 81, p. 2299-2316.
- Sharma, T., and R.N. Clayton, 1965, Measurement of O^{18}/O^{16} ratios of total oxygen of carbonates, Geochim. Cosmochim. Acta, 29, p. 1347-1353.
- Sharp, R.P., 1943, Geology of the Wolf Creek area, St. Elias Range, Yukon Territory, Canada, Geol. Soc. Amer. Bull., 5, p. 625-650.
- Sheppard, S.M.F., R.L. Nielsen, and H.P. Taylor, Jr., 1971, Hydrogen and oxygen isotope ratios in minerals from porphyry copper deposits, Econ. Geol., 66, 515-542.
- Sheppard, S.M.F., R.L. Nielsen, and H.P. Taylor, Jr., 1969, Hydrogen and oxygen isotope ratios of clay minerals from porphyry copper deposits, Econ. Geol., 64, 755-777.
- Sheppard, S.M.F., and H.P. Schwarcz, 1970, Fractionation of carbon and oxygen isotopes and magnesium between coexisting metamorphic calcite and dolomite, Contr. Mineral. Petrol., 26, p. 161-198.
- Sheppard, S.M.F., and H.P. Taylor, Jr., 1974, Hydrogen and oxygen isotope evidence for the origins of water in the Boulder batholith and the Butte ore deposits, Montana, Econ. Geol., 69, p. 926-946.
- Sheppard, S.M.F., and H.P. Taylor, Jr., 1973, Hydrogen and oxygen isotope evidence for the origins of water in the Boulder batholith and the Butte ore deposits, Montana, (abs.), Geol. Soc. Amer. Annual Meeting, Dallas, Abstracts with Programs, p. 805.
- Shieh, Y.N., and H.P. Schwarcz, 1974, Oxygen isotope studies of granite and migmatite, Grenville Province of Ontario, Canada, Geochim. Cosmochim. Acta, 38, p. 21-45.
- Shieh, Y.N., and H.P. Taylor, Jr., 1969a, Oxygen and hydrogen isotope studies of contact metamorphism in the Santa Rosa range, Nevada and other areas, Cont. Mineral. Petrol., 20, p. 306-356.
- Shieh, Y.N., and H.P. Taylor, Jr., 1969b, Oxygen and carbon isotope studies of contact metamorphism of carbonate rocks, Jour. Petrol., 10, p. 307-331.

- Silver, L.T., C.R. McKinney, and L.A. Wright, 1961, Some Precambrian ages in the Panamint Death Valley, California (abs.), Geol. Soc. America Spec. Paper 68, p. 55.
- Silverman, S.R., 1951, The isotope geology of oxygen, Geochim. Cosmochim. Acta, 2, p. 26-42.
- Spooner, E.T.C., and W.S. Fyfe, 1973, Sub-sea-floor metamorphism, heat and mass transfer, Contr. Mineral. Petrol., 42, p. 287-304.
- Stewart, A.D., 1966, An unconformity in the Torridonian, Geol. Mag., 103, p. 462-464.
- Stewart, F.H., 1965, Tertiary igneous activity, in Craig, G.Y., (ed.), The Geology of Scotland, Hander, Con., Archon Books, p. 417-465.
- Sugisaki, R., and M.L. Jensen, 1971, Oxygen isotopic studies of silicate minerals with special reference to hydrothermal mineral deposits, Geochem. Jour., 5, p. 7-21.
- Suzuoki, T., and S. Epstein, 1974, Hydrogen isotope fractionation between OH-bearing silicate minerals and water, Geochim. Cosmochim. Acta, (in press).
- Suzuoki, T., and S. Epstein, 1970, Hydrogen isotope fractionation factors (α 's) between muscovite, biotite, hornblende and water, Amer. Geophys. Union Trans., 51, p. 451-452.
- Tan, F.C., 1969, Carbon and oxygen isotope studies of the Great Estuarine series (Jurassic) of Scotland, Ph.D. Thesis, The Pennsylvania State University.
- Tan, F.C., and J.D. Hudson, 1971, Carbon and oxygen isotopic relationships of dolomites and coexisting calcites, Great Estuarine series (Jurassic), Scotland, Geochim. Cosmochim. Acta, 35, p. 755-767.
- Tarling, D.H., and N.H. Gale, 1968, Isotopic dating and paleomagnetic polarity in the Faeroe Islands, Nature, 218, p. 1043-1044.
- Taylor, H.P., Jr., 1975, Oxygen and hydrogen isotopes in petrology, Springer-Verlag monograph, in preparation.
- Taylor, H.P., Jr., 1974a, Oxygen and hydrogen isotope evidence for large-scale circulation and interaction between ground waters and igneous intrusions, with particular reference to the San Juan volcanic field, Colorado, Carnegie Institution of Washington, Conference on Geochemical Transport and Diffusion (in press).
- Taylor, H.P., Jr., 1974b, The application of oxygen and hydrogen isotope studies to problems of hydrothermal alteration and ore deposition, Econ. Geol., 69, p. 843-883.
- Taylor, H.P., Jr., 1973, $^{18}\text{O}/^{16}\text{O}$ evidence for meteoric-hydrothermal alteration and ore deposition in the Tonopah, Comstock Lode, and Goldfield Mining Districts, Nevada, Econ. Geol., 68, p. 747-764.

- Taylor, H.P., Jr., 1971, Oxygen isotope evidence for large-scale interaction between meteoric ground waters and Tertiary granodiorite intrusions, Western Cascade Range, Oregon, Jour. Geophys. Res., 76, p. 7855-7874.
- Taylor, H.P., Jr., 1969, Oxygen isotope studies of anorthosites with special reference to the origin of bodies in the Adirondack Mountains, New York, in Origin of Anorthosites, N.Y. State Museum and Science Service Mem., 18, p. 111-134.
- Taylor, H.P., Jr., 1968, The oxygen isotope geochemistry of igneous rocks, Contr. Mineral. Petrol., 19, p. 1-71.
- Taylor, H.P., Jr., and S. Epstein, 1968, Hydrogen isotope evidence for influx of meteoric ground water into shallow igneous intrusives (abs.), Geol. Soc. Amer. Annual Meeting, Mexico City, Abstracts with Programs, p. 294.
- Taylor, H.P., Jr., and S. Epstein, 1966, Deuterium-hydrogen ratios in coexisting minerals of metamorphic and igneous rocks (abs.), Amer. Geophys. Union Trans., 47, p. 213.
- Taylor, H.P., Jr., and S. Epstein, 1963, O^{18}/O^{16} ratios in rocks and coexisting minerals of the Skaergaard intrusion, Jour. Petrol., 4, p. 51-74.
- Taylor, H.P., Jr., and S. Epstein, 1962a, Relationship between O^{18}/O^{16} ratios in coexisting minerals of igneous and metamorphic rocks, Part I, Principles and experimental results, Geol. Soc. Amer. Bull., 73, p. 461-480.
- Taylor, H.P., Jr., and S. Epstein, 1962b, Relationship between O^{18}/O^{16} ratios in coexisting minerals of igneous and metamorphic rocks, Part II, Application to petrological problems, Geol. Soc. Amer. Bull., 73, p. 675-693.
- Taylor, H.P., Jr., and R.W. Forester, 1973, An oxygen and hydrogen isotope study of the Skaergaard intrusion and its country rocks, Amer. Geophys. Union Trans. (abs.), 54, p. 500.
- Taylor, H.P., Jr., and R.W. Forester, 1971, Low- O^{18} igneous rocks from the intrusive complexes of Skye, Mull, and Ardnamurchan, western Scotland, Jour. Petrol., 12, p. 465-497.
- Taylor, H.P., Jr., J. Frechen, and E.T. Degens, 1967, Oxygen and carbon isotope studies of carbonatites from the Laacher See District, West Germany, and the Alno District Sweden, Geochim. Cosmochim. Acta, 31, p. 407-430.
- Thompson, R.N., 1969, Tertiary granites and associated rocks of the Marsco area, Isle of Skye, Quart. Jour. Geol. Soc. London, 124, p. 349-385.
- Thompson, R.N., J. Esson, and A.C. Dunham, 1972, Major element chemical variation in the Eocene lavas of the Isle of Skye, Scotland, Jour. Petrol., 13, p. 219-253.

- Thompson, T.E.K., 1960, Shallow temperature surveying in the Wairakei-Taupo area, N.Z. Jour. Geol. Geophys., 3, p. 553-562.
- Thompson, T.E.K., C.J. Banwell, G.B. Dawson, and D.J. Dickinson, 1961, Prospecting of hydrothermal areas by surface thermal surveys, U.N. Conf. on New Sources of Energy, Rome, Paper G54.
- Tilley, C.E., 1951, The zoned contact-skarns of the Broadford area, Skye, a study of boron-fluorine metasomatism in dolomites, Min. Mag., 29, p. 621-666.
- Tilley, C.E., 1949, An alkali facies of granite at granite-dolomite contacts in Skye, Geol. Mag., 86, p. 81-93.
- Tomasson, J., and H. Kristmannsdottir, 1972, High temperature alteration minerals and thermal brines, Reykjanes, Iceland, Contr. Mineral. Petrol., 36, p. 123-134.
- Tomkeieff, S.I., and M. Longstaff, 1961, The magmatic complex at Kingscross Point, Isle of Arran, Trans. Edinb. Geol. Soc., 18, p. 194-201.
- Turi, B., and H.P. Taylor, 1971a, An oxygen and hydrogen isotope study of a granodiorite pluton from the Southern California batholith, Geochim. Cosmochim. Acta, 35, p. 383-406.
- Turi, B., and H.P. Taylor, 1971b, $^{18}\text{O}/^{16}\text{O}$ ratios of the Johnny Lyon granodiorite and Texas Canyon quartz monzonite plutons, Arizona and their contact aureoles, Contr. Mineral. Petrol., 32, p. 138-146.
- Tuttle, O.F., and M.L. Keith, 1954, The granite problem: evidence from the quartz and feldspar of a Tertiary granite, Geol. Mag., 91, p. 61-72.
- Turner, F., 1968, Metamorphic Petrology, McGraw-Hill, New York.
- Tyrrell, G.W., 1928, The geology of Arran, Mem. Geol. Surv. Scotland.
- Urey, H.C., 1947, The thermodynamic properties of isotopic substances, Jour. Chem. Soc., p. 562-581.
- Urey, H.C., H.A. Lowenstam, and C.R. McKinney, 1951, Measurement of paleotemperatures and temperatures of the Upper Cretaceous of England, Denmark and the Southeastern United States, Geol. Soc. Amer. Bull., 62, p. 399.
- Urey, H.C., and D. Rittenberg, 1933, Jour. Chem. Phys., 1, p. 137.
- Van Hise, C.R., 1902, Some principles controlling the deposition of ore: in The Genesis of Ore Deposits, Trans. Amer. Inst. Mining Eng., 23 and 24, p. 282-432.
- Vogel, D.E. and G.D. Garlick, 1970, Oxygen-isotope ratios in metamorphic eclogites, Contr. Mineral. Petrol., 28, p. 183-191.

- Wager, L.R., and G.M. Brown, 1967, Layered Igneous Rocks, Freeman, San Francisco.
- Wager, L.R., E.A. Vincent, G.M. Brown, and J.D. Bell, 1965, Marscoite and related rocks of the Western Red Hills complex, Isle of Skye, Phil. Trans. R. Soc. London, ser. A, 257, p. 273-307.
- Wager, L.R., D.S. Weedon, and E.A. Vincent, 1953, A granophyre from Coire Uaigneich, Isle of Skye, containing quartz paramorphs after tridymite, Min. Mag., 30, p. 263-275.
- Walker, G.P.L., 1970, The distribution of amygdule minerals in Mull and Movern (Western Scotland), West Commemoration Volume, p. 181-194.
- Wasserberg, G.J., G.W. Wetherill, and L.A. Wright, 1959, Ages in the Precambrian terrane of Death Valley, California, Jour. Geol., 67, p. 702-708.
- Weedon, D.S., 1965, The layered ultrabasic rocks of Sgurv Dubh, Isle of Skye, Scott. Jour. Geol., 1, p. 41-68.
- Weedon, D.S., 1961, Basic igneous rocks of the Southern Cuillin, Isle of Skye, Trans. Geol. Soc. Glasg., 24, p. 190-212.
- Wenner, D.B., 1970, Hydrogen and oxygen isotopic studies of serpentinization of ultramafic rocks, Ph.D. Thesis, California Institute of Technology.
- Wenner, D.B., and H.P. Taylor, Jr., 1974, $^{18}\text{O}/^{16}\text{O}$ and D/H studies of serpentinization of ultramafic rocks, Geochim. Cosmochim. Acta (in press).
- Wenner, D.B., and H.P. Taylor, Jr., 1973, Oxygen and hydrogen isotope studies of the serpentinization of ultramafic rocks in oceanic environments and continental ophiolite complexes, Amer. Jour. Sci., 273, p. 207-239.
- White, D.E., 1973, Characteristics of geothermal resources, in Kruger, P., and C. Otte, editors, Geothermal Energy, Stanford University Press, Stanford, p. 69-94.
- White, D.E., 1968a, Hydrology, activity, and heat flow of the Steamboat Springs thermal system, Washoe County, Nevada, U.S. Geol. Surv. Prof. Paper 458-C, p. C1-C109.
- White, D.E., 1968b, Environments of generation of some base-metal ore deposits, Econ. Geol., 63, p. 301-335.
- White, D.E., 1965, Geothermal energy, U.S. Geol. Surv. Circ. 519.
- White, D.E., 1957, Thermal waters of volcanic origin, Geol. Soc. Amer. Bull., 68, p. 1637-1658.
- White, D.E., I. Barnes, and J.R. O'Neil, 1973, Thermal and mineral waters of non-meteoritic origin, California Coast Ranges, Geol. Soc. Amer. Bull., 84, p. 547-560.

- White, D.E., H. Craig, and F. Begemann, 1963, Summary of the geology and isotope geochemistry of Steamboat Springs, Nevada, in Nuclear Geology on Geothermal Areas, (Ed. E. Tongiorgi), Spoletto, Italy, p. 9-16.
- White, D.E., G.A. Thompson, and C.H. Sandberg, 1964, Rocks, structure, and geologic history of Steamboat Springs thermal area, Washoe County, Nevada, U.S. Geol. Surv. Prof. Paper 458-B.
- Wilson, A.F., D.C. Green, and L.R. Davidson, 1970, The use of oxygen isotope geothermometry on the granulites and related intrusives, Musgrave Range, Central Australia, Contr. Mineral. Petrol., 27, p. 166-178.
- Wooding, R.A., 1957, Steady state free thermal convection of liquid in a saturated permeable medium, Jour. Fluid Mech., 2, p. 273-285.